AN *IN-SITU* APPROACH FOR CHARACTERIZATION AND MODELING OF TRANSPONDER PACKAGING TECHNIQUES IN RADIO FREQUENCY INDENTIFICATION SYSTEMS

by

Leonid Mats

B.S. in Computer Science, University of Pittsburgh, 1997

B.S. in Electrical Engineering, University of Pittsburgh, 1997

M.S. in Electrical Engineering, University of Pittsburgh, 2001

Submitted to the Graduate Faculty of

School of Engineering in partial fulfillment

of the requirements for the degree of

Doctor of Philosophy

University of Pittsburgh

2007

UNIVERSITY OF PITTSBURGH

SCHOOL OF ENGINEERING

This dissertation was presented

by

Leonid Mats

It was defended on

March 20, 2007

and approved by

Michael R. Lovell, Associate Professor, Department of Industrial Engineering

J. Robert Boston, Professor, Department of Electrical and Computer Engineering, Department of Bioengineering, Department of Communications Science and Disorders

Ronald G. Hoelzeman, Associate Professor, Department of Electrical and Computer Engineering

James T. Cain, Professor, Department of Electrical and Computer Engineering

Dissertation Director: Marlin H. Mickle, Nickolas A. DeCecco Professor, Department of Electrical and Computer Engineering

Copyright © by Leonid Mats

2007

AN *IN-SITU* APPROACH FOR CHARACTERIZATION AND MODELING OF TRANSPONDER PACKAGING TECHNIQUES IN RADIO FREQUENCY INDENTIFICATION SYSTEMS

Leonid Mats, PhD

University of Pittsburgh, 2007

In a typical Radio Frequency Identification system, the tag-reader communication is the most important characteristic of success or failure. In this system, the tag represents the weakest link in the equation and must be selected with great care. It is also important to recognize that a passive RFID tag derives its power from the RF energy generated by the reader. In turn, it communicates to the reader by modulation of the incident RF energy to create a backscatter signal, where any power loss between the antenna and the integrated circuit chip limits the maximum distance from which the tag can be read. Because the typical assembly flow of the RFID labels requires multiple steps, different assembly methodologies are being used to lower the final cost of the RFID label. Packaged parasitic components can significantly degrade the performance of the RFID tags. Today, the most insidious problem is the loss of energy due to the mismatch between the antenna and the IC chip. The final cost and fabrication requirements for the RFID tag impose a set of criteria on the assembly of the tag, where the typical methods for extracting and characterizing parasitic components of the packaging are not feasible. This research develops the theoretical mechanism for measuring and modeling the packaging parasitic components of the passive Ultra High Frequency RFID tags. The research is based on proven antenna theory and antenna measurement methods, which in turn will provide a benchmark for the current and future assembly methods for manufacturing of the RFID labels.

TABLE OF CONTENTS

LIST OF TABLES

LIST OF FIGURES

1.0 INTRODUCTION

1.1 CURRENT AND RELATED WORK

The wireless industry is undergoing tremendous growth spurred in part by emerging technologies that rely on Radio Frequency (RF) energy harvesting for powering autonomous devices such as Radio Frequency Identification (RFID) transponders (tags) and Active Remote Sensing (ARS) devices [1]. In these systems, antennas are among the most important components that impose stringent restrictions on the performance of the whole system.

A non-destructive and non-invasive method for accurate measurement of the antenna input impedance and the related characteristics in-situ is presented in this dissertation. Previously, similar approaches have been presented in the literature for measuring large scale antennas with the standard non-reactive loads. This dissertation presents a new technique in order to extend the concept of the previous work.

RFID systems are used in various fields of identifying and tracking objects as in the case of process control in semiconductor industries [2], healthcare applications [3], monitoring of oil drill pipe [4], logistic applications [5], and mainly supply chain management [6], which in turn has become the main driver for the RFID technology. The demand for high volume, low cost, small size RFID systems is increasing rapidly.

RFID is a method utilized to send and receive data without contact between the readers and the tags that is achieved through the use of electromagnetic waves. The RFID tags can hold

significantly more information than any other data carrier systems and do not require strict optical line of site in order to be read [6]. This is only one of the reasons why RFID is expected to become a dominant alternative system for controlling individual product information and tracking of production history of manufacturing products.

The operation of RFID systems and their features depend on the type of tag system used. There are several types of RFID tags: active, passive and semi-passive which differ depending on whether they have their own power system [7].

Active RFID tags, which have both an on-tag power source and an active transmitter, offer superior performance. Because they are connected to their own battery, they can be read at a much longer range, but they are larger and more expensive. These tags are suitable for manufacturing, such as tracking of larger components on an assembly line, or for logistics, where the tag device is reused.

A passive RFID tag lacks a power source, although its typical read range can be more than ten meters [7]. These tags offer the most potential for lowest cost, making them suitable for mass production and single-use applications.

The first passive tags were designed to operate at both low and high frequencies (125 kHz, 136.4 kHz or 13.56 MHz) using coils as antennas. These tags operate in the magnetic near field [8] of the base station's coil antenna, and their reading distance is typically limited to about one meter [7].

Due to demand for a longer reading distance and smaller antenna sizes, there is a strong interest in UHF frequency band for RFID tags, which operate in 850 MHz to 960 MHz frequency range. Also, the backscatter principle [9, 10] is more suitable for the UHF type tags

[7] because the tag is normally operating in the far field [8] of the reader's antenna, where size of the antenna becomes significant.

The typical flow of manufacturing of RFID labels involves multiple stages, where an inlay (inlets) is an unfinished RFID label [11]. The assembly of the chip with the antenna is one of the last stages in manufacturing the inlay. After that, inlays are processed by label converters (special printers) which make them into "smart labels". Figure 1.1 details the anatomy of a smart label [12]. "Smart labels" extend the basic tag functionality by combining human-readable information and bar code technology with RFID. A smart label consists of an adhesive label that is embedded with an ultra-thin RFID tag inlay.

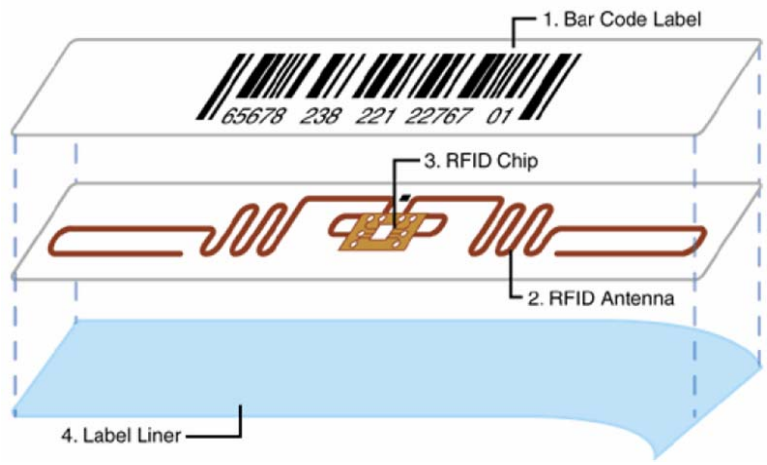

Figure 1.1: Anatomy of a smart label

Thus, the antenna design is the key competitive factor in the final product because it affects such crucial design and manufacturing characteristics as operating frequency, power requirements, reliability, and cost. Accurate design specification of the antenna in the final

package (form) is the essential component for the high performance of the RFID tag in terms of consistent performance and quality control.

1.2 RESEARCH MOTIVATION

The motivation for this research can be attributed to two principle issues, which are the unequal performance characteristics of the tags due to different packaging methods and the non-trivial ways for measuring and modeling parasitic components.

Omron Corporation [13], which is a major RFID tag manufacturing company, reports the read range results for their tags. This report points out a problem with the significant variation in the communication distance between the interrogator (reader) and the transponder (tag) for the two packaging methods: Jomful and ACP. The variations in the read distance are demonstrated in Table 1.1, where the packaging method of ACP exhibits a 61% variation in the reading distance for the tags of the same type [14].

Table 1.1: Variations in the read distance of RFID tags

Method	Variation Range	Communication Distance	Quantity of Samples
Jomful (Omron's manufacturing technology) [15]	± 14%	1.8~3.5m	233
ACP (Anisotropic Conductive Paste) [14]	± 61%	0.1~3.5m	98

A similar problem, but with the variance in the optimal operating frequency of the RFID tag has also been shown for the flip-chip assembly. The frequency spread was due to the flip-chip attachment process, which affects the package parasitic components and adds variations to the imaginary part of the packaged chip impedance. According to the referenced material, the difference in operating frequency between the two tags is as much as 20 MHz [16], as illustrated in Figure 1.2. This constitutes a problem because the total UHF frequency band allocation for North America region is only 26 MHz.

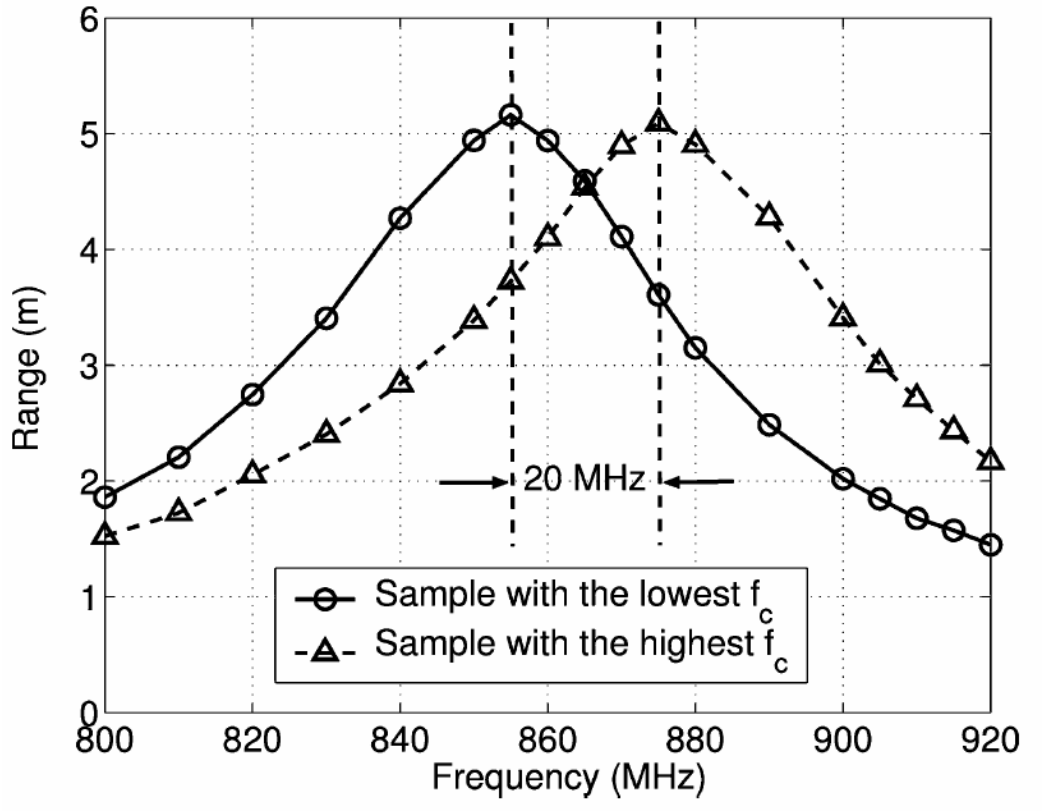

Figure 1.2: The maximum read range versus frequency

Presently, the packaging issues are resolved by the iterative methods of either adjusting the antenna layout or the positioning of the chip. For instance, the antenna layout is experimentally trimmed and tuned to the proper operating frequency [16] in order to achieve an optimal performance of the tag, while the positioning of the chip method is based on changing the positioning of the RFID chip relative to the antenna in order to meet the required read range performance criteria [17]. Thus, it is imperative to have a lumped element model (the SPICE model) of the packaging parasitic components and the interconnects between the chip and the antenna. By using the model, the tag's antenna can be correctly designed such that it would eliminate the iterative approaches of optimizing the performance of the RFID tag that are only based on the trial and error methods.

In the design of the RFID tag, the IC chip and the antenna co-design flow require an electrical model that includes both the packaging parasitic components and the interconnects. Such a model does not exist for the RFID tags. Presently, there is no information available that describes any approach for extracting or modeling packaging that is derived specifically for the RFID tags. Typically, there are two approaches that are used for extracting and modeling a standard IC chip package.

A first approach is based on using the electromagnetic (EM) field solvers. However, these simulations require such detailed information as the three-dimensional (3D) package, the bonding structure, the accurate dimension as well as the material parameters that are frequency dependent. Additionally, this information is extremely complex, proprietary to the package vendor and may not be available.

The second method is based on the measurements in the frequency domain, which are used as the direct package modeling approach. Typically, this method requires specific

mechanical fixtures and de-embedding techniques to reveal the parts of interest. In addition, the encapsulated internal package features cannot be measured from the outside due to the unique material and innovative packaging methods of the RFID tags [18]. As the result, the typical package measurement setups are not capable of taking into account the real IC package configuration.

The proposed research provides the analytic basis and methodology for measuring and modeling the packaging parasitic components of the passive UHF RFID tags.

1.3 OVERALL RESEARCH OBJECTIVES

The proposed research provides a method to obtain a complete solution for analyzing and evaluating of the tag's performance with respect to various packaging methods. The following are the key objectives of the proposed research:

Develop a mathematical formulation in order to extract the IC chip interconnect of the RFID label. The extracted data are represented as the two-port model defined by a scattering matrix.

Verify the formulation of the proposed method by modeling the RFID tag antenna and measuring its Radar Cross Section (RCS) with the load in the full-wave electromagnetic solver (Ansoft HFSS). For all selected tags, a three planer model of the antenna will be designed in Sonnet (electromagnetic solver). The RCS simulation will be performed for the three different lump elements (loads), which are inserted between the two input terminals of the antenna. By applying the proposed method the input impedance of the antenna is extracted from the

simulation results, which is verified by performing the standard design and simulation procedure for the evolution of the antenna with the wave port.

Perform test measurements of the scatter parameters with the Vector Network Analyzer (VNA). The RCS measurements will be performed for different types of tags. The measured data will be used to extract packaging information by using the proposed formulation. The results will be correlated to the simulation results

Convert RFID tags into "smart labels" by using RFID printers from Zebra Technologies [19] and Paxar Corporation [20]. Then, perform the extraction of the packaging information in order to analyze the mechanical properties of the physical interconnect between the chip and the antenna. The mechanical properties of the interconnect are critical during the printing process which is due to bending and pressure that is applied to the interconnect. The tag's specification typically defines the maximum tape tension, bending diameter and static pressure that the tags can withstand [21].

Perform a statistical analysis of the measured data in order to investigate the influence of the deviation in the reflection coefficient, which directly correlates to the quality of the packaging techniques.

Using the measured data, generate a circuit model of the package interconnect in order to provide a qualitative measure of its electrical performance for different packaging methods. A generic circuit that is proposed to model the packaging interconnects between the antenna and the chip. The interconnect model includes the inductance as the reactive components. Also, the parasitic capacitance component is present due to the antenna radial and the IC chip's substrate overlap.

Analyze the circuit model components in order to relate circuit elements to the physical packaging method in order to provide an intuitive understanding of their effects on the tag, and recommend possible design improvements that can potentially reduce the effects of these parasitic components.

1.4 DISSERTATION OUTLINE

The remainder of this dissertation is organized as follows. Chapter 2 contains an introduction of the current state of passive RFID systems along with the measurement techniques for capturing the physical communication channel using standard frequency and time domain type measurement equipment. The manufacturing flow and the application procedures for passive RFID tags are presented as the differentiating factors for the selected RFID tags.

Chapter 3 develops the mathematic model for the proposed methodology in order to extract the RFID antenna impedance and characterize the dynamic effects of the manufacturing and application flows for the tag. The initial verification of the developed equations is obtained from the simulation of the modeled RFID system in the three-dimensional electromagnetic simulation environment.

Chapter 4 involves the development of the proposed measurement method with the complete test system, which is comprised of the high precision test instrument (Vector Network Analyzer) and the controlled environment (test cell and the tag rig). A software program will be designed and implemented and used to facilitate the robust flow of the test measurements and data interpolation in real time.

Chapter 5 presents measured results for the selected types of RFID tags. The population of the identical type of tags is split into two sets. The first set of tags will be tested as received from the manufacturer. However, the second set of tags will be preprocessed using RFID printers that mechanically move a roll of tags to print the information. The effect of this operation will also be evaluated using the characterization method being developed. As a part of the proposed method, an original technique will be developed for identifying the absolute minimum operating power of passive RFID tag, which was applied in order elevate the accuracy of the measured data.

Chapter 6 presents the development of the model of the interconnect between the RFID antenna and the chip. As no comparable methodology currently exists, the simulation results are correlated to the measured data with the proposed model. The two step procedure is presented to correlate the measured results with the electromagnetic simulation solution by classical impedance transformation network. Using the transformation network, a designer can compensate for the dynamic effect of the manufacturing method and process. Then, the de-embedding technique is applied in order to extract the dynamic variations in the electrical characteristic of the interconnection between the antenna and the chip.

Chapter 7 covers the statistical analysis as the way to evaluate measured results and provide the quality control for the electrical and mechanical performance of the RFID tags with respect to different manufacturing process. The power analysis is presented in support of the statistical analysis and the sample size selection.

Chapter 8 summarizes the contributions of this effort and describes additional work that can be performed to advance the state of the proposed technique and models.

2.0 PASSIVE RFID SYSTEM

2.1 INTRODUCTION

In the classical Radio Detection and Ranging (radar) applications, radar detects the presence of objects by detecting the reflected radio waves (frequencies). Objects reflect radio frequencies in a similar manner as they do the light [22]. The radio waves and the light are similar in the sense that they are both a flow of electromagnetic energy. The only difference between the two is that light is at much higher frequency.

The reflected radio frequencies are scattered in all directions. Object detection occurs when a significant portion of it is scattered back in the direction from which it originally generated, which is back in the direction of the radar's receiving antenna.

In a typical passive RFID system, a single reader acts as the transmitter and the receiver. This system is referred to as Monostatic radar system [23], which uses the backscatter energy as the input into the reader for detection. The process of reading the RFID tag begins with the antenna radiating a modulated continuous wave (CW) signal generated by the reader. In the mean time, the modulated tag's echo is picked up and decoded by a receiver in the reader. If an echo is detected by the reader, the tag's information may be retrieved. The tag transmits data by alternating its impedance between two states which in turn varies the radar cross-section of the antenna. Typically, the state impedances are different in order to provide distinct changes in the backscattered signal.

In order to successfully read a passive RFID tag, there are two important physical requirements that must to be met. The first requirement is the forward power transfer, where sufficient power must be transferred into the tag to energize its circuitry. This is described using the Friis transmission equation (Appendix A.1) [23]. The Friis transmission equation relates the power, which is fed to the transmitting antenna (reader), to the power, which is received by the receiving antenna (tag).

The second requirement is the backscatter power where the reader must be able to detect and resolve the small fraction of energy returned to it. This requirement is described by the radar transmission equation (Appendix A.2) [23]. The radar transmission equation depends on the RCS of the tag. The RCS is defined as an equivalent area from which the energy is collected by the target and then re-radiated back to the reader (Appendix A.3) [24].

Both equations, Friis and radar transmission, depend on a magnitude of the reflection coefficient that defines in part how well the tag's antenna impedance is matched to the chip. The increase in variations of the reflection coefficient degrades the performance of the communication in the RFID system. The communication channel between the reader and a tag is demonstrated in Figure 2.1.

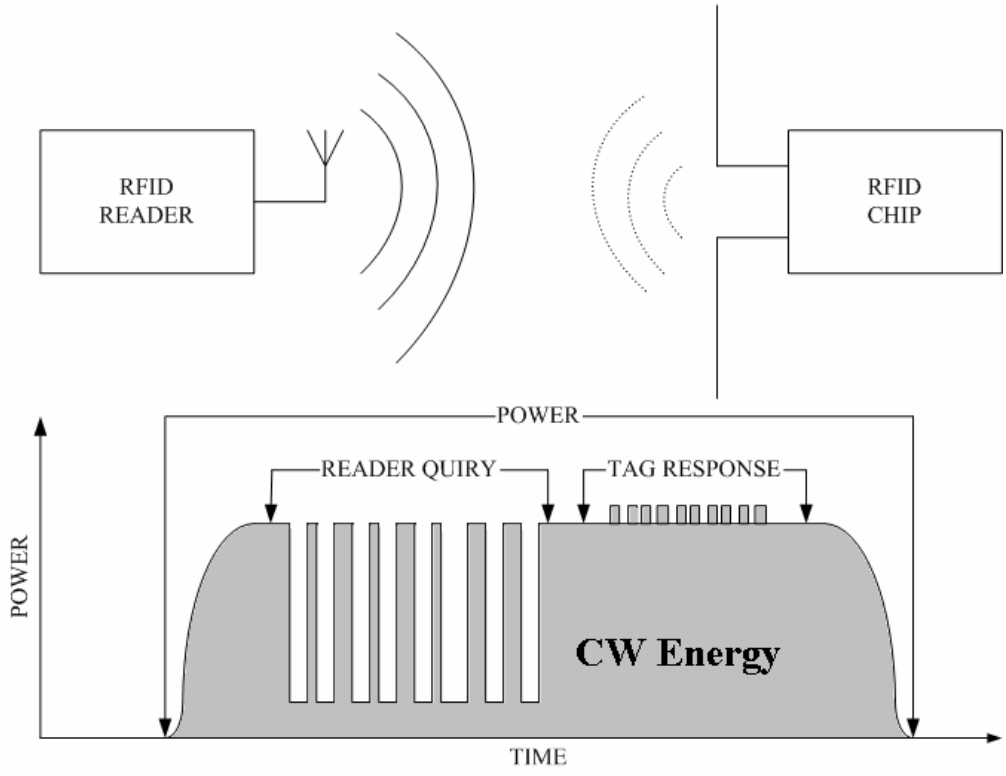

Figure 2.1: RF Communication Envelop of a Passive RFID System

In order minimize the detuning effects of the tag's antenna due to proximity to various objects, the RFID reader performs frequency hopping within the specified frequency band. The tag will not be detected unless its echoes are strong enough to be discerned above the background noise and the reader sensitivity level, which is typically around -80 dB for the commercial type RFID reader.

2.2 THEORY AND MEASURMENT OF TAG BACKSCATTERING

There are significant technical challenges in the RFID testing of the physical layer which is the air interface of the tag. These challenges include the ability to simultaneously measure the

complete communication envelope for the reader and the tag. In the case of a passive tag, the reader provides the RF power to the tag to energize the circuit and measure the response or backscatter signal from the tag. The reader's transmitter may have an output power level on the order of several orders of magnitude higher then the signal level from the response of the tag. This requires a measurement solution that has a high dynamic range and the ability to capture a single or multiple RFID data packets to characterize the RF, timing and modulation quality.

Due to these challenges, highly specialized equipment is required in order to perform the test measurements either in frequency or time domain environment. Figure 2.2 illustrates the complete capture of the communication between the reader and a tag using Tektronix's Real Time Spectrum Analyzer (RSA3408A) which performs the test measurements in the frequency domain by measuring the power at specific frequencies.

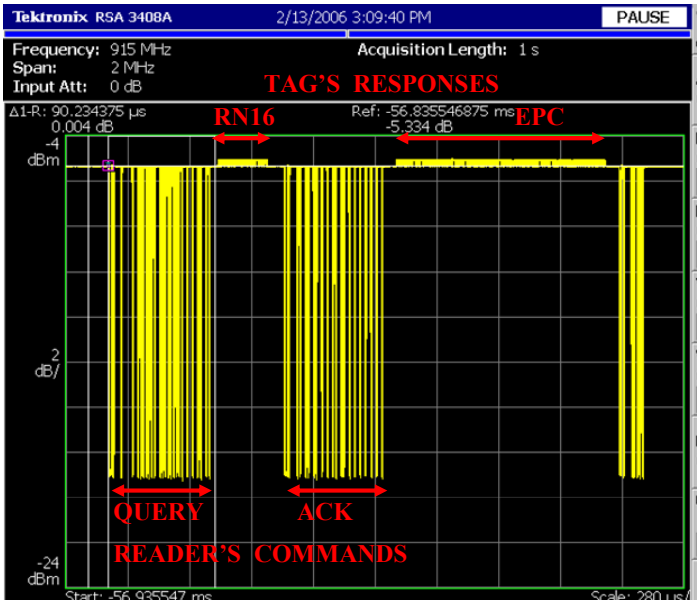

Figure 2.2: Measured RF Communication Envelop of a Passive RFID System

Using the high performance spectrum analyzer from Agilent, the backscatter power level can be captured and analyzed for the quality of the response from a tag, which is shown in Figure 2.3.

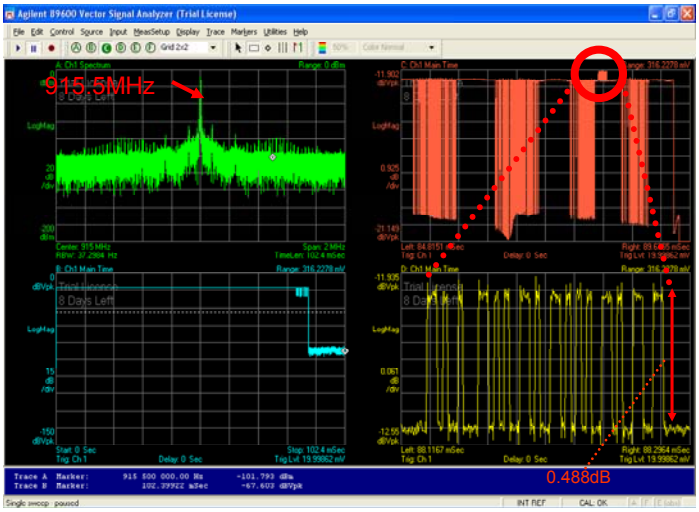

Figure 2.3: Measured backscatter signal from a tag

The oscilloscope is the most widely used piece of equipment that is used for measuring signals in the time domain environment. A scope with the high sampling rate can be used to capture the physical communication channel of the RFID system. Figure 2.4 illustrates the signal transmitted during the reader-to-tag communication which contains both continuous wave (CW) and the modulated commands. The communication channel is captured with the high sampling scope that provides $20 \cdot 10^9$ samples per second on two channels simultaneously. There is a phase shift in the re-radiated signal from the tag with respect to signal which is transmitted by the reader.

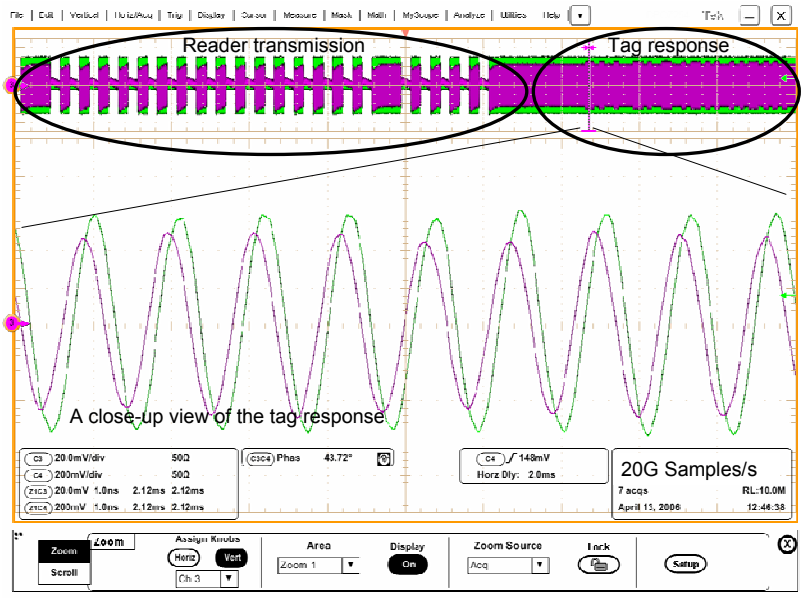

Figure 2.4: The communication channel between an RFID reader and a tag in time-domain

In order to better understand how an RFID tag sends data back to the reader by simply switching its input impedance and thus performing an amplitude or phase modulation of the backscatter signal, the simplified test configuration was set up. This setup demonstrates a phenomenon of radar cross-section from a loaded antenna that is the total re-radiated power from an antenna which was the function of a load attached to the terminals of the antenna. When different terminations are attached to the antenna, the back scattered signal will have a distinctive amplitude and phase shift with respect to the signal impinging on the antenna which represents the fundamental method for sending the data from the tag to the reader.

In order to demonstrate the desired phenomenon, the three standard microwave terminations of the HP3567A calibration kit (open short and matched load) were used for terminating the tuned dipole antenna manufactured by A.H. Systems (Figure 1.2).

Figure 2.5: The tuned dipole antenna (model FCC-4) from A.H. Systems

The measurement system is presented in Figure 2.6. The transmission part of the test system consists of a horn antenna and a signal generator with the amplifier. The transmitting signal was at 915 MHz, and the output power level was set to 5 Watt. The receiving part was based on the fast sampling oscilloscope (Tektronix DPO7254) connected to the receiving antenna located above the dipole under the test. Both antennas were part of the ETS-Lindgren Model AMS-8050 Antenna Measurement System that is the compact and fully anechoic RF enclosure for antenna pattern measurements in Figure 2.6. The dipole antenna under the test was placed 1.5 m from the transmitting antenna and about 1 meter from the receiving antenna, well located in the far field. The antenna was securely position on a specially built support which facilitates the accurate position of the antenna for all measurements (Figure 2.7).

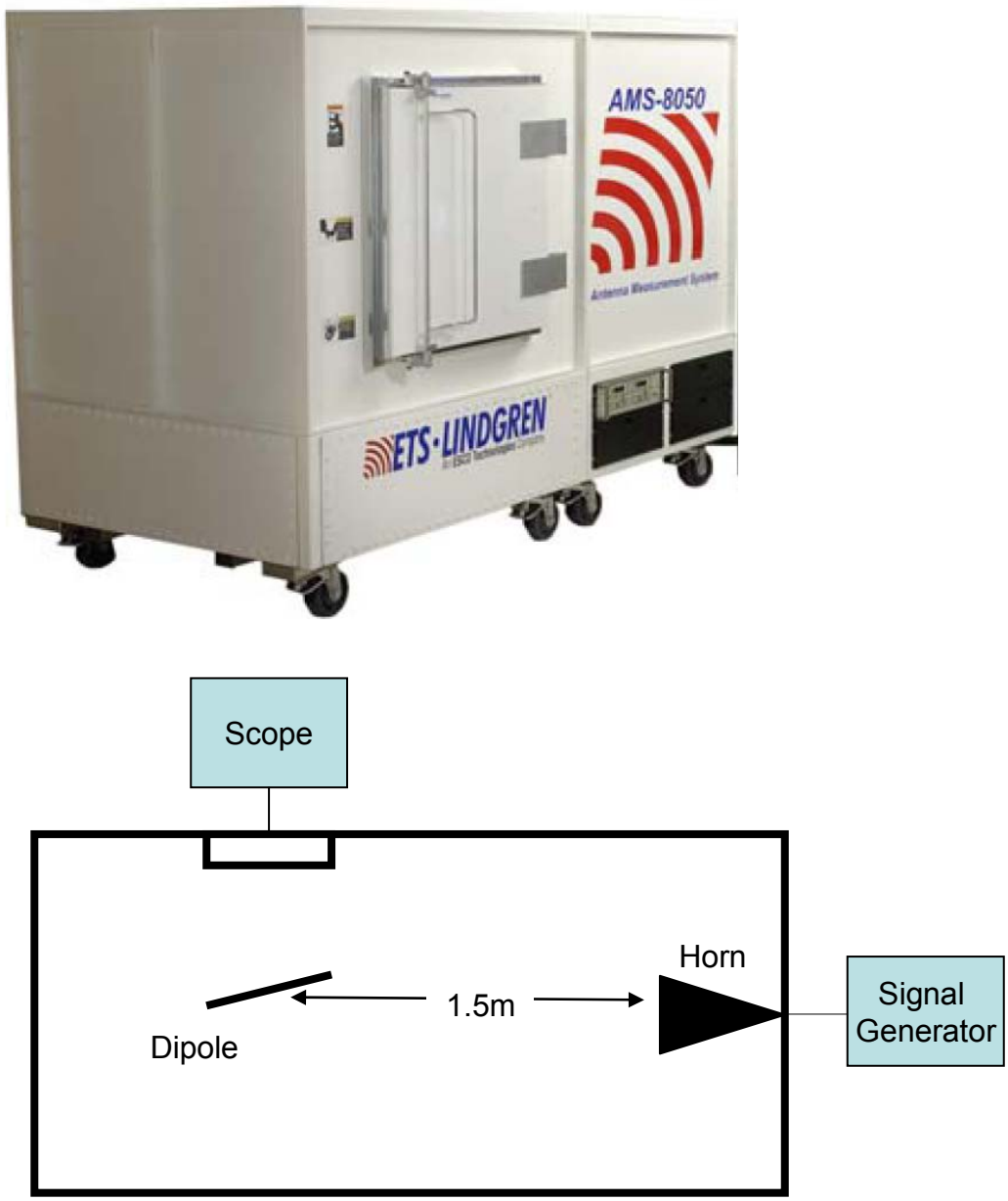

Figure 2.6: The side view of the ETS-Lindgren test system for measuring RCS of the antenna

Figure 2.7: The dipole antenna under the test on the support

The measured results, which are presented in Table 2.1, confirm the fact that the phase and the magnitude of the re-radiated signal are different for various loads attached to the dipole antenna which agreed to the theoretical calculations in [23].

Table 2.1: The measured results for the dipole with three different termination cases

Termination	V_{rms}, mV	Phase, Degree
OPEN	182	178
SHORT	162	161
LOAD	175	167

The measured results of the dipole antenna show that the total scattered RCS is smaller when the short circuit termination is attached. The reason for this is most likely due to the balance-to-unbalanced transmission line which is attached to the dipole in order to allow for the coaxial connection to the unbalanced test instruments (i.e. Network Analyzer). This reinforces the benefits of the proposed measurement technique which does not require the access to the antenna terminals which in turn minimizes the uncertainty of the measurements.

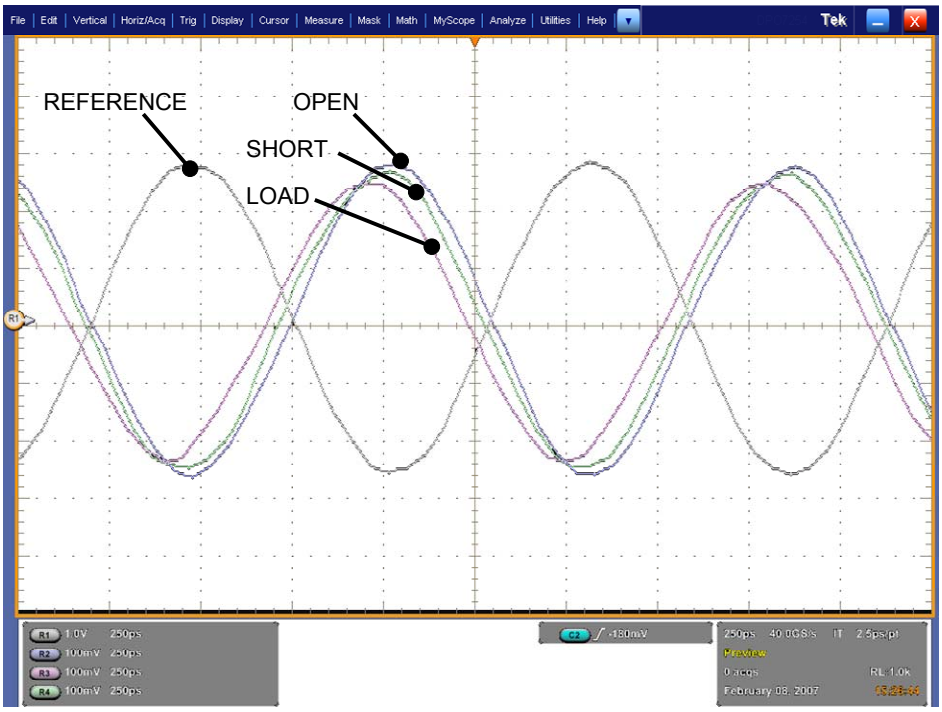

Figure 2.8: The re-radiated signals of the dipole antenna for three different termination cases

2.3 MANUFACTURING OF RFID TAGS

The demand for RFID tags has recently increased dramatically, where over 1.3 billion RFID tags were produced in 2005, 2.5 billion is expected in 2006 [25], and by 2010, that figure will soar to

33 billion [26]. Due to this fact, there is a need for manufacturing methods and quality conformance measurements that can provide highly reliable inlays at low cost.

The typical flow for manufacturing of passive RFID tags is illustrated in Figure 2.9 [13]. The overall design is split in different stages of an assembly line where the integrated circuit (IC) chip is designed and manufactured first. Then, the antenna is designed and manufactured. In the last two stages, the IC chip and antenna are assembled together and packaged for the final product. The final product is the RFID label.

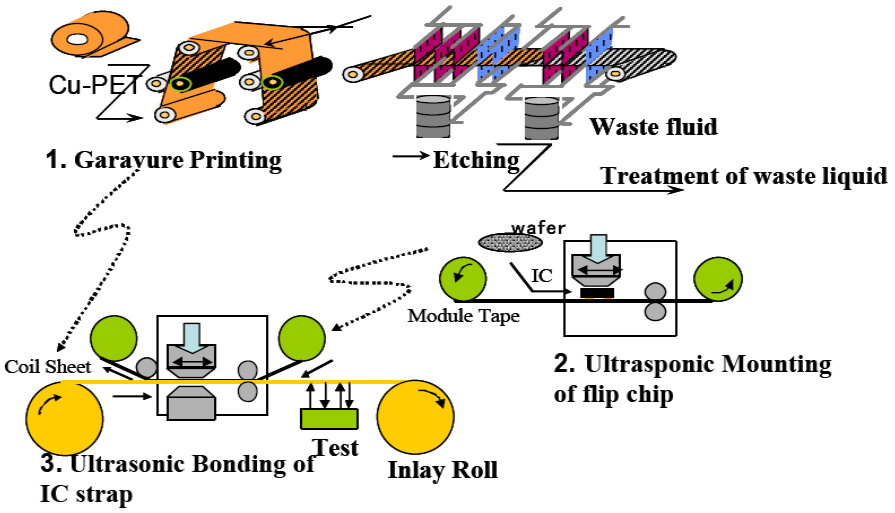

Figure 2.9: The typical flow for manufacturing of passive RFID tags

Because the manufacturing of the RFID tag is split in stages (Figure 2.10), the accountability of all package parasitic components due to integration of the antenna and IC chip becomes paramount to the overall quality of the final RFID label.

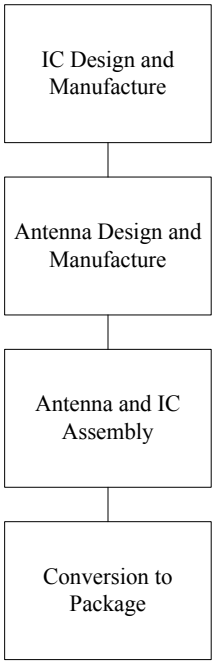

Figure 2.10: Manufacturing Flow of a Low Cost RFID Tag

2.3.1 Integrated Circuit (IC) Design and Manufacture

The main performance objective in the IC chip design is placed in achieving the maximum read distance by minimizing its power consumption [27] and maximizing available power delivered to the IC. One of the latest IC chip designs [6] for RFID tags is implemented in an industry-standard 0.25µ logic CMOS process and implements the electronic product code (EPC) Class-1 Generation-2 protocol [28]. The International Standards Organization (ISO) has approved this protocol, which was published as an amendment to its 18000-6C standard RFID air interface for item management using devices that operate in the 860 MHz to 960 MHz of the Industrial Scientific and Medical (ISM) band. To this date, there is one IC chip that dominatesis all tags that are manufactured.

The typical architecture of the passive RFID chip consists of the antenna interface, circuitry to rectify and convert incident RF energy to DC, demodulator oscillator and digital logic with nonvolatile memory [6].

The critical part of the RFID chip is in the front-end analog circuitry. The typical UHF type RFID chips are designed to be used with a dipole antenna. Therefore, there are at least two connection points.

2.3.2 Antenna Design and Manufacture

In a typical passive RFID tag, the antenna plays a dual role. First, the antenna is responsible for sending and receiving data, which is accomplished by the microchip that changes the electrical load on the antenna to reflect back the carrier signal backscatter. Secondly, the tag antenna collects and emits (reflects) energy in the form of electromagnetic waves. Energy collected by a tag's antenna is used to power the tag's microchip. Maximizing collected energy is essential to increasing the range and robustness of a passive system.

The characteristics of an antenna are fundamental to an understanding of the antenna and how it is used in a passive device for both radio communications system and energy harvesting. These most important characteristics include gain, radiation pattern, and polarization. The input impedance is one of characteristics, which is of fundamental importance. It is necessary to match the impedance of an antenna to a load in order to efficiently couple the RF power. This can be achieved by using the maximum power transfer theorem.

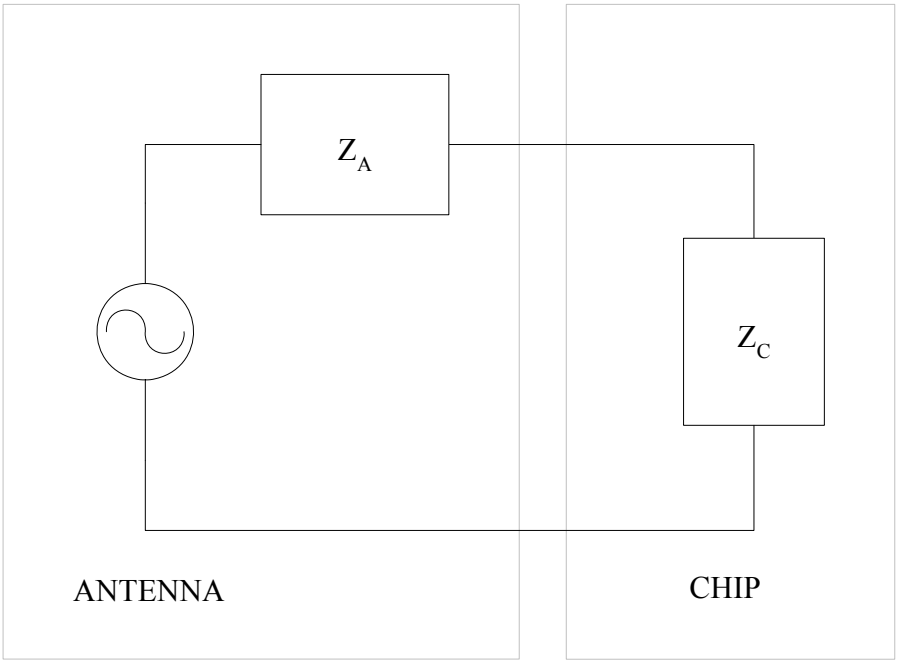

Figure 2.11: Passive RFID tag

The maximum power transfer theorem states that, for a linear network with fixed source impedance, the maximum power is delivered from the source to the load when the load impedance is the complex conjugate of the source impedance, that is

$$Z_L = Z_S^* \qquad \textbf{(2.1)}$$

Where $Z_L = R_L + jX_L$ and $Z_S = R_S - jX_S$

Thus, $R_L = R_S$ and $jX_L = -jX_S$; and in this case, the circuit is said to be conjugately matched.

2.3.3 Antenna and IC chip assembly

The method of assembling a chip onto a substrate has been developed and optimized for decades and is known as conventional die bonding technology. Initially, this technology was adopted for manufacturing and RFID tags [18]. The technology was based on the wire bonding of the application specific integrated circuit (ASIC) pad with either ultrasonic or thermosonic method using aluminum, silver or gold wire [29]. New assembly technologies are being explored, because ultrasonic and thermosonic require mechanically stable support from the substrate. This is not easy to achieve with low-cost materials like the polyethylene terephthalate (PET) at thicknesses of 50μ [21]. The PET is the most commonly used substrate for the RFID tags. Also, the multiple steps and expensive materials were adding to the final cost of the RFID tags.

From a designer's point of view, the advantage of conventional chip bonding is very accurate wire-bond modeling, which has been thoroughly tested and simulated within EM Software tools, like Ansoft HFSS [30], Sonnet [31] and IE3D [32]. The 3D interconnects and their SPICE equivalent models are shown in **Error! Reference source not found.** [32] . The models are typically supplied by the industry [33]. The model parameters can be converted into a SPICE netlist. The SPICE netlist can be imported into a SPICE simulator for time domain simulation.

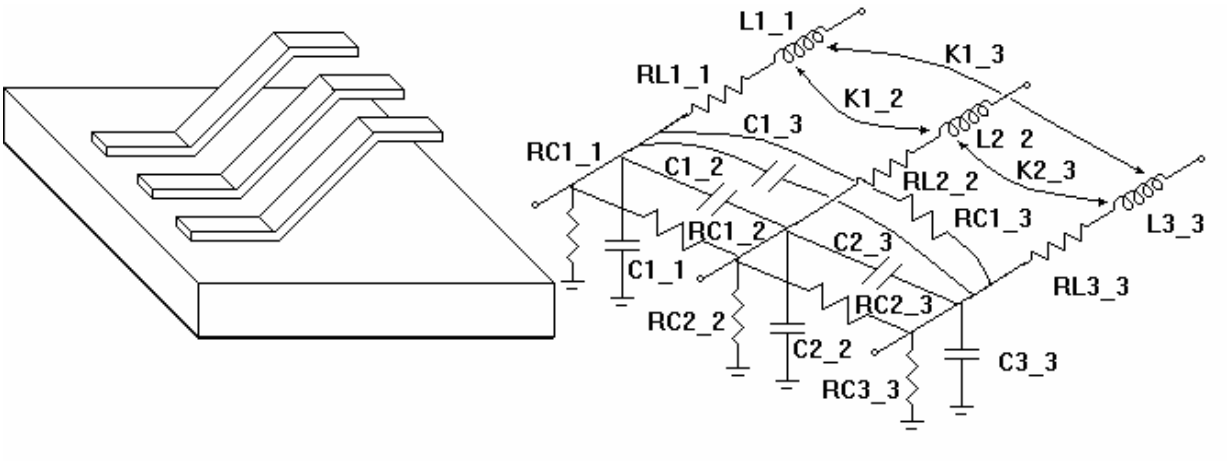

Figure 2.12: An example of the RLC equivalent circuit model for three bonding wires

Because the manufacturing price appears to be a significant benchmark for RFID tags to be commercially accepted into the industry, alternative approaches have been investigated to offer a low cost solution.

There are two principle types of the RFID chip assembly methods that exist; they are the direct and indirect chip assembly. Typically, an IC chip has "bumps" formed by an off line process on the active surface of the chip, which are made of gold or a gold alloy [34]. Bumps provide convenient connection points between the chip and antenna. In direct assembly, the chip's bumps are positioned and placed directly onto the antenna connections by means of flip-chip technology [35]. Usually, the IC has four bumps on a chip, which are connected to the corresponding four connection pads on the antenna. These bumps are pushed into the antenna connection pads and then the chip is secured with some type of adhesive. This manufacturing process typically uses a robotic arm to assemble RFID tags one at a time.

As an alternative, some manufacturers employ indirect RFID chip assembly. Initially, a chip is applied onto a positioning strip called interposer or strap (Figure 2.13), which is typically

a flexible substrate [36] that contains a die. Then, the strap is mounted on the antenna, which can be typically done by crimping. Indirect assembly is advantageous because the interposer is not as gentle or as fragile as a bare die for attaching to the antenna. Also, the form factor is much larger than a die, which makes it easier to handle with the machinery that performs the assembly of the tag.

In order to increase the throughput in tag production, an alternative process, pick-and-place robots are replaced with the fluidic self assembly [37] manufacturing process that involves flowing IC chips in a special fluid over a base with holes shaped to catch the chips. The process is designed to mass assemble billions of RFID tags at a very low cost.

There is another alternative technique known as vibratory assembly [11], where a special drum vibrates until chips slide into cavities on a substrate where they can be connected to the nodes on packages and then bonded to an antenna. The system is similar to fluidic self-assembly where the goal is to provide a low cost mass production.

Once the IC chip is positioned, different connection methods are used for making an Ohmic contact between the IC chip and antenna. For example, ultrasonic bonding technology has been adopted at the processes of IC chip mounting to the strap and that of the strap bonding to the antenna [38, 39]. The IC chip mounting method is provided Figure 2.13 [34]. The IC strap is produced by etching aluminum on the PET substrate.

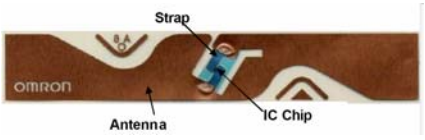

Figure 2.13: RFID inlay

By adding physical pressure from the upper side to the IC chip, where the gold bumps are formed, the ultrasonic technique is applied. Next, the gold and aluminum are joined by breaking the oxide layer on the aluminum electrode.

Figure 2.14 shows welded area between the conductive circuit (aluminum circuit) and the electrodes of the IC chip in the attachment process where the IC chip electrodes were removed for the picture [14].

Figure 2.14: Melted metal of the interconnect

Another attachment method is based on applying a conductive paste between the electrode and the antenna. Two tags which were manufactured using the same packaging method, but have some interconnect differences are illustrated in Figure 2.15 and Figure 2.16.

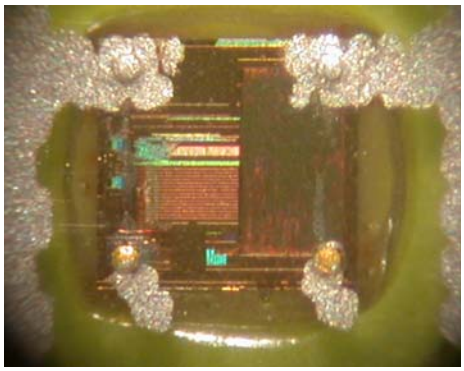

Figure 2.15: Sample Tag A

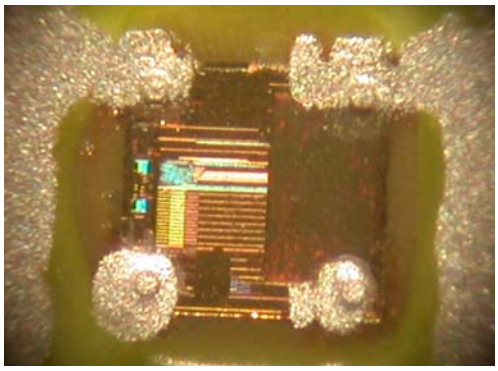

Figure 2.16: Sample Tag B

The goal of the packaging technique is to be stable so that the communication distance is stable and the connection is not broken. Mounting an IC chip on a substrate forms parasitic components between the IC and the conductive circuits as shown in Figure 2.17 [14]. The circuit parasitic components greatly influence the working performance of the RFID Tags.

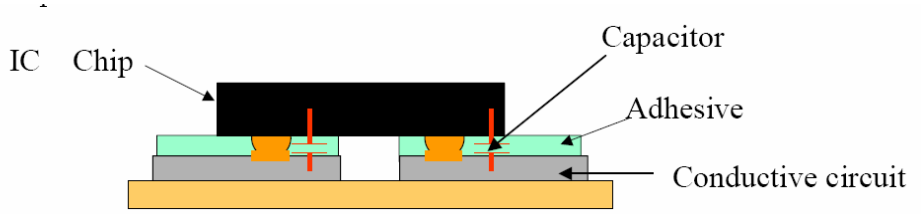

Figure 2.17: A parasitic capacitors between the IC and the conductive circuit

The typical assembly paradigm puts most emphasis on the cost and mechanical characteristics of the package while disregarding the RF performance. Any new package design must have the RF performance at least at the same priority as the mechanical concerns because

the assembly structure and parasitic components of the materials can cause the package to seriously degrade the RFID tag performance if not it render the tag to be unusable.

The ideal package creates a transparent link between the antenna connection and the IC chip. Any deviation from the ideal package causes the input signal to be degraded. This degradation manifests itself in two ways, which are the power insertion loss and return loss. The RF input signal energy is either reflected or transmitted from the antenna to the IC inputs. The return loss (RL) at the port of a network is deind as

$$RL = -20\log(|\Gamma|) \tag{2.2}$$

For a perfectly transparent interconnect where the reflection coeeficient (Γ) is zero, the return loss will be infinite. If the interconnect is completely destroyed, for instance presenting a short or an open circuit, than all of the signal will be returned (none will be transmitted to a load) and the return loss wll be zero. A larger value is preferred for the return loss. The insertion loss (IL) defines how much of a signal is lost as it goes through interconnect, which is also a measure of the attenuation resulting from insertion of a parasitic component (resistance) between an antenna and a chip. A smaller value is desired for the insertion loss. The insertion loss is defined as

$$IL = -20\log(1 - |\Gamma|) \tag{2.3}$$

where Γ is the reflection coefficient from the leads of the package. The quantity |Γ| is the ratio of reflected voltage wave magnitude to incident voltage wave magnitude which is defined as follows, where Z_1 is the impedance toward the source, Z_2 is the impedance toward the load:

$$\Gamma = \frac{Z_2 - Z_1}{Z_2 + Z_1} \tag{2.4}$$

Power loss (PL) due to lead package parasitic is given by:

$$P_L = 1 - |\Gamma|^2 \tag{2.5}$$

Figure 2.18 shows the relationship between maximum read range and the reflection coefficient, which is not linear. If a circuit is perfectly matched, Γ=0, the maximum possible power will be transferred from the line to the load hence achieving maximum read range. On the other hand, the impedance matching with the Γ = 0.5 corresponds to about 80% of the maximum attainable read range.

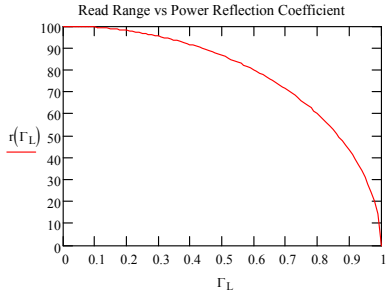

Figure 2.18: Relationship between Reflection Coefficient and Read Range of the Tag

2.4 APPLICATION OF RFID TAGS

Typically, RFID tags can be encoded with a stand-alone reader/antenna configuration. However, in real-world applications that function is accomplished within the RFID-enabled printer or a printer/applicator. In RFID implementation, the tag can be encoded, verified, printed and even applied to the box by one machine.

The RF inlay adds a level of complexity to an otherwise fairly straightforward process of printing additional information on the RFID label. Both the microchip itself and the edges of the inlay cause “bumps” in the otherwise flat label surface. This can cause print distortion. There is a floating head technology that is used to lift the print head over the chip in the label, thus reducing the risk of impact damage to the chip.

Another issue is that the RF environment inside each RFID printer is different. Therefore, the differences between the inner cavity of the printer and the reader antenna location often require unique inlay orientation and placement for labels used on different printers in order to perform the encoding of the chip, and then verifies the miscoded and unreadable RFID labels.

Also, spacing between the smaller labels often needs to be increased to prevent more than one tag from being programmed at the same time. Stand-alone printers can try more than once to program a tag. However, a printer/applicator must keep up with cartons moving along the conveyor and therefore must discard tags it cannot program the first time.

There are a number of options available for automatically dispensing and applying the tag. Factors that affect the selection of an applicator include label size, carton speed, carton placement, and height variation and placement accuracy requirements. The preferred methods are semi-automated or automated "print-and-apply" processes. In these systems, cartons are fed to the label applicator by hand or preferably by conveyor. The label printer at the end of the

process prints a pallet level label which is applied before the pallet moves through the RFID portal. The attached tags are read as they move through supply chain from manufacturing plant to the retailer.

2.5 STATEMENT OF THE PROBLEM

The preceding elements regarding the performace of an RFID tag will now be incorporated to summarize and define the problem which will be solved as part of this research.

- The proposed research will provide the methodology for a non-invasive *in-situ* measurement of the interconnection effect between the antenna and the chip in an RFID tag.
- The proposed interconnect characterization and model will be developed using a classical two-port network model.
- The proposed methodology will be validated with the electromagnetic simulation.
- The characterization method will be demonstrated using RFID tags from different manufacturers.
- Because tags can be documented using an RFID printer that mechanically moves a roll of tags. The effect of this operation will also be evaluated against the original tags using the proposed characterization method that will be developed.

- As no comparable methodology currently exists, one benchmark for approximate demonstration and correlation of the results will be based on the antenna modeling of the selected RFID tags using the commercial RF software simulation package.
- The antenna/chip interconnect model will be developed to make it possible for the antenna designer to compensate for the dynamic effect of the manufacturing method and process.
- Based on the test results from the selected RFID tags, the method and the results will be evaluated using statistics, where the statistical methodology will be found and a corresponding analysis will be performed in order to evaluate the minimum sample size of the testing results.
- The sensitivity and realism of the method will be justified through the physical evaluation of the RFID tag analog front-end as the means for measuring the absolute minimum operating power level of the RFID tag.
- Based on the proposed method, the complete test system that is comprised of the control environment and software will be realized. This system will provide a quality control of the manufacturing process for the on-line and in real time environment due to the non-invasive nature of the research results.

3.0 THE PROPOSED MEASUREMENT METHODOLOGY

Currently, RFID readers with variable output power are used to evaluate tag performance in manufacturing with respect to operating difference. However, due to the differences in the architecture of the RFID readers the test results are subject to inconsistencies. Antenna patterns and receiver sensitivities are two factors which can produce different results with different readers. The following methodology provides a "baseline" for other characterization RFID test systems which are based on the standard RF test equipment (i.e. vector network analyzer and real-time spectrum analyzer).

3.1 THEORETICAL BACKGROUND

A typical UHF RFID system combines the physical operating principle of the radio broadcast technology and radar [9]. The scattering and radiating properties of the target are related [40, 41]. The total scattered RCS of a target (object) defined as [42]

$$\sigma = \lim_{R\to\infty} 4\pi R^2 \frac{\left|E_{scat}\right|^2}{\left|E_{inc}\right|^2} \quad \textbf{(3.1)}$$

where

σ is the total radar cross section or echo area

R is the distance from the target

E_{scat} is the scattered electric field

E_{inc} is the incident field

In the past, the fields scattered by the antenna have been represented with the electric field scattered by the antenna with the load impedance [24, 43, 44], where the electromagnetic waves backscattered by an antenna depend not only on the antenna geometry, but also on the antenna load defined [45]. Consequently, the radar cross-section of the antenna is expressed as [24]

$$\sigma = \frac{1}{\pi}\left|\frac{2\pi RE_{short}}{E_{inc}} - (1+\Gamma_A)\frac{\pi RE_{ant}}{E_{inc}}\right|^2 \quad \textbf{(3.2)}$$

where

E_{inc} is the impinging electric field on the antenna (tag)

E_{short} is the received electric field at the receiver (reader) by short-circuited antenna (tag)

E_{ant} is the received electric field radiated by the antenna (tag)

R is the distance between the transmitting antenna (reader) and receiving antenna (tag)

Γ_A is the antenna reflection coefficient, which is defined as

$$\Gamma_A = \frac{Z_L - Z_A}{Z_L + Z_A} \tag{3.3}$$

where

Z_L is the load impedance

Z_A is the antenna input impedance

Based on equation (3.2), the radar cross section of the short-circuited antenna (Γ_A=-1) can be reduced to the equation (3.1), which is the defined for an arbitrary object (target). The open-circuited antenna generates the minimum radar cross section (Γ_A=+1). In the complex conjugate case (Γ_A=0), the radar cross section would be lower than in the short circuit antenna, but larger than in the open circuit antenna. The simulated radar cross section for a half-wave dipole with three different terminations is demonstrated in Figure 3.1.

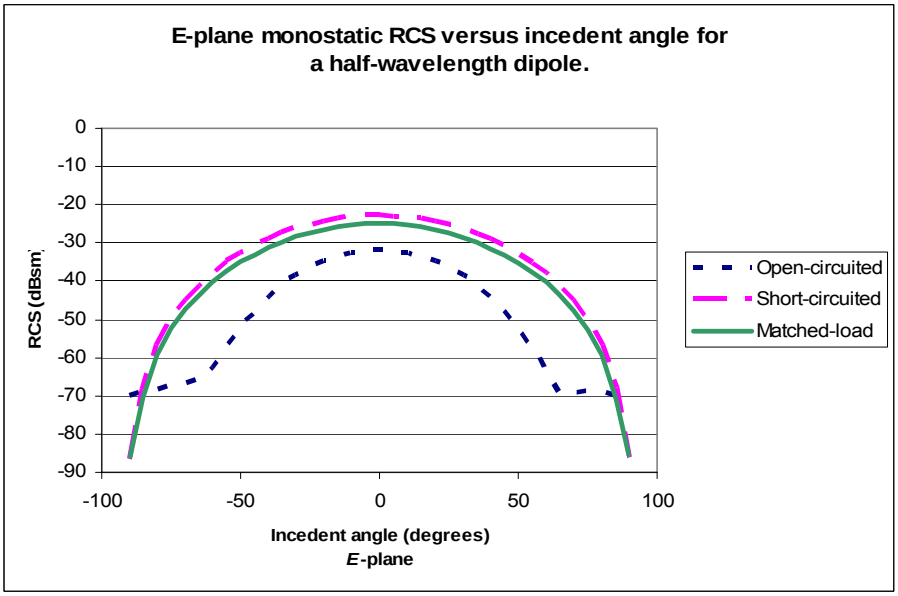

Figure 3.1: The radar cross section of a loaded half-wave dipole

The available power to the antenna can also be determined by examining the incident wave. The power density in the incoming wave is related to electric field as

$$E = \sqrt{120\pi S} \tag{3.4}$$

where

E is the electric field

S is the power density

Then the radar cross section of the antenna in the free space can be written as

$$\sigma = \frac{1}{\pi}\left|2\pi R\sqrt{\frac{S_{short}}{S_{inc}}} - (1+\Gamma_A)\pi R\sqrt{\frac{S_{ant}}{S_{inc}}}\right|^2 \tag{3.5}$$

where

S_{inc} is the impinging electric field density on the antenna (tag)

S_{short} is the received electric field density at the receiver (reader), which is reradiated by short-circuited antenna (tag)

S_{ant} is the received electric field density radiated by the antenna (tag)

The first term in equation (3.5) represents the "structural scattering" of the antenna, which is due to the currents induced by the incident field when antenna is short-circuited, and it is independent of the load impedance. The second term represents the "antenna mode" scattering

term, which represents the radiation characteristics of the antenna, which depend on the power absorbed in the load and the power which is reradiated due to the mismatch (Γ_A). The total radar cross-section of the transponder antenna with the load impedance (Z_L) can be represented with the formula given in [23]

$$\sigma = \left| \sqrt{\sigma^s} - (1+\Gamma_A)\sqrt{\sigma^a} e^{j\phi_r} \right|^2 \quad \textbf{(3.6)}$$

where

σ is the total RCS with antenna terminated with Z_L

σ^s is the RCS due to structural term

σ^a is the RCS due to the antenna mode term

φ_r is the relative phase between the structural and antenna mode terms

Given the previously presented derivations, it is possible to quantify the changes in loading connected to the input terminals of the tag's antenna. In other words, the total RCS is determined by changes in the reflection coefficient defined in the equation (3.6). Therefore, it is possible to apply the relationship between the RCS and the load in order to derive the input impedance of the tag's antenna from the RCS measurement concept, which in turn is adopted from the method of connecting at least three known loads to the feed point of the antenna [43].

The critical advantage of the proposed method is the fact that it eliminates any direct probe connection to the terminals of the antenna. Because there is no physical connection, it becomes useful for the measurement of the input impedance of the antenna which is integrated within the package such as RFID tags [9].

Assuming that there is a set of known load impedances, the input impedance of the antenna can be quantified at the reader side where a tag-reader system can be modeled as a two-port network. The transfer function between the input (reader) and the output (tag) ports is expressed in terms of the scattering parameters of the equivalent two-port network [46, 47]. An equivalent two-port network is demonstrated in Figure 3.2.

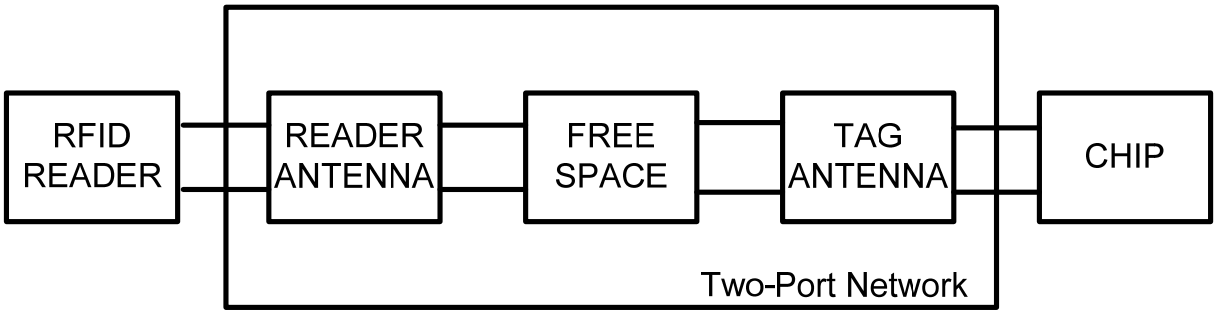

Figure 3.2: Two-port model of the tag-reader system

3.2 THE TWO-PORT MODEL

In this work, it is sufficient to assume a system with only one RFID reader and one tag, which in turn can be represented with two circuits, one for each. The transfer function between the two circuits will be expressed in terms of the two-port network.

In a linear two-port system, any type of hybrid matrix (for example, impedance [Z], admittance [Y], or scattering [S] parameters) is theoretically adequate for modeling multi-port linear networks. RF and microwave circuits are traditionally described by S-parameters even though Z-parameters provide some physical meaning of the network, so the S-parameter or Z-

parameter description is the logical choice for a proposed measurement method. The approach described in this work, therefore, uses both S-parameters and Z-parameters for two-port characterization. Due to conversion relations, however, any n-port hybrid matrix theoretically can be used [46]. The proposed equivalent two-port network is illustrated in Figure 3.3.

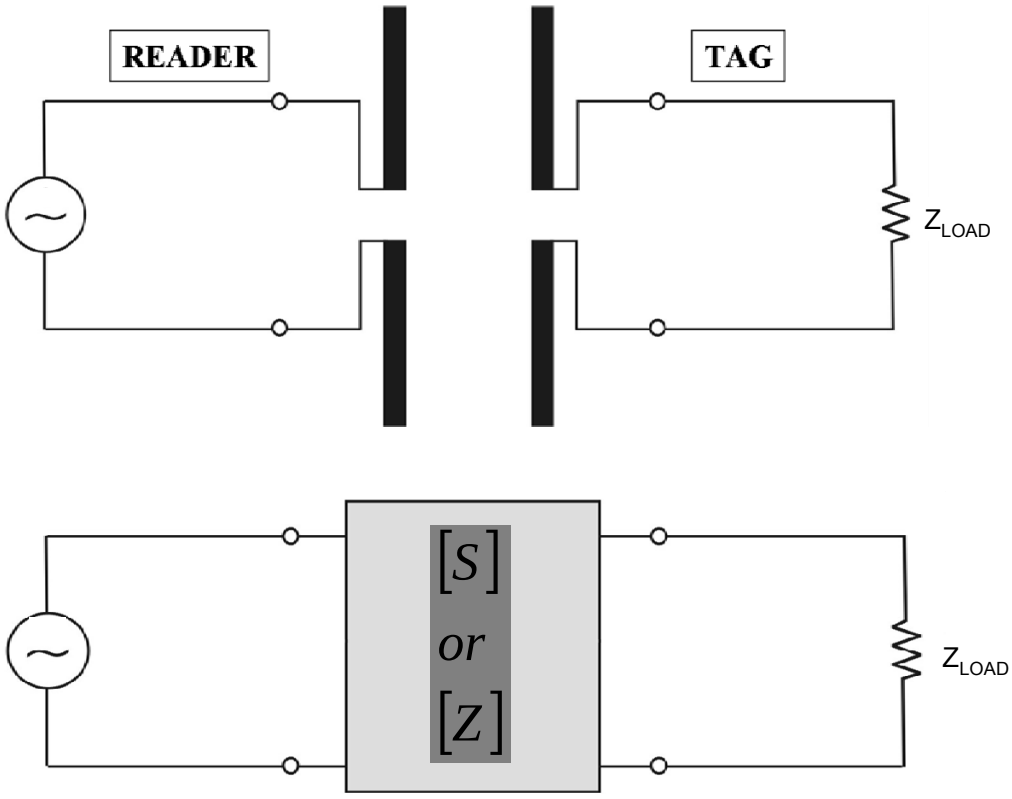

Figure 3.3: An equivalent two-port network representation

3.2.1 Z-Parameters

Based on this reciprocity principle, any complex passive linear two-port network can be modeled by either a T-network or a PI-network. Therefore, the two-port network can be represented by the equivalent symmetrical T-network shown in Figure 3.4.

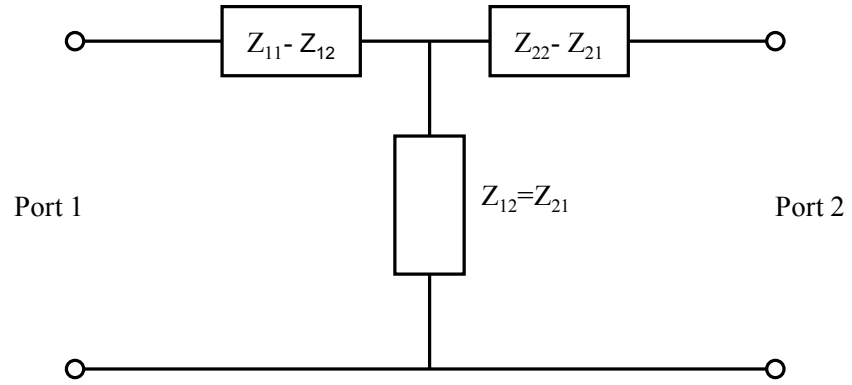

Figure 3.4: T-network

Where Z is defined as

$$\begin{bmatrix} Z_{11} = \left.\frac{V_1}{I_1}\right|_{I_2=0} & Z_{12} = \left.\frac{V_1}{I_2}\right|_{I_1=0} \\ Z_{21} = \left.\frac{V_2}{I_1}\right|_{I_2=0} & Z_{22} = \left.\frac{V_2}{I_2}\right|_{I_1=0} \end{bmatrix} \quad \textbf{(3.7)}$$

Applying circuit theory, the Z matrix can be defined as following, where Z_1=Z_{11}-Z_{12}, Z_2=Z_{22}-Z_{21} and Z_3=Z_{12}=Z_{21}

$$\begin{bmatrix} Z_{11} = Z_1 + Z_3 & Z_{12} = Z_3 \\ Z_{21} = Z_3 & Z_{22} = Z_2 + Z_3 \end{bmatrix} \quad \textbf{(3.8)}$$

Given a two port reciprocal network, its behavior is uniquely determined by a three impedance T-network. When a Z_{load} is connected at the output port, the impedance seen at the

input port is given by equitation (3.9). The impedances that makes up the T-network can be determine by connecting at least three different loads to the output of the two-port network and solving a system of three equations for the unknown impedances Z_1, Z_2, and Z_3.

$$Z_{IN} = (Z_{11} - Z_{12}) + \frac{Z_{12} \cdot \left[(Z_{22} - Z_{21}) + Z_{OUT} \right]}{Z_{21} + \left[(Z_{22} - Z_{21}) + Z_{OUT} \right]} \tag{3.9}$$

$$Z_{IN} = (Z_{11} - Z_{12}) + \frac{Z_{12} \cdot Z_{22} - Z_{12} \cdot Z_{12} + Z_{12} \cdot Z_{OUT}}{Z_{21} + Z_{OUT}} \tag{3.10}$$

$$Z_{OUT} \cdot Z_{11} - Z_{IN} \cdot Z_{22} + Z_{11} \cdot Z_{22} = Z_{IN} \cdot Z_{OUT} + Z_{12}^2 \tag{3.11}$$

By assuming three known terminations (i.e. open, short and load), the following set of equation can be derived

$$\begin{cases} Z_{OUT\_LOAD} \cdot Z_{11} - Z_{IN\_LOAD} \cdot Z_{22} + Z_{11} \cdot Z_{22} = Z_{IN\_LOAD} \cdot Z_{OUT\_LOAD} + Z_{12}^2 \\ Z_{OUT\_OPEN} \cdot Z_{11} - Z_{IN\_OPEN} \cdot Z_{22} + Z_{11} \cdot Z_{22} = Z_{IN\_OPEN} \cdot Z_{OUT\_LOAD} + Z_{12}^2 \\ Z_{OUT\_SHRT} \cdot Z_{11} - Z_{IN\_SHRT} \cdot Z_{22} + Z_{11} \cdot Z_{22} = Z_{IN\_SHRT} \cdot Z_{OUT\_SHRT} + Z_{12}^2 \end{cases} \tag{3.12}$$

The system of two equations can be formulated by subtracting first equation from the second and the third

$$\begin{cases} (Z_{OUT\_OPEN} - Z_{OUT\_LOAD}) Z_{11} - (Z_{IN\_LOAD} - Z_{IN\_OPEN}) Z_{22} = Z_{IN\_OPEN} Z_{OUT\_OPEN} - Z_{IN\_LOAD} Z_{OUT\_LOAD} \\ (Z_{OUT\_SHRT} - Z_{OUT\_LOAD}) Z_{11} - (Z_{IN\_LOAD} - Z_{IN\_SHRT}) Z_{22} = Z_{IN\_SHRT} Z_{OUT\_SHRT} - Z_{IN\_LOAD} Z_{OUT\_LOAD} \end{cases} \tag{3.13}$$

The derived equations can be represented in matrix notation by

$$A = \begin{bmatrix} Z_{OUT\_OPEN} - Z_{OUT\_LOAD} & Z_{IN\_LOAD} - Z_{OPEN} \\ Z_{OUT\_SHRT} - Z_{OUT\_LOAD} & Z_{IN\_LOAD} - Z_{SHRT} \end{bmatrix} \quad \textbf{(3.14)}$$

$$B = \begin{bmatrix} Z_{IN\_OPEN} \cdot Z_{OUT\_OPEN} - Z_{IN\_LOAD} \cdot Z_{OUT\_LOAD} \\ Z_{IN\_SHRT} \cdot Z_{OUT\_SHRT} - Z_{IN\_LOAD} \cdot Z_{OUT\_LOAD} \end{bmatrix} \quad \textbf{(3.15)}$$

$$Ax = B \quad \textbf{(3.16)}$$

With the unknown X is defined as flowing, where $Z_{11}=Z_1+Z_3$, and $Z_{22}=Z_2-Z_3$

$$X = \begin{bmatrix} Z_{11} \\ Z_{22} \end{bmatrix} \quad \textbf{(3.17)}$$

In order to solve for Z_{22} (antenna impedance), the X can be expressed as

$$\left(A^{-1}\right) \cdot A \cdot X = \left(A^{-1}\right) \cdot B \quad \textbf{(3.18)}$$

$$X = A^{-1} \cdot B \quad \textbf{(3.19)}$$

3.2.2 S-Parameters

An alternative approach for the two-port model is based on the scattering matrix [S] that captures the relationship between the reader and the tag in the free space [48] as illustrated in Figure 3.5. The S-parameters quantify the relationship between the incident and the reflected waves as

shown in equation (3.19). As indicated previously, providing three different terminations (short, open and load), the frequency dependent S-parameters can be determined. Based on the collected data, all elements of a two port S-matrix are calculated requiring only the one-port measurements.

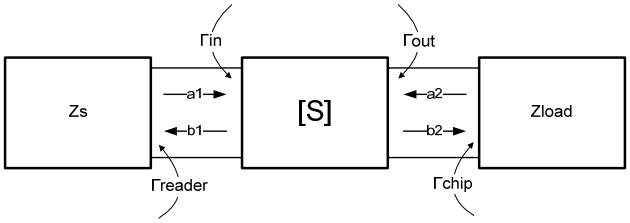

Figure 3.5: Equivalent S-parameters of a tag-reader system

The two-port scattering matrix [S] captures the relationship between the reader and the tag in the free space [48]. By providing three different terminations (Γ_{chip}), the frequency dependent S-parameters sets can be determined. Based on the collected data, all elements of a two-port S-matrix will be calculated from one-port measurements only. The two-port scattering matrix is represented as follows:

$$\begin{bmatrix} b_1 \\ b_2 \end{bmatrix} = \begin{bmatrix} S_{11} & S_{12} \\ S_{21} & S_{22} \end{bmatrix} \begin{bmatrix} a_1 \\ a_2 \end{bmatrix} \quad \textbf{(3.20)}$$

where a_i and b_j are the inward and outward propagating wave vectors. The S_{ii} parameters represent the reflection of the wave vector a_i to b_i and S_{ij} ($i \neq j$) represents the transmission from

a_j to b_i. Figure 3.6 demonstrates the network concept of the proposed measurement system including the two-port scattering parameters.

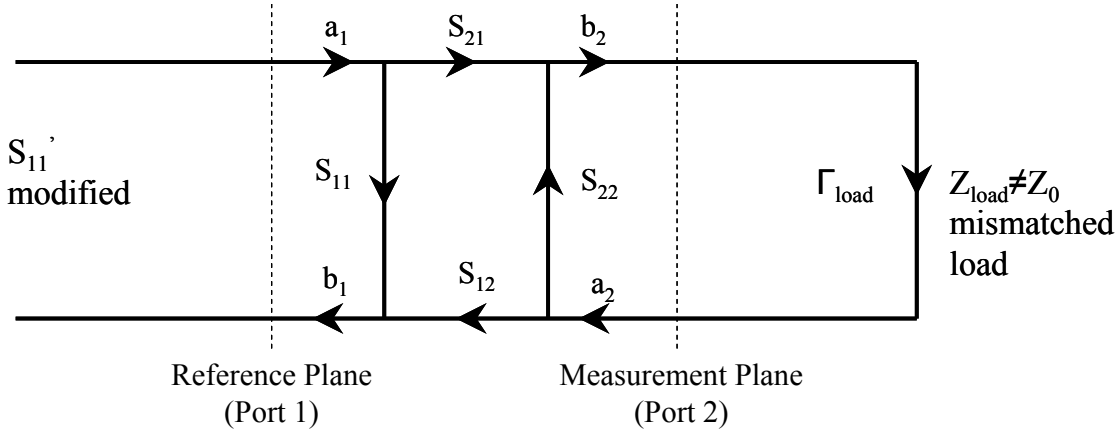

Figure 3.6: The signal flow graph for the Monostatic setup, modeled by the two port network

Evaluating the scattering matrix results in the following equations:

$$b_1 = S_{11}a_1 + S_{12}a_2 \quad \textbf{(3.21)}$$

$$b_2 = S_{21}a_1 + S_{22}a_2 \quad \textbf{(3.22)}$$

Dividing equation (3.20) by a_1 yields the following

$$\Gamma_m = \frac{b_1}{a_1} = S_{11} + S_{12}\left(\frac{a_2}{a_1}\right) \quad \textbf{(3.23)}$$

Dividing equation (3.21) by a_2 yields the following equation

$$\frac{1}{\Gamma_{load}} = \frac{b_2}{a_2} = S_{22} + S_{21}\left(\frac{a_1}{a_2}\right) \tag{3.24}$$

Rearranging equation (3.22) results in the following relation between a_2 and a_1:

$$\frac{a_2}{a_1} = \frac{\Gamma_{load} S_{21}}{1 - \Gamma_{load} S_{22}} \tag{3.25}$$

Substituting equation (3.23) into equation (3.21) yields the following equation for the reflection coefficient at the reference plane in terms of the reflection coefficient at the measurement plane and the scattering parameters:

$$\Gamma_m = S_{11} + \frac{S_{12} S_{21} \Gamma_{load}}{1 - S_{22} \Gamma_{load}} \tag{3.26}$$

If it is assumed that Port 1 is terminated with a matched load, the input impedance at Port 2 is given by

$$Z_{in} = \frac{1 + S_{22}}{1 - S_{22}} Z_{matched} \tag{3.27}$$

where $Z_{matched}$ is the matched impedance of Port 2 and S_{22} is given by

$$S_{22} = \left.\frac{a_2}{b_2}\right|_{a1=0} \tag{3.28}$$

The reflection coefficient looking into the load side is Γ_{load} when Port 2 is loaded with Z_{load}, because the incident wave is b_2 and the reflected wave is a_2, we have

$$\Gamma_{load} = \frac{a_2}{b_2} = \frac{Z_{matched} - Z_{in}}{Z_{matched} + Z_{in}} \tag{3.29}$$

The input impedance of the tag antenna can be determined by analyzing S_{11}, the s-parameter at the reader antenna input port. The variations in phase and magnitude can be directly observed from the behavior of the S_{11}.

$$S_{11}^{'} = S_{11} + \frac{S_{12}S_{21}\Gamma_L}{1 - S_{22}\Gamma_L} \tag{3.30}$$

As prescribed, the three known terminations are connected at Port 2. Thus, equation (3.28) provides three independent relationships, where $S_{12}=S_{21}$ due to reciprocity:

$$S_{open} = S_{11} - \frac{S_{12}^2}{S_{22} - 1} \tag{3.31}$$

$$S_{short} = S_{11} - \frac{S_{12}^2}{S_{22} + 1} \tag{3.32}$$

$$S_{load} = S_{11} - \frac{S_{12}^2}{S_{22} - \Gamma_{load}^{-1}} \tag{3.33}$$

Based on the above equations, the following formulation is obtained, which is used to determine the input impedance of the antenna

$$\frac{S_{short} - S_{load}}{S_{open} - S_{load}} = \frac{1+\Gamma_{load}}{1-\Gamma_{load}} \frac{1-S_{22}}{1-S_{22}} \tag{3.34}$$

Now, from equation (3.25),

$$\frac{1+\Gamma_{load}}{1-\Gamma_{load}} = \frac{Z_{load}}{Z_{matched}}$$

Z_{in} can be calculated as follows from equation (3.27)

$$Z_{in} = -\frac{S_{short} - S_{load}}{S_{open} - S_{load}} \cdot Z_{load} \tag{3.35}$$

The above equation can be used to calculate the input impedance that is based on the backscatter data S_{open}, S_{short}, and S_{load}. Also, all scatter parameter of the two-port network can be determined from the derived equations.

3.3 SIMULATION AND VALIDATION OF THE MODEL

Prior to performing the measurements, a rigorous three-dimensional (3D) electromagnetic simulation is required to conceptually validate the proposed method.

In the past few years, tremendous improvements in the accuracy of the numerical evaluation of antenna characteristics have been achieved. Some of the popular antenna analysis methods employ numerical techniques to directly solve Maxwell's equations such as the method of moments (MoM), the finite element method (FEM), and the finite-difference time-domain method (FDTD).

Therefore, the goal is to simulate a close-to-reality test system with an RF generator and the antenna under test. The electromagnet software package selected for the effort is Ansoft's HFSS Finite Element Method (FEM) 3D electromagnetic solver. This simulator was selected because of its ability to simulate 3D model by performing a discretization (meshing) of a large 3D space.

Ansoft HFSS evaluates the electromagnetic fields within a structure using a mesh of the simulated antenna made from tetrahedral which is the four-sided pyramid (Figure 3.7). The field quantities at the vertices of each pyramid are calculated to interpolate the electric and magnetic vector field quantities at points within the tetrahedron.

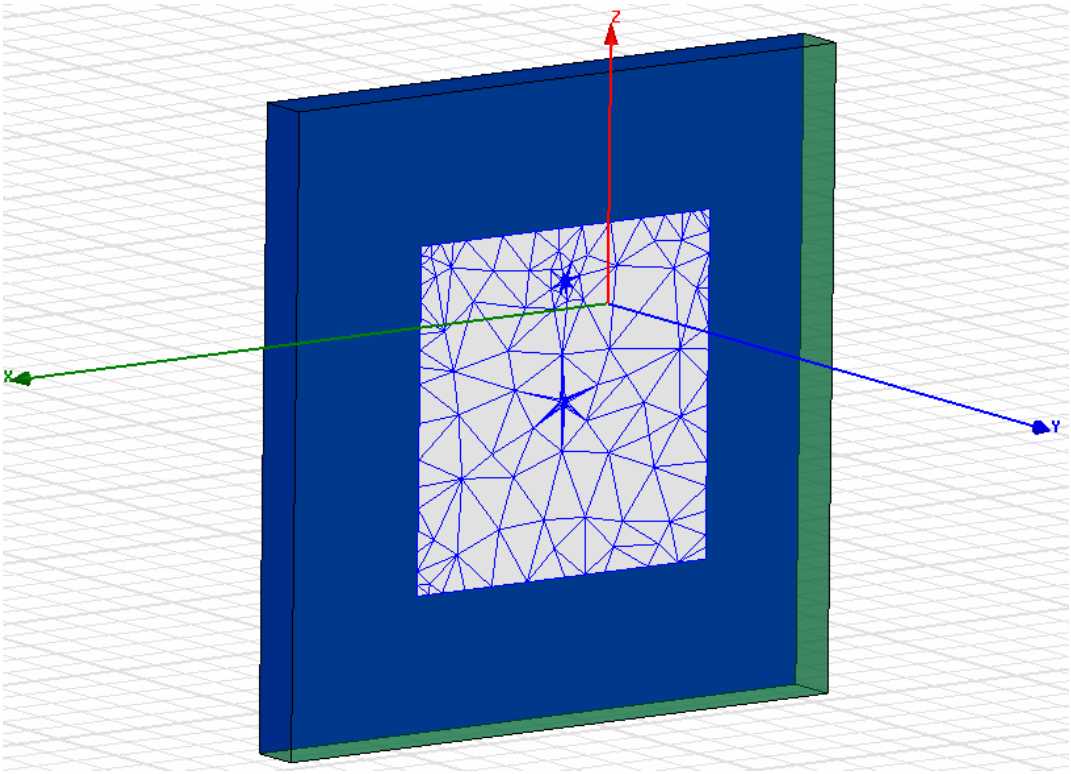

Figure 3.7: The design of the patch antenna

At each vertex, the software provides the components of the field that are tangential to the three edges of the tetrahedron. These values are then interpolated in order to generate the field quantities for each particular tetrahedron. This technique allows the system to represent Maxwell's equations in the matrix form that is solved with the numerical methods.

The conversion of the model to obtain a discretisize description of an arbitrary structure can be a non-trivial process. Therefore, the solution accuracy depends primarily on the size of each of the individual tetrahedra. However, because the field quantities are produced by inverting a matrix with approximately as many elements as the number of tetrahedra nodes, the inversion can require a significant amount of computing power and physical memory, especially

for a problem space that involves modeling two antennas, which are placed about one meter apart in order to evaluate antennas in the far-field for each other.

Fortunately, the increase in the computational speeds and the reduction in the computer hardware costs (i.e. physical memory), along with the improvements in the numerical analysis methods, allow rapid analysis of large antenna systems.

Also, Ansoft HFSS uses an adaptive analysis process in which the mesh is automatically refined in critical regions of the simulation space. First, it generates a solution based on a coarse mesh and then refines it in areas of high error density. The automatic mesh generator constructs a network of tetrahedra that conforms to the electrical performance of the device, which means the mesher automatically adjusts the total number of tetrahedra to produce the most accurate and efficient mesh as possible for a given structure. The S-parameters of the device under test are compared between each meshing operation and when the S-parameter differential reaches the limit which is set by a user, the solution has converged and the mesh is used to complete the simulation. Based on converge criteria, Ansoft HFSS terminates the simulation process and reports the last mesh for determining the final solution [30].

The simulation model is shown in **Error! Reference source not found.**. The model consists of the patch antenna (RF source) and the transponder antenna (tag). For the selected tag, a three dimensional model of the antenna was designed in Ansoft HFSS. The electromagnetic simulator such as Ansoft HFSS generates a 2x2 S-parameter matrix based on the geometric and material properties of the physical model.

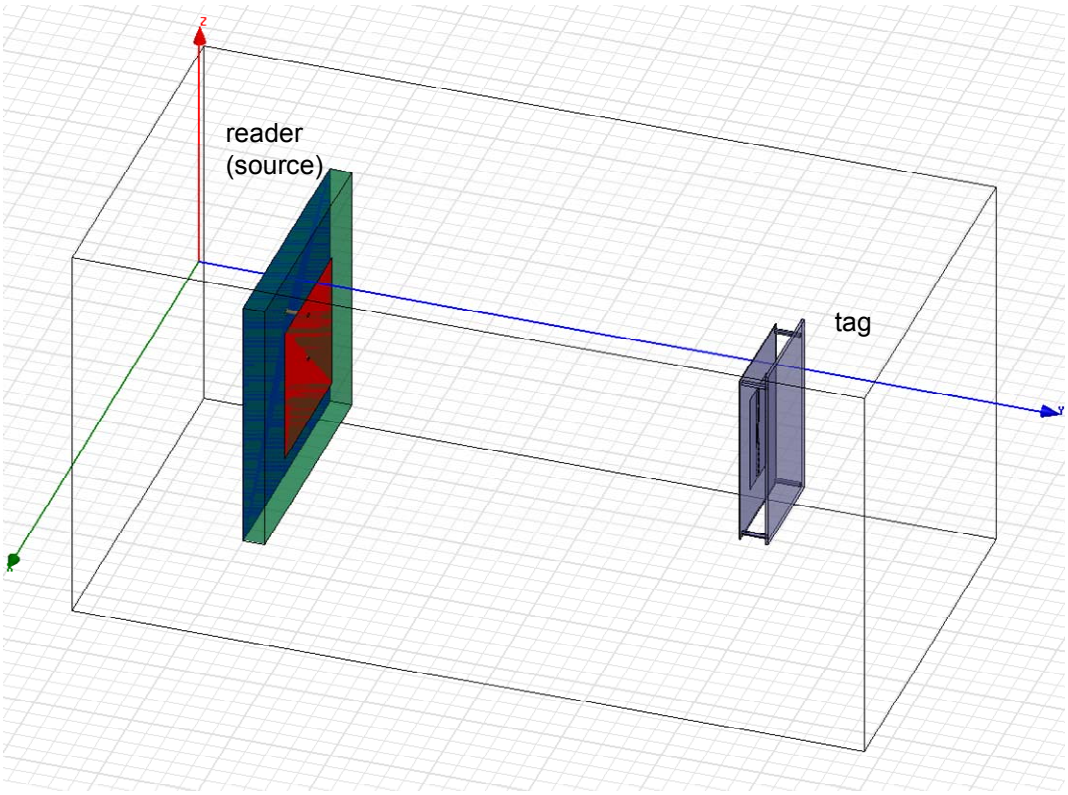

Figure 3.8: The three-dimensional model in Ansoft HFSS

The static S-parameter file of the simulation results was exported from the electromagnetic field solver in to the circuit simulator (Ansoft Designer) that support S-parameters "black-box" model. The model is inserted into Ansoft Designer circuit schematic using Ansoft dynamic link (Figure 3.9). This feature allows to dynamically co-simulate between full-wave extraction and circuit analysis.

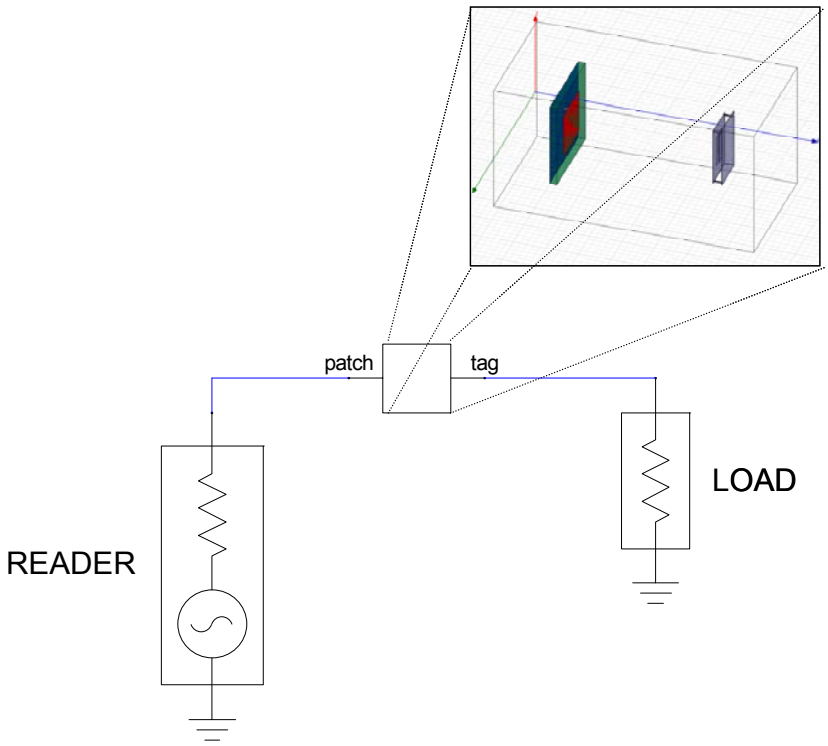

Figure 3.9: Schematic diagram of the measurement system

The resulting two-terminal "black-box" symbol is automatically created and inserted into the circuit schematic with the source (reader) and the chip (load) where each terminal corresponds to a port in Ansoft HFSS. This is an important feature for this work. In order to validate the proposed measurement technique, the simulation is performed for the three different lumped-elements (loads), which were inserted between the two input terminals as the circuit elements (Figure 3.10).

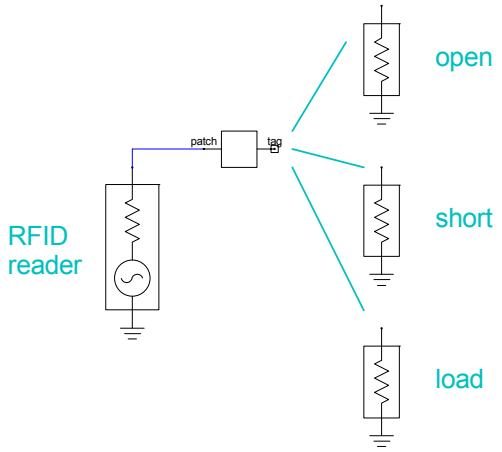

Figure 3.10: The schematic with the proposed three-loads

By applying the proposed method, the input impedance of the antenna was calculated from the simulations results. For comparison purposes, the tag antenna was simulated using Ansoft HFSS following the standard procedure. The simulated antenna impedance is shown in Figure 3.11.

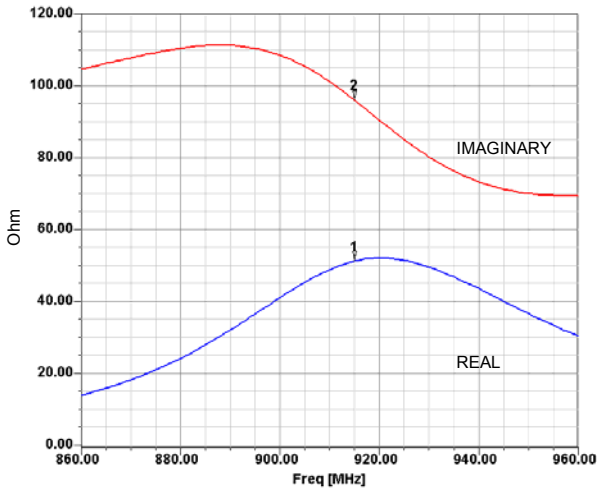

Figure 3.11: The simulated antenna impedance

The input impedance was calculated using Z and S parameters. The calculated and simulated results are reported for S and Z parameters in the Table 3.3 and Table 3.4 respectively.

Table 3.1: The simulates S-parameters

S-Domain		
	Real	Imaginary
Open	0.109717	-0.071732
Short	0.122849	-0.041433
Load	0.07658	-0.04239

Table 3.2: The simulated Z-parameters

Z-Domain		
	Real	Imaginary
Open	61.59934	-8.991852
Short	63.75167	-5.373141
Load	58.06526	-4.961388

The percent difference to determine the similarity of the simulation results is now obtained. This is found by dividing the absolute difference of the two measured values by their average, or

$$PercentDifference = \frac{\left|measured_1 - measured_2\right|}{\left(\frac{measured_1 + measured_2}{2}\right)} \cdot 100\% \qquad \textbf{(3.36)}$$

Table 3.3: The calculated antenna impedance in S-domain

S-Domain			
	Calculated	Simulated	Error
Real	49.46134	49.16504	0.60%
Imaginary	100.1077	99.45942	0.65%

Table 3.4: The calculated antenna impedance in Z-domain

Z-Domain			
	Calculated	Simulated	Error
Real	51.869	49.16504	5.50%
Imaginary	96.753	99.45942	2.72%

Using S-parameter for calculating the impedance, generates a less than 1% difference between the expected and calculate values. The small difference can be attributed to the meshing of the antennas. When calculating impedance with the Z-parameters, the error is much greater than it is with the S-parameter formulation. The S-parameter calculation provides better results because the solution has eight degrees of freedom, as opposed to the Z-parameter solution with only six degrees of freedom. Therefore, the presented methodology is based on the solution using S-parameters.

This concept was demonstrated by examining the Ansoft Designer circuit model that incorporated the Ansoft HFSS S-parameter two-port model. The results demonstrate the validity of the equation that is part of the proposed measurement method. It is clear that the analytical derivations are sound and based upon the proven mathematical framework of Maxwell's equations. However, significant distortions may exist in a real world test system such as air humidity, connector discontinuities and, random errors. This substantiates the need for measurement results, and correspondingly, accurate measurement techniques.

4.0 MEASUREMENT SYSTEM

4.1 NETWORK ANALYZER

The integral part of the measurement system that implements the proposed measurement methodology is the Vector Network Analyzer (VNA). The VNA has been successfully demonstrated in industry and academia to measure RCS of the RFID tags [49, 50]. The system is based on the 8753 VNA from Agilent Technologies (model 8753). The measurement systems feature phase and amplitude measurement capabilities and about 100 dB dynamic range. The hardware platform of the VNA is ideal for performing RCS measurement with minimum error due to its architecture. The VNA provides the Monostatic measurement with a stable RF generator that is capable of sampling amplitude and phase of the reflected signal within the same instrument. Also, the VNA can be switched into a continuous wave (CW) operating mode, which corresponds to the working of the RFID reader. Figure 4.1 illustrates the model of the test system, which represents the proposed measurement technique using the VNA.

The errors in measurements depend on the VNA accuracy, the residual systematic errors, the dynamic range, and noise. The typical error of the VNA is approximately ±0.001 dB in amplitude and 0.5º in phase with the 10 Hz intermediate frequency (IF) bandwidth to minimize data acquisition times and no data averaging.

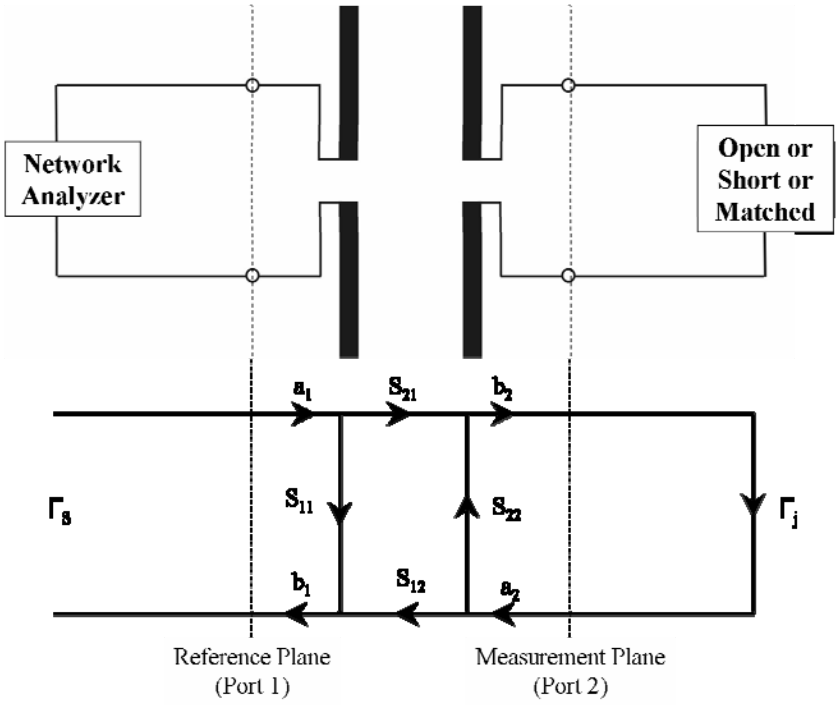

Figure 4.1: The measurement system and model

4.2 GIGA-HERTZ TRANSVERSE ELECTROMAGNETIC TEST CELL

The control environment is a vital part of the measurement system, where the computer controlled VNA is connected to the Giga-Hertz Transverse Electromagnetic (GTEM) cell. The GTEM cell provides the controlled environment for accurate antenna measurements [51, 52].

The antenna under test should be placed in a well controlled environment. Because the received wave will be a composite signal, containing, mixed with the direct signal from the transmitter, spurious signals produced by interaction between the antenna under test and its surroundings. Therefore, the GTEM cell is an ideal candidate for the table top control

environment, which has been successfully used in measuring the maximum read range of the RFID tags [2], where the results were in agreement with the testing in an anechoic chamber [16].

The proposed method employs a GTEM Cell (Figure 4.2). A typical UHF TEM cell generates the electromagnetic field for testing small RF devices such as wireless pager, GPS receiver, portable phone, etc. Through the input port, an external test signal may be applied to generate predictable electro-magnetic field inside the cell. The radiation field can also be picked up through the input port using a test receiver. The unique design of the GTEM cell is intended for accurate measurements beyond the standard TEM Cell frequency range.

The GTEM is an absorber lined broad-band TEM Cell which can be used for wide range of applications. This product provides small internal reflection that is required for accurate measurement. This is specifically designed for characterization of devices up to 3 GHz range [53]. Because the cell is highly broadband, it has many applications in the area of electromagnetic interference (EMI) and electromagnetic shielding (EMS). Also, it is well suited for general transceiver characterization, where transmitter Effective Radiated Power (ERP) and receiver Effective Received Signal Strength (ERSS). Therefore, the GTEM presents a cost effective alternative to the anechoic chamber environment for highly integrated testing small wireless devices.

The UHF GTEM cell is made to work beyond the typical TEM Cell, where the operating frequency range is limited by the cell resonance. A typical TEM Cell is a two-port symmetrical device, where the RF signal is applied to one port while the other port has terminated the match load while maintaining a standard (50 Ohm) characteristic impedance along the length of the cell. When the wave propagates beyond a certain frequency, the cell structure starts resonating. In order to eliminate the resonance problem, half of the cell is replaced by the wave absorbing

material. The typical size of the GTEM design allows for accommodating typical small wireless devices.

The operating principle is essentially the same as in TEM Cell environment. The electromagnetic field inside the test volume is proportional to the input voltage and inversely proportional to the cell height. If a radiating object is placed inside the cell, the radiated wave toward input port is guided by the transmission line and picked up at the input with a receiver such as Spectrum Analyzer or Network Analyzer. With this method, radiation characteristics of a radiating device can be measured quantitatively

The GTEM cell is a wide band TEM Cell with absorber termination. The large absorber wall eliminates potential resonance inside the cell and makes wide band operation. When a small radiating object (RFID tag) is placed at the test position, a part of its radiated energy couples into TEM mode and the guided wave appears at the cell input port. Inversely, if an RF signal is injected into the TEM Cell input port, the predictable TEM mode field is generated at the test position. The GTEM Cell is an accurate, broad band RF coupler that also offers high quality shielding as well.

Because the system is passive and reciprocal, the transfer function from the input port to the antenna port maintains the two-port S-parameter relations given by $S_{12}=S_{21}$, for any antenna. When a radiating object is placed inside the TEM cell, the device's radiated power travels equally to both ends of the cell.

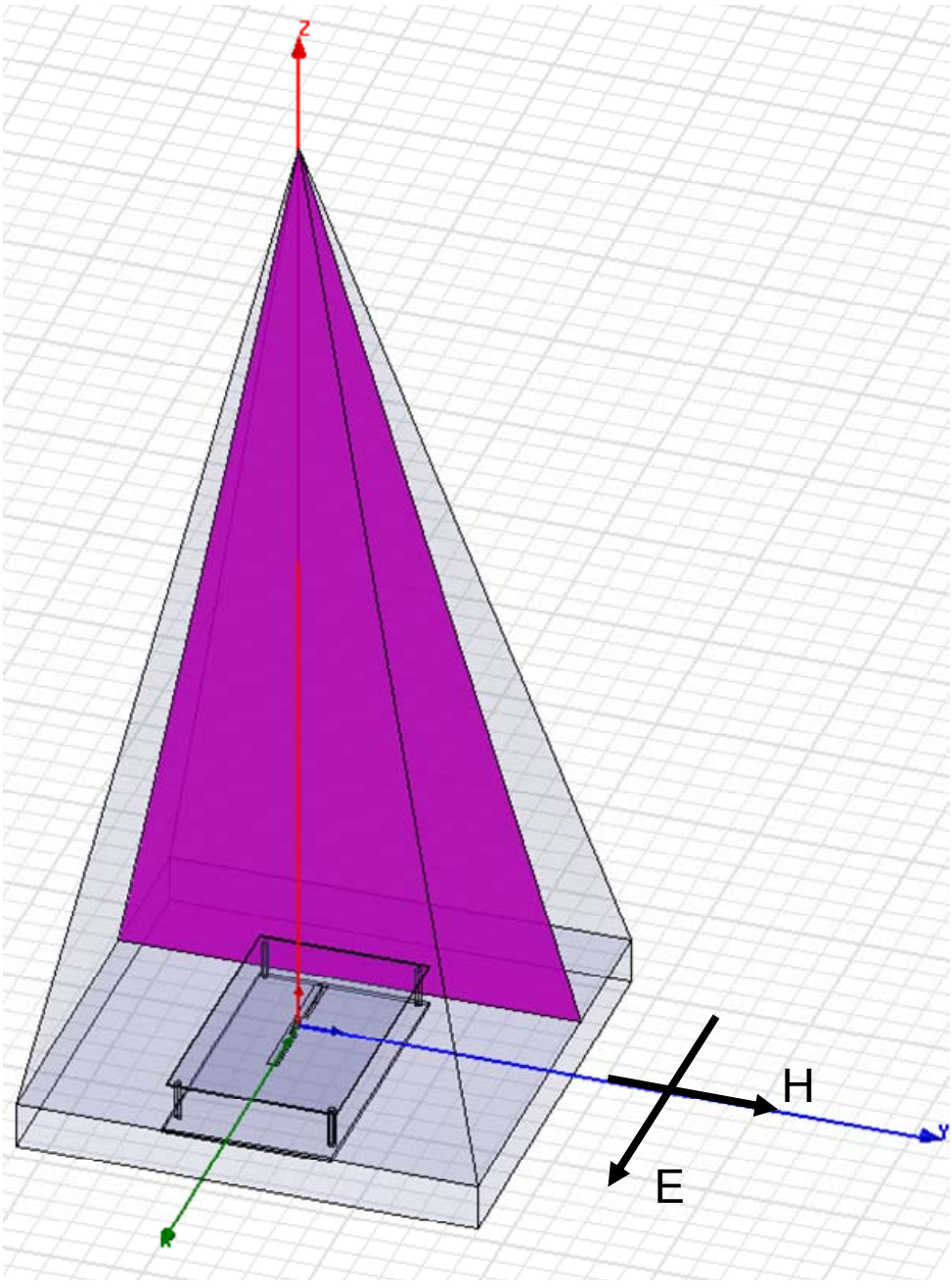

Figure 4.2: The GTEM Cell three-dimensional model

Standard E-field generation inside the cell is shown in Figure 4.2. The reciprocity theorem assures that the gains/attenuation in both directions, S_{21} and S_{12}, are exactly the same, i.e., for the receiver testing and transmitter testing. Under normal conditions, the coupling between the tag input to the TEM Cell input remains constant regardless of direction of energy flow.

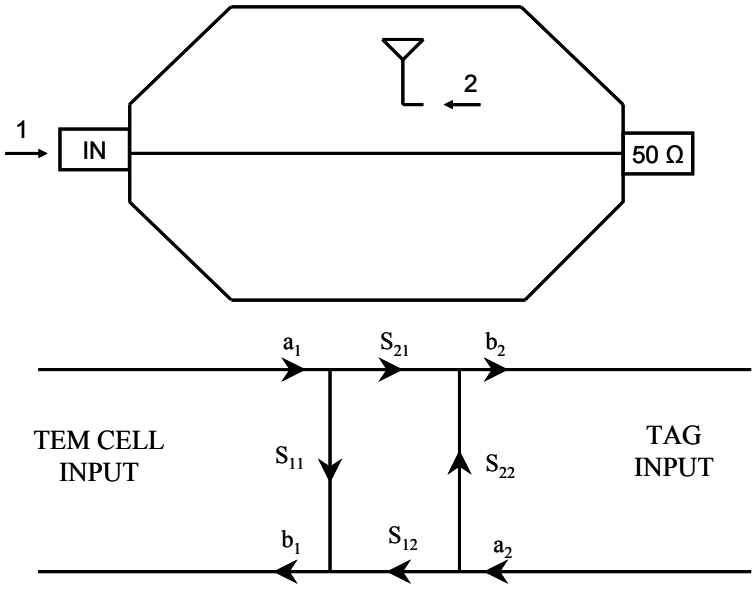

Figure 4.3: The GTEM Cell and the tag as two-port network

In order to test the quality of the GTEM cell, the standing wave ratio (SWR) of the empty GTEM cell was measured for the frequencies starting from 800 MHz to 1 GHz using Vector Network Analyzer (8753ES). As shown in Figure 4.4, the SWR is below 1.5 for the desired operating range, which constitutes a very good match.

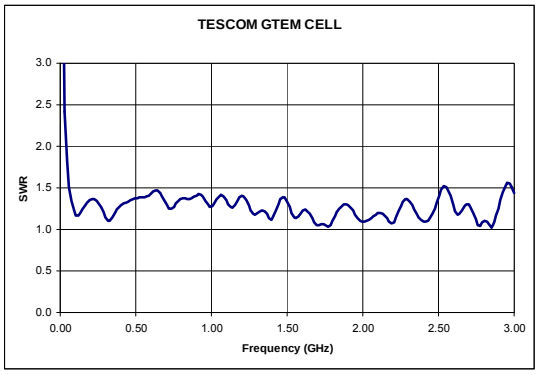

Figure 4.4: The GETM cell SWR plot

Another important test was performed in order to evaluate the characteristic impedance of the GTEM cell as maintained over its full length, which was measured by the pulse response of the cell using Time Domain Reflectometry (TDR) instrument from Tektronix. **Error! Reference source not found.** demonstrates the measurement result. There is a small deviation of the impedance, which is slightly above 50 Ohm.

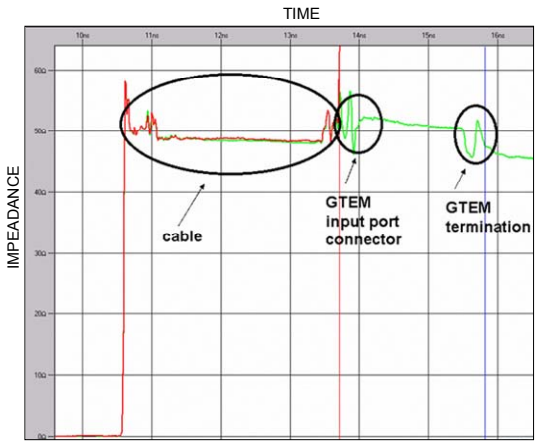

Figure 4.5: The characteristic impedance of the GTEM cell

The length of the GTEM cell can be measured on the basis of the time between input connector and the termination, which is found to be 2.11 ns. The calculated length is 633 mm, which is determined by multiplying time transition from the input connector to the inside termination of the GTEM cell by the speed of light. The specified length of the GTEM cell (640 mm) is in agreement with the measured results, where the difference can be attributed to the termination material on the bottom of the cell.

4.3 RFID TAG HOLDER

A specially designed tag holder was constructed in order to reduce the number of random errors, which usually result from the experimenter's inability to take the same measurement in exactly the same way in order to get exact the same number.

The holder is required to provide consistent means of positioning the tag from one tag measurement to another. RFID tags attached to products with different electromagnetic properties will affect the antenna impedance because of changes in the resonant (operating) frequency and the matching between the antenna and the chip. Therefore, the tag holder (Figure 4.6) was constructed using specifically selected materials, Roha-cell foam and FR4, in order to provide parameters close to the reality of the actual operating environment for the tag.

The permittivity of the Roha-cell is 1.07 at microwave frequencies. The loss tangent of the Roha-cell structure is less than 0.001 at UHF frequencies. Its radar cross section is below −35 dBm. Therefore, it does not affect the test measurements to any significant degree. Also, the placement of the antenna under the test and the measurement distance is constantly maintained with the tag holder in order to minimize the possible physical errors in measurements.

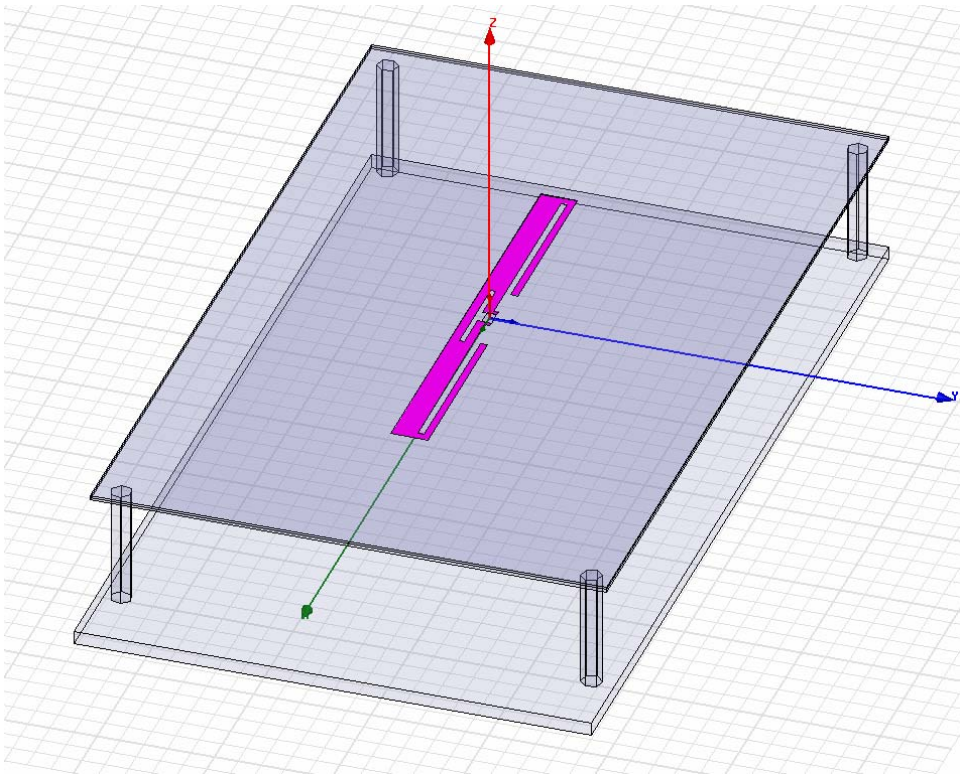

Figure 4.6: The three-dimensional model of the tag holder

Figure 4.7 illustrates the tag's holder position (center), which was securely attached to the bottom of the GTEM cell. Also, **Error! Reference source not found.** is the photo of the complete test system.

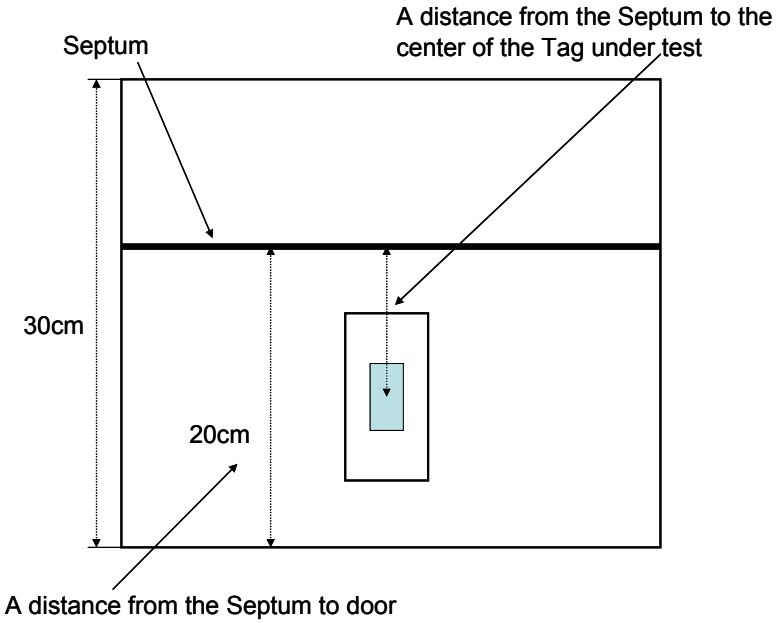

Figure 4.7: The position of the tag holder inside the GTEM cell

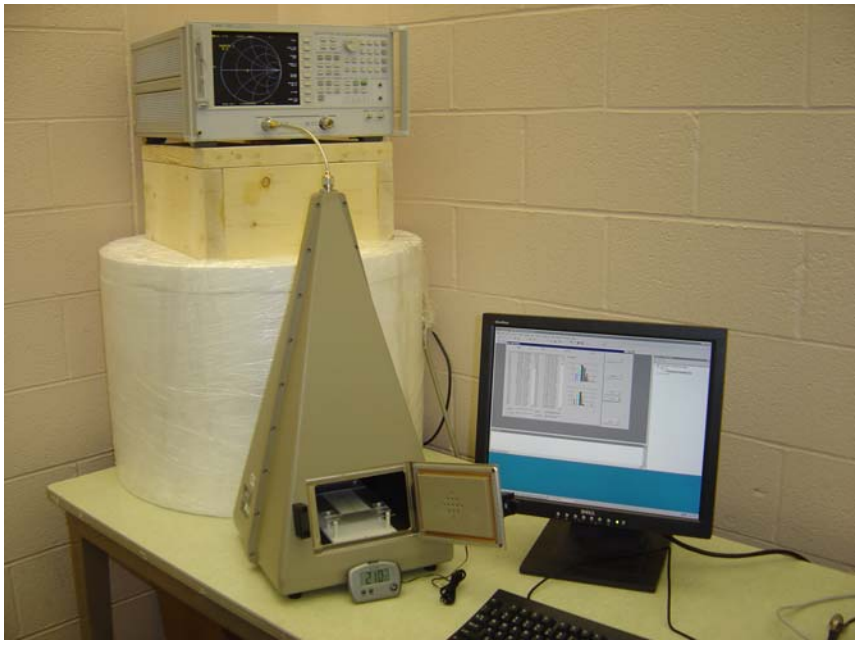

Figure 4.8: The complete test system

4.4 SOFTWARE

In order to test a large number of tags, a semi-automated system was developed. A computer program controls the VNA, which allows data acquisition for a large number of tags as well as the required calculation in essentially real time. Based on the mathematical derivations, the software performs the data extraction and the calculations. All computations were performed on the collected data to extract the statistical data, which were interpolated to quantitatively measure the quality of the assembly and contact methods.

The implemented software program totally implements the proposed technique. This software was implemented using Microsoft Visual Basic (Appendix I) in conjunction with the Agilent IntuiLink ActiveX/COM object. The software has the capability to fully control the VNA and retrieve the measurement instrument data into the PC. The data are retrieved in term of the scatter parameters, which can be directly used following the proposed methodology for determining the impedance of the antenna.

During the initialization phase, the software provides the identification and connection to the VNA using National Instruments' GPIB interface (IEEE 488).

Then, the software selects the operating frequency (915MHz), power level and the operating mode (continuous wave). At this point, the user is required to perform at least three different measurements in order for the software to compute the input impedance of the tag's antenna. The five step process is demonstrated in Figure 4.9.

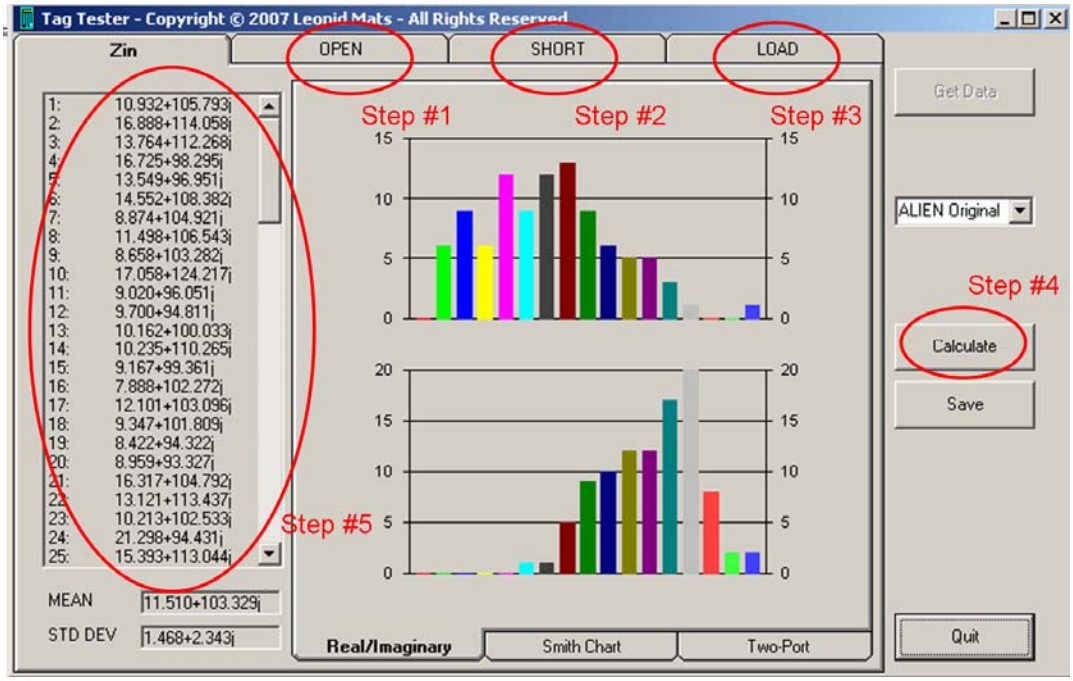

Figure 4.9: The main view of the software

The two step process is required to perform a measurement of the antenna with the load (chip). Initially, the software performs a power sweep in order to identify the absolute minimum turn on power level of the chip, which is done by identifying a non-linear change in the phase and the magnitude as described in Section 5.4. The change in the data is recognized by calculating the first derivative and then identifying the maximum change along all measured points.

Figure 4.10 illustrates the graphical representation of the magnitude and phase versus power index as the waveform. The user has the ability to control the precision of the results by adjusting start, stop and step the power values in the software where smaller power steps provide a more accurate power level at the cost of time sweeping selected power levels. The following figures demonstrate the software environment.

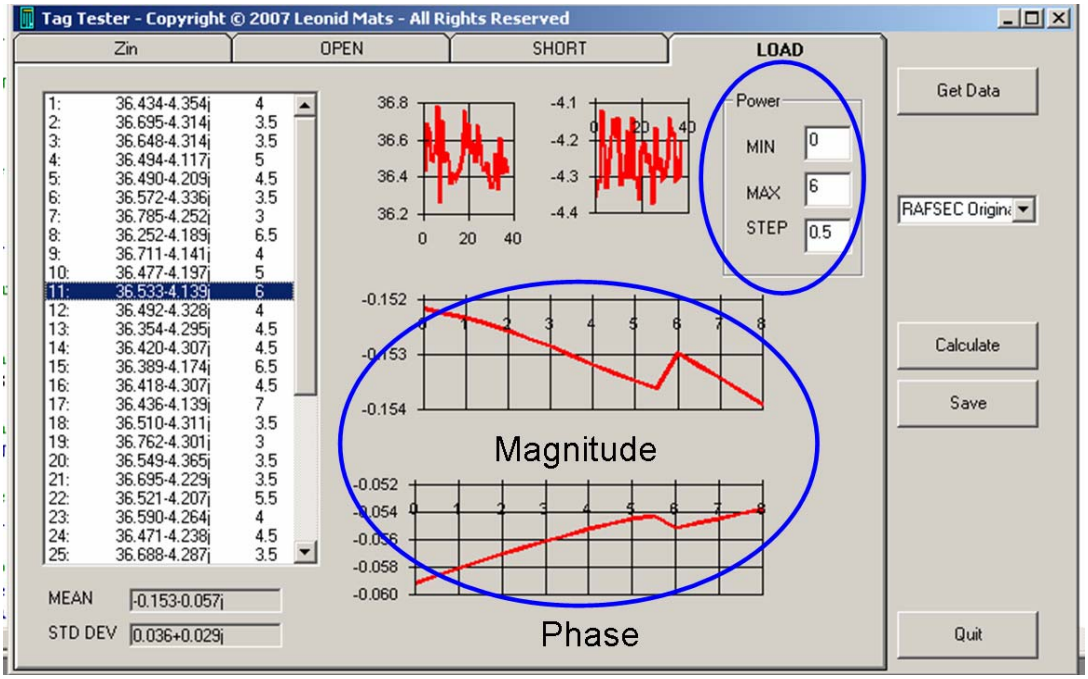

Figure 4.10: The software control for the determination of the lowest operating power

As the software calculates the impedance of the antenna, the data are preprocessed and presented to the user in terms mean, variance and histograms that represent measured and calculated data.

In order to provide a user with the graphical feed back of the measured impedance with respect to the optimal and simulated impedance. The Smith Chart window can be select to plot all measured data along with the predefined optimal and simulate values.

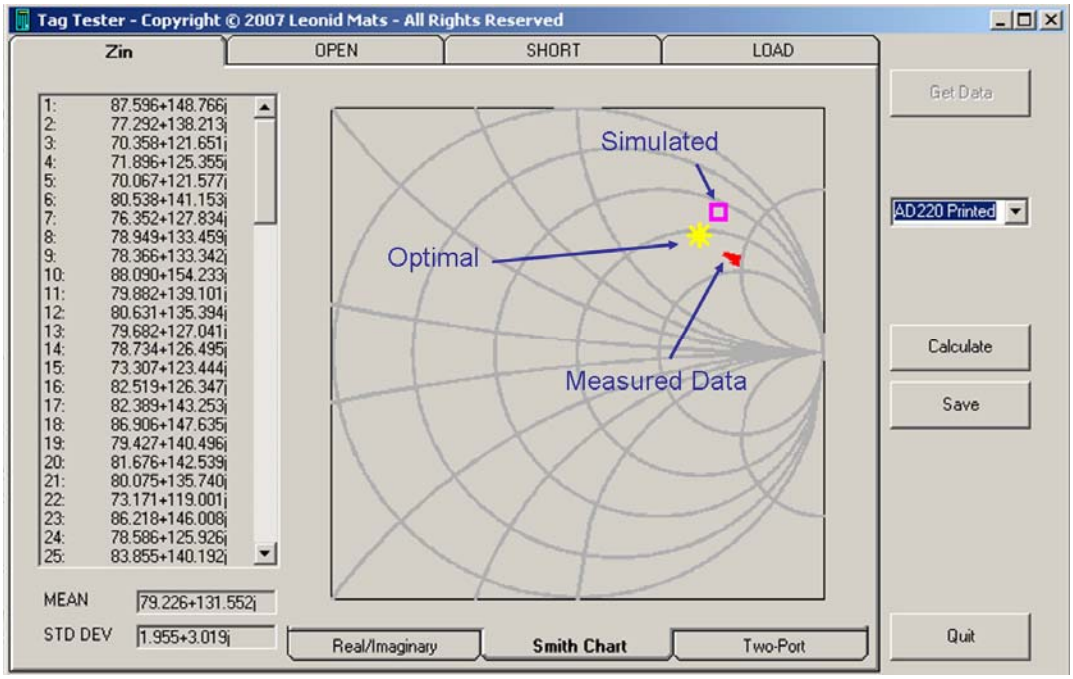

Figure 4.11: The Smith Chart with the measured and simulated results

The software provides the automatic on-line determination of the proposed virtual matching between the simulated and the measured results, which are presented in terms of the "L-match" and the two-port residual network. The virtual match is dynamically adjusted with respect to the measured data that allows users continuous monitoring of the measured data with respect to the simulated data.

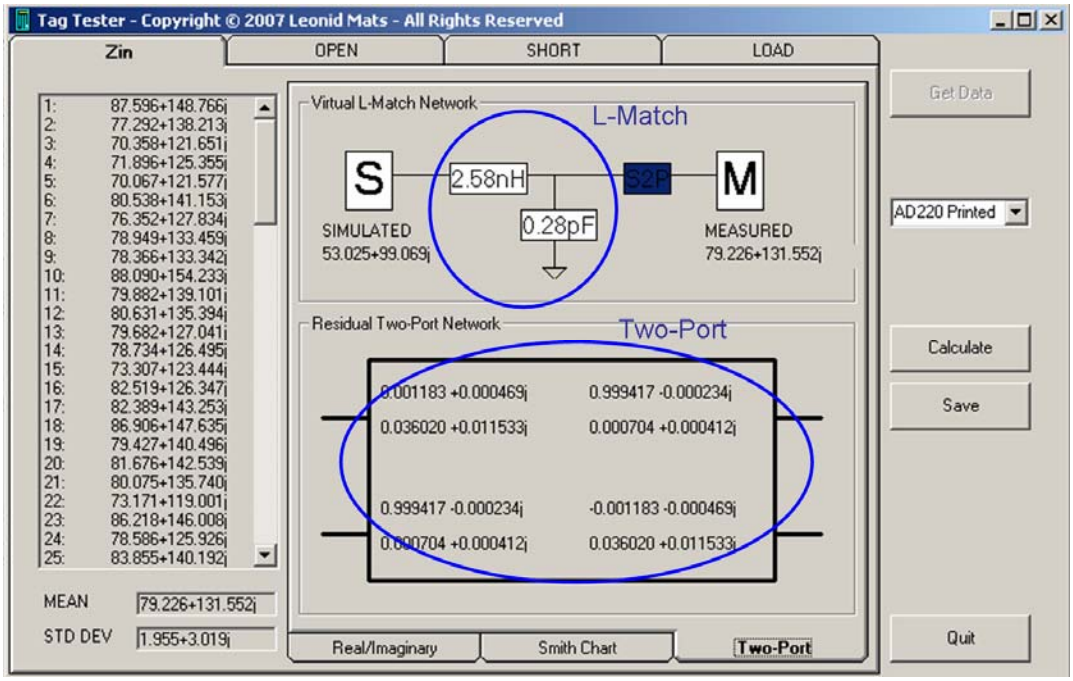

Figure 4.12: The "L-match" and the residual two-port network in the software implementation

The software stores all measured and calculated data in order to be used offline for the post processing of the data. The stored data can be imported into a statistical software package for the advanced analysis.

5.0 RESEARCH RESULTS

5.1 TAG SELECTION

Four production quality RFID tags from different manufactures were acquired for the evaluation of the proposed measurement technique. These tags have different antenna designs, construction materials, base antenna material, and the interconnections of the IC chip to the antenna technologies. Also, these tags are manufactured by four different companies. Three out of four tags were manufactured using flip-chip technology, where the chip is placed directly on top of the antenna connection terminals. The other RFID tag was manufactured using the indirect assembly by means of interposer as the chip carrier. Within each group of tags, the tags have been split into equal groups in order to provide a control group and a group to run through the RFID printers where identical information was printed on the label side of the selected tags. Two commercially available printers were used to print the data on the labels.

The first tag has been manufactured by the Avery Denison Corporation [54], which uses the AD-220 inlay. In this study it is referred to AD220. This is a general purpose RFID tag that is designed to be used on cartons. The antenna is printed on a substrate using silver ink. The tag's nominal operating frequency range is 902 MHz to 928 MHz. Figure 5.1 illustrates the AD-220 tag. The chip attachment is based on the strap solution.

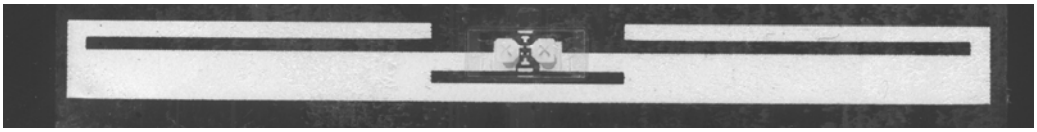

Figure 5.1: Avery Dennison AD-220

The second selected RFID tag, Alien Squiggle Antenna, was manufactured by Alien Technologies [55], which used an assembly method based on the flip-chip technology. In this study the tag is referred to as Alien. The base antenna material is etched copper, which is optimized to work on most packaging surfaces including products containing metal and water. This tag has a nominal operating frequency range from 860 MHz to 960 MHz. Figure 5.2 illustrates the tag.

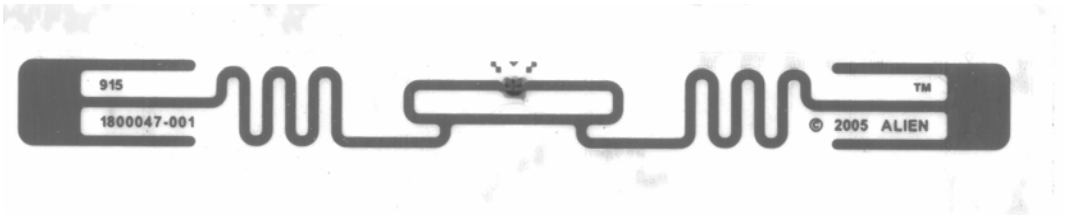

Figure 5.2: Alien Squiggle Antenna Tag

The third tag was from Texas Instruments [56] with the flip-chip attachment technology, which is referred to as the TI tag in this document (Figure 5.3). The base antenna material is printed silver ink. The tag antenna was designed with the nominal operating frequency of the tag being from 860 MHZ to 960 MHz.

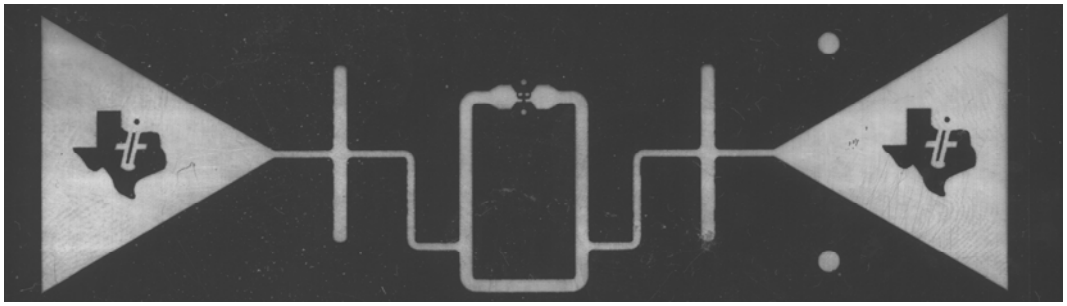

Figure 5.3: TI tag

The last tag selected was the Rafsec Short Dipole Antenna (Figure 5.4), which is manufactured by UPM Rafsec [57]. The base antenna material is etched aluminum. The nominal operating frequency range of the tag is 902 MHz to 928 MHz. The antenna design is tailored for mainly consumer market solutions such as retail/supply chain management, pharma, apparel, and airlines (tickets, baggage tags).

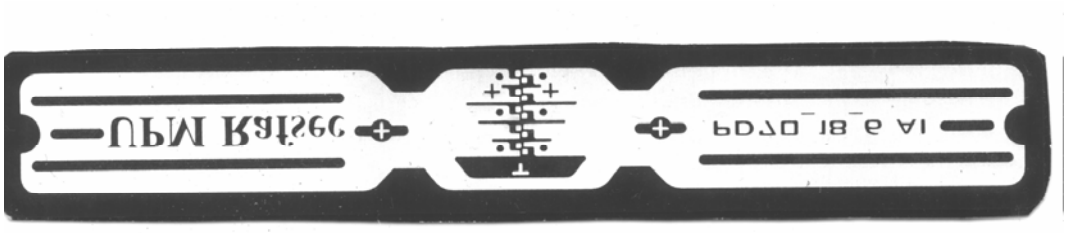

Figure 5.4: Rafsec Short Dipole

All selected tags were using the same RFID chip that supports the EPC UHF Class 1 Generation 2 specification (ISO-1800 Part 6C standard) [28]. At present time, there is primarily one IC chip commercially available for the manufacturing of the RFID tags that support Class 1 Generation 2 specification from the EPC Global. Therefore, the selected tags employ the IC chip

manufactured by Impinj, Inc [58]. Because of the commonality of the chips, it can be assumed that there is no major variation in design from one tag to another within the same family of tags due to the highly consistent internal circuitry of the IC chip. Also, there are no differing effects from the data modulation or encoding algorithm, which are implemented in the IC chip.

5.2 SIMULATION RESULTS FOR THE SELECTED TAGS

The selected antennas were designed and analyzed with the aid of Sonnet software, which is based on Method of Moments (MoM). The method is implemented as the numerical solution of integral equations for currents induced on the antenna by sources. This software is well suited for the simulation of the planar type antennas because it avoids many of the simplifying assumptions required by other methods for performing electromagnetic analysis. The simulation results are very useful in providing an approximate value for the antenna impedance. The simulation results for the antenna impedance at 915 MHz are given in Table 5.1.

Table 5.1: The simulation results of the tag's antennas

Tag	Impedance
AD220	53.025+99.069j
Alien	12.203+104.030j
TI	14.728+145.973j
Rafsec	23.111+142.961j

The corresponding Smith chart illustrates the simulation of the antenna impedance looking into the terminals. In this simulation, the resonant impedance falls almost on the real axis. That is the point at which the antenna source impedance yields maximum power transfer to the chip [6]. The numbered markers (1 - 3) highlight the simulated input impedance versus the frequency performance at the upper limit of the European band (Marker 3), and the limits of the North American band (Marker 1 and 2).

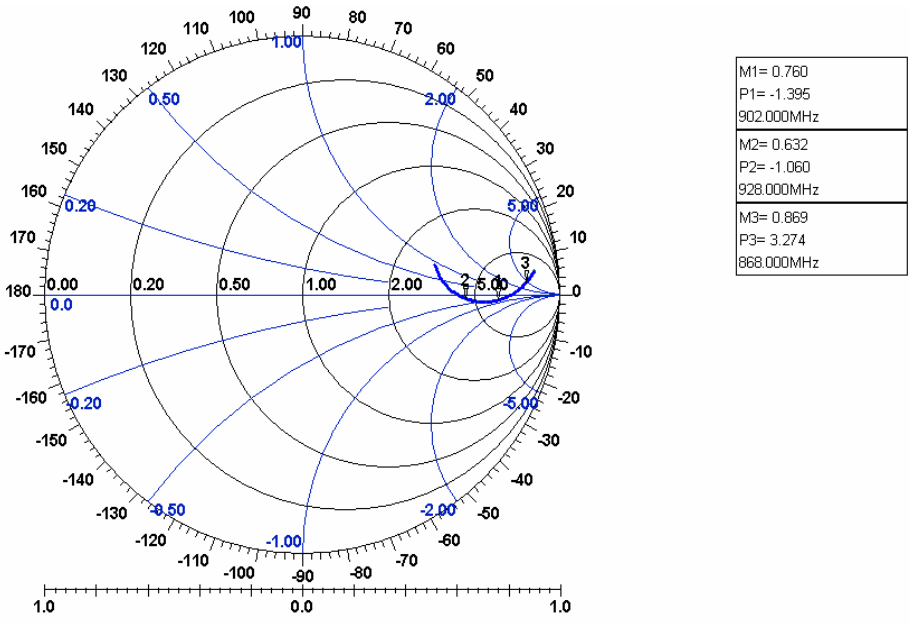

Figure 5.5: The Smith chart of the simulated antenna impedance

5.3 THE TEST LOAD SELECTION

The basis of the backscatter testing procedure implies three independent loads are required to be connected to the terminal of the antenna in order to determine its input impedance. The open, short and RFID chip load were chosen as the most viable selection of the required number of different loads.

The open circuit loading was achieved by removing the RFID chip from the tag. Figure 5.6 demonstrates an example of the open-circuited antenna as one of the required termination for the proposed measurement technique.

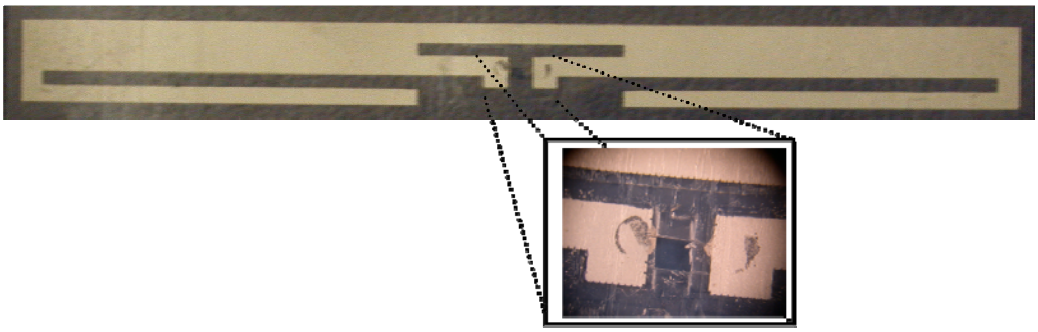

Figure 5.6: The photo of the open-circuited antenna

The short circuit loading has been accomplished by removing the RFID chip and connecting the terminals with highly conductive silver ink [59]. Figure 5.7 illustrates the short-circuit antenna.

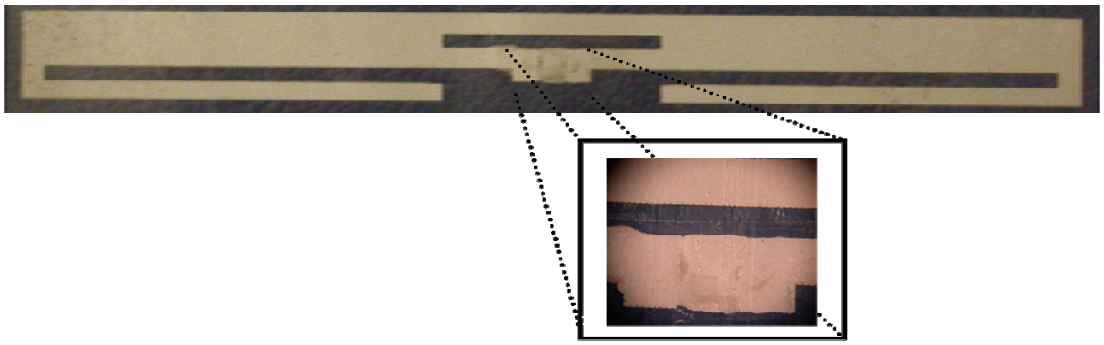

Figure 5.7: The photo of the short-circuited antenna

The third load was simply the actual RFID chip, where the chip acts as the load of the antenna (Figure 5.8). This load selection provides the most important information about the tag's characteristics. The open and the short samples are fixed with respect to the various tags (third load). Therefore, any variation in the tags can be measured and quantified.

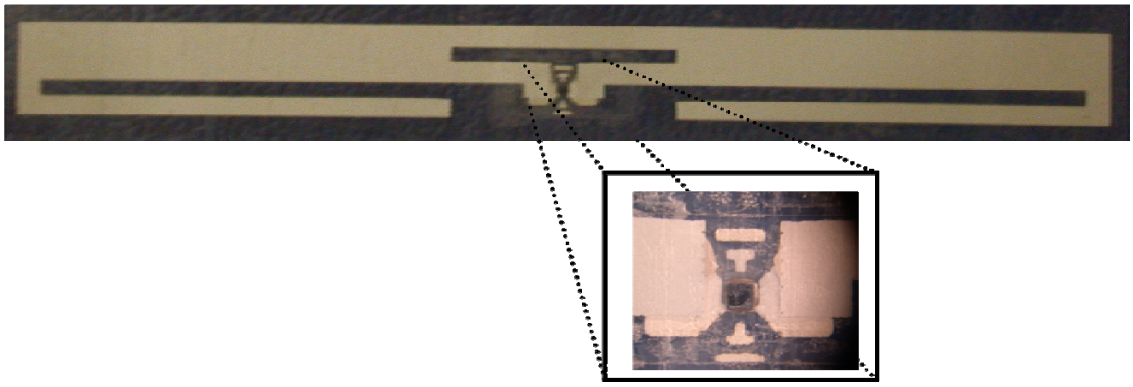

Figure 5.8: The photo of the antenna with the chip

The measurement with the chip as a load depends on the input power level into the chip. This is due to the non-linearity of the RF front-end circuitry of the chip, which draws a non-sinusoidal current.

This third required termination was chosen as the impedance of the chip, which is typically specified by the manufacturere for the lowest operating power level of the chip. There are several different approaches that can be employed in order to determine the lowest power level. One of the methods is based on determining the minimum turn-on power level at which the tag can successfully respond to the RFID reader command. The measured result is extrapolated using the Friis free-space formula [23] in order to predict the maximum operating distance of the tag on the basis of the minimum turn-on power. In this research, the measured result is used as the indicator for the value of the load impedances at particular power.

The measurement method encompasses some degree of uncertainty in terms of the ability to evaluate tag's performance. This uncertainty is due to the fact that different reader systems do not have the same receiver sensitivity (recognition) capabilities, which in turn could be attributed to the system architecture of the receiver. While corrective terms can be included to compensate for receiver sensitivity, the calibration of antenna gains and accurate reflection coefficients tend to make it difficult to obtain accurate and consistent comparisons from reader to reader.

As part of this work, a novel alternative approach for identifying the absolute minimum power level is presented. This method will provide a reader-independent measure of tag's performance using a Vector Network Analyzer (VNA), which is a fundamental commercial RF measuring instrument that can be accurately calibrated.

5.4 THE ABSOLUTE MINIMUM OPERATING POWER OF THE TAG

Typically, the front–end of the RFID tag is a rectifier design based on voltage doubler circuit topology [7]. This front-end section acts as a peak detector Figure 5.9.

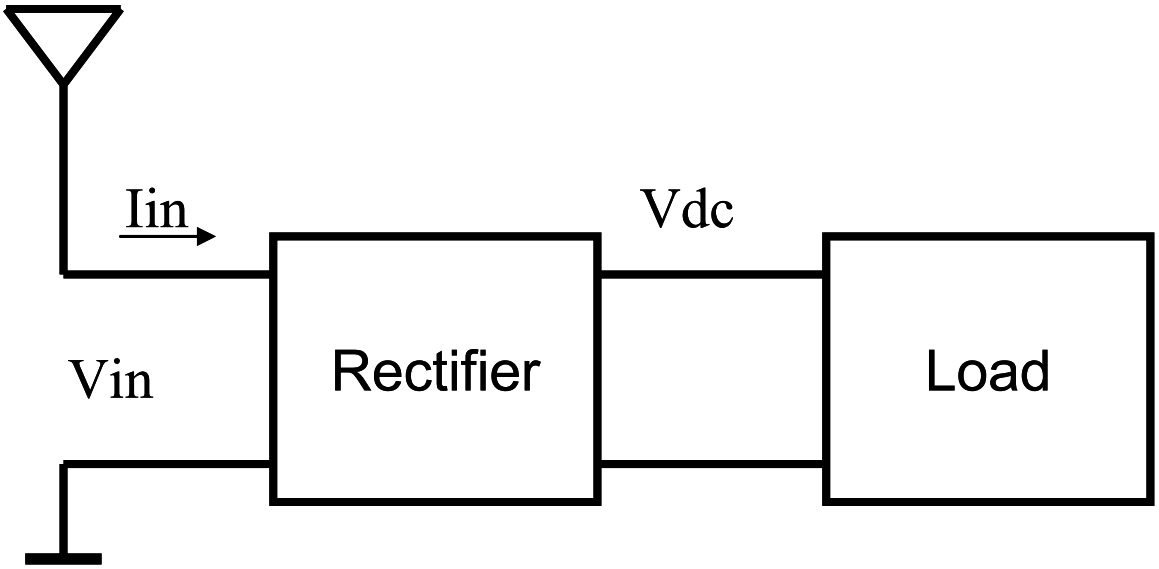

Figure 5.9: Passive RFID tag model

The voltage doubler architecture is based on non-linear devices (diodes). Therefore, it is extremely difficult to analyze the transient response of the tag front-end, where the incident RF signal from the receiving antenna is rectified to charge the load capacitor as long as the instantaneous AC voltage exceeds the voltage on the load capacitor. As a result, the supplied current is pulsing (Figure 5.10). However, as the reader generates a continuous wave (CW) signal, or maintains the power supply to the tag, the rectifier enters the steady-state mode. The load draws the energy store inside the load capacitor and at the same time the same amount of

energy is restored back by the rectifier, where the output current is approximately constant. This model of operation simplifies the circuit analysis of the RF front-end of the tag [60].

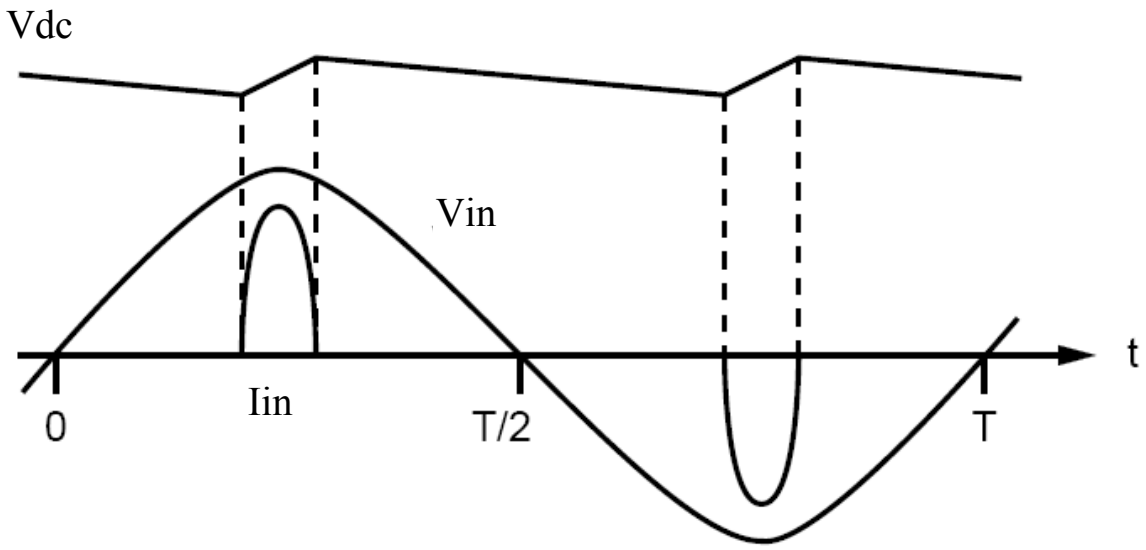

Figure 5.10: The input and the output waveforms of the signals

In order for the rectifier to operate in a steady-mode, a specific power level must be reached. This power level becomes the absolute minimum power level for the chip to be operational or ready to respond to the reader's commands, which in turn is used to accurately characterize the RFID tag (i.e. the antenna input impedance, operating range and radiation pattern).

A computer controlled VNA is used to measure the RCS of a tag under test (TUT) as a function of the frequency and the power. The reflected signal amplitude and phase are

measured. Figure 5.11 and Figure 5.12 are generated to represent the computer generated data for a single power sweep at the specific frequency after some initial processing. The plots are of the first order differences in the data, i.e., the numerical derivative of phase and magnitude at the indicated power levels.

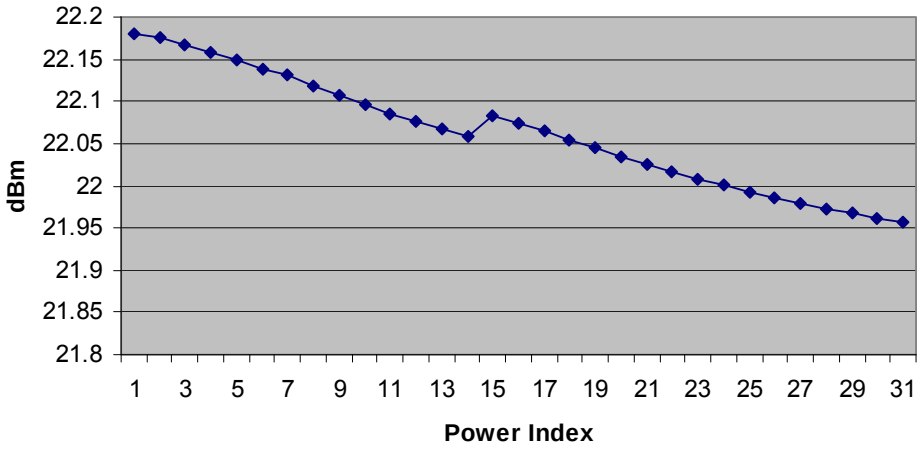

Figure 5.11: The magnitude versus power of the tag's RCS

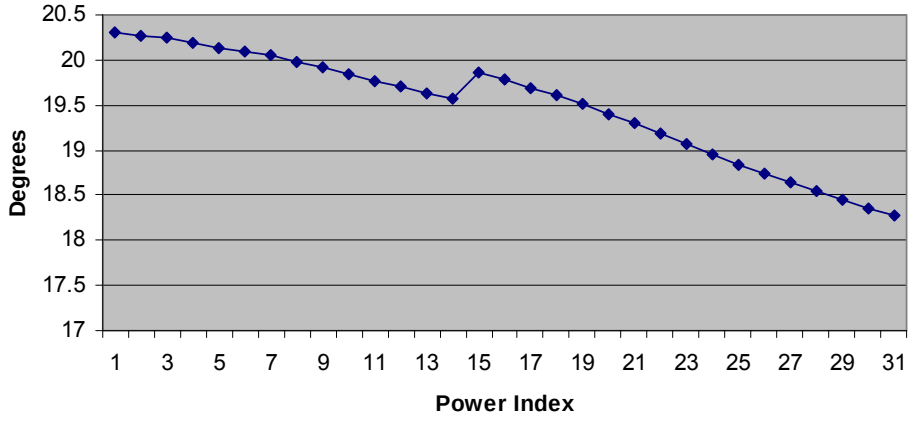

Figure 5.12: The phase verses power of the tag's RCS

The magnitude and phase measurements demonstrate a linear dependence with respect to power change except for one single power transition. There is a distinct change in the magnitude and phase of the reflected signal when a tag just turns on before it starts to operate in the steady-state. This power level represents the lowest level at which the tag can operate.

A software procedure that computes first derivative was written in order to precisely identify a single point for the magnitude and phase change.

In order to determine additional characteristics concerning the backscatter results, the numerical derivatives (differences) are calculated as shown in Figure 5.13 for the entire range.

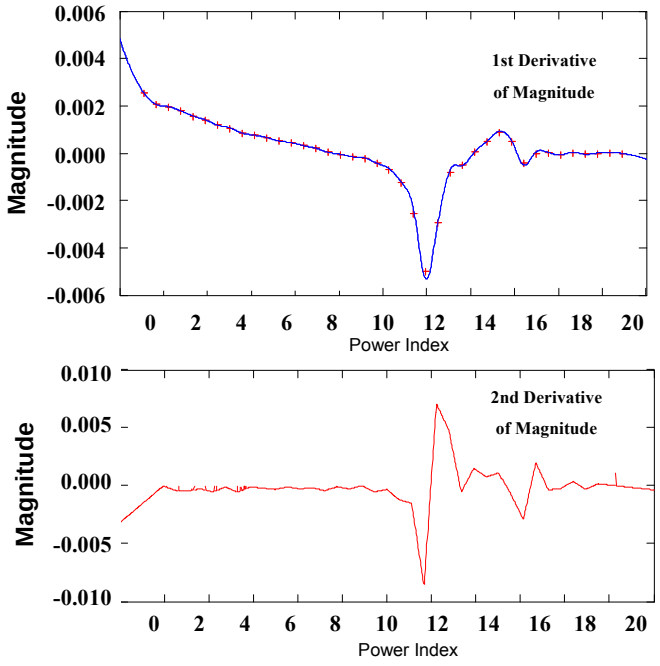

Figure 5.13: The 1st and 2nd derivatives

In order to validate the proposed method, the turn on power level was measured for various passive RFID tags with the RFID reader and the VNA (HP8753) in the same environment. Figure 5.14 and Figure 5.15 demonstrate the results for two different production quality tags, which are in agreement with the tests results, which were collected using commercially available RFID readers.

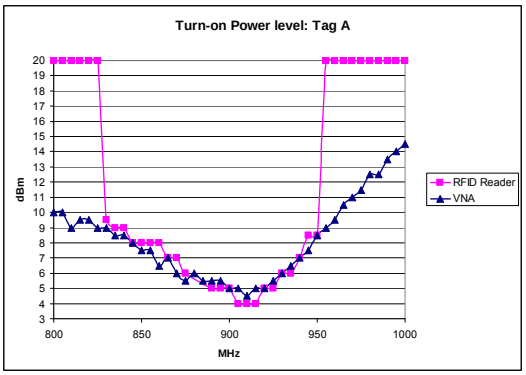

Figure 5.14: The minimum power required to communicate with Tag A versus frequency

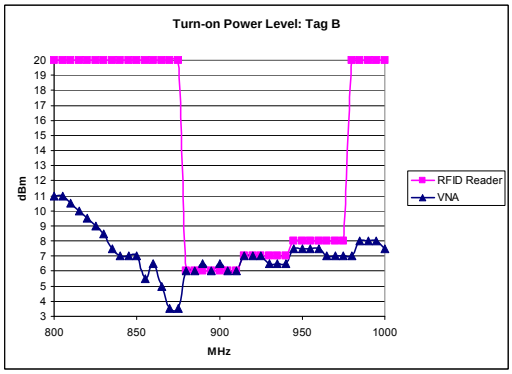

Figure 5.15: The minimum power required to communicate with Tag B versus frequency

The reported measurement technique was used to accurately identify the turn-on power level, which in turn improved accuracy of the measured results with respect to the measurements of the antennas with load (chip).

5.5 MEASUREMENT RESULTS

The experimental testing involved four production quality tags from different manufacturers and was carried out to test the validity of the measuring method. The selected tags were manufactured using different technologies for manufacturing antennas and for bonding chip to the antenna such as flip-chip (Alien, TI and Rafsec) and strap (AD220) [35]. However, the same RFID chip was used in all tags, which in turn allowed for characterization of the antenna, materials and packaging. Thus, it is expected that the load impedance is consistent across all four tag types.

The experimental measurements have been performed using one hundred candidate tags of each type that were randomly selected for each type of tag. Table 5.2 contains the summarized simulation and experimentally measured (mean with standard deviation) results for the input impedance of the tag antenna at 915 MHz, where Appendix E has all measured data for all tags. Appendix F contains the calculated result for the input impedance of the tags.

The exact parameters to accurately model and simulate the RFID tags are (as expected) unknown (undocumented). Therefore, typical values for passive UHF type tags [61] were used to model and simulate RFID antennas in Sonnet.

Table 5.2: The simulated and measured results for the selected tags

Alien		
	Real	Imaginary
Sonnet	12.20337	104.0298
Measured Original	11.510 (±1.468)	103.329 (±2.343)
Measured Printed	11.372 (±1.375)	104.245 (±2.249)
AD220		
	Real	Imaginary
Sonnet	53.02508	99.069274
Measured Original	74.120 (±2.021)	133.366 (±2.463)
Measured Printed	79.226 (±1.955)	131.552 (±3.019)
TI		
	Real	Imaginary
Sonnet	14.74812	145.9728
Measured Original	11.711 (±1.481)	163.354 (±2.417)
Measured Printed	9.845 (±1.262)	157.107 (±2.021)
Rafsec		
	Real	Imaginary
Sonnet	23.11096	142.9606
Measured Original	22.932 (±2.197)	168.723 (±2.742)
Measured Printed	24.822 (±2.677)	172.088 (±2.889)

The differences between the results can be primarily attributed to the packaging of the tag, which is not normally included in the electromagnetic modeling of the tag antenna.

The same types of tags were selected for testing after the tags were converted into "smart labels" by using two commercial RFID printers from Zebra Corporation [19] and Paxar Corporation (Monarch) [20] to print the same information on candidate tags. Then, the measurement of the input impedance of the antennas was performed, which in turn allowed the analysis of the mechanical properties of the physical interconnect between the chip and the antenna.

The testing of printed verses non-printed tags shows slight improvement in variance of the antenna impedance after the exposure to the environmental stress testing for the TI tags. The result coincides with the conclusions provided by the manufactures of the novel conductive inks [62]. Figure 5.16 illustrates the simulated and measured data plotted on a Smith Chart. There is a much bigger difference between simulation and measured results for tag Type B (AD220) that other tags, which was mainly due to the strap interconnect that was not modeled in the Ansoft HFSS.

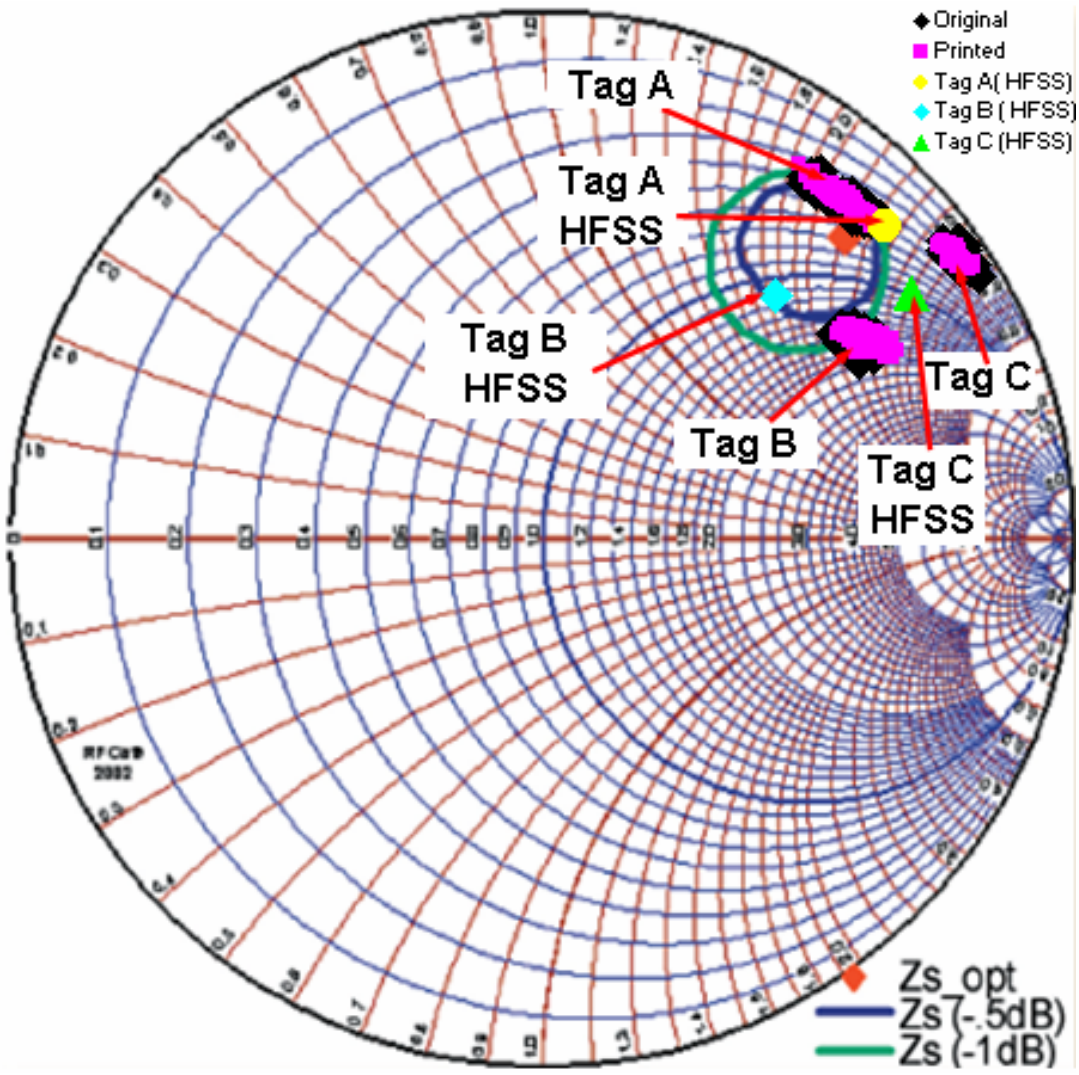

Figure 5.16: The Smith Chart with the simulated and measured results for three different tags

6.0 RFID ANTTENA TO CHIP INTERCONNECT METHODOLOGY

6.1 INTRODUCTION

One important result of this work is the conceptual modeling methodology for the interconnection between the antenna and the chip. The interconnection actually contains two separate models in tandem.

The accurate model of the antenna/chip interconnection can only be obtained from a manufactured tag. The question becomes which tag performs better in presence of normal variations in manufacturing. This is the basis of the two models in tandem. The first is the characterization of the interconnect embodied as the mean of the measured set of tags. This is the most accurate way of determining what actually should happen in a consistent process. This is the model of the interconnect process.

The second model contains the statistical variations which constitute the parameters that characterizing the process variations around the nominal interconnection which can only be produced in the manufactured state.

This capability provides a mechanism to support both quality control and the process variations that can be taken into account by the antenna designer to provide accommodation for the most robust design possible accounting for the manufacturing process producing the actual RFID tags.

Thus, we have a method to model and calibrate the distributed characteristics of the interconnect mechanism and the expected variations of these characteristics in the manufacturing environment.

6.2 IMPIDANCE TRANSFORMATION

In the context of understanding any variation between simulated and measured results, it is necessary to transform the simulation results of the ideal antenna impedance to a value which is measured.

The typical impedance matching (transformation) networks include: lumped element matching circuits, a transformer matching networks, and distributive networks with transmission lines. The analytical analyses on these networks have been studied in depth [46, 63].

The matching technique with the lumped elements, specifically the "L-match" network, is applied in this study. A single stage "L-match" is shown in Figure 6.1 composed of a capacitor and an inductor providing a way to transform the simulated impedance into measured one. This allows for the virtual modeling of unaccounted parameters of the simulations (i.e. unknown material parameters and roughness of the surface). Figure 6.1 demonstrates a single stage "L-match" with a parallel capacitor and a series inductor

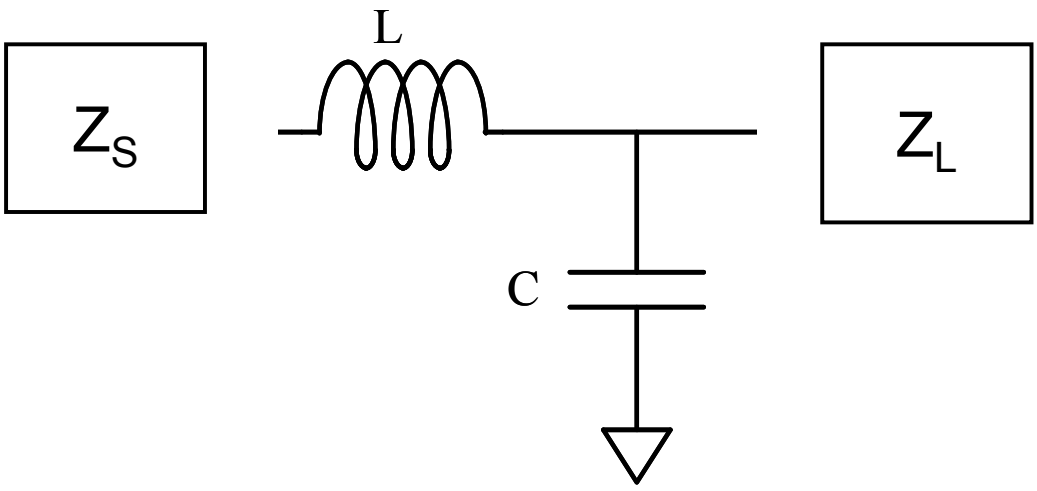

Figure 6.1: The "L-match" model

The “L-match” circuit is the simplest matching network, which provides two degrees of freedom and the Q of the circuit can not be selected. The “L-match” circuit is chosen in order to reduce the degrees of freedom which could introduce errors into analysis procedure. Q is proportional to the ratio of the load and source resistance. The mathematical calculations for the “L-match” network are given by the following formulations. The “L-match” network is designed to provide maximum power transfer at one frequency, that is

$$\omega = 2\pi f \tag{6.1}$$

The first step in synthesizing an impedance matching network is to de-embed the source and load complex parts. Because the matching network consists of an inductor in series with the source, the source impedance is converted into an equivalent series resistance and inductance. The equivalent series inductance and resistance of source impedance are given

$$R_s = \mathrm{Re}(Z_s) \tag{6.2}$$

$$L_s = \frac{\mathrm{Im}(Z_s)}{\omega} \tag{6.3}$$

De-embedding the load complex part by converting the input impedance to an admittance, so that the equivalent parallel capacitance and resistance of load impedance are determine as

$$Q_L = -\frac{\mathrm{Im}(Z_L)}{\mathrm{Re}(Z_L)} \tag{6.4}$$

$$R_L = \mathrm{Re}(Z_L)(Q_L^2 + 1) \tag{6.5}$$

$$C_L = \frac{Q_L}{\omega R_L} \tag{6.6}$$

Because the source and load resistances must be equal for the impedance transfromation, the Q's of the source and load sides must be equal. Setting the source impedance and load impidance equal to each other, and setting the Q's equal gives the following forumal to deterime the Q

$$Q = \sqrt{\frac{R_L}{R_S} - 1} \tag{6.7}$$

Given the Q of the source and load half sides of the network, and the effective source and load impedances, the matching network inductance and capacitance can be determined as

$$L_T = \frac{QR_s}{\omega} \tag{6.8}$$

$$C_T = \frac{Q}{\omega R_L} \tag{6.9}$$

The final impedance network is found by subtracting the source inductance from the matching inductance and the load capacitance from the matching capacitance.

$$L = L_T - L_S \tag{6.10}$$

$$C = C_T - C_S \tag{6.11}$$

Table 6.1 demonstrates the calculated values of the matching network for each tag that was measured and simulated. Some of the tags were matched with only a series inductor, where the series inductor was a sufficient lumped element for the impedance transformation network. Also, the value of the series inductance represents the relative distance between the simulated and the measured. When, the simulated and measured results are relatively close in value, the series inductance is small.

Table 6.1: The matching network values for the tags

Tags	Simulated Impedance	Measured Impedance (mean)	L (nH)	C (pF)
AD220 Original	53.025+99.069j	74.120+133.366j	3.23	0.23
AD220 Printed	53.025+99.069j	79.226+131.552j	2.58	0.28
Alien Original	12.203+104.030j	11.510+103.329	0.4	-
Alien Printed	12.203+104.030j	11.372+104.245j	0.68	-
TI Original	14.728+145.973j	11.711+163.354	2.99	-
TI Printed	14.728+145.973j	9.845+157.107j	2.28	-
Rafsec Original	23.111+142.961j	22.932+168.723j	4.59	-
Rafsec Printed	23.111+142.961j	24.822+172.088j	4.04	0.04

Some of the tags were matched with only a series inductor, where the series inductor was a sufficient lumped element for the impedance transformation network. Also, the value of the series inductance represents the relative distance between the simulated and the measured. When, the simulated and measured results are relatively close in value, the series inductance is small.

The Ansoft Designer includes the graphical tool, Smith Tool. The tool lets the user select lumped elements interactively and designs any type of impedance transformation network. Through the Smith Chart tool, the calculated matching network was verified for the tags.

Appendix D contains the Smith Tools results, which were in agreement with the calculated values for the matching network.

6.3 RESIDUAL INTERCONNECT VARIATION

The second part of the interconnect model is derived as the two-port residual network following the "L-match" network (Figure 6.2). The two-port network represents the residual variation of the measured data, which can be used to evaluate the tag.

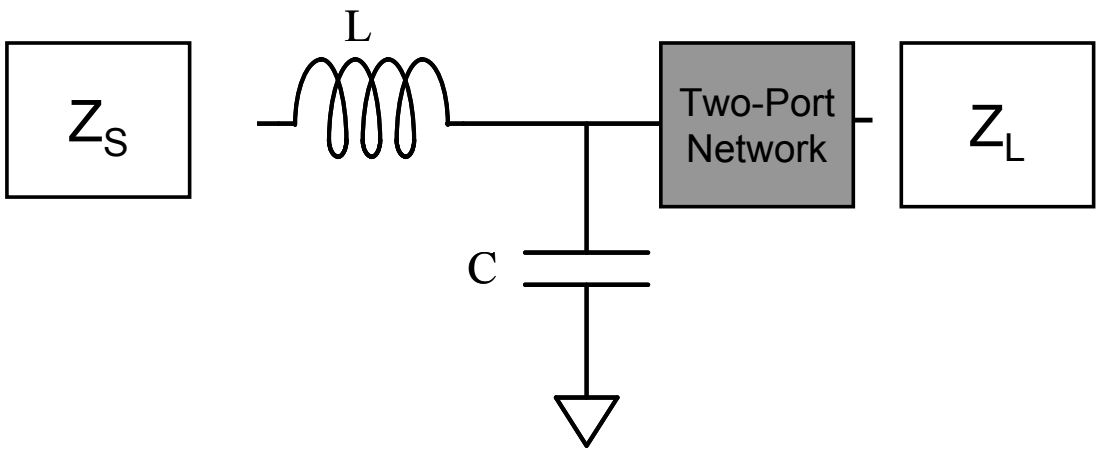

Figure 6.2: The residual two-port network

Measurements of a device under test (DUT) may not always be performed in a desirable test environment. This is because it may be practically impossible to measure a DUT in the desired

test environment. Accordingly, a DUT is often measured in a different environment for reasons of expediency and/or practicality, thereby requiring the use of embedding or de-embedding techniques to correct the effects of the test environment.

In this configuration, the tag under test is coupled to the VNA via septum of the GTEM cell, thereby requiring the removal of the effects of the GTEM from the measured data for a truer picture of actual tag's antenna performance. De-embedding techniques allow this task (i.e., removal of effects) to be performed computationally. This concept is shown in Figure 6.3.

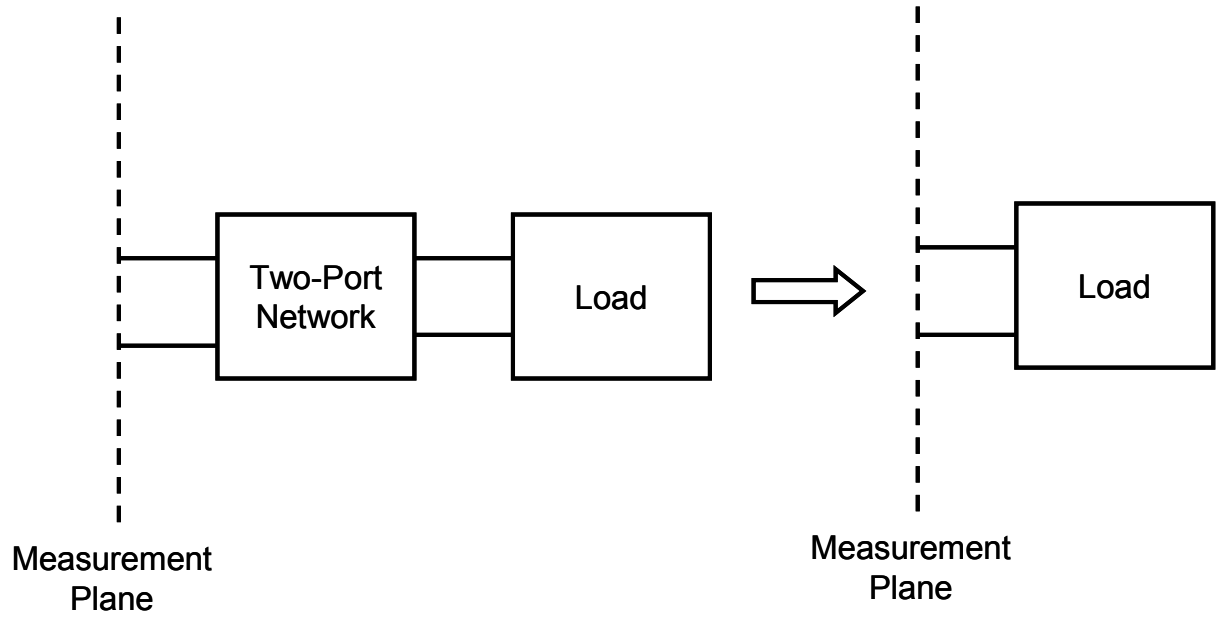

Figure 6.3: The normal measurement situation

For the two port devices, a chain matrix or cascading computation using transfer matrices has been used to perform embedding and de-embedding. The concept is to re-arrange standard scattering-parameters (s-parameters) to form a pair of new matrices (termed T for transfer matrices) that can be multiplied for embedding and forming the equivalent to the networks being

concatenated or cascaded (i.e., one network being embedded). Multiplying by the inverse of the T-matrix (i.e., T^{-1}) is the equivalent of de-embedding. A key-point is that the outputs from one stage map directly to the inputs of the next stage thereby allowing the matrix multiplication to make sense.

Transfer-matrices (also known to as transmission matrices) are made up of T-parameters (also known as chain-scattering-parameters and scattering-transfer-parameters) that are defined in a manner analogous to s-parameters except the dependencies have been switched to enable the cascading discussed above. In both cases the wave variables are defined as shown in the definition of s-parameters.

The T-formulation is a bit different to allow for cascading. More specifically, for a two port network, the T-parameters are defined as

$$\begin{bmatrix} a_1 \\ b_1 \end{bmatrix} = \begin{bmatrix} T_{11} & T_{12} \\ T_{21} & T_{22} \end{bmatrix} \begin{bmatrix} b_2 \\ a_2 \end{bmatrix} \tag{6.12}$$

The equations for computing the T-parameters in terms of the s-parameters (and vice versa) can be mathematically derived. The results are shown below [64]

$$\begin{bmatrix} T_{11} & T_{12} \\ T_{21} & T_{22} \end{bmatrix} = \frac{1}{S_{21}} \begin{bmatrix} 1 & -S_{22} \\ S_{11} & S_{22}S_{12} - S_{11}S_{22} \end{bmatrix} \tag{6.13}$$

$$\begin{bmatrix} S_{11} & S_{12} \\ S_{21} & S_{22} \end{bmatrix} = \frac{1}{T_{11}} \begin{bmatrix} T_{21} & T_{11}T_{22} - T_{21}T_{12} \\ 1 & -T_{12} \end{bmatrix} \tag{6.14}$$

Consider a two-port DUT where the networks to be added or subtracted are still two ports (Figure 6.4).

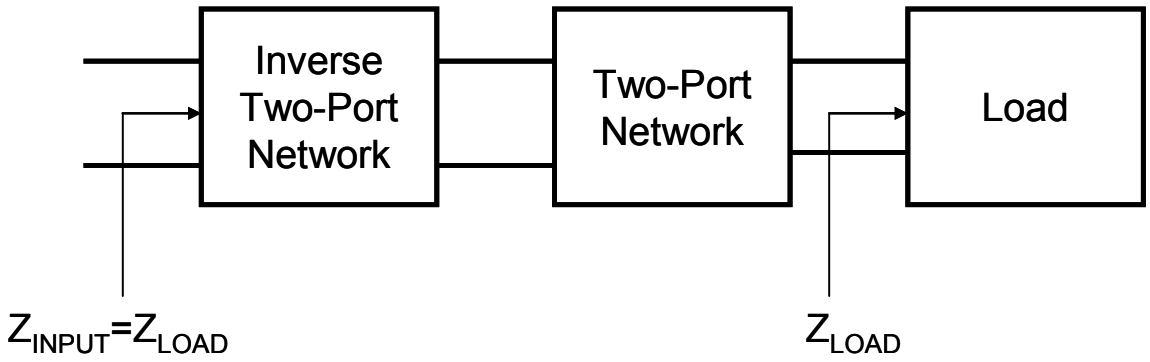

Figure 6.4: The cascade inverse of the embedding network

Embedding and de-embedding techniques have been in existence for number of years, which were applied primarily to de-embedding a test fixture attached directly to the test equipment. However, the proposed method has produced a need to apply the de-embedding method.

In accordance with the present research, a method is provided for virtually de-embedding a "mean" (average) two-port network from measured networks. The *mean* two-port network is generated using mean values for the measured data. This method includes the steps of acquiring a set of scattering-parameters for the measured two-port network (Appendix G) and then generating a transfer-matrix based on the set of scattering-parameters. A set of scattering-parameters for the two-port network to be de-embedded is also calculated. In this case, it is represented by a mean two-port network. A corresponding transfer-matrix is then generated for the two-port network that is to be de-embedded. Each transfer-matrix being generated is based

on the corresponding set of acquired scattering-parameters. The transfer-matrix for the measured two-port network is then multiplied by the inverse of the transfer-matrix associated with the mean network to be de-embedded, to thereby produce a composite transfer-matrix. Finally, a set of composite scattering-parameters is generated based on the composite transfer-matrix. The set of composite scattering-parameters is representative of the residual two-port network (Appendix H).

The calculated two-port parameters of the mean residual scattering matrix are tabulated in Table 6.2. Due to the de-embedding technique, the resulted matrix is reciprocal. Therefore, the scattering parameters for the input port (Port 1) are the same as for the output port (Port 2). Also, the S_{11} and S_{22} parameters are close to zero and S_{12} and S_{21} are close to one. Thus, the selection of the mean vector for the de-embedding procedure was accurate for all tags.

Table 6.2: The calculated residual two port network (mean values) for the tested tags

		S11		S12		S21		S22	
		Real	Imaginary	Real	Imaginary	Real	Imaginary	Real	Imaginary
AD220	Printed	0.0008	0.0000	0.9996	0.0000	0.9996	0.0000	0.0008	0.0000
	Original	0.0012	0.0005	0.9994	0.0002	0.9994	0.0002	0.0012	0.0005
ALIEN	Printed	0.0009	0.0001	0.9995	0.0001	0.9995	0.0001	0.0009	0.0001
	Original	0.0008	0.0000	0.9996	0.0000	0.9996	0.0000	0.0008	0.0000
TI	Printed	0.0004	0.0001	0.9998	0.0000	0.9998	0.0000	0.0004	0.0001
	Original	0.0002	0.0000	0.9999	0.0000	0.9999	0.0000	0.0002	0.0000
RAFSEC	Printed	0.0005	0.0001	0.9997	0.0001	0.9997	0.0001	0.0005	0.0001
	Original	0.0002	0.0002	0.9999	0.0001	0.9999	0.0001	0.0002	0.0002

Looking at the standard deviation of each scattering parameter in the residual two-port network Table 6.3, the transmission parameters (S_{12} and S_{21}) are close to zero, because there were no distortions in the signal from the input to the output port for all tested tags. However,

there are deviations in the matching which represent the variation in the manufacturing of the tags with respect to interconnect between the antenna and the chip.

Table 6.3: The calculated standard deviation of the scattered parameters

		S11		S12		S21		S22	
		Real	Imaginary	Real	Imaginary	Real	Imaginary	Real	Imaginary
AD220	Printed	0.0291	0.0101	0.0007	0.0003	0.0007	0.0003	0.0291	0.0101
	Original	0.0362	0.0116	0.0007	0.0004	0.0007	0.0004	0.0362	0.0116
ALIEN	Printed	0.0329	0.0121	0.0007	0.0004	0.0007	0.0004	0.0329	0.0121
	Original	0.0301	0.0108	0.0006	0.0004	0.0006	0.0004	0.0301	0.0108
TI	Printed	0.0219	0.0082	0.0003	0.0002	0.0003	0.0002	0.0219	0.0082
	Original	0.0164	0.0066	0.0002	0.0001	0.0002	0.0001	0.0164	0.0066
RAFSEC	Printed	0.0283	0.0168	0.0006	0.0004	0.0006	0.0004	0.0283	0.0168
	Original	0.0293	0.0267	0.0008	0.0009	0.0008	0.0009	0.0293	0.0267

7.0 STATISTICAL ANALYSIS

The typical statistical analysis of measurements can be performed according to the internationally accepted guidelines [65, 66]. However, there are no alternative guidelines that can be applied to complex valued quantities (i.e. impedance), which are very common in RF measurements including this work. As a result, there are different methods that have been proposed [67-69], which are fundamentally based on the classical multivariate statistics [70-72]. In this study, the classical multivariate analysis is applied for evaluating the measured results.

7.1 BACKGROUND

By assuming multivariate normal distribution, the analysis can be represented by the generalized T^2 statistics [72], which is the multivariate extension of the Student's t for the hypotheses on means involving p dependent variables. For the purpose of this study, the bivariate analysis is performed, where p is limited to special case of two dependent variables in the context of either the one or two sample test. These designs are referred to as the one or two samples cases of the Hotelling's T^2 (also referred to simply as T^2) [70-73].

In this study, all measured data (antenna impedances) are represented with two numbers: real and imaginary, which are independent parameters. The real and imaginary values can be combined by calculating the magnitude, which could be used for the statistical analysis based on

the classical Student's t approach. However, based on the research results from previous works [70-72] and the recommendations from the statistical consultation services [74], the multivariate statistical analysis is used. Figure 7.1 demonstrates the probability density function (pdf) for a normal bivariate distribution.

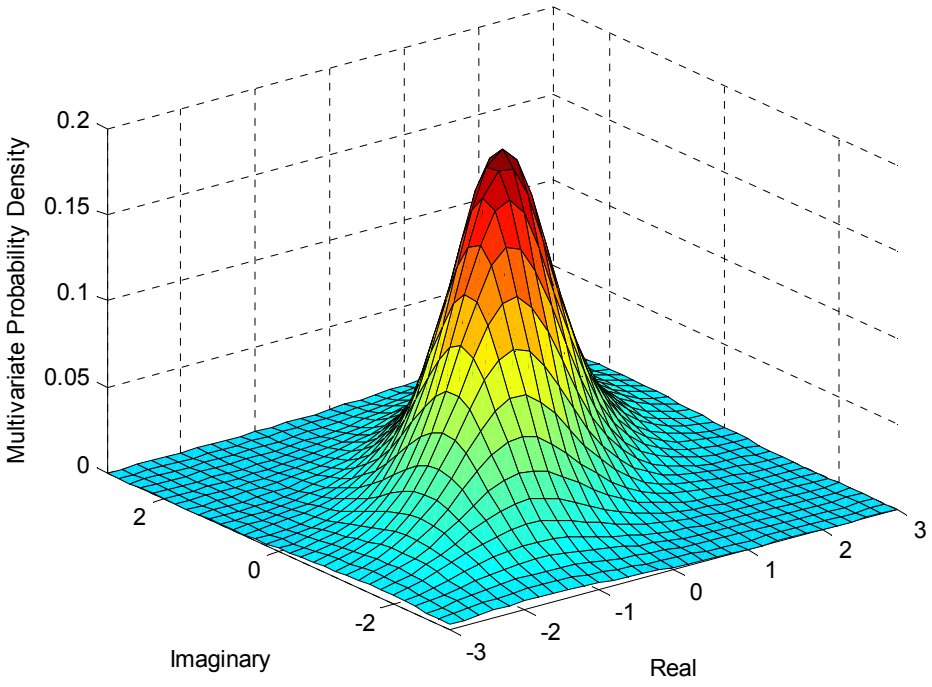

Figure 7.1: The normal bivariate distribution

7.2 INFERENCE ABOUT THE IMPEDANCE OF THE TAGS

The important question in multivariate statistics is related to the problem concerning the mean of a given distribution when the population covariance matrix is unknown. On the basis of a single sample, one may wish to statistically test whether the mean vector μ_0 is equal to a desired mean vector $\mu_{0.}$ The answer depends on the hypothesis testing such as

$$\mathbf{H_o: \mu = \mu_0} \quad (7.1)$$

$$\mathbf{H_a: \mu \neq \mu_0} \quad (7.2)$$

where μ_0 is the original population mean, and μ is the population mean of the sample in question.

If the distribution sampled is from a multivariate normal population with the mean vector μ and covariance matrix Σ then Hotelling's T^2 is given as:

$$T^2 = n(\underset{\sim}{\bar{x}} - \underset{\sim}{\mu_o})^T \Sigma^{-1} (\underset{\sim}{\bar{x}} - \underset{\sim}{\mu_o}) \quad (7.3)$$

where

$$\underset{\sim}{\bar{x}} = \begin{bmatrix} \bar{x}_1 \\ \bar{x}_2 \\ \vdots \\ \bar{x}_p \end{bmatrix} \qquad \underset{\sim}{\mu_o} = \begin{bmatrix} \mu_{o_1} \\ \mu_{o2} \\ \vdots \\ \mu_{op} \end{bmatrix}$$

Σ^{-1} is the inverse of the sample covariance matrix, Σ,

$$\Sigma = \begin{bmatrix} \sigma_R^2 & \sigma_{R,I} \\ \sigma_{R,I} & \sigma_I^2 \end{bmatrix} \tag{7.4}$$

n is the sample size upon which each x_i, i = 1, 2, ..., p, is based. The diagonal elements of Σ are the variances, and the off-diagonal elements are the covariance for the p variables. And, T^2 is a scalar value that gives the statistical distance away from the desired mean of the multivariate data set.

It is rare, in multivariate situations, to be content with the test of the null hypothesis, where all of the mean vector components are specified under the null hypothesis [70]. This is especially true in this research and is due to the fact that the desired (mean) impedance of the antenna is not reported by the manufactures. Also, simulation results are not sufficiently accurate to be used as the target value for the input impedance of the measured antennas. Ordinarily, it is preferred to find regions of mean values that are plausible in light of the observed data [70].

Therefore, the simultaneous confidence regions are computed on the basis of T^2 in order to make statistical inference from a sample about the mean value for the measured input impedance. In this case, the region shape is an ellipsoid centered at mean value, where the ellipsoid defines the 100(1-α) % (i.e. α=0.05 or 95%) simultaneous confidence region for real and imaginary values of the impedance. The simultaneous interval (T^2 – interval) for the i's value of the mean vector is defined as

$$\bar{x}_i - \sqrt{\frac{p(n-1)}{(n-p)}F_{p,n-p}(\alpha)} \cdot \sqrt{\frac{s_{ii}}{n}} \le \mu_i \le \bar{x}_i - \sqrt{\frac{p(n-1)}{(n-p)}F_{p,n-p}(\alpha)} \cdot \sqrt{\frac{s_{ii}}{n}} \quad \textbf{(7.5)}$$

or

$$\bar{x}_i \pm \sqrt{\frac{p(n-1)}{(n-p)}F_{p,n-p}(\alpha)} \cdot \sqrt{\frac{s_{ii}}{n}} \quad \textbf{(7.6)}$$

The T^2 statistic is computed using the fact that the change in T^2 is related to the F-distribution using the following formula

$$T^2_{p,n,\alpha} = \frac{p(n-1)}{(n-p)}F_{p,n-p,\alpha} \quad \textbf{(7.7)}$$

where $F_{p,n-p,\alpha}$ representing the F distribution with p degrees of freedom for the numerator and n - p for the denominator, *n* is the number of samples. Table 7.1 illustrates the critical values for the T^2 statistics, which were calculated according to the equation (7.7) for n=100 and p=2.

Table 7.1: The critical values for 100 samples

90% CRITICAL VALUE	4.71508
95% CRITICAL VALUE	6.178407
99% CRITICAL VALUE	9.65703

The 95% simultaneous T^2 intervals were calculated for all measured tags. The calculated results for the real and imaginary components of the antenna impedance are demonstrated in Table 7.2.

Table 7.2: The 95% simultaneous T^2 intervals tabulated for all tags

Alien (N=100 tags)		
	Real	Imaginary
Measured Original	$10.83 < \mu < 12.19$ or 11.51 ± 0.68	$101.63 < \mu < 105.03$ or 103.33 ± 1.70
Measured Printed	$10.76 < \mu < 11.98$ 11.37 ± 0.61	$102.67 < \mu < 105.82$ 104.25 ± 1.57
AD220 (N=100 tags)		
	Real	Imaginary
Measured Original	$72.77 < \mu < 75.47$ or 74.12 ± 1.35	$131.36 < \mu < 135.37$ or 133.37 ± 2.01
Measured Printed	$78.03 < \mu < 80.42$ or 79.23 ± 1.20	$128.86 < \mu < 134.25$ or 131.55 ± 2.69
TI (N=100 tags)		
	Real	Imaginary
Measured Original	$11.01 < \mu < 12.42$ or 11.72 ± 0.71	$161.59 < \mu < 165.12$ or 163.29 ± 1.78
Measured Printed	$9.32 < \mu < 10.37$ or 9.84 ± 0.52	$155.82 < \mu < 158.39$ or 157.11 ± 1.29
Rafsec (N=38 tags)		
	Real	Imaginary
Measured Original	$20.55 < \mu < 25.31$ or 22.93 ± 2.38	$164.67 < \mu < 172.78$ or 168.72 ± 4.06
Measured Printed	$21.07 < \mu < 28.57$ or 24.82 ± 3.75	$167.73 < \mu < 176.44$ or 172.09 ± 4.35

The simultaneous T^2 confidence intervals are ideal for "data snooping" [70]. The simultaneous T^2 confidence intervals of the bivariate statistics can be plotted on the same chart, which can be bound by an ellipse.

7.3 QUALITY CONTROL CHARTS

In order to improve the quality of products (RFID tags), data need to be examined for cases of variations. The control chart is used to identify occurrences of special causes of variations that arise from out of control limits.

The control limits are chosen based on the assumption that the underlying data are approximately normal. In the manufacturing industry, the control limits are typically set to be ± 3 sigma [70, 75, 76]. The most common multivariate chart is the ellipse format chart. This is due to the fact that the ellipse type chart for a bivariate control region creates intuitive representations of the data while only being limited to two variables. In this study, the two characteristics of the impedance (real and imaginary parts) are plotted as a pair (Real, Imaginary). The 95% quality ellipse charts were generated for the measured tags, which consist of all x_j point that satisfy

$$(x_j - \bar{x})' \Sigma^{-1} (x_j - \bar{x}) \leq \frac{p(n-1)}{(n-p)} F_{p,n-p,\alpha} \qquad \textbf{(7.8)}$$

For the four candidate tags, the T^2 was plotted on the ellipse type control charts in order to identify tags that were statistically different from the sample population. The charts were

generated using statistical software package Minitab. The charts are shown in Appendix C. The summary of the results is presented in Table 7.3.

Table 7.3: The out-of-control RFID tags

Tags	The tag number that is outside of the ellipse	Total number of the out of control points
ALIEN Original	10, 24, 48	3
ALIEN Printed	22, 30, 55, 59, 75, 78	6
AD220 Original	49, 60, 71, 72	4
AD220 Printed	68,27,90	3
TI Original	6, 8, 97	3
TI Printed	6, 81, 82, 91	4
RAFSEC Original	8	1
RAFSEC Printed	37	1

Based on the results, most of the variables are in control, where the outer border of the ellipsoid is used as the confidence limit on checking if the data points are significantly different tfrom the mean. However, there are a few special cases of tags that were outside of the quality control 95% ellipse. These cases will be examined as point of illustration of the usefulness of this research.

For all tested manufacturers, the original tags that were identified to be outside of 95% control border were examined under a microscope in order to identify the possible reasons for the drastic deviation from the sample population.

From the following figures, the Alien tags do not have any visible features that can be responsible for the variation in the tags. The assumption is that the variation are due to the micro fractures or adhesive position that hold the chip. In the close examination of the AD220 tags that were out-of-control ellipse, the strap position of the tag is the main cause of the tag variability. The following figures illustrate the shift in the strap position with respect the antenna terminals. The shift in the starp can be due to the quality of the conductive adhesive that holds the strap in place. The TI tags have a visible shift in chip position, which can be seen from the position of the connection bumps. The following figures demonstrate the close up view of the chips that were identified as out-of-control. The Rafsec tags do not show any visible problems

Another observation was made with regard to the difference in the chip attachment methods (i.e. direct and indirect). From the quality control chart of AD220, the indirect attachment process provides much tighter statistical dispersion of the values for the real part of the measured impedance. All other tags (Alien, TI and Rafsec) with the direct chip attachment have a wide spread of the data values in comparison to the AD220. Because of the large standard deviation for the direct attachment process, the outlier's tags of the quality control of 95% ellipse might not exhibit the critical issues of attachment process such as thickness of the attachment material. Also, the wide spread of the direct attachment data can be attributed to the fact that the assembly process has to deal with the much smaller feature size than with that of the indirect attachment process where the chip is initially attached to the strap and only then to the antenna terminals. As the result, the strap attachment process seems to be more robust in terms

of the standard deviation of the complex magnitude of the interconnect value. However, any out-of-control data points present the "failure" in the attachment of the chip. Thus, the close-up figures are presented in this chapter to allow for a physical examination of the out-of control tags.

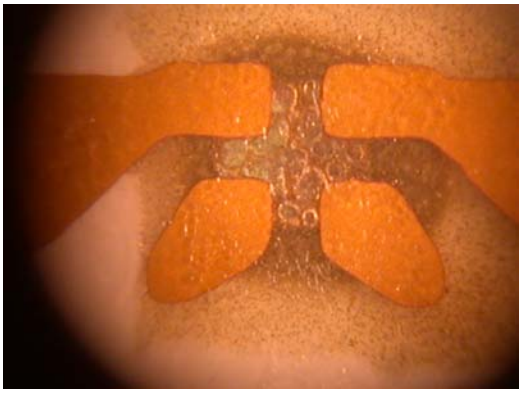

Figure 7.2: The Alien Original Tag #10

Figure 7.3: The Alien Original Tag #24

Figure 7.4: The Alien Original Tag #48

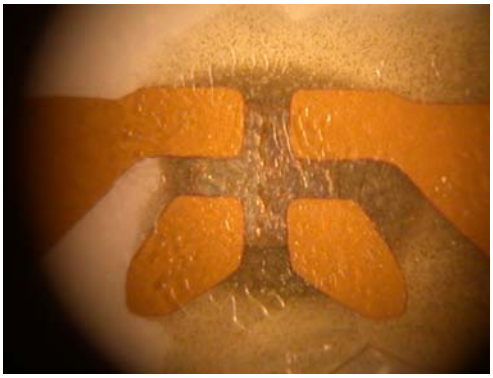

Figure 7.5: The Alien Original Tag #87 (MEAN)

Figure 7.6: The AD220 Original Tag #49

Figure 7.7: The AD220 Original Tag #60

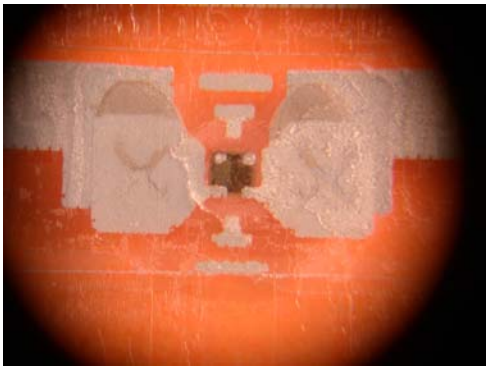

Figure 7.8: The AD220 Original Tag #71

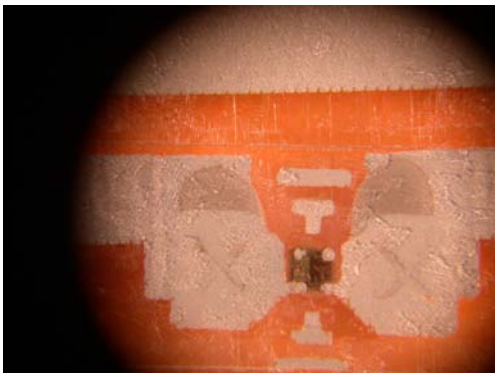

Figure 7.9: The AD220 Original Tag #72

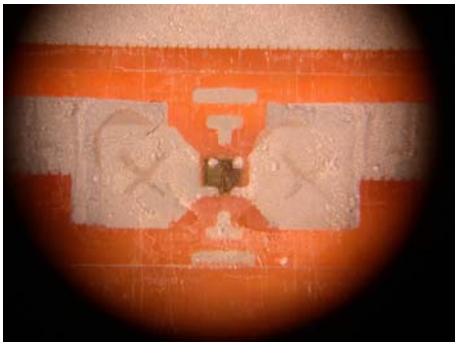

Figure 7.10: The AD220 Original Tag #39 (MEAN)

Figure 7.11: The TI Original Tag #6

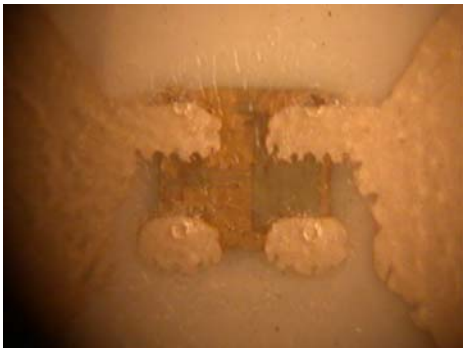

Figure 7.12: The TI Original Tag #8

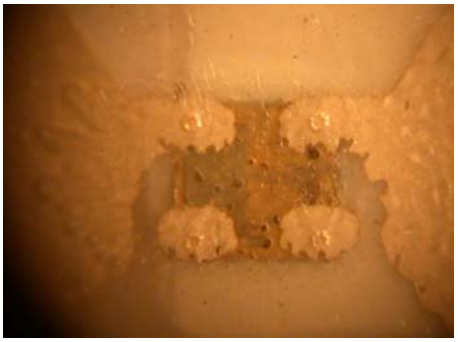

Figure 7.13: The TI Original Tag #97

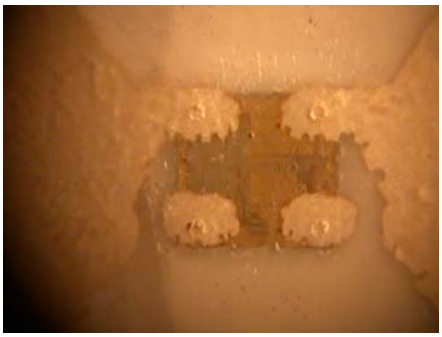

Figure 7.14: The TI Original Tag #95 (MEAN)

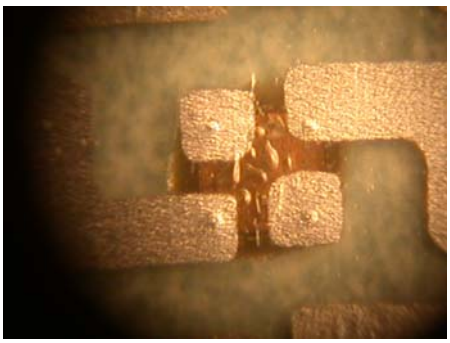

Figure 7.15: The Rafsec Original Tag #8

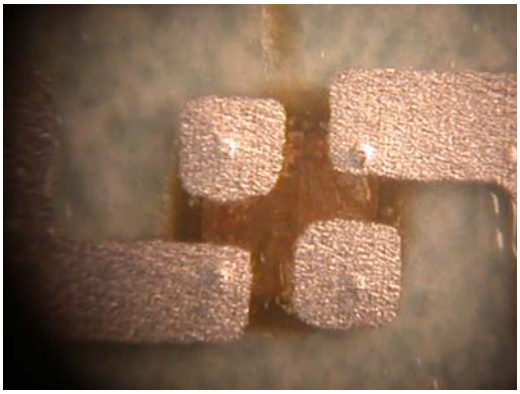

Figure 7.16: The Rafsec Original Tag #29 (MEAN)

7.4 COMPARISON OF ORIGINAL AND PRINTED TAGS

The comparison of the original and printed tags is performed in order to determine whether running tags through the RFID printers actually affects the tags. This is hypothesis test: where the null hypothesis states that there is no significant difference between tags prior and past the RFID printers. This becomes a two-sample Hotelling's T^2 test with two independent sets of tags.

The Hotelling's T^2 is used to test whether two mean vectors from multivariate normal population are equal (i.e. H_o: $\mu_1 = \mu_2$ and H_a: $\mu_1 \neq \mu_2$). Hotelling's T^2 is determine as

$$T^2 = \frac{n_1 n_2}{n_1 + n_2}(\bar{x}_1 - \bar{x}_2)' \Sigma^{-1} (\bar{x}_1 - \bar{x}_2) \qquad \textbf{(7.9)}$$

where x1 and x2 are the two sample mean vectors of size n1 and n2 respectively, Σ is a pooled covariance matrix, and Hotellin's T^2 is distributed as

$$\frac{2(n_1+n_2-2)}{(n_1+n_2-3)}F_{2,n_1+n_2-3} \quad \textbf{(7.10)}$$

Using data collected as part of this research for identifying the printing effects, the T^2 statistic is calculated for the selected tags and tabulated in Table 7.4.

Table 7.4: The T^2 statistics for the original versus printed tags

Tag	Printer	N1/N2	Variables	T^2	F	p
AD220	Zebra	100	2	153.1035	76.1651	<0.001
ALIEN	Paxar	100	2	1.5842	0.7881	0.4561
TI	Paxar	100	2	62.2566	30.9711	<0.001
RAFSEC	Paxar	38	2	3.6024	1.7769	0.1764

where N is the number of samples in the set per each tag, which was the same for all tags, each sample was represented by an item of two variable (real and imaginary part of the antenna impedance), T^2 (Hotelling's T^2 statistics) was calculated based on equation (7.9) which relates to the F-distribution, and P defines the probability that H_o is true.

Base on statistical analysis of the measured data for the ALIEN and the RAFSEC tags, the difference in the input impedance is not statistically significant (nothing visible). Thus there is no evidence to reject the hypothesis that the tags are not affected by printing. However, for the AD220 and the TI there is strong evidence of a difference in mean impedance of the original and

printed tags. This can be attributed to the properties of the material (conductive ink) which is used the manufacturing of the antennas in the AD220 and the TI tags.

7.5 THE POWER OF THE T^2 TEST

The purpose of analyzing the power of a statistical test is to determine the probability that the test will reject a false null hypothesis. The power of a test is the probability of rejecting H_0 when H_a is in fact true, which is Type II error. Power measures how likely a test is to detect a specific alternative.

There are two kinds of error, classified as Type I error and Type II error, depending upon which hypothesis has been incorrectly identified as being true. Type I error (alpha error) occurs when a null hypothesis is rejected when it is actually true. Type II error (beta error) occurs when there is an error of not rejecting a null hypothesis, but the alternative hypothesis is true.

It is important to perform the power calculation in order to verify that the sample sizes are adequate to detect differences among means. Power calculations are used to evaluate and interpret the results of the analysis which H_0 was not rejected.

The power increases with an increase in the value of the alpha (usually equal to 0.05), the sample size and the non-centrality parameter, λ. The non-centrality parameter measures how far apart the true parameter values from the hypothesized parameter values of the means. For T^2-tests, the non-centrality parameter is obtained for the one-sample case as follows:

$$\lambda = n(\mu - \mu_0)' \Sigma^{-1} (\mu - \mu_0) \quad \textbf{(7.11)}$$

and for the two-sample test, it is given by

$$\lambda = \frac{n_1 n_2}{n_1 + n_2}(\mu_1 - \mu_2)' \Sigma^{-1}(\mu_1 - \mu_2) \qquad \textbf{(7.12)}$$

If the means are all equal, $\lambda=0$. A large value of λ points to an alternative hypothesis far from the null hypothesis, which in turn increases the power. Because T^2 is related to the F-distribution, the power can be determine using statistical software packages [77] and tables [78].

Table 7.5: The power of the one-sample T^2 test

Power	N	Alpha	Beta	DF1	DF2
0.0228	5	0.01	0.9772	2	3
0.172	15	0.01	0.828	2	13
0.4032	25	0.01	0.5968	2	23
0.6219	35	0.01	0.3781	2	33
0.8414	50	0.01	0.1586	2	48
0.9737	75	0.01	0.0263	2	73
0.9968	100	0.01	0.0032	2	98
0.1054	5	0.05	0.8946	2	3
0.4122	15	0.05	0.5878	2	13
0.6751	25	0.05	0.3249	2	23
0.8399	35	0.05	0.1601	2	33
0.9525	50	0.05	0.0475	2	48
0.9952	75	0.05	0.0048	2	73
0.9996	100	0.05	0.0004	2	98
0.1966	5	0.1	0.8034	2	3
0.5589	15	0.1	0.4411	2	13
0.791	25	0.1	0.209	2	23
0.9102	35	0.1	0.0898	2	33
0.9778	50	0.1	0.0222	2	48
0.9983	75	0.1	0.0017	2	73
0.9999	100	0.1	0.0001	2	98

In Table 7.5, the N is the sample size, alpha is the probability of rejecting a true null hypothesis, beta is the probability of accepting a false null hypothesis, DF1 is the number of response variables, and DF2 is the second degree of freedom of T^2.

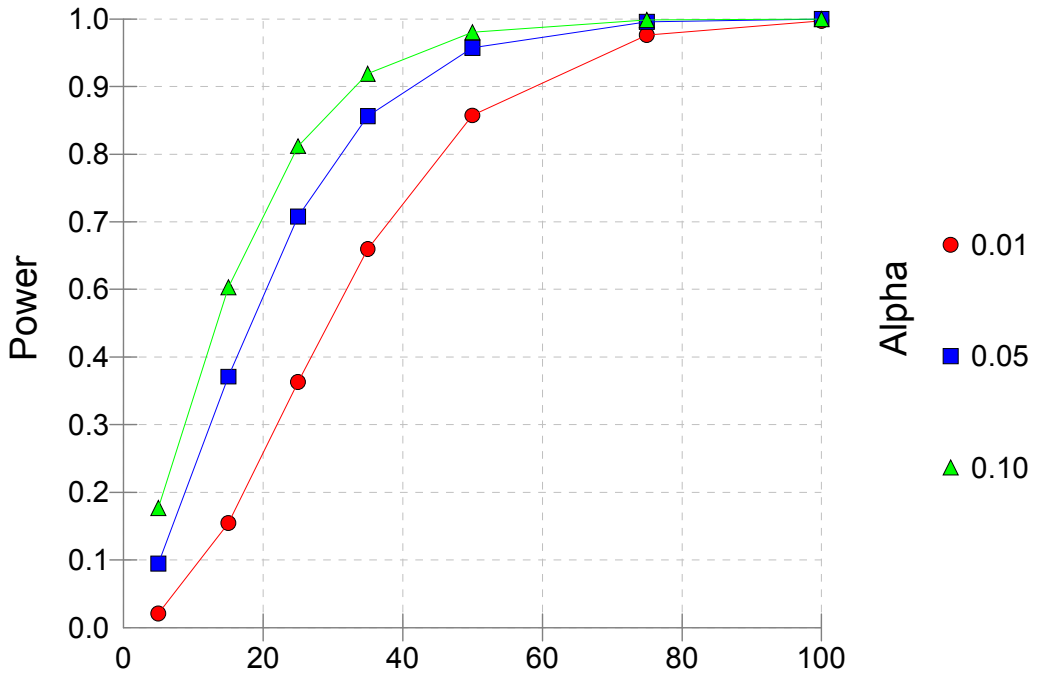

Figure 7.17: The power plot for one-sample T^2 test

A sample size of one hundred achieves 99% power which is needed to accurately detect the Type II errors for cases where the statistical analysis has failed to reject the null hyposisis, where the one-sample Hotelling's T^2 test statistic is used with a significance level of 0.05. Ideally, power should be at least 80% to detect a reasonable departure from the null hypothesis. On the other hand, a very large sample size may suggest that differences detected could be

irrelevant. In this case, a different hyposisis testing can potentially be performed using the measured data in Appendix E.

Table 7.6: The power of the two-sample T^2 test

Power	N1	N2	Alpha	Beta	DF1	DF2
0.0221	5	5	0.01	0.9779	2	7
0.0901	15	15	0.01	0.9099	2	27
0.1892	25	25	0.01	0.8108	2	47
0.3052	35	35	0.01	0.6948	2	67
0.4834	50	50	0.01	0.5166	2	97
0.7263	75	75	0.01	0.2737	2	147
0.8738	100	100	0.01	0.1262	2	197
0.0942	5	5	0.05	0.9058	2	7
0.2484	15	15	0.05	0.7516	2	27
0.4071	25	25	0.05	0.5929	2	47
0.5511	35	35	0.05	0.4489	2	67
0.7221	50	50	0.05	0.2779	2	97
0.8898	75	75	0.05	0.1102	2	147
0.9611	100	100	0.05	0.0389	2	197
0.1711	5	5	0.1	0.8289	2	7
0.3677	15	15	0.1	0.6323	2	27
0.5392	25	25	0.1	0.4608	2	47
0.6764	35	35	0.1	0.3236	2	67
0.8197	50	50	0.1	0.1803	2	97
0.939	75	75	0.1	0.061	2	147
0.9814	100	100	0.1	0.0186	2	197

In Table 7.6, N1 and N2 are the sample sizes of the two groups, alpha is the probability of rejecting a true null hypothesis, beta is the probability of accepting a false null hypothesis, DF1 is the number of response variables, and DF2 is the second degrees of freedom of T^2.

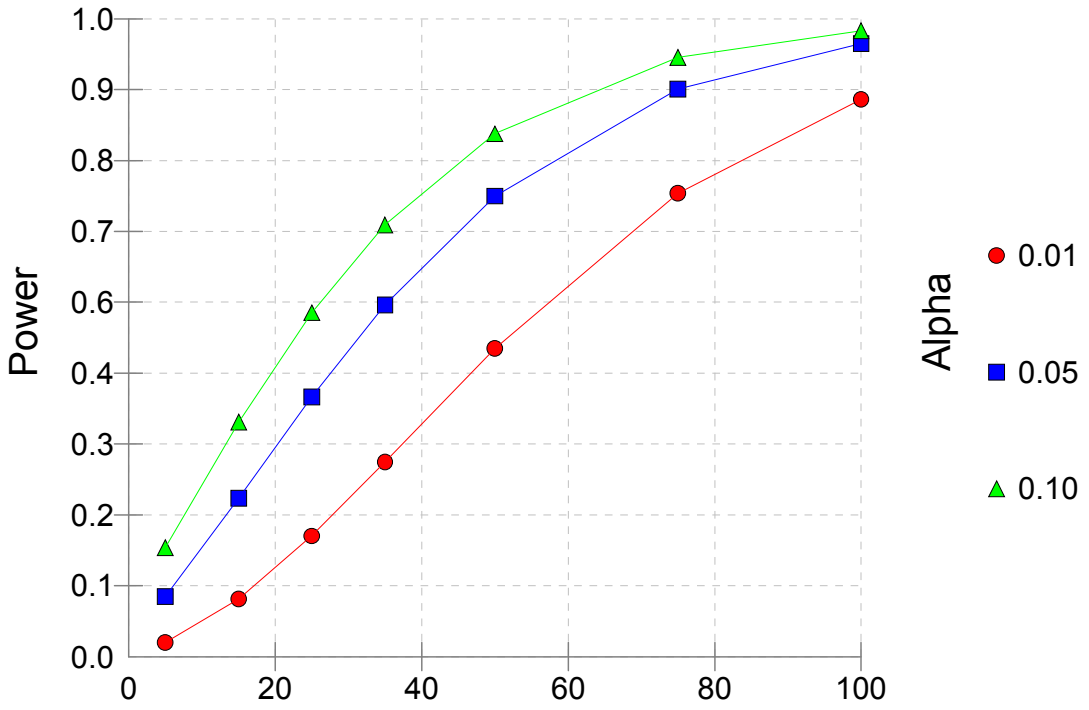

Figure 7.18: The power plot for two-sample T^2 test

Sample sizes of one hundred in group of original tags (group one) and one hundred in group of printed tags (group two) achieve 97% power to detect the Type II errors. The two-sample Hotelling's T^2 test statistic is used with a significance level of 0.05. A power calculation confirms that the sample size in that study was adequate for detecting a relevant difference for the selected tags with the exception of Rafsec, which has smaller sample (38 tags) size due to the availability.

8.0 CONCLUSIONS

The original methodology for a non-invasive in-situ measurement of the input impedance and the effect of the connection manufacturing of the antenna to the chip in RFID tags has been accomplished. The technique involves the measurement of the amplitude and phase of the scattered field of the antenna in order to characterize the RFID transponder chip and antenna interconnection. The method of scattering measurements is independent of contact mechanisms implying a more accurate, than conventional measurement technique. The developed methodology in this research is valid on the basis of direct measurement using the commercial test equipment and mathematic first principles.

8.1 RESEARCH RESULTS AND ORIGINAL CONTRIBUTIONS

The contributions of the dissertation are listed below.

1. A non-invasive *in-situ* approach for characterization and modeling.

This dissertation has developed the mathematical model along with the practically realizable system and methodology for performing the real time non-invasive *in-situ* measurements and analysis of the RFID antenna for the purpose of monitoring and evaluating of the manufacturing methods and variations of the RFID tags.

2. The two-port model representation.

It was determined that the two-port model was the best suited model for the proposed technique. Using a classical two-port network as the representation of the interface between the antenna and the chip, the interconnect characterization of the antenna/chip is presented.

3. The validation of the proposed methodology.

The three-dimensional electro-magnetic simulation was performed using Ansoft's Finite Element Method (FEM) field simulator in order to provide the conceptual validation of the proposed methodology. The numerical simulations have been used in association with the physical measurements in order to analyze and evaluate the method developed. Any observed discrepancy between the electromagnetic (EM) simulations and the measurements can be attributed to a few specific factors. Most notably, the EM simulations are as good as the antenna model and its surrounding environment, which are both only approximated due to the fact that the physical characteristics of the tag and the surroundings can not be accurately modeled.

4. The demonstration of the proposed methodology.

Experimental conformation of the technique is presented using measurements on the commercially available tags. The quantities such as antenna impedance determined in this dissertation are difficult to measure with standard RF test instruments (i.e. venctor network analyzer). The results indicate that the derived technique provides the information for characterizing and evaluating the performance of the tags.

5. The demonstration of the evaluation of mechanical quality of the RFID tag packaging.

The proposed method is applied for the quantitative evaluation of the mechanical effects due to running tags under test through the two commercial RFID printers.

6. The simulation of the selected RFID tags.

Due to the lack of comparable methodologies, the simulation results of the selected RFID tags are demonstrated as the approximation of the expected results, which are correlated to the measured results.

7. The antenna/chip interconnect model.

The tandem model of the antenna/chip interconnection is developed. The first part of the model demonstrates the "mean" transformation network that provides the antenna designer with the virtual "distance" between the simulated and the measured results in the form of the "L-match" impedance transformation network. The extraction of the second part of the interconnect model is achieved with a robust and relatively simple microwave de-embedding technique. It presents the evaluation and characterization of the process variations in the manufacturing process.

8. A statistical analysis of the test results.

A statistical analysis has been performed which presents the quality control approach for the manufacturing configuration of RFID tags. The statistical analysis is based on the hypothesis testing. Therefore, the statistical power analysis has been presented in support of the sample size selection in order to ensure that the provided results are adequate (i.e. sufficiently powerful) for the testing of the null hypothesis. The results of the characterization presented in conjunction

with the method being developed make it possible for the antenna designer to compensate for the dynamic effect of the manufacturing technique process. Also, this makes it possible for the manufacturer to monitor the manufacturing process on-line and in real-time, because of the non-invasive results of this research.

9. The test procedure for quantifying the absolute minimum operating power level of RFID tags. The sensitivity and realism of the method is justified through the physical evaluation of the RFID tag analog front-end with the novel technique for identifying the absolute lowest operating power level of the RFID tags. The measurements presented provide the most complete information regarding antenna characteristics, interconnect and RF scattering obtained with one single measurement and commercial test equipment configuration.

10. The complete test system based on the proposed methodology.

The realized test system is comprised of a Vector Network Analyzer (VNA), Giga-Hertz Transverse Electromagnetic (GTEM) cell and the control software that facilitates a semi-automated robust measurement and analysis flow. The system provides the in-situ and non-destructive environment for the RFID tag evaluation where no reference cables or probes from the antenna to the receiver are necessary. Therefore, the research result avoids the difficulties usually experienced with the other antenna measurement techniques due to unwanted electromagnetic coupling between antenna and measurement probe at the antenna structures.

11. The collection of measured data as the reference for the future studies.

The presented test system is one of the first technical test procedures that can provide the quantitative data for evaluating any packaging technique on the basis of their quality and reliability. While there have been a few papers discussing the problems addressed in this dissertation, they are incomplete and data are not available to the general public. The collected data can be utilized in the future studies as the reference, which is independent of the RFID equipment (i.e. readers), because all measurements are performed with the high precision RF test instrument (i.e. vector network analyzer).

8.2 FUTURE RESEARCH

The proposed technique may be applied to a moderately difficult problem, such as that of the antenna design with multiple input ports. The measurement of the N-port antennas is a difficult problem because the input impedance of an N-port antenna cannot be measured directly with only two-port vector analyzer. Even though the vector network analyzers with four ports are commercially available, these four-port analyzers are expensive due to their complexity. Therefore the proposed methodology can be potentially extended to allow for the characterization of the antennas with a large number of ports by using the vector analyzers with only two ports. Thus, the results of the current dissertation provide the scientific basis to address the problem of N-ports using available equipment as opposed to an N which would require a corresponding N-port Netork Analyzer. Also, the proposed methodology for antenna characterization across multiple frequencies can be accomplished given the more detailed specification for the RFID chips. Lastly, an observation made during the course of this effort

was the discovery of the fact that the proposed technique could be improved by utilizing the redundant measurements in order to reduce experimental error.

APPENDIX A

ANTENNA CALCULATIONS

A.1 FRIIS TRANSMISSION FORMULA

$$\frac{P_R}{P_T} = \left(\frac{\lambda}{4\pi R}\right)^2 G_T G_R \left|\hat{\rho}_T \bullet \hat{\rho}_R\right|^2 \left(1 - \left|\Gamma_T\right|^2\right)\left(1 - \left|\Gamma_R\right|^2\right) \tag{A1}$$

where the variables are defined as shown in Table 8.1:

Table 8.1: Friis transmission equation variables

Variable	Definition
λ	wavelength
G_T	gain of the transmitting antenna
G_R	gain of the receiving antenna
P_T	power received by the tag
P_R	power transmitted by the reader
$\hat{\rho}_T$	polarization of the transmitting antenna
$\hat{\rho}_R$	polarization of the receiving antenna
Γ_T	reflection coefficient of the transmitting antenna
Γ_R	reflection coefficient of the receiving antenna
R	distance measured from the reader to the tag

A.2 RADAR TRANSMISSION EQUATION

$$\frac{P_R}{P_T} = \sigma \frac{G_T G_R}{4\pi} \left[\frac{\lambda}{4\pi R_T R_R} \right]^2 \tag{A2}$$

where the variables are defined as shown in Table 8.2:

Table 8.2: Radar transmission equation variables

Variable	Definition
λ	wavelength
G_R	gain of the receiving antenna
G_T	gain of the transmitting antenna
σ	radar cross section of the tag
P_R	power received by the receiving antenna
P_T	power transmitted by the transmitting antenna
R	distance measured from the reader to the tag

A.3 RADAR CROSS SECTION

$$\sigma = \frac{1}{\pi} \left| \frac{2\pi R E_{struct}}{E_{inc}} - (1 - \Gamma_T) \frac{\pi R E_{ant}}{E_{inc}} \right|^2 \tag{A3}$$

where the variables are defined as shown in Table 8.3:

Table 8.3: RCS equation variables

Variable	Definition
R	distance between the transmitting and receiving antenna
E_{struct}	the electric field at the receiver in the short circuit case
E_{inc}	the electric field incident at the target (tag)
E_{ant}	the electric field of the antenna mode at the receiver
Γ_T	the tag antenna reflection coefficient

APPENDIX B

SELECTED RFID TAG FOR TESTING

B.1 ALIEN TAG

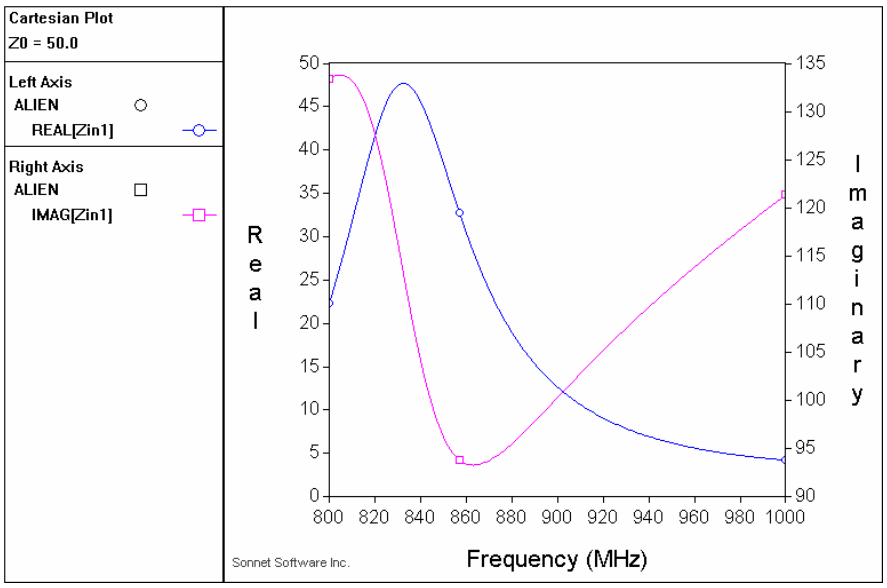

Figure 8.1: Input Impidance for the Alien Tag

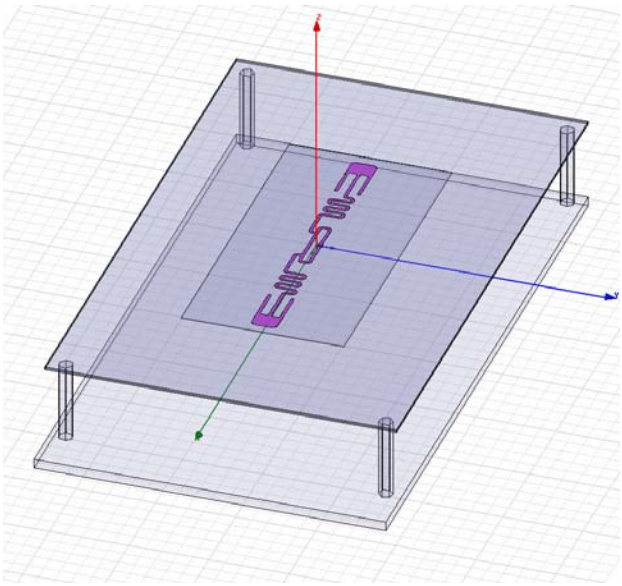

Figure 8.2: The Alien Tag

B.2 AD220 TAG

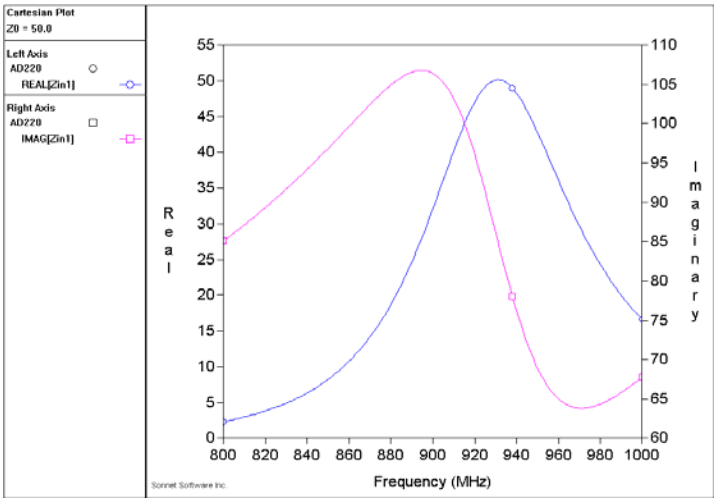

Figure 8.3: The input impidance for the AD220 tag

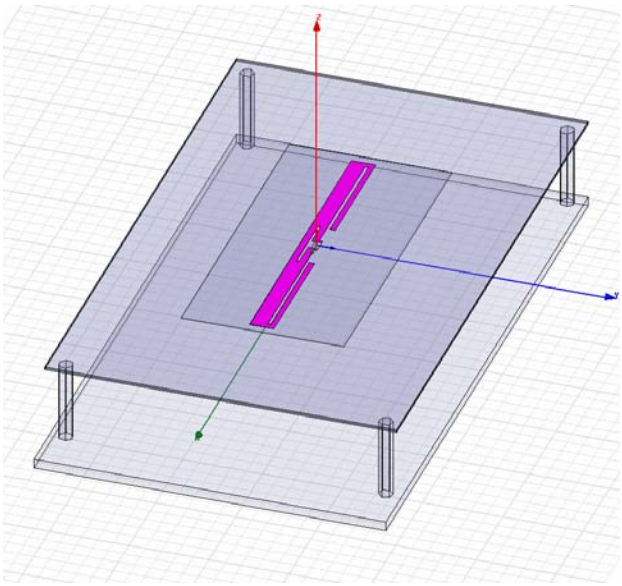

Figure 8.4: The AD220 tag

B.3 TI TAG

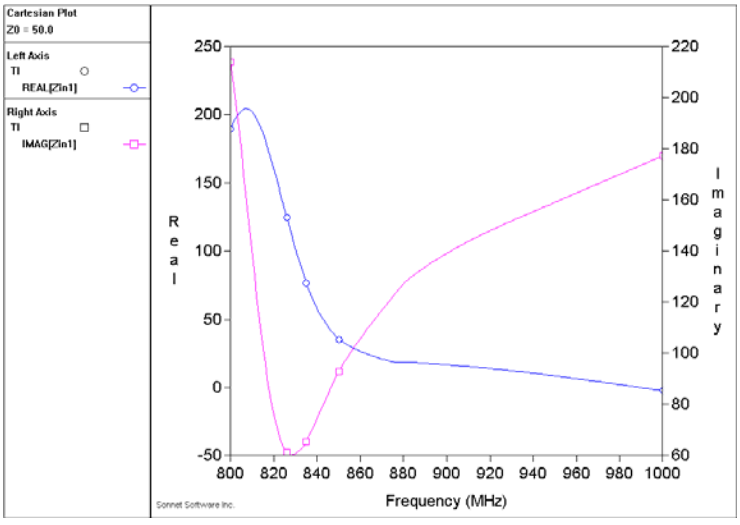

Figure 8.5: The input Impidance for the TI tag

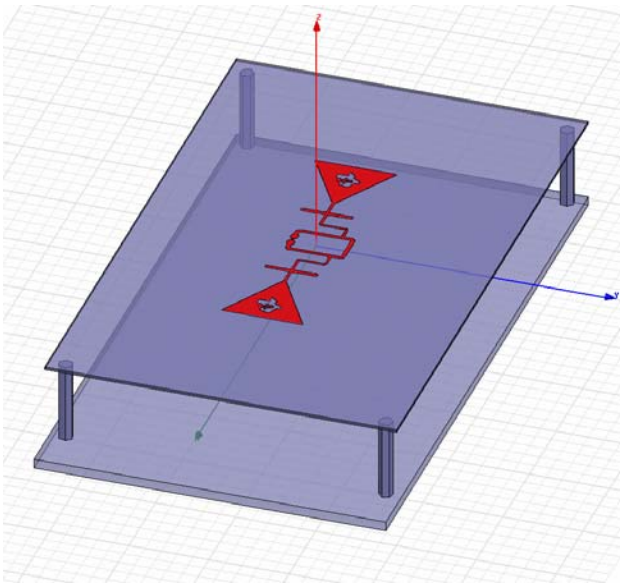

Figure 8.6: TI Tag

B.4 RAFSEC TAG

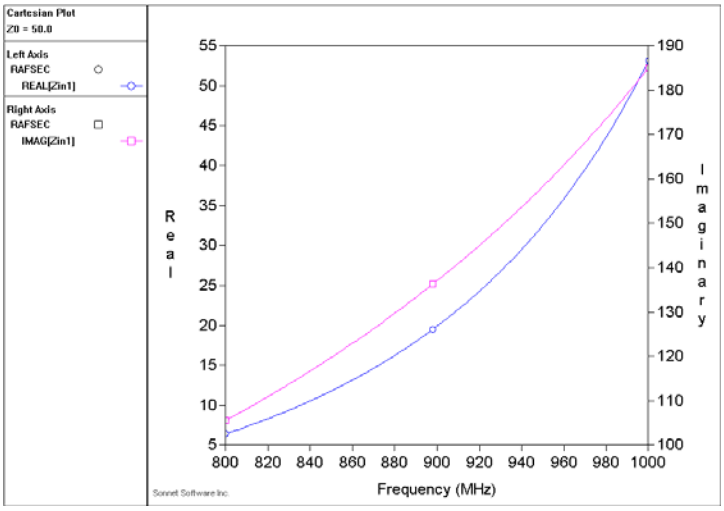

Figure 8.7: The input impidance for the Rafsec tag

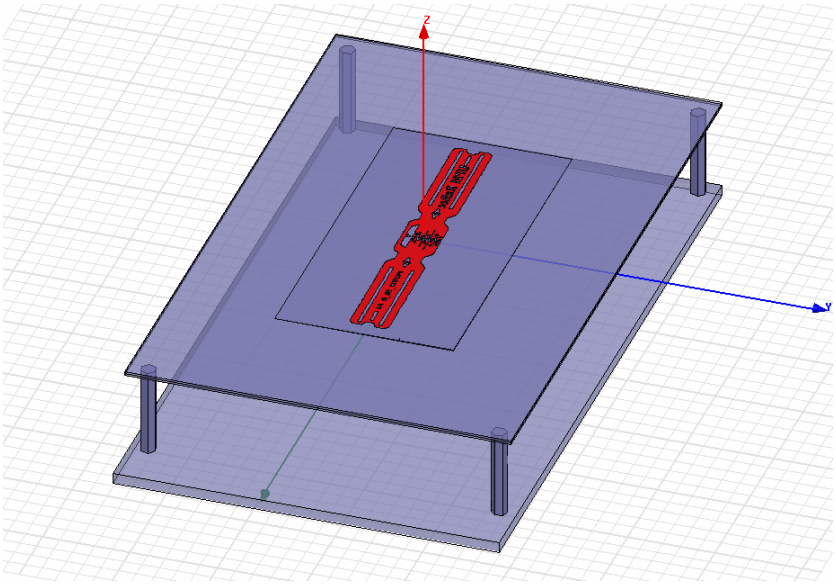

Figure 8.8: The Rafsec tag

APPENDIX C

THE QUALITY CONTROL 95% ELLIPSE TYPE CHARTS

C.1 ALIEN TAG

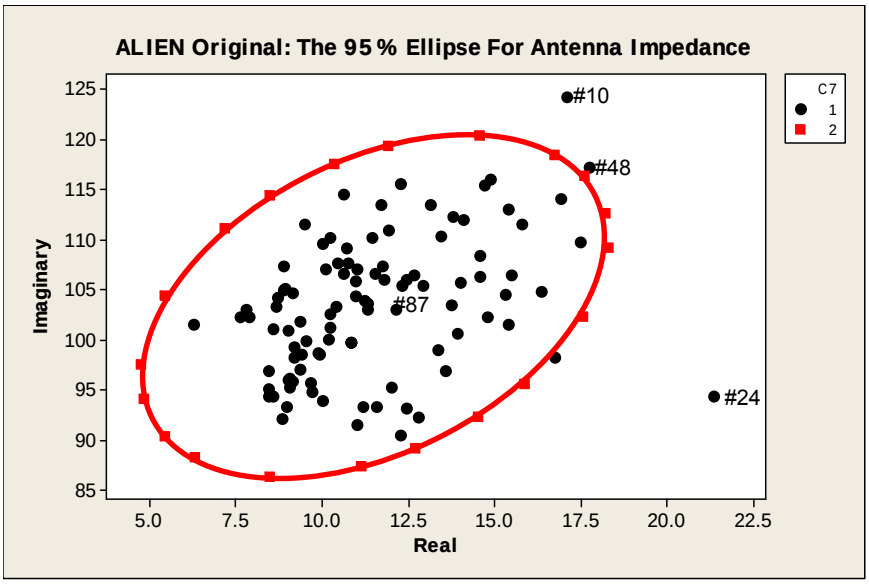

Figure 8.9: The Alien tag original

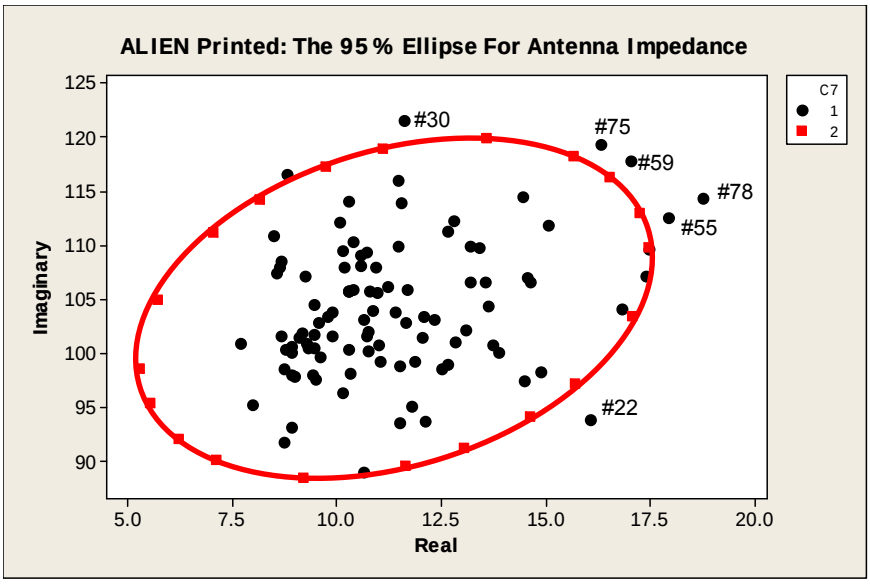

Figure 8.10: The Alien tag printed

C.2 AD220 TAG

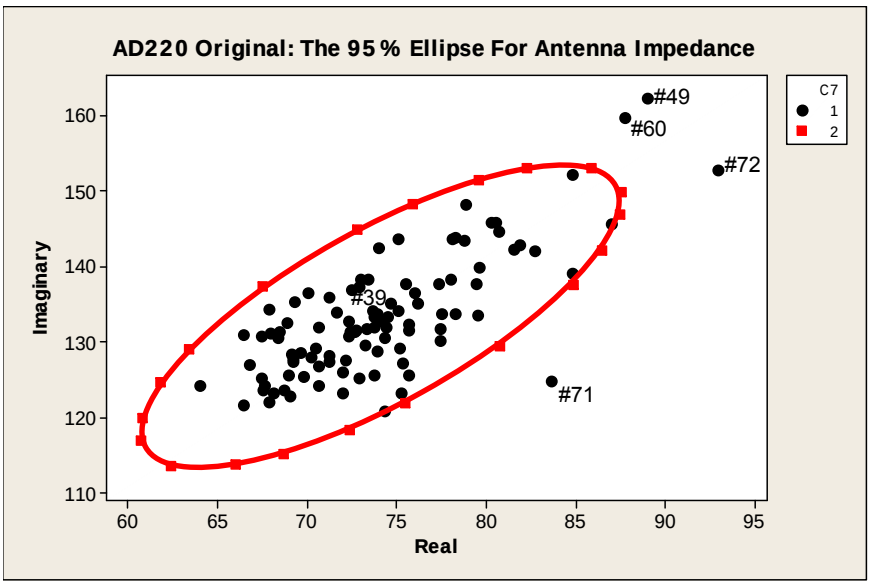

Figure 8.11: The AD220 original tag

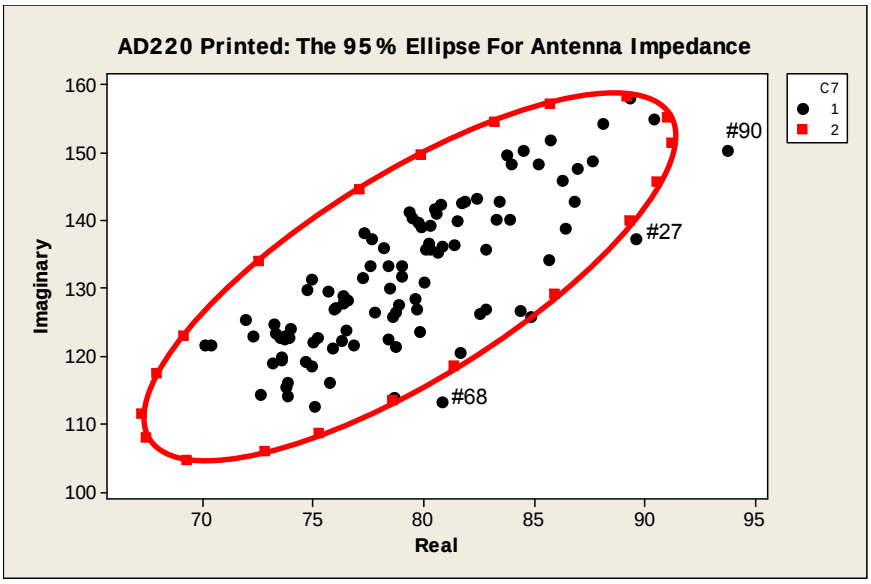

Figure 8.12: The AD220 printed tag

C.3 TI TAG

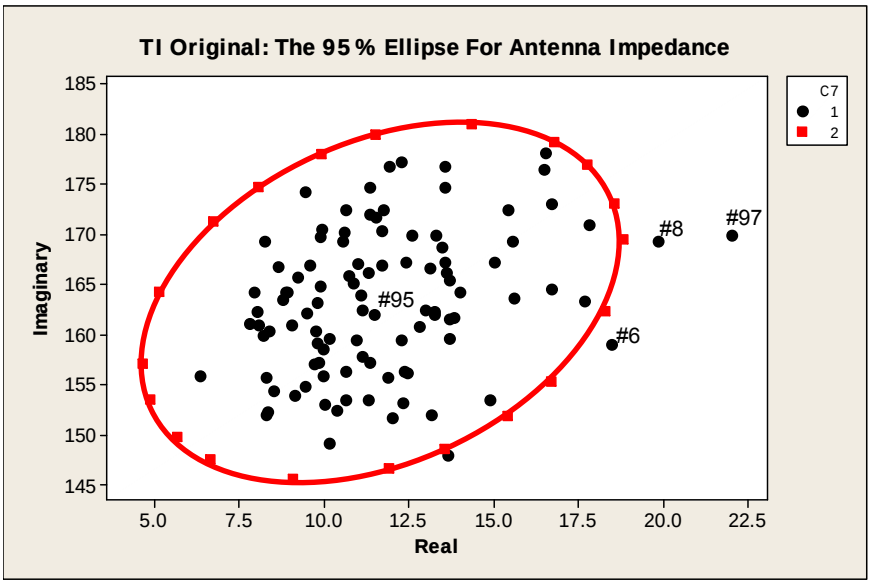

Figure 8.13: The TI original tag

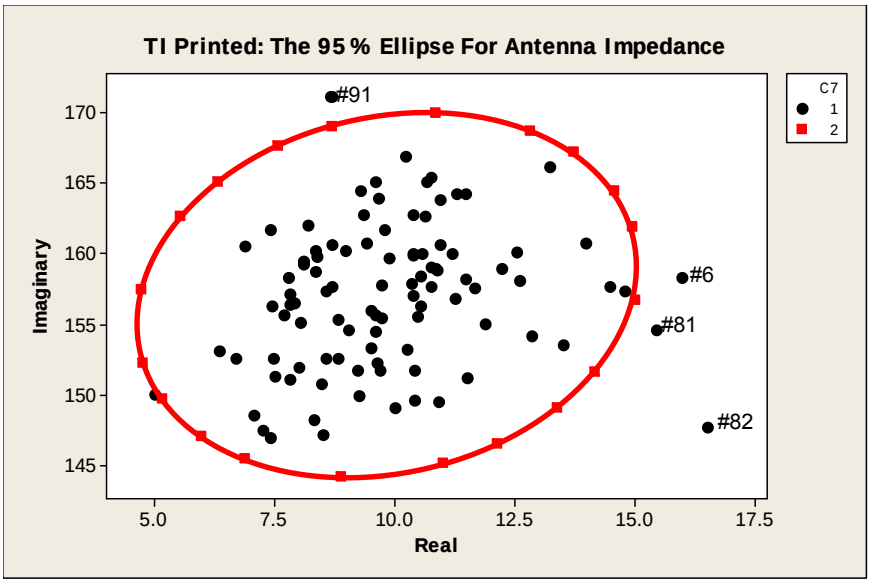

Figure 8.14: The TI printed tag

C.4 RAFSEC TAG

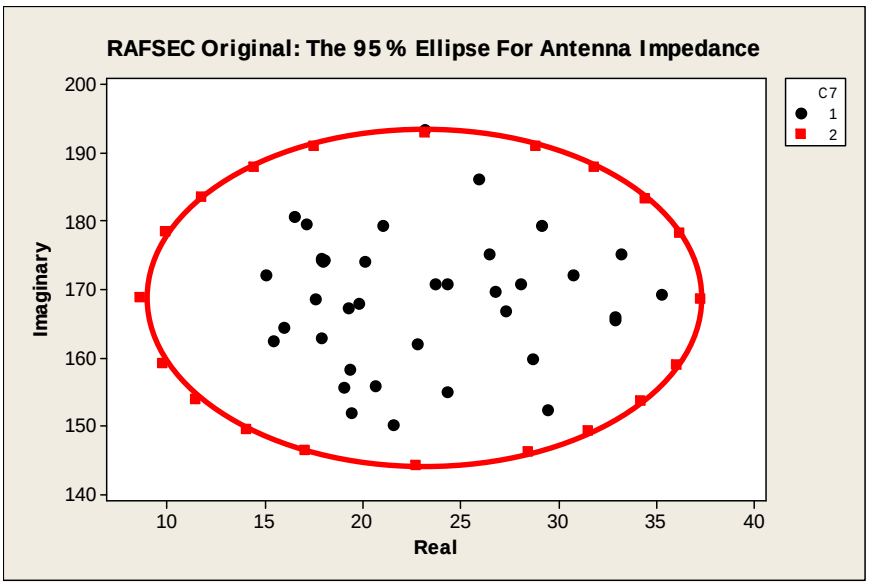

Figure 8.15: The Rafsec original tag

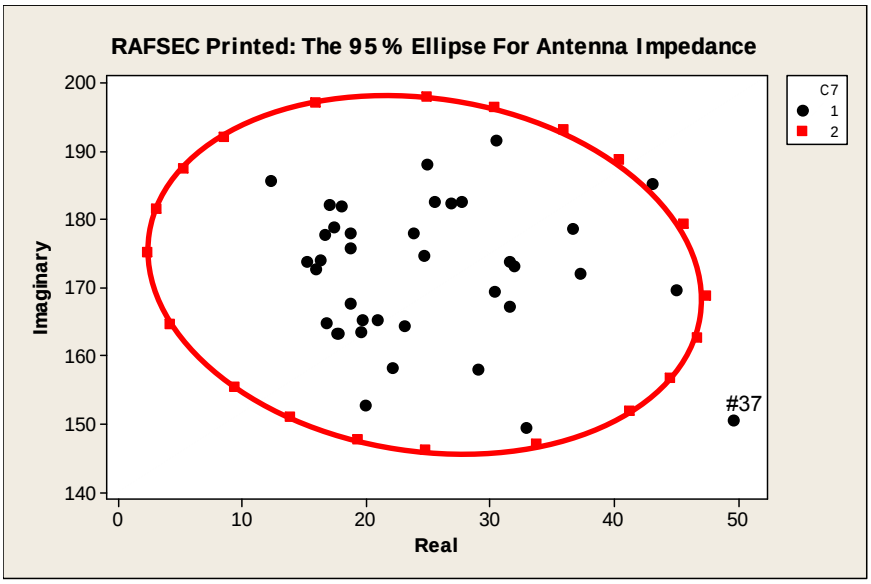

Figure 8.16: The Rafsect printed tag

APPENDIX D

IMPIDANCE TRANSFORMATION NETWORK

D.1 AD220 ORIGINAL

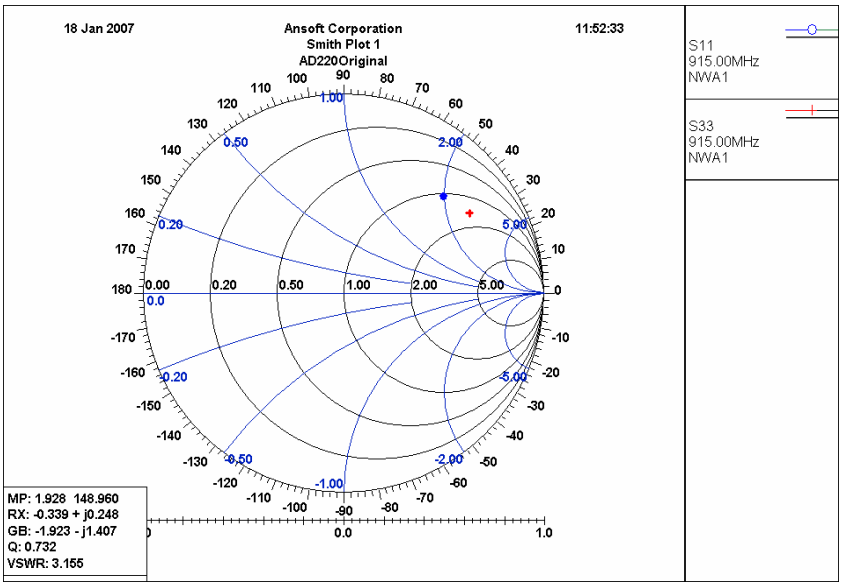

Figure 8.17: The original AD220 Smith Chart

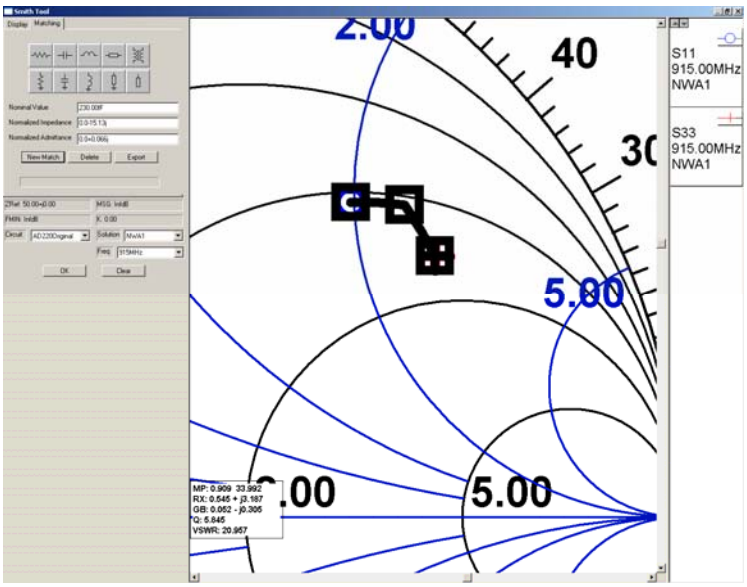

Figure 8.18: The original AD220 match

D.2 AD220 PRINTED

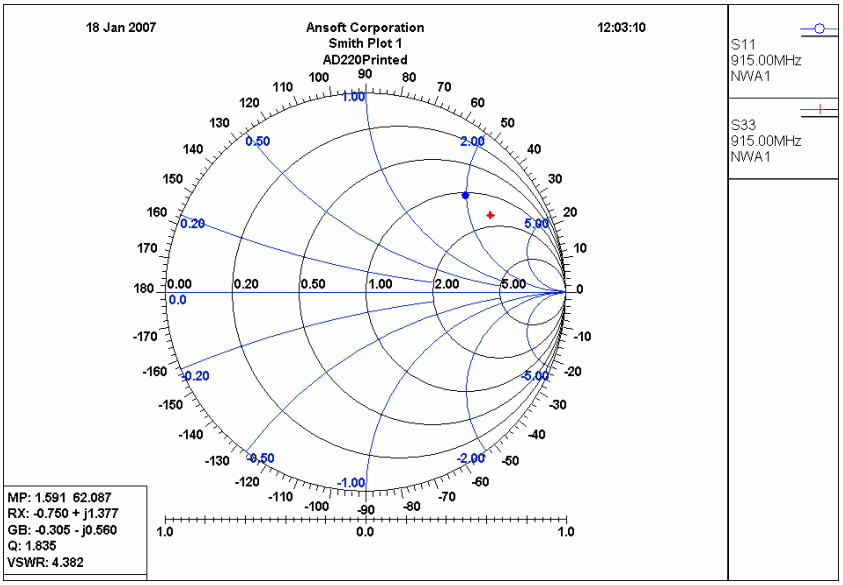

Figure 8.19: The printed AD220 Smith Chart

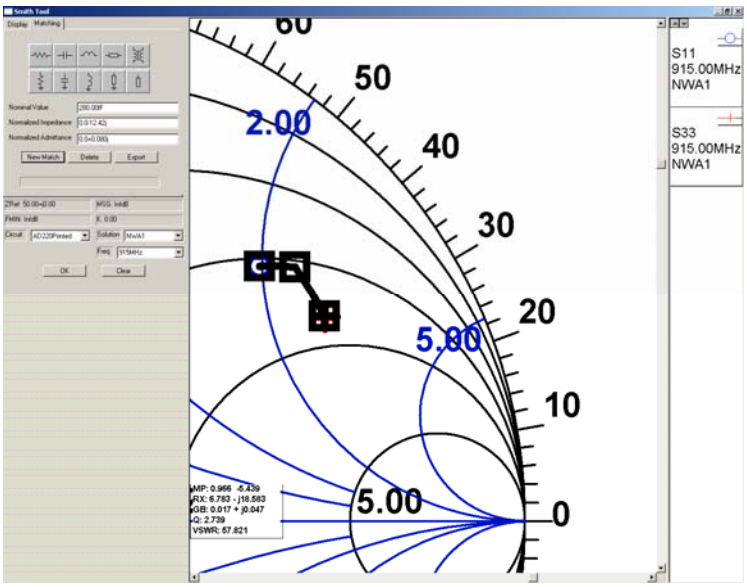

Figure 8.20: The printed AD220 match

D.3 ALIEN ORIGINAL

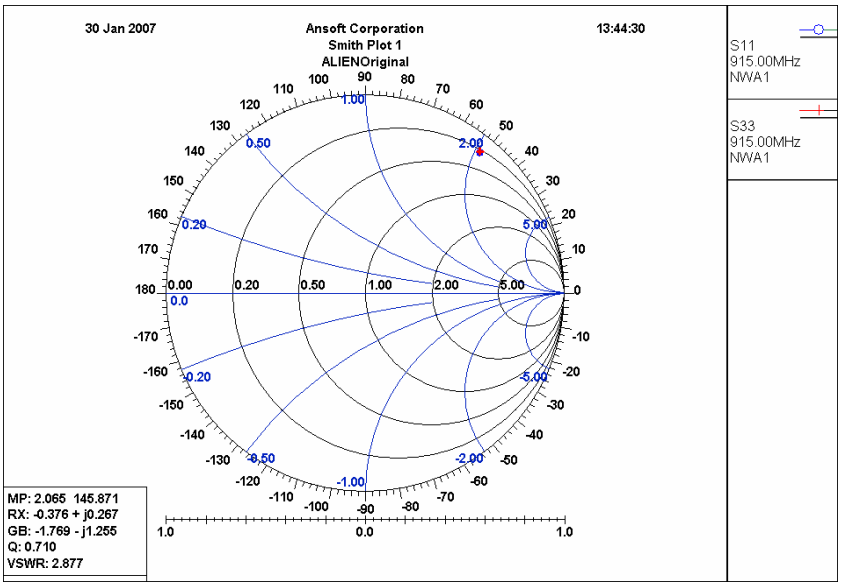

Figure 8.21: The original Alien Smith Chart

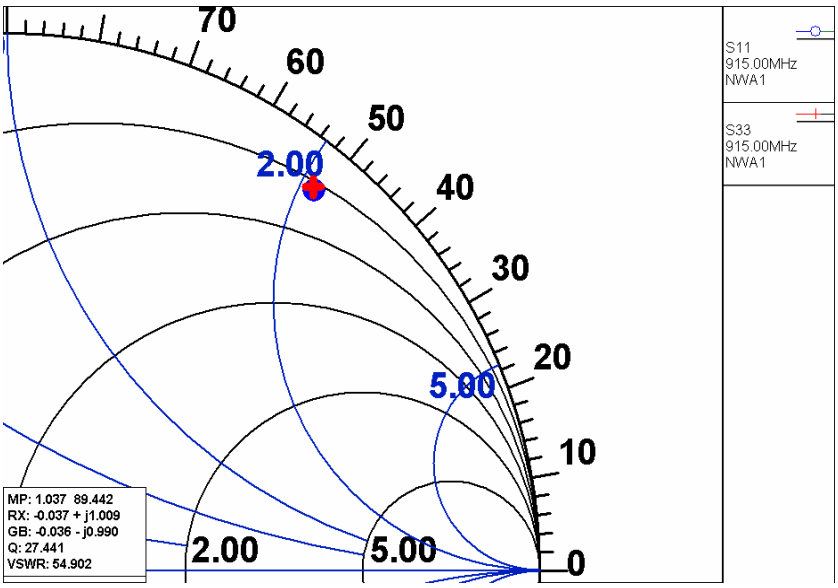

Figure 8.22: The original Alien match

D.4 ALIEN PRINTED

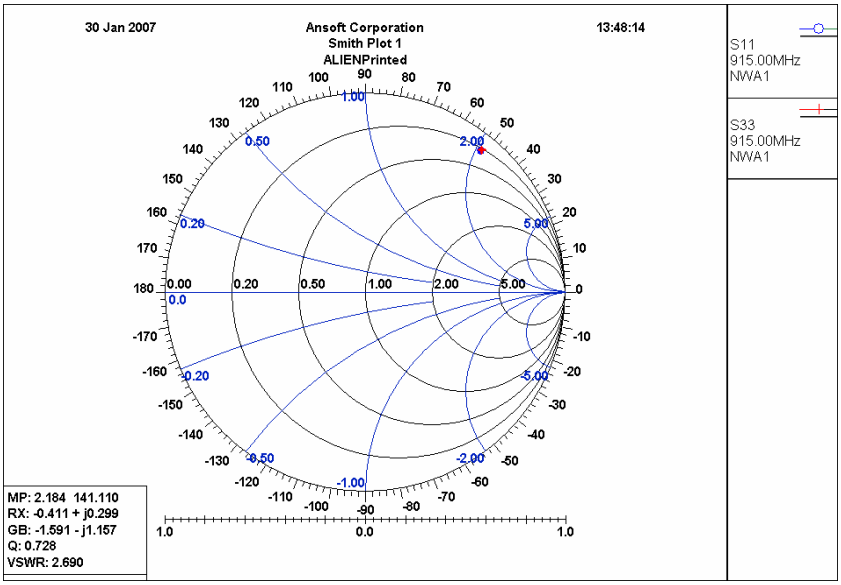

Figure 8.23: The printed Alien Smith Chart

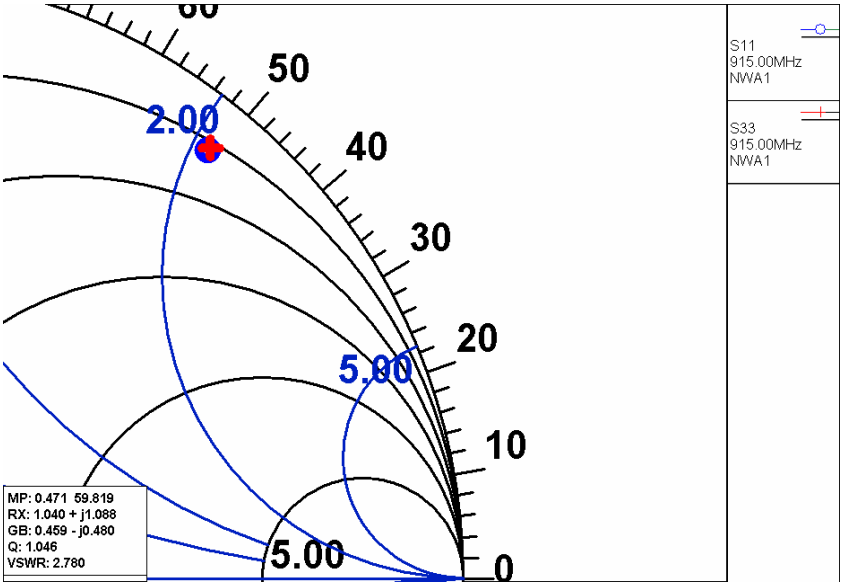

Figure 8.24: The printed Alien match

D.5 TI ORIGINAL

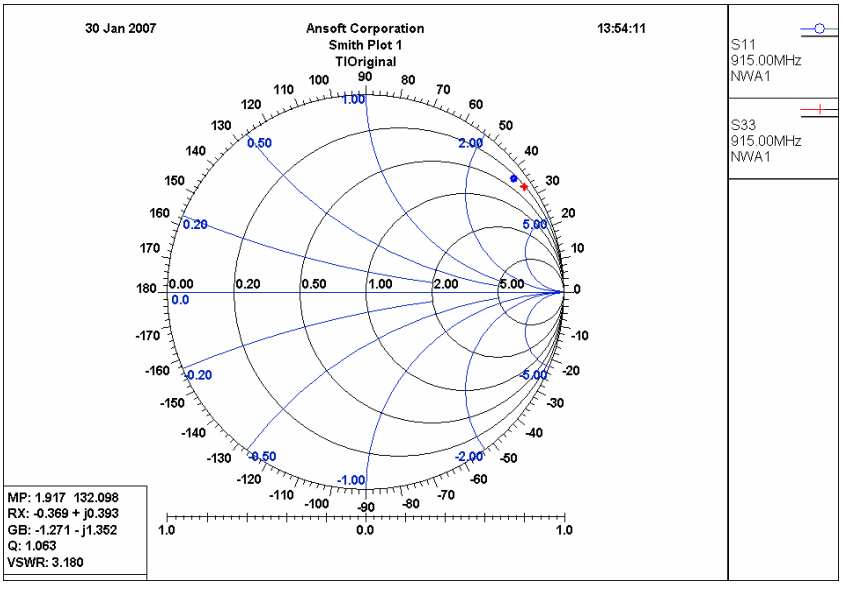

Figure 8.25: The original TI Smith Chart

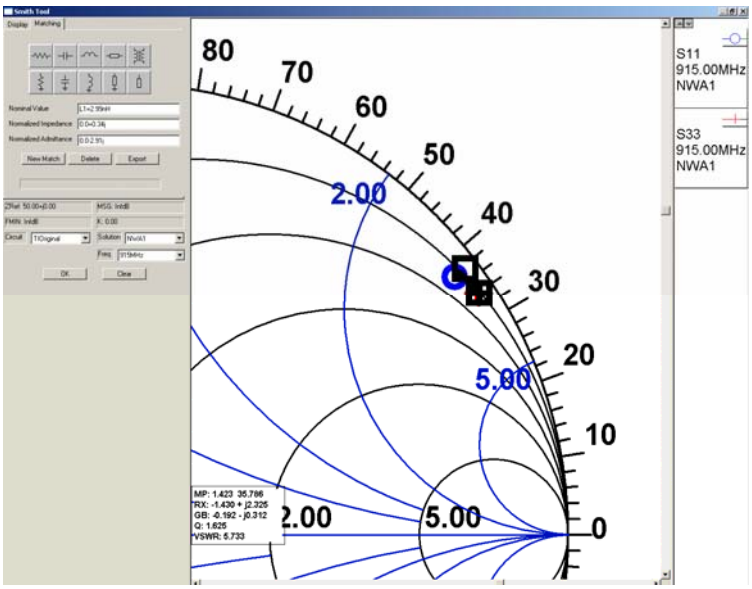

Figure 8.26: The original TI match

D.6 TI PRINTED

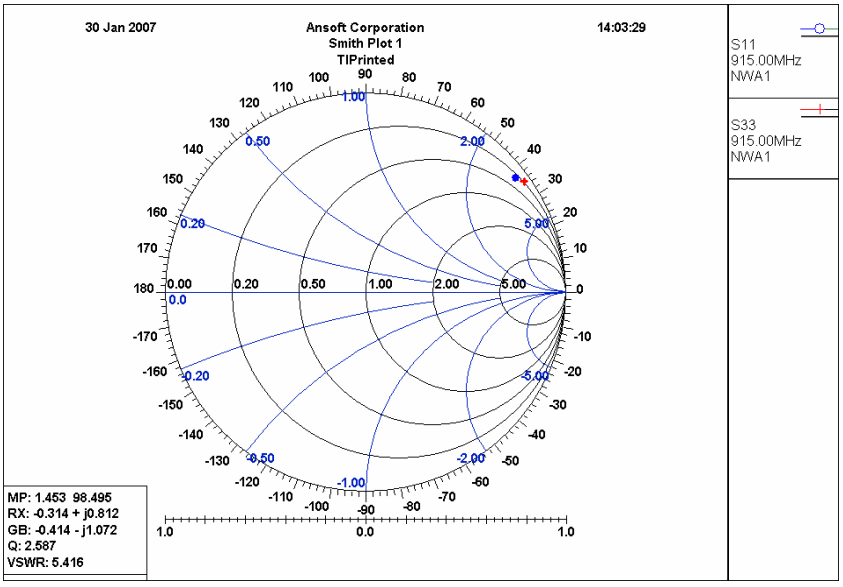

Figure 8.27: The printed TI Smith Chart

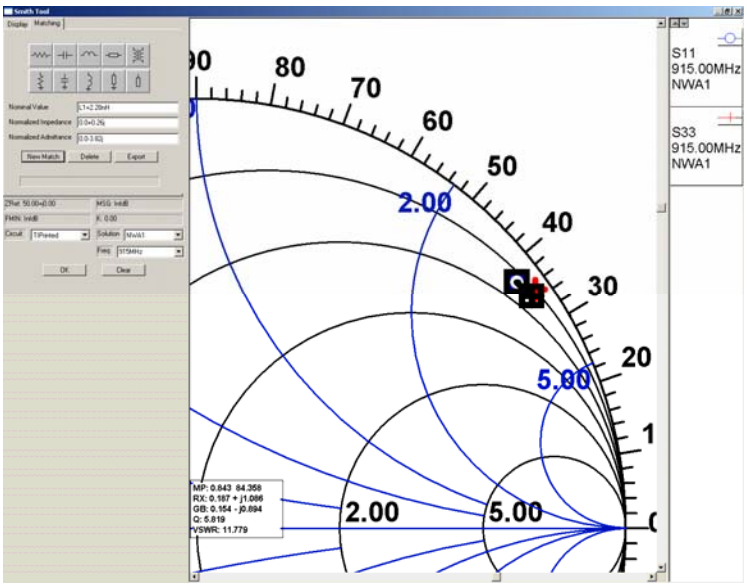

Figure 8.28: The printed TI match

D.7 RAFSEC ORIGINAL

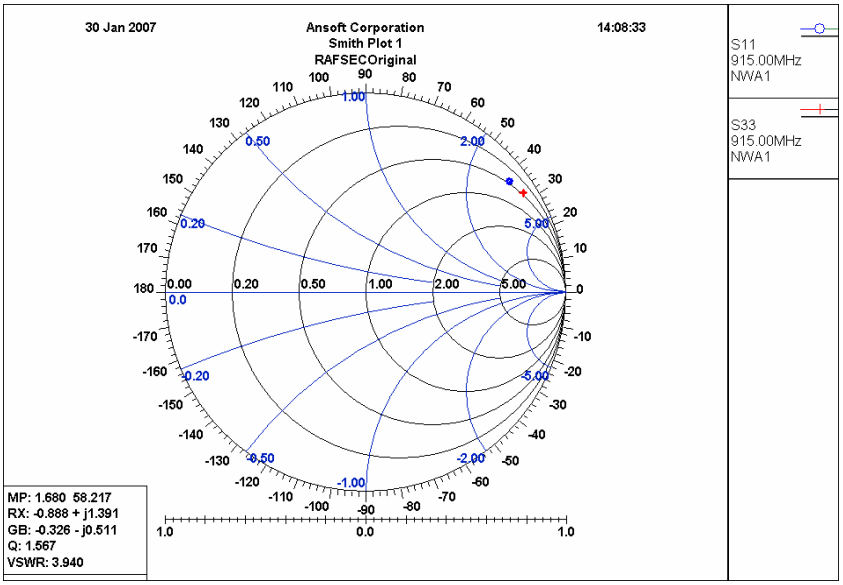

Figure 8.29: The original Rafsec Smith Chart

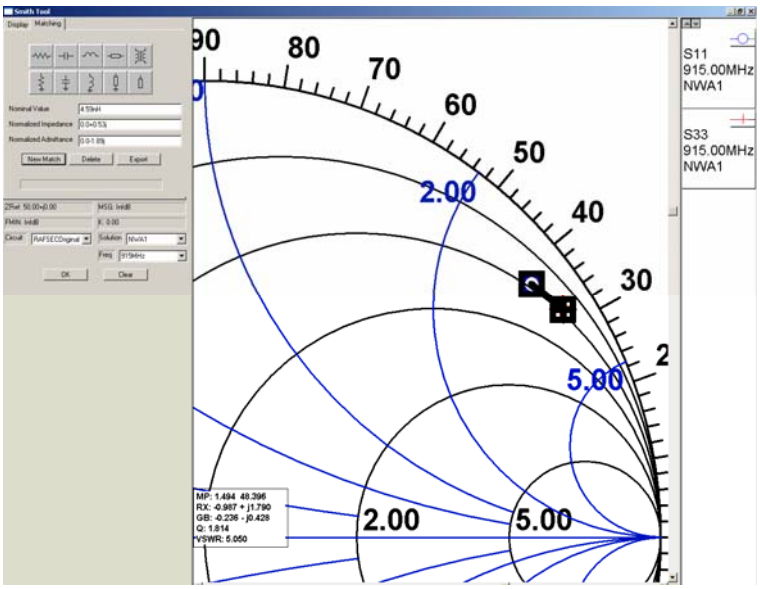

Figure 8.30: The original Rafsec match

D.8 RAFSEC PRINTED

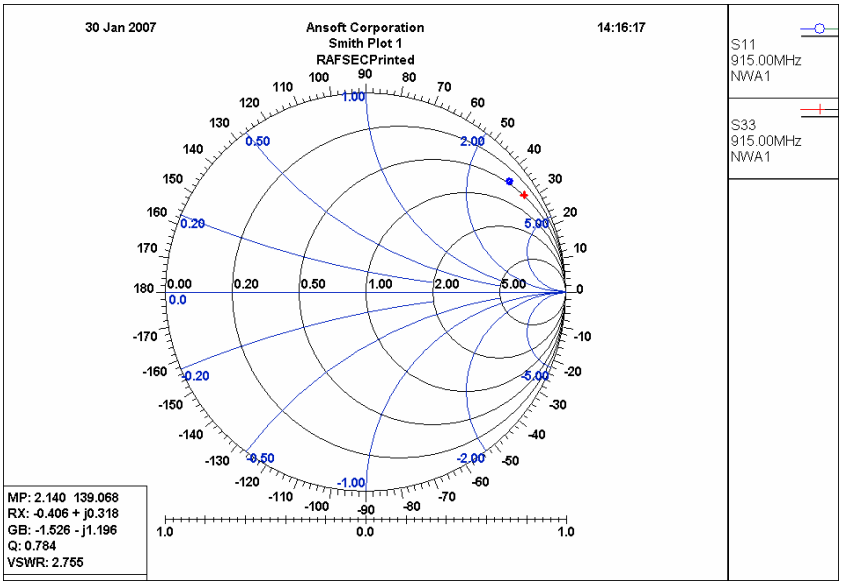

Figure 8.31: The printed Rafsec Smith Chart

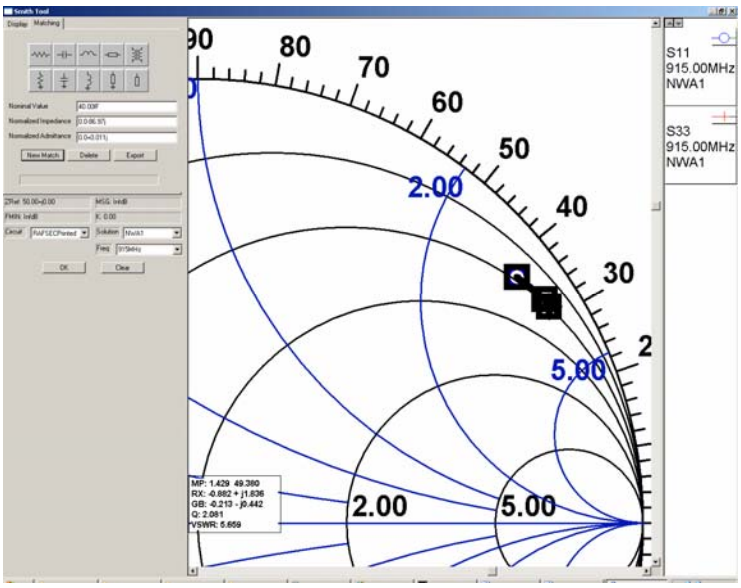

Figure 8.32: The printed Rafsec match

APPENDIX E

MEASURED DATA

E.1 AD220 TAG

AD220 - LOAD									
Tag #	Original		Printed		Tag #	Original		Printed	
	Real	Imaginary	Real	Imaginary		Real	Imaginary	Real	Imaginary
1	-0.155487	-5.92E-02	-0.157364	-5.30E-02	51	-0.153435	-5.79E-02	-0.155304	-5.47E-02
2	-0.156403	-5.70E-02	-0.156792	-5.58E-02	52	-0.154457	-5.90E-02	-0.153831	-0.057556
3	-0.156372	-0.05838	-0.153847	-5.88E-02	53	-0.154686	-0.059265	-0.156792	-5.52E-02
4	-0.154549	-0.057922	-0.154625	-0.058136	54	-0.156502	-5.55E-02	-0.152176	-0.058228
5	-0.155823	-0.057587	-0.153847	-0.058838	55	-0.155487	-5.75E-02	-0.152878	-5.78E-02
6	-0.15493	-5.88E-02	-0.15696	-5.49E-02	56	-0.157684	-5.50E-02	-0.151703	-0.057159
7	-0.154266	-5.90E-02	-0.154831	-5.70E-02	57	-0.155342	-5.81E-02	-0.153976	-5.79E-02
8	-0.154099	-5.98E-02	-0.155739	-0.055969	58	-0.155884	-0.056061	-0.153732	-5.65E-02
9	-0.158035	-5.56E-02	-0.155769	-0.056091	59	-0.155937	-5.62E-02	-0.154404	-5.79E-02
10	-0.157326	-5.66E-02	-0.15802	-5.24E-02	60	-0.158714	-5.18E-02	-0.155861	-5.62E-02
11	-0.157318	-5.74E-02	-0.156677	-5.53E-02	61	-0.15625	-5.70E-02	-0.155083	-5.69E-02
12	-0.156563	-0.058167	-0.155945	-0.055481	62	-0.15757	-5.50E-02	-0.157913	-5.35E-02
13	-0.15712	-5.82E-02	-0.154427	-0.056335	63	-0.156631	-5.62E-02	-0.156311	-5.59E-02
14	-0.156464	-0.058899	-0.154381	-5.66E-02	64	-0.15477	-5.81E-02	-0.153885	-5.54E-02
15	-0.156723	-5.59E-02	-0.154083	-5.79E-02	65	-0.15686	-5.52E-02	-0.153564	-5.69E-02
16	-0.154434	-0.059204	-0.154106	-5.58E-02	66	-0.155945	-5.75E-02	-0.153938	-5.79E-02
17	-0.156349	-5.87E-02	-0.157104	-5.44E-02	67	-0.154961	-5.92E-02	-0.155098	-0.056366
18	-0.155128	-5.79E-02	-0.15728	-5.33E-02	68	-0.154556	-5.93E-02	-0.15152	-0.056702
19	-0.156113	-5.70E-02	-0.156967	-5.52E-02	69	-0.15773	-5.44E-02	-0.158348	-5.18E-02
20	-0.156509	-0.056641	-0.157066	-5.46E-02	70	-0.156883	-5.45E-02	-0.157059	-0.054871
21	-0.157059	-5.72E-02	-0.156059	-5.55E-02	71	-0.153748	-5.57E-02	-0.153992	-5.72E-02
22	-0.156364	-5.85E-02	-0.153053	-0.058228	72	-0.157333	-5.20E-02	-0.154701	-5.71E-02
23	-0.156265	-5.74E-02	-0.15712	-0.053528	73	-0.15477	-5.72E-02	-0.156212	-5.54E-02
24	-0.157089	-0.056885	-0.154274	-5.66E-02	74	-0.155823	-0.056732	-0.153847	-5.79E-02
25	-0.156891	-0.056213	-0.156464	-0.054474	75	-0.157051	-5.46E-02	-0.157135	-5.51E-02
26	-0.157272	-0.056519	-0.153641	-5.74E-02	76	-0.156761	-5.57E-02	-0.156067	-5.55E-02
27	-0.157127	-0.057739	-0.155495	-5.38E-02	77	-0.155571	-5.84E-02	-0.154472	-0.056763
28	-0.155579	-0.058533	-0.153008	-0.056305	78	-0.155243	-5.71E-02	-0.152336	-5.82E-02
29	-0.155357	-5.86E-02	-0.156029	-5.42E-02	79	-0.156204	-5.44E-02	-0.156509	-5.46E-02
30	-0.154427	-5.73E-02	-0.154198	-5.57E-02	80	-0.156334	-5.64E-02	-0.153694	-0.057648
31	-0.154999	-6.02E-02	-0.153328	-5.69E-02	81	-0.156151	-0.056854	-0.151474	-0.057983
32	-0.154449	-5.85E-02	-0.154922	-0.056885	82	-0.157745	-0.054443	-0.154579	-5.65E-02
33	-0.155655	-5.81E-02	-0.158005	-5.30E-02	83	-0.157005	-5.35E-02	-0.155151	-5.60E-02
34	-0.155602	-0.057159	-0.153412	-5.75E-02	84	-0.155243	-5.74E-02	-0.152267	-5.78E-02
35	-0.154137	-5.83E-02	-0.156082	-5.54E-02	85	-0.155937	-5.74E-02	-0.156952	-5.43E-02
36	-0.155373	-5.83E-02	-0.156677	-5.52E-02	86	-0.154816	-5.86E-02	-0.151978	-5.85E-02
37	-0.158287	-5.44E-02	-0.157875	-5.20E-02	87	-0.15815	-5.30E-02	-0.155441	-5.61E-02
38	-0.157135	-5.67E-02	-0.157928	-5.33E-02	88	-0.155853	-5.70E-02	-0.153465	-5.73E-02
39	-0.156296	-5.69E-02	-0.155373	-5.72E-02	89	-0.15567	-0.056793	-0.155548	-0.056458
40	-0.157967	-0.055908	-0.155708	-5.70E-02	90	-0.157509	-5.45E-02	-0.15696	-5.21E-02
41	-0.15657	-5.74E-02	-0.157585	-5.34E-02	91	-0.156067	-0.057037	-0.153038	-5.79E-02
42	-0.153923	-0.057526	-0.154037	-5.82E-02	92	-0.155724	-5.59E-02	-0.155273	-5.70E-02
43	-0.155449	-5.86E-02	-0.154205	-0.057739	93	-0.156235	-5.67E-02	-0.156052	-0.055267
44	-0.155945	-5.74E-02	-0.151901	-5.83E-02	94	-0.15554	-5.64E-02	-0.1558	-5.51E-02
45	-0.156166	-5.85E-02	-0.154716	-5.63E-02	95	-0.155151	-0.058136	-0.15667	-5.49E-02
46	-0.156235	-5.78E-02	-0.154053	-5.55E-02	96	-0.15712	-5.45E-02	-0.156593	-0.055847
47	-0.154549	-5.77E-02	-0.157158	-5.47E-02	97	-0.155945	-5.73E-02	-0.154655	-0.057129
48	-0.155083	-0.058319	-0.153893	-5.79E-02	98	-0.157677	-0.054993	-0.157097	-5.45E-02
49	-0.158852	-0.051361	-0.1577	-5.36E-02	99	-0.155922	-0.057159	-0.156609	-5.38E-02
50	-0.154129	-5.94E-02	-0.153267	-5.81E-02	100	-0.155251	-0.056549	-0.153152	-5.81E-02

AD220 - OPEN		
Tag #	Real	Imaginary
1	-0.127007	-4.21E-02
2	-0.128128	-4.01E-02
3	-0.128281	-3.97E-02
4	-0.127586	-4.11E-02
5	-0.12841	-4.00E-02
6	-0.127884	-4.06E-02
7	-0.127159	-0.041351
8	-0.127121	-4.20E-02
9	-0.128471	-3.96E-02
10	-0.127419	-4.11E-02

AD220 - SHORT		
Tag #	Real	Imaginary
1	-0.14991	-3.28E-02
2	-0.149956	-0.032867
3	-0.151222	-3.29E-02
4	-0.14991	-3.27E-02
5	-0.150253	-3.28E-02
6	-0.148476	-3.26E-02
7	-0.149391	-0.032684
8	-0.149666	-3.28E-02
9	-0.148613	-0.032532
10	-0.14994	-3.29E-02

E.2 ALIEN TAG

ALIEN - LOAD									
Tag #	Original		Printed		Tag #	Original		Printed	
	Real	Imaginary	Real	Imaginary		Real	Imaginary	Real	Imaginary
1	-0.14547	-5.06E-02	-0.148384	-5.04E-02	51	-0.151016	-5.43E-02	-0.145248	-5.10E-02
2	-0.140129	-5.36E-02	-0.148941	-0.05191	52	-0.146339	-0.052734	-0.139687	-5.23E-02
3	-0.141075	-5.18E-02	-0.145493	-5.02E-02	53	-0.149101	-5.06E-02	-0.147278	-5.03E-02
4	-0.14814	-5.54E-02	-0.147781	-0.052216	54	-0.147011	-0.049408	-0.144325	-0.048553
5	-0.149666	-0.054413	-0.149529	-5.07E-02	55	-0.145416	-5.34E-02	-0.140884	-5.41E-02
6	-0.143372	-5.24E-02	-0.153824	-5.45E-02	56	-0.152718	-0.056335	-0.143013	-4.95E-02
7	-0.146507	-4.94E-02	-0.153206	-5.39E-02	57	-0.144798	-4.98E-02	-0.149071	-5.28E-02
8	-0.144882	-5.08E-02	-0.148788	-5.02E-02	58	-0.146614	-5.11E-02	-0.150642	-5.20E-02
9	-0.147697	-0.049652	-0.143883	-4.99E-02	59	-0.144302	-5.01E-02	-0.138153	-0.054016
10	-0.135063	-5.52E-02	-0.148987	-0.053314	60	-0.152893	-0.05545	-0.148438	-5.06E-02
11	-0.151825	-5.26E-02	-0.149551	-0.049774	61	-0.151703	-5.53E-02	-0.147675	-5.03E-02
12	-0.152115	-5.35E-02	-0.145111	-5.07E-02	62	-0.150337	-5.17E-02	-0.142593	-5.16E-02
13	-0.149239	-5.16E-02	-0.148361	-5.09E-02	63	-0.150589	-0.051727	-0.142464	-5.39E-02
14	-0.142487	-4.95E-02	-0.15155	-5.49E-02	64	-0.14241	-5.40E-02	-0.145561	-5.06E-02
15	-0.149986	-5.13E-02	-0.151901	-5.48E-02	65	-0.144341	-5.08E-02	-0.15271	-5.25E-02
16	-0.148628	-4.95E-02	-0.144089	-0.049683	66	-0.15197	-0.054901	-0.149162	-0.051025
17	-0.146889	-5.19E-02	-0.146965	-0.050293	67	-0.151855	-5.58E-02	-0.139908	-5.04E-02
18	-0.148445	-5.06E-02	-0.146652	-4.98E-02	68	-0.148544	-5.13E-02	-0.153877	-5.64E-02
19	-0.152924	-5.31E-02	-0.142586	-5.04E-02	69	-0.149773	-0.048615	-0.143066	-4.99E-02
20	-0.153107	-5.38E-02	-0.147858	-5.13E-02	70	-0.144325	-4.99E-02	-0.144341	-5.27E-02
21	-0.145126	-0.053864	-0.147141	-5.26E-02	71	-0.144524	-5.27E-02	-0.144737	-4.86E-02
22	-0.140335	-5.14E-02	-0.150101	-5.64E-02	72	-0.142929	-4.94E-02	-0.143242	-0.049835
23	-0.147728	-5.09E-02	-0.146667	-5.09E-02	73	-0.1521	-5.47E-02	-0.149651	-5.09E-02
24	-0.14846	-0.058136	-0.141006	-5.12E-02	74	-0.146339	-4.93E-02	-0.150551	-5.13E-02
25	-0.14064	-5.28E-02	-0.148605	-0.054565	75	-0.151886	-0.052765	-0.137238	-5.39E-02
26	-0.146683	-0.053528	-0.143837	-4.85E-02	76	-0.149193	-5.21E-02	-0.148987	-5.08E-02
27	-0.151695	-5.30E-02	-0.150818	-5.17E-02	77	-0.149185	-5.21E-02	-0.144135	-5.26E-02
28	-0.150154	-5.20E-02	-0.149246	-5.10E-02	78	-0.149178	-0.052124	-0.139999	-5.46E-02
29	-0.144989	-5.24E-02	-0.149376	-5.27E-02	79	-0.146805	-0.05127	-0.14537	-5.42E-02
30	-0.147179	-5.08E-02	-0.13504	-0.051727	80	-0.1464	-0.050873	-0.146667	-5.18E-02
31	-0.153679	-0.054382	-0.146584	-5.13E-02	81	-0.144325	-0.053162	-0.141289	-5.26E-02
32	-0.151726	-0.052551	-0.147186	-5.09E-02	82	-0.151672	-5.20E-02	-0.137711	-4.88E-02
33	-0.149185	-5.03E-02	-0.149353	-0.052368	83	-0.141281	-5.20E-02	-0.148468	-5.18E-02
34	-0.144791	-4.89E-02	-0.149597	-0.051422	84	-0.152512	-5.27E-02	-0.142014	-0.048157
35	-0.142418	-5.03E-02	-0.144524	-5.21E-02	85	-0.152855	-0.053192	-0.142342	-4.96E-02
36	-0.151176	-5.23E-02	-0.141685	-5.11E-02	86	-0.144936	-5.02E-02	-0.1455	-5.05E-02
37	-0.145332	-5.19E-02	-0.149254	-5.07E-02	87	-0.14547	-5.15E-02	-0.150826	-5.22E-02
38	-0.139488	-4.98E-02	-0.145622	-5.01E-02	88	-0.145203	-0.051056	-0.151138	-5.43E-02
39	-0.138901	-5.10E-02	-0.145576	-5.01E-02	89	-0.141472	-5.30E-02	-0.141121	-4.93E-02
40	-0.152191	-0.052948	-0.145599	-0.05011	90	-0.147148	-0.051422	-0.145775	-5.24E-02
41	-0.14505	-0.051453	-0.148705	-5.05E-02	91	-0.141899	-0.050629	-0.143738	-5.41E-02
42	-0.140251	-5.05E-02	-0.148979	-5.16E-02	92	-0.143272	-4.99E-02	-0.1492	-5.34E-02
43	-0.139214	-5.25E-02	-0.142525	-5.15E-02	93	-0.14698	-5.40E-02	-0.148064	-5.36E-02
44	-0.141548	-4.89E-02	-0.146751	-0.051971	94	-0.142242	-5.16E-02	-0.151192	-5.30E-02
45	-0.148109	-4.91E-02	-0.150169	-0.052368	95	-0.14959	-5.13E-02	-0.139717	-4.96E-02
46	-0.146645	-4.96E-02	-0.144577	-5.18E-02	96	-0.148727	-4.93E-02	-0.138489	-5.06E-02
47	-0.144707	-5.15E-02	-0.148079	-0.051422	97	-0.14875	-0.05365	-0.144753	-4.91E-02
48	-0.138512	-5.43E-02	-0.143997	-5.02E-02	98	-0.144653	-5.04E-02	-0.14711	-5.16E-02
49	-0.138931	-5.27E-02	-0.149147	-5.47E-02	99	-0.152397	-5.40E-02	-0.150894	-5.18E-02
50	-0.147797	-5.35E-02	-0.147766	-5.34E-02	100	-0.150116	-5.20E-02	-0.147789	-0.052765

ALIEN - OPEN		
Tag #	Real	Imaginary
1	-0.152245	-7.72E-02
2	-0.152481	-7.71E-02
3	-0.15213	-7.73E-02
4	-0.152084	-0.077332
5	-0.152046	-7.73E-02
6	-0.151985	-0.077393
7	-0.152481	-7.71E-02
8	-0.152313	-0.077179
9	-0.152283	-7.72E-02
10	-0.152008	-7.74E-02

ALIEN - SHORT		
Tag #	Real	Imaginary
1	-0.141846	-8.05E-02
2	-0.142647	-8.03E-02
3	-0.141922	-8.06E-02
4	-0.139557	-8.04E-02
5	-0.140556	-0.080688
6	-0.142632	-8.03E-02
7	-0.141769	-8.06E-02
8	-0.141136	-8.07E-02
9	-0.139999	-0.079773
10	-0.139771	-8.09E-02

E.3 TI TAG

TI - LOAD									
Tag #	Original		Printed		Tag #	Original		Printed	
	Real	Imaginary	Real	Imaginary		Real	Imaginary	Real	Imaginary
1	-0.136658	-7.10E-02	-0.133972	-0.06781	51	-0.135719	-0.069	-0.135391	-0.068756
2	-0.135132	-0.067474	-0.134674	-6.82E-02	52	-0.135414	-6.69E-02	-0.13517	-6.93E-02
3	-0.134979	-0.0672	-0.133194	-0.066956	53	-0.135109	-6.94E-02	-0.135841	-6.85E-02
4	-0.136559	-6.93E-02	-0.135765	-6.89E-02	54	-0.138008	-7.11E-02	-0.134666	-0.067413
5	-0.136177	-7.00E-02	-0.135048	-6.79E-02	55	-0.134903	-6.79E-02	-0.134628	-6.84E-02
6	-0.137375	-6.84E-02	-0.136909	-6.84E-02	56	-0.135223	-6.85E-02	-0.135139	-6.91E-02
7	-0.135757	-6.69E-02	-0.134636	-6.86E-02	57	-0.137039	-7.19E-02	-0.135483	-6.85E-02
8	-0.138214	-0.070221	-0.13401	-6.76E-02	58	-0.137512	-7.05E-02	-0.134949	-0.066376
9	-0.136772	-7.12E-02	-0.135162	-6.81E-02	59	-0.135811	-6.81E-02	-0.136375	-0.070038
10	-0.135139	-6.82E-02	-0.135109	-6.63E-02	60	-0.134918	-6.74E-02	-0.135948	-0.069305
11	-0.136261	-6.91E-02	-0.135803	-6.92E-02	61	-0.13636	-6.88E-02	-0.13475	-6.86E-02
12	-0.135185	-6.85E-02	-0.135551	-6.87E-02	62	-0.134735	-6.77E-02	-0.13591	-0.067566
13	-0.137108	-7.06E-02	-0.135275	-6.99E-02	63	-0.135208	-0.069489	-0.134926	-0.067566
14	-0.135612	-6.84E-02	-0.134407	-6.69E-02	64	-0.136269	-7.13E-02	-0.134956	-6.91E-02
15	-0.136772	-7.05E-02	-0.133797	-6.57E-02	65	-0.136024	-0.070801	-0.136009	-7.01E-02
16	-0.138008	-7.06E-02	-0.136131	-7.04E-02	66	-0.136436	-0.069489	-0.135368	-6.68E-02
17	-0.135774	-6.57E-02	-0.135948	-6.91E-02	67	-0.135651	-7.01E-02	-0.134766	-0.068604
18	-0.136284	-6.72E-02	-0.134598	-6.65E-02	68	-0.137238	-7.02E-02	-0.135452	-6.94E-02
19	-0.135651	-6.97E-02	-0.136002	-0.070313	69	-0.135834	-6.99E-02	-0.136078	-6.98E-02
20	-0.137451	-6.93E-02	-0.1353	-6.95E-02	70	-0.136032	-7.03E-02	-0.134712	-0.067108
21	-0.137344	-6.96E-02	-0.135452	-6.83E-02	71	-0.135406	-6.90E-02	-0.134186	-6.60E-02
22	-0.13472	-6.62E-02	-0.135078	-0.067047	72	-0.135612	-6.86E-02	-0.135269	-6.94E-02
23	-0.135422	-6.95E-02	-0.13694	-7.02E-02	73	-0.135536	-6.91E-02	-0.136459	-7.07E-02
24	-0.136505	-0.069214	-0.135803	-0.069672	74	-0.135765	-7.03E-02	-0.134781	-0.068604
25	-0.134323	-6.72E-02	-0.135757	-6.89E-02	75	-0.13414	-0.068542	-0.133774	-6.58E-02
26	-0.137192	-7.14E-02	-0.135712	-6.79E-02	76	-0.135797	-6.81E-02	-0.13488	-6.72E-02
27	-0.137688	-0.071564	-0.13549	-6.99E-02	77	-0.135353	-7.00E-02	-0.134865	-6.71E-02
28	-0.137077	-7.13E-02	-0.136581	-6.83E-02	78	-0.135155	-0.069702	-0.134201	-6.57E-02
29	-0.135315	-6.74E-02	-0.135155	-6.83E-02	79	-0.136612	-7.05E-02	-0.135117	-6.88E-02
30	-0.135582	-6.73E-02	-0.135139	-6.93E-02	80	-0.137085	-7.14E-02	-0.135048	-6.87E-02
31	-0.136482	-0.069427	-0.136414	-7.00E-02	81	-0.138268	-0.071564	-0.136597	-0.067535
32	-0.134354	-6.73E-02	-0.134369	-0.067291	82	-0.136887	-0.07016	-0.136742	-6.57E-02
33	-0.134605	-6.79E-02	-0.134232	-6.70E-02	83	-0.136841	-7.00E-02	-0.135612	-6.92E-02
34	-0.136848	-7.03E-02	-0.135689	-6.84E-02	84	-0.13768	-7.20E-02	-0.135376	-6.81E-02
35	-0.135353	-6.82E-02	-0.136337	-7.03E-02	85	-0.136208	-0.070709	-0.136093	-0.068817
36	-0.135635	-0.067993	-0.133781	-6.62E-02	86	-0.136803	-6.98E-02	-0.13459	-6.74E-02
37	-0.137192	-0.070862	-0.134804	-6.62E-02	87	-0.135384	-6.89E-02	-0.13575	-6.89E-02
38	-0.136047	-6.97E-02	-0.134254	-6.75E-02	88	-0.136604	-7.12E-02	-0.136528	-6.83E-02
39	-0.136452	-6.94E-02	-0.13604	-0.069824	89	-0.137894	-7.19E-02	-0.134895	-6.80E-02
40	-0.137367	-7.18E-02	-0.136268	-7.00E-02	90	-0.136009	-7.05E-02	-0.135628	-6.86E-02
41	-0.135765	-0.070282	-0.135155	-6.82E-02	91	-0.135567	-7.04E-02	-0.136673	-7.16E-02
42	-0.135193	-0.069641	-0.136116	-6.86E-02	92	-0.13707	-7.09E-02	-0.135437	-6.95E-02
43	-0.136269	-7.02E-02	-0.135643	-6.88E-02	93	-0.137024	-0.071533	-0.134148	-0.067139
44	-0.137764	-7.20E-02	-0.136627	-6.91E-02	94	-0.135521	-6.93E-02	-0.135765	-6.92E-02
45	-0.134666	-6.83E-02	-0.136391	-7.03E-02	95	-0.13607	-6.95E-02	-0.134995	-6.97E-02
46	-0.136505	-7.06E-02	-0.135857	-6.87E-02	96	-0.136963	-7.11E-02	-0.13575	-6.92E-02
47	-0.136314	-7.04E-02	-0.135612	-6.95E-02	97	-0.138603	-0.07019	-0.135139	-6.75E-02
48	-0.137054	-6.95E-02	-0.134827	-6.88E-02	98	-0.136978	-7.04E-02	-0.136047	-6.74E-02
49	-0.136459	-7.04E-02	-0.135818	-6.99E-02	99	-0.136017	-6.89E-02	-0.13668	-0.071574
50	-0.136688	-7.13E-02	-0.13626	-6.90E-02	100	-0.137764	-0.071075	-0.134911	-6.82E-02

TI - OPEN		
Tag #	Real	Imaginary
1	-0.158096	-7.11E-02
2	-0.15818	-7.10E-02
3	-0.158119	-7.10E-02
4	-0.158066	-7.11E-02
5	-0.158104	-7.10E-02
6	-0.158005	-7.12E-02
7	-0.158165	-0.070953
8	-0.157959	-7.12E-02
9	-0.158073	-7.11E-02
10	-0.158104	-7.10E-02

TI - SHORT		
Tag #	Real	Imaginary
1	-0.15065	-7.60E-02
2	-0.15033	-7.61E-02
3	-0.15052	-7.59E-02
4	-0.150558	-0.07608
5	-0.150597	-7.61E-02
6	-0.150665	-7.60E-02
7	-0.150375	-7.63E-02
8	-0.150368	-7.62E-02
9	-0.139999	-0.079773
10	-0.139771	-8.09E-02

E.4 RAFSEC TAG

RAFSEC - LOAD				
Tag #	Original		Printed	
	Real	Imaginary	Real	Imaginary
1	-0.15403	-5.81E-02	-0.15255	-5.79E-02
2	-0.15062	-5.73E-02	-0.154518	-0.057373
3	-0.151215	-5.73E-02	-0.149986	-5.69E-02
4	-0.153549	-5.49E-02	-0.151314	-0.056732
5	-0.153481	-5.62E-02	-0.151588	-5.54E-02
6	-0.152168	-5.77E-02	-0.153465	-5.56E-02
7	-0.149483	-5.63E-02	-0.154327	-5.78E-02
8	-0.156639	-5.62E-02	-0.155472	-5.73E-02
9	-0.15062	-5.49E-02	-0.152649	-5.74E-02
10	-0.153641	-0.055969	-0.153168	-0.055389
11	-0.152969	-5.51E-02	-0.150452	-5.41E-02
12	-0.153297	-0.057739	-0.153961	-5.47E-02
13	-0.155144	-5.75E-02	-0.15551	-0.05426
14	-0.154289	-0.057526	-0.152657	-0.057129
15	-0.154854	-5.58E-02	-0.153931	-5.37E-02
16	-0.154297	-5.75E-02	-0.156242	-0.055481
17	-0.154297	-5.53E-02	-0.155983	-5.62E-02
18	-0.15303	-5.74E-02	-0.152237	-5.78E-02
19	-0.149727	-5.70E-02	-0.155273	-5.61E-02
20	-0.152504	-5.81E-02	-0.155525	-5.74E-02
21	-0.150734	-5.61E-02	-0.154091	-5.79E-02
22	-0.153038	-5.60E-02	-0.155327	-5.62E-02
23	-0.152054	-5.67E-02	-0.154732	-5.66E-02
24	-0.153648	-5.66E-02	-0.155266	-0.055969
25	-0.150742	-5.69E-02	-0.152245	-0.05777
26	-0.152069	-5.83E-02	-0.15625	-5.78E-02
27	-0.153862	-5.56E-02	-0.154846	-5.73E-02
28	-0.154221	-5.72E-02	-0.155045	-5.75E-02
29	-0.153618	-5.67E-02	-0.154327	-0.058014
30	-0.154274	-5.75E-02	-0.152512	-0.056732
31	-0.155342	-0.057526	-0.152321	-5.74E-02
32	-0.154984	-5.69E-02	-0.1549	-5.76E-02
33	-0.153038	-5.52E-02	-0.15477	-5.49E-02
34	-0.155754	-5.61E-02	-0.154121	-5.55E-02
35	-0.151878	-5.56E-02	-0.154037	-5.54E-02
36	-0.154358	-5.75E-02	-0.154221	-5.65E-02
37	-0.153152	-0.057343	-0.152161	-0.052094
38	-0.154289	-0.056213	-0.15313	-5.75E-02

RAFSEC - OPEN		
Tag #	Real	Imaginary
1	-0.160675	-7.73E-02
2	-0.152481	-7.71E-02
3	-0.15213	-7.73E-02

RAFSEC - SHORT		
Tag #	Real	Imaginary
1	-0.163086	-0.047302
2	-0.163086	-0.047302
3	-0.161922	-0.047602

APPENDIX F

CALCULATED DATA

F.1 ALIEN TAG

ALIEN

	Original		Printed	
Tag #	Real	Imaginary	Real	Imaginary
1	10.9318	105.7935	9.175679	101.992517
2	16.88849	114.058	10.7391	100.213765
3	13.76398	112.2682	10.35984	105.924377
4	16.72475	98.29534	12.01484	101.583463
5	13.5491	96.95129	8.772062	100.382255
6	14.55171	108.3818	8.742733	91.8147779
7	8.874048	104.9212	8.89795	93.1603208
8	11.49814	106.543	8.654037	101.631133
9	8.65844	103.2816	10.5702	108.235203
10	17.05794	124.2166	12.62774	98.9883299
11	9.019713	96.05092	7.675568	100.999289
12	9.699858	94.81068	11.20361	106.266827
13	10.16185	100.0328	9.888466	101.665848
14	10.2349	110.2651	12.09492	93.8072723
15	9.166697	99.3612	11.47495	93.5580829
16	7.888271	102.2723	10.16777	108.01249
17	12.1013	103.096	9.868293	103.875615
18	9.347265	101.8087	9.434618	104.510153
19	8.422462	94.32196	11.44472	110.01707
20	8.95861	93.32686	10.72304	102.080337
21	16.31687	104.792	13.07276	102.236296
22	13.12113	113.4374	16.02837	93.9413912
23	10.2129	102.5331	10.8288	103.965283
24	21.29784	94.43106	12.77613	112.366198
25	15.39344	113.0439	14.85253	98.394488
26	14.78703	102.3457	8.673212	108.622256
27	9.656965	95.74809	8.897041	98.0765831
28	9.912492	98.55489	9.29261	100.537442
29	13.98098	105.7156	11.50332	98.945198
30	10.38313	103.3341	11.58559	121.618444
31	8.840358	92.06484	11.39757	103.88324
32	9.058349	96.21607	10.61627	103.22407
33	8.556299	101.0619	11.01339	99.301006
34	8.863799	107.308	9.604347	99.7526983
35	11.40981	110.2685	13.54721	106.621908
36	9.336231	97.06232	12.63575	111.309404
37	12.90092	105.4376	8.913497	100.746496
38	10.60098	114.4966	10.27651	105.755815
39	12.23897	115.5946	10.25327	105.830672
40	9.027319	95.28997	10.25449	105.796342
41	12.4057	106.0414	9.092142	101.529659
42	11.67248	113.4765	10.26106	100.424932
43	14.68247	115.451	13.17776	109.953201
44	9.476244	111.5924	12.32884	103.237866
45	7.779755	103.079	10.30801	98.2482296
46	9.132808	104.6314	13.18942	106.617619
47	12.65597	106.5338	10.71041	101.716515
48	17.71253	117.2792	10.92974	108.002877
49	14.86704	115.9686	14.47368	97.4505558
50	13.89458	100.6056	13.70778	100.761371

	Original		Printed	
Tag #	Real	Imaginary	Real	Imaginary
51	11.97105	95.18406	11.6568	105.9301
52	13.73723	103.4083	14.43642	114.6125
53	9.011123	100.9378	9.77098	103.4358
54	8.707579	104.2616	8.608839	107.9871
55	15.28767	104.5592	17.88777	112.6773
56	12.26334	90.48264	10.10947	109.5404
57	10.0762	107.015	11.84914	99.30871
58	11.19782	103.9099	9.410968	98.01488
59	10.71522	107.5954	17.00806	117.8264
60	10.99664	91.51889	9.458109	101.7639
61	12.42622	93.09681	9.547269	102.9209
62	9.392458	98.58633	13.37421	109.8245
63	9.15841	98.29877	17.4315	109.6652
64	17.46979	109.7637	10.9584	105.6454
65	11.71576	107.3284	7.988707	95.21655
66	11.54815	93.31428	9.438575	100.5917
67	12.78814	92.3211	11.50977	113.9755
68	10.19924	101.1997	10.64396	89.08014
69	6.253831	101.5005	10.70946	109.3931
70	10.45197	107.6161	14.61185	106.6895
71	14.54027	106.3846	8.547078	107.4516
72	10.01744	109.6681	10.56995	109.1587
73	11.17618	93.37492	8.902084	100.1009
74	8.928155	105.1414	8.733824	98.67342
75	9.138458	95.82029	16.30015	119.4105
76	10.80243	99.72527	9.269423	100.9779
77	10.80857	99.73532	14.522	107.0693
78	10.83482	99.73311	18.7282	114.4695
79	11.28664	103.5661	16.80797	104.1589
80	10.94546	104.3442	12.07577	103.4816
81	15.45998	106.5221	15.04303	111.9128
82	8.452024	96.84311	8.806021	116.6648
83	14.07793	111.9307	11.00285	100.8975
84	8.451506	95.17296	8.462908	111.0163
85	8.577801	94.31032	10.38919	110.4568
86	10.62007	106.6819	10.77999	105.7912
87	12.29493	105.3909	9.482553	97.61804
88	11.75349	105.9754	11.76424	95.08736
89	15.74528	111.5843	10.04242	112.1707
90	11.30238	102.9953	13.58731	104.4651
91	11.90043	111.0114	17.35949	107.224
92	10.68273	109.0997	12.5006	98.6445
93	15.388	101.4955	13.84045	100.1083
94	13.42132	110.3869	10.13566	96.3739
95	9.51582	99.82148	10.26005	114.1362
96	7.606906	102.2698	11.45246	116.0917
97	13.32544	99.03098	9.222595	107.2781
98	10.99575	107.0128	11.63792	102.9158
99	10.01263	93.86023	8.989697	97.86698
100	9.850952	98.66756	12.8071	101.1757

F.2 AVERY DENNISON (AD220) TAG

AD220

	Original		Printed	
Tag #	Real	Imaginary	Real	Imaginary
1	66.76	127.10	87.60	148.77
2	73.58	134.17	77.29	138.21
3	68.40	131.47	70.36	121.65
4	72.83	125.33	71.90	125.35
5	72.24	130.79	70.07	121.58
6	68.92	125.64	80.54	141.15
7	69.04	122.99	76.35	127.83
8	66.39	121.61	78.95	133.46
9	75.08	143.71	78.37	133.34
10	72.96	138.43	88.09	154.23
11	70.02	136.62	79.88	139.10
12	68.83	132.51	80.63	135.39
13	67.87	134.48	79.68	127.04
14	66.46	130.94	78.73	126.50
15	77.27	137.83	73.31	123.44
16	68.11	123.39	82.52	126.35
17	67.40	130.91	82.39	143.25
18	72.13	127.63	86.91	147.64
19	73.87	132.91	79.43	140.50
20	74.61	135.24	81.68	142.54
21	71.22	136.07	80.08	135.74
22	67.93	131.22	73.17	119.00
23	72.30	132.87	86.22	146.01
24	72.44	136.93	78.59	125.93
25	75.45	137.66	83.85	140.19
26	73.40	138.43	76.24	122.27
27	69.28	135.30	89.55	137.24
28	69.10	128.40	81.64	120.54
29	69.16	127.49	86.37	138.94
30	75.63	125.69	82.77	126.91
31	63.95	124.24	78.74	121.44
32	70.61	124.20	76.53	128.34
33	70.47	129.28	85.67	151.97
34	74.28	130.66	75.86	121.14
35	71.97	123.29	80.79	136.24
36	70.21	127.96	80.30	139.35
37	78.85	148.20	90.35	155.08
38	72.88	137.41	84.50	150.41
39	73.88	133.80	74.70	129.76
40	73.96	142.51	74.89	131.44
41	71.63	133.97	85.14	148.46
42	75.21	123.27	72.26	122.95
43	69.15	127.87	74.00	124.18
44	72.70	131.57	73.80	114.25
45	68.33	130.56	79.60	128.47
46	70.64	131.93	84.32	126.64
47	73.71	125.62	80.77	142.50
48	70.59	126.86	73.89	122.77
49	88.91	162.38	83.92	148.31
50	67.84	122.11	73.58	119.99

	Original		Printed	
Tag #	Real	Imaginary	Real	Imaginary
51	74.27	120.87	85.65	134.18
52	68.69	123.65	75.19	122.85
53	67.61	124.23	79.72	139.66
54	79.41	137.83	73.76	115.40
55	73.18	129.66	74.92	118.59
56	78.03	143.79	78.62	113.87
57	71.17	128.20	73.68	123.08
58	78.26	133.89	79.79	123.65
59	77.45	133.77	73.23	124.82
60	87.68	159.76	77.57	133.44
61	73.67	133.48	76.34	129.03
62	78.72	143.59	83.70	149.64
63	75.94	136.59	78.15	136.09
64	71.91	125.99	84.84	125.91
65	79.54	139.95	78.35	122.46
66	72.35	131.40	73.50	122.87
67	67.45	125.26	78.45	129.95
68	67.48	123.68	80.82	113.22
69	80.51	145.89	89.31	158.17
70	82.66	142.05	80.49	141.72
71	83.55	124.79	76.45	123.94
72	92.92	152.77	76.00	127.10
73	75.33	127.18	80.22	136.66
74	75.60	132.32	73.73	122.53
75	81.52	142.34	79.30	141.40
76	77.99	138.45	80.29	135.89
77	69.64	128.58	77.73	126.60
78	75.16	129.33	73.83	116.08
79	84.76	139.12	83.28	140.13
80	76.13	135.15	74.96	122.18
81	74.49	133.40	75.08	112.55
82	80.28	145.82	78.87	127.52
83	86.94	145.73	80.02	130.86
84	73.87	128.82	75.70	116.05
85	72.60	131.48	83.37	142.94
86	69.74	125.44	72.63	114.44
87	84.73	152.25	78.98	131.92
88	74.41	131.92	76.82	121.62
89	75.64	131.59	77.25	131.70
90	80.68	144.61	93.68	150.32
91	73.93	132.72	74.66	119.23
92	79.44	133.61	75.64	129.67
93	75.08	134.11	81.33	136.35
94	77.42	131.74	82.80	135.68
95	71.19	127.38	81.51	140.03
96	81.85	142.99	77.60	137.31
97	73.29	131.84	75.91	126.85
98	78.26	143.91	81.85	142.84
99	73.72	131.93	86.76	142.91
100	77.40	130.28	73.56	119.50

F.3 TI TAG

TI

	Original		Printed	
Tag #	Real	Imaginary	Real	Imaginary
1	10.54	169.37	6.36	153.14
2	10.63	153.56	8.03	155.13
3	10.35	152.54	5.00	150.07
4	13.82	161.83	10.83	158.94
5	11.07	163.95	9.58	154.51
6	18.46	159.02	15.96	158.29
7	13.17	152.00	7.43	156.34
8	19.81	169.35	6.69	152.54
9	10.58	170.34	9.71	155.44
10	9.97	155.89	10.92	149.50
11	12.80	160.91	10.56	160.00
12	9.69	157.18	10.34	157.90
13	13.47	168.81	7.42	161.71
14	11.32	157.34	8.45	150.77
15	12.37	167.36	7.41	147.02
16	17.80	170.99	9.58	165.10
17	13.62	147.99	11.18	160.02
18	14.86	153.57	9.24	149.91
19	9.48	162.15	9.27	164.50
20	17.65	163.44	8.33	160.16
21	16.69	164.62	10.52	156.28
22	10.16	149.21	10.41	151.78
23	9.02	161.04	13.22	166.16
24	13.67	161.56	9.78	161.74
25	8.29	152.08	10.86	158.79
26	11.71	172.53	11.88	155.05
27	13.54	174.73	8.19	162.07
28	11.53	171.72	14.76	157.40
29	11.27	153.58	9.51	155.94
30	12.31	153.24	8.09	159.28
31	13.24	162.40	11.47	164.20
32	8.32	152.34	8.01	151.99
33	8.51	154.46	7.81	151.13
34	13.11	166.75	11.26	156.85
35	10.62	156.39	10.66	165.04
36	11.88	155.81	7.07	148.58
37	13.27	170.05	10.01	149.12
38	11.12	162.55	7.46	152.59
39	13.23	162.07	10.39	162.74
40	11.31	174.74	10.93	163.85
41	8.84	164.36	9.59	155.71
42	8.05	160.98	12.59	158.12
43	10.84	165.28	10.53	158.41
44	12.25	177.27	13.95	160.76
45	8.28	155.74	10.74	165.39
46	11.00	167.21	11.47	158.25
47	10.72	165.92	9.42	160.71
48	15.56	163.64	7.82	157.11
49	11.27	166.30	9.36	162.72
50	9.91	170.58	12.52	160.10

	Original		Printed	
Tag #	Real	Imaginary	Real	Imaginary
51	10.95	159.56	9.73	157.82
52	12.01	151.70	8.10	159.51
53	8.19	159.98	11.64	157.56
54	16.67	173.18	8.82	152.62
55	9.45	154.82	7.69	155.61
56	9.82	157.23	8.36	158.69
57	9.41	174.27	10.38	157.06
58	15.54	169.40	10.39	149.59
59	12.44	156.23	11.28	164.21
60	10.02	153.03	10.94	160.62
61	13.68	159.69	7.81	156.44
62	9.14	153.92	12.84	154.16
63	8.36	160.49	9.50	153.33
64	8.25	169.41	7.80	158.31
65	8.63	166.87	9.65	163.89
66	12.95	162.57	11.49	151.22
67	8.78	163.48	7.85	156.49
68	14.98	167.29	8.96	160.20
69	9.79	163.23	10.63	162.60
70	9.87	164.86	9.21	151.71
71	9.80	159.15	8.30	148.25
72	11.12	157.91	8.37	159.82
73	10.14	159.65	10.23	166.91
74	8.89	164.27	7.90	156.50
75	6.34	155.86	7.26	147.50
76	12.35	156.36	9.63	152.27
77	8.01	162.38	9.69	151.77
78	7.81	161.12	8.50	147.23
79	11.69	167.02	8.70	157.68
80	11.34	172.08	8.58	157.33
81	16.44	176.63	15.43	154.55
82	13.57	166.23	16.49	147.70
83	13.67	165.51	9.86	159.73
84	11.92	176.90	10.46	155.57
85	9.55	166.96	12.20	158.99
86	14.00	164.33	8.56	152.62
87	9.95	158.56	10.74	159.00
88	9.89	169.88	14.47	157.64
89	13.53	176.86	9.03	154.55
90	9.20	165.83	10.74	157.65
91	7.94	164.24	8.66	171.10
92	12.55	170.03	8.69	160.63
93	10.64	172.52	7.49	151.36
94	9.75	160.39	10.38	160.05
95	11.46	162.04	6.87	160.48
96	11.68	170.41	10.36	159.94
97	22.01	170.00	10.26	153.27
98	13.52	167.33	13.48	153.58
99	12.25	159.49	8.70	171.10
100	15.38	172.60	8.81	155.36

F.4 RAFSEC TAG

RAFSEC

	Original		Printed	
Tag #	Real	Imaginary	Real	Imaginary
1	15.01	172.25	16.76	164.79
2	19.03	155.81	18.70	175.87
3	19.30	158.41	19.89	152.88
4	35.20	169.23	22.10	158.39
5	26.73	169.85	28.91	158.07
6	17.84	162.96	30.30	169.43
7	21.54	150.14	16.19	174.20
8	23.12	193.49	17.91	182.11
9	29.40	152.36	19.66	165.32
10	28.03	170.81	31.47	167.24
11	32.84	165.62	32.83	149.48
12	17.57	168.64	37.20	172.02
13	17.09	179.58	43.02	185.33
14	18.03	174.33	20.90	165.33
15	29.08	179.49	44.94	169.79
16	17.89	174.35	30.45	191.71
17	33.17	175.16	24.90	188.06
18	19.24	167.32	17.66	163.29
19	19.42	151.92	26.73	182.54
20	15.97	164.54	17.00	182.21
21	24.29	154.99	15.90	172.77
22	27.25	167.03	25.49	182.77
23	22.78	162.01	23.79	178.10
24	24.26	170.97	27.64	182.60
25	20.63	156.02	17.63	163.33
26	15.40	162.51	12.30	185.70
27	30.74	172.13	18.61	177.97
28	20.06	174.22	17.35	178.99
29	23.65	170.77	15.20	173.99
30	17.96	174.22	22.97	164.42
31	16.48	180.76	19.46	163.66
32	20.96	179.40	16.65	177.85
33	32.84	166.09	36.52	178.79
34	25.88	186.33	31.53	173.95
35	28.65	159.82	31.88	173.31
36	17.87	174.72	24.64	174.67
37	19.75	167.99	49.49	150.61
38	26.43	175.22	18.65	167.82

APPENDIX G

THE EXTRACTED TWO-PORT NETWORK FOR ALL TESTED TAGS

	AD220 - Original							
	S11		S12		S21		S22	
	Real	Imaginary	Real	Imaginary	Real	Imaginary	Real	Imaginary
1	-0.147138	-0.039021	0.095208	-0.047094	0.095208	-0.047094	0.608034	0.426699
2	-0.14727	-0.03868	0.092646	-0.046714	0.092646	-0.046714	0.628594	0.403239
3	-0.147263	-0.038892	0.093987	-0.047421	0.093987	-0.047421	0.621772	0.419989
4	-0.146983	-0.038831	0.094592	-0.045508	0.094592	-0.045508	0.601131	0.406979
5	-0.14718	-0.038774	0.09355	-0.046495	0.09355	-0.046495	0.618592	0.408103
6	-0.147051	-0.038967	0.095172	-0.046381	0.095172	-0.046381	0.60263	0.419817
7	-0.146953	-0.039002	0.095717	-0.045908	0.095717	-0.045908	0.593677	0.419801
8	-0.146942	-0.039123	0.096477	-0.046239	0.096477	-0.046239	0.589249	0.429167
9	-0.147536	-0.038492	0.090462	-0.047679	0.090462	-0.047679	0.65541	0.395927
10	-0.147413	-0.038635	0.091838	-0.047437	0.091838	-0.047437	0.641337	0.403782
11	-0.147403	-0.038755	0.092629	-0.047817	0.092629	-0.047817	0.637073	0.413116
12	-0.14729	-0.03886	0.093696	-0.047484	0.093696	-0.047484	0.62491	0.41829
13	-0.147371	-0.038859	0.093405	-0.047984	0.093405	-0.047984	0.631405	0.420546
14	-0.147277	-0.038966	0.094402	-0.047769	0.094402	-0.047769	0.620761	0.426409
15	-0.147331	-0.038513	0.091381	-0.046468	0.091381	-0.046468	0.638374	0.391627
16	-0.146982	-0.039031	0.095793	-0.046177	0.095793	-0.046177	0.595152	0.422944
17	-0.14726	-0.038935	0.094265	-0.047554	0.094265	-0.047554	0.620297	0.423385
18	-0.147074	-0.038824	0.094229	-0.046026	0.094229	-0.046026	0.608624	0.409013
19	-0.147226	-0.038689	0.092865	-0.04647	0.092865	-0.04647	0.624741	0.402643
20	-0.147289	-0.038632	0.092278	-0.046653	0.092278	-0.046653	0.63151	0.399923
21	-0.147367	-0.038726	0.09258	-0.047482	0.09258	-0.047482	0.634987	0.409737
22	-0.147262	-0.038912	0.094115	-0.047485	0.094115	-0.047485	0.62112	0.42157
23	-0.147247	-0.038741	0.093105	-0.046793	0.093105	-0.046793	0.624984	0.407444
24	-0.147374	-0.038674	0.092227	-0.047341	0.092227	-0.047341	0.637112	0.405813
25	-0.147352	-0.038571	0.091661	-0.046817	0.091661	-0.046817	0.638362	0.396859
26	-0.147406	-0.038622	0.091781	-0.047345	0.091781	-0.047345	0.64117	0.402524
27	-0.147373	-0.0388	0.093022	-0.047792	0.093022	-0.047792	0.633364	0.415873
28	-0.147146	-0.038917	0.094549	-0.046791	0.094549	-0.046791	0.611675	0.41864
29	-0.147114	-0.038929	0.094733	-0.046632	0.094733	-0.046632	0.608712	0.418636
30	-0.146959	-0.038729	0.094064	-0.045001	0.094064	-0.045001	0.602195	0.398
31	-0.147082	-0.039172	0.09632	-0.047243	0.09632	-0.047243	0.599061	0.437171
32	-0.146974	-0.038927	0.095193	-0.045783	0.095193	-0.045783	0.59761	0.414369
33	-0.147155	-0.038856	0.094142	-0.046636	0.094142	-0.046636	0.614215	0.414014
34	-0.147146	-0.038708	0.093268	-0.04605	0.093268	-0.04605	0.617808	0.401804
35	-0.146922	-0.03889	0.095154	-0.045346	0.095154	-0.045346	0.594483	0.4099
36	-0.147114	-0.038885	0.094465	-0.046483	0.094465	-0.046483	0.610014	0.415128
37	-0.147604	-0.038322	0.089097	-0.047449	0.089097	-0.047449	0.665885	0.384291
38	-0.147383	-0.038653	0.092064	-0.047316	0.092064	-0.047316	0.638398	0.404363
39	-0.147254	-0.038676	0.09268	-0.046599	0.09268	-0.046599	0.627418	0.402431
40	-0.147518	-0.038542	0.090851	-0.047762	0.090851	-0.047762	0.65254	0.399464
41	-0.147293	-0.038745	0.092969	-0.047094	0.092969	-0.047094	0.628522	0.40916
42	-0.146879	-0.038774	0.094614	-0.044687	0.094614	-0.044687	0.594442	0.399277
43	-0.147127	-0.038924	0.094654	-0.046696	0.094654	-0.046696	0.609948	0.418608
44	-0.147199	-0.038747	0.093319	-0.046514	0.093319	-0.046514	0.620883	0.406509
45	-0.147233	-0.038909	0.094198	-0.047295	0.094198	-0.047295	0.618875	0.420498
46	-0.147242	-0.03881	0.09355	-0.047005	0.09355	-0.047005	0.622529	0.412798
47	-0.146982	-0.038796	0.094389	-0.045375	0.094389	-0.045375	0.602013	0.404109
48	-0.14707	-0.038889	0.094637	-0.046226	0.094637	-0.046226	0.606383	0.414097
49	-0.147818	-0.037886	0.085334	-0.046992	0.085334	-0.046992	0.695805	0.3556
50	-0.146938	-0.039061	0.096114	-0.046014	0.096114	-0.046014	0.590803	0.424042
51	-0.146803	-0.038838	0.095251	-0.044467	0.095251	-0.044467	0.586501	0.402189
52	-0.146983	-0.039005	0.095636	-0.046096	0.095636	-0.046096	0.595977	0.420899
53	-0.147021	-0.039036	0.095697	-0.046428	0.095697	-0.046428	0.598111	0.424505
54	-0.147302	-0.038449	0.091091	-0.046041	0.091091	-0.046041	0.63796	0.38561
55	-0.147128	-0.038759	0.093643	-0.046125	0.093643	-0.046125	0.614882	0.40538
56	-0.147495	-0.038407	0.09008	-0.047086	0.09008	-0.047086	0.654601	0.387922
57	-0.147108	-0.038848	0.094261	-0.046317	0.094261	-0.046317	0.610611	0.411984
58	-0.147196	-0.038535	0.092031	-0.045721	0.092031	-0.045721	0.626902	0.389467
59	-0.147203	-0.038563	0.092171	-0.045867	0.092171	-0.045867	0.626665	0.391856
60	-0.147773	-0.037947	0.085935	-0.046969	0.085935	-0.046969	0.690451	0.359179
61	-0.147247	-0.038687	0.092777	-0.046594	0.092777	-0.046594	0.626486	0.40313
62	-0.147479	-0.03839	0.090034	-0.046923	0.090034	-0.046923	0.653864	0.386131
63	-0.147312	-0.038571	0.091814	-0.046568	0.091814	-0.046568	0.635135	0.395706
64	-0.147019	-0.038855	0.094606	-0.045806	0.094606	-0.045806	0.603347	0.409901
65	-0.147363	-0.038417	0.090654	-0.046295	0.090654	-0.046295	0.643795	0.384818
66	-0.147199	-0.038761	0.093405	-0.046564	0.093405	-0.046564	0.620464	0.407627
67	-0.147061	-0.039026	0.095498	-0.046637	0.095498	-0.046637	0.601658	0.42483
68	-0.147002	-0.03905	0.095838	-0.046362	0.095838	-0.046362	0.596254	0.425048
69	-0.147519	-0.038309	0.089359	-0.046848	0.089359	-0.046848	0.659403	0.380746
70	-0.147383	-0.0383	0.089845	-0.045956	0.089845	-0.045956	0.648822	0.376027
71	-0.146839	-0.038467	0.092973	-0.043343	0.092973	-0.043343	0.60025	0.373523
72	-0.147546	-0.037904	0.086669	-0.045305	0.086669	-0.045305	0.673438	0.349067
73	-0.147014	-0.038719	0.093813	-0.045298	0.093813	-0.045298	0.606894	0.398895
74	-0.147182	-0.038641	0.092732	-0.046028	0.092732	-0.046028	0.622634	0.397544
75	-0.147406	-0.038328	0.089931	-0.046214	0.089931	-0.046214	0.649832	0.378978
76	-0.14734	-0.038483	0.091158	-0.046408	0.091158	-0.046408	0.639983	0.389459
77	-0.147144	-0.038896	0.094423	-0.046704	0.094423	-0.046704	0.612147	0.416844
78	-0.14709	-0.038697	0.093405	-0.045668	0.093405	-0.045668	0.613603	0.399269
79	-0.147274	-0.038275	0.090132	-0.045181	0.090132	-0.045181	0.640789	0.370847
80	-0.147265	-0.038586	0.092082	-0.046329	0.092082	-0.046329	0.63091	0.395484
81	-0.147232	-0.038662	0.092675	-0.046414	0.092675	-0.046414	0.626072	0.400688
82	-0.14752	-0.038317	0.089403	-0.046885	0.089403	-0.046885	0.659268	0.381378
83	-0.147433	-0.038137	0.088624	-0.045596	0.088624	-0.045596	0.657559	0.364409
84	-0.14709	-0.038747	0.093709	-0.045852	0.093709	-0.045852	0.612152	0.403337
85	-0.147197	-0.038752	0.093352	-0.046524	0.093352	-0.046524	0.620649	0.406847
86	-0.147032	-0.03894	0.095077	-0.046174	0.095077	-0.046174	0.601848	0.417122
87	-0.14763	-0.038114	0.087649	-0.046754	0.087649	-0.046754	0.674024	0.368361
88	-0.147185	-0.038686	0.09299	-0.046212	0.09299	-0.046212	0.621627	0.401198
89	-0.147158	-0.03865	0.092876	-0.045913	0.092876	-0.045913	0.620425	0.39755
90	-0.147481	-0.038322	0.089592	-0.04666	0.089592	-0.04666	0.656009	0.380668
91	-0.147218	-0.03869	0.092896	-0.04643	0.092896	-0.04643	0.624144	0.402514
92	-0.147172	-0.038502	0.091917	-0.045449	0.091917	-0.045449	0.62597	0.386081
93	-0.147247	-0.038633	0.092444	-0.046395	0.092444	-0.046395	0.628062	0.398783
94	-0.147139	-0.03859	0.092581	-0.045576	0.092581	-0.045576	0.620668	0.392179
95	-0.147079	-0.03886	0.094432	-0.046183	0.094432	-0.046183	0.607957	0.412075
96	-0.14742	-0.03831	0.089765	-0.04623	0.089765	-0.04623	0.651464	0.377973
97	-0.147199	-0.038724	0.093174	-0.046432	0.093174	-0.046432	0.621592	0.40464
98	-0.147495	-0.038399	0.090027	-0.047054	0.090027	-0.047054	0.654854	0.387258
99	-0.147196	-0.038708	0.093092	-0.046356	0.093092	-0.046356	0.621779	0.403315
100	-0.147092	-0.03861	0.092874	-0.045363	0.092874	-0.045363	0.616305	0.39237

	AD220 - Printed							
	S11		S12		S21		S22	
	Real	Imaginary	Real	Imaginary	Real	Imaginary	Real	Imaginary
1	-0.147505	-0.038084	0.087984	-0.045828	0.087984	-0.045828	0.664922	0.362279
2	-0.147342	-0.038507	0.0913	-0.046515	0.0913	-0.046515	0.639463	0.391471
3	-0.146884	-0.038973	0.095771	-0.045399	0.095771	-0.045399	0.589012	0.415404
4	-0.146997	-0.038864	0.09474	-0.045706	0.09474	-0.045706	0.601287	0.410026
5	-0.146885	-0.038985	0.095838	-0.045447	0.095838	-0.045447	0.588771	0.416401
6	-0.147385	-0.038372	0.090289	-0.046255	0.090289	-0.046255	0.646854	0.381862
7	-0.147023	-0.038676	0.093522	-0.045197	0.093522	-0.045197	0.608894	0.395694
8	-0.147174	-0.038519	0.092018	-0.045524	0.092018	-0.045524	0.625574	0.38752
9	-0.147178	-0.038539	0.092125	-0.045622	0.092125	-0.045622	0.625296	0.38923
10	-0.147637	-0.038006	0.086917	-0.046335	0.086917	-0.046335	0.677785	0.359881
11	-0.147334	-0.038418	0.090778	-0.046117	0.090778	-0.046117	0.641391	0.384062
12	-0.147213	-0.038443	0.091402	-0.045468	0.091402	-0.045468	0.630945	0.382512
13	-0.146956	-0.038573	0.093157	-0.044421	0.093157	-0.044421	0.606511	0.385477
14	-0.146949	-0.038612	0.093411	-0.044519	0.093411	-0.044519	0.604789	0.388337
15	-0.14691	-0.03884	0.094898	-0.045099	0.094898	-0.045099	0.594957	0.405491
16	-0.146902	-0.038486	0.092847	-0.043777	0.092847	-0.043777	0.604715	0.376874
17	-0.147421	-0.038292	0.089646	-0.046159	0.089646	-0.046159	0.65205	0.376502
18	-0.147484	-0.038115	0.088273	-0.045827	0.088273	-0.045827	0.662289	0.364177
19	-0.147381	-0.038413	0.090561	-0.04639	0.090561	-0.04639	0.645313	0.385021
20	-0.14741	-0.038321	0.089874	-0.046208	0.089874	-0.046208	0.650318	0.378531
21	-0.14723	-0.038455	0.091411	-0.045624	0.091411	-0.045624	0.631984	0.384043
22	-0.146747	-0.038902	0.095817	-0.044358	0.095817	-0.044358	0.580083	0.4057
23	-0.147449	-0.038153	0.088658	-0.045765	0.088658	-0.045765	0.658376	0.366176
24	-0.146931	-0.038624	0.093545	-0.044457	0.093545	-0.044457	0.603027	0.388759
25	-0.147316	-0.038288	0.090047	-0.045491	0.090047	-0.045491	0.643729	0.37314
26	-0.14683	-0.038749	0.09464	-0.044317	0.09464	-0.044317	0.591278	0.395876
27	-0.147168	-0.038157	0.089847	-0.044053	0.089847	-0.044053	0.635738	0.358235
28	-0.146711	-0.038574	0.094062	-0.043005	0.094062	-0.043005	0.586812	0.378362
29	-0.147251	-0.03823	0.089955	-0.044856	0.089955	-0.044856	0.640202	0.366573
30	-0.146918	-0.038472	0.092703	-0.043816	0.092703	-0.043816	0.60642	0.376193
31	-0.146772	-0.038669	0.09438	-0.043694	0.09438	-0.043694	0.588967	0.387711
32	-0.147038	-0.038664	0.093394	-0.04524	0.093394	-0.04524	0.61044	0.395126
33	-0.147611	-0.038094	0.0876	-0.046546	0.0876	-0.046546	0.67309	0.366194
34	-0.146794	-0.038776	0.094924	-0.0442	0.094924	-0.0442	0.587568	0.396976
35	-0.147237	-0.038427	0.091216	-0.045554	0.091216	-0.045554	0.633304	0.381978
36	-0.147336	-0.038402	0.090673	-0.046067	0.090673	-0.046067	0.642002	0.382856
37	-0.147631	-0.037941	0.086525	-0.04601	0.086525	-0.04601	0.679184	0.354483
38	-0.147586	-0.038144	0.088024	-0.046596	0.088024	-0.046596	0.669636	0.369445
39	-0.14711	-0.038706	0.093389	-0.045827	0.093389	-0.045827	0.614967	0.400643
40	-0.147163	-0.038677	0.093018	-0.046043	0.093018	-0.046043	0.620084	0.399835
41	-0.147527	-0.038152	0.088322	-0.046254	0.088322	-0.046254	0.664687	0.368364
42	-0.146906	-0.038884	0.095174	-0.045229	0.095174	-0.045229	0.593347	0.408944
43	-0.146927	-0.038806	0.094634	-0.045082	0.094634	-0.045082	0.597361	0.403239
44	-0.146555	-0.038933	0.096636	-0.043365	0.096636	-0.043365	0.563768	0.402594
45	-0.147005	-0.03856	0.092896	-0.044658	0.092896	-0.044658	0.610811	0.385798
46	-0.146893	-0.038423	0.092514	-0.043491	0.092514	-0.043491	0.605877	0.3716
47	-0.147421	-0.038347	0.089996	-0.046381	0.089996	-0.046381	0.650407	0.380954
48	-0.146878	-0.038827	0.094935	-0.044868	0.094935	-0.044868	0.592766	0.403558
49	-0.147538	-0.038186	0.088492	-0.046469	0.088492	-0.046469	0.664607	0.371434
50	-0.146779	-0.038874	0.095546	-0.044451	0.095546	-0.044451	0.583491	0.404418
51	-0.147118	-0.038304	0.090934	-0.044348	0.090934	-0.044348	0.627389	0.36857
52	-0.146864	-0.03878	0.094701	-0.044622	0.094701	-0.044622	0.593088	0.399327
53	-0.147353	-0.038415	0.090688	-0.046223	0.090688	-0.046223	0.642966	0.384395
54	-0.146601	-0.038922	0.096421	-0.043588	0.096421	-0.043588	0.567781	0.403031
55	-0.14671	-0.038841	0.095588	-0.043939	0.095588	-0.043939	0.578933	0.399719
56	-0.146492	-0.038748	0.095812	-0.042389	0.095812	-0.042389	0.564145	0.38588
57	-0.146892	-0.038831	0.09491	-0.044963	0.09491	-0.044963	0.593771	0.40428
58	-0.146839	-0.038608	0.093788	-0.043861	0.093788	-0.043861	0.596099	0.384791
59	-0.14696	-0.038824	0.094631	-0.045344	0.094631	-0.045344	0.599457	0.405718
60	-0.147191	-0.038563	0.09222	-0.045794	0.09222	-0.045794	0.62567	0.391545
61	-0.147064	-0.038661	0.093285	-0.045386	0.093285	-0.045386	0.612586	0.395683
62	-0.147576	-0.038174	0.08826	-0.046662	0.08826	-0.046662	0.667973	0.371604
63	-0.147266	-0.03851	0.091608	-0.046054	0.091608	-0.046054	0.633272	0.389467
64	-0.146864	-0.038414	0.092569	-0.043282	0.092569	-0.043282	0.603808	0.369937
65	-0.146813	-0.038671	0.094251	-0.04394	0.094251	-0.04394	0.592146	0.38914
66	-0.146886	-0.03884	0.094982	-0.044962	0.094982	-0.044962	0.593063	0.404848
67	-0.147067	-0.03858	0.092782	-0.045106	0.092782	-0.045106	0.615251	0.389234
68	-0.146448	-0.038669	0.095528	-0.041874	0.095528	-0.041874	0.562943	0.378262
69	-0.147716	-0.037929	0.086067	-0.046513	0.086067	-0.046513	0.686424	0.356026
70	-0.147402	-0.038366	0.090183	-0.046336	0.090183	-0.046336	0.648384	0.381858
71	-0.146887	-0.038722	0.094278	-0.044553	0.094278	-0.044553	0.596645	0.39534
72	-0.147003	-0.038698	0.093724	-0.04515	0.093724	-0.04515	0.60661	0.396798
73	-0.147257	-0.038439	0.091211	-0.045722	0.091211	-0.045722	0.634562	0.383511
74	-0.146871	-0.038837	0.095012	-0.04486	0.095012	-0.04486	0.591955	0.404101
75	-0.147409	-0.038404	0.090399	-0.046531	0.090399	-0.046531	0.647791	0.385159
76	-0.147232	-0.038447	0.091352	-0.045604	0.091352	-0.045604	0.632391	0.383419
77	-0.146964	-0.038645	0.093547	-0.04473	0.093547	-0.04473	0.605084	0.391422
78	-0.146627	-0.038912	0.096274	-0.043701	0.096274	-0.043701	0.570175	0.402953
79	-0.147321	-0.038306	0.090133	-0.045592	0.090133	-0.045592	0.643641	0.374671
80	-0.146843	-0.038796	0.094873	-0.044554	0.094873	-0.044554	0.590876	0.400035
81	-0.146474	-0.0389	0.096717	-0.042799	0.096717	-0.042799	0.55823	0.397525
82	-0.146982	-0.038595	0.093191	-0.044652	0.093191	-0.044652	0.607922	0.387962
83	-0.147078	-0.038517	0.092368	-0.044936	0.092368	-0.044936	0.617933	0.384538
84	-0.146605	-0.038839	0.095938	-0.043333	0.095938	-0.043333	0.570528	0.396512
85	-0.1474	-0.038268	0.089584	-0.045932	0.089584	-0.045932	0.651044	0.373998
86	-0.146576	-0.038977	0.096818	-0.043628	0.096818	-0.043628	0.564136	0.406744
87	-0.147125	-0.038538	0.092316	-0.045295	0.092316	-0.045295	0.621078	0.387567
88	-0.1468	-0.038736	0.09467	-0.044093	0.09467	-0.044093	0.589227	0.393917
89	-0.14714	-0.038596	0.092614	-0.045605	0.092614	-0.045605	0.620569	0.392703
90	-0.147477	-0.037912	0.08702	-0.044902	0.08702	-0.044902	0.667707	0.347635
91	-0.146738	-0.038843	0.095507	-0.044104	0.095507	-0.044104	0.581065	0.400692
92	-0.147094	-0.038676	0.093263	-0.045623	0.093263	-0.045623	0.614599	0.397758
93	-0.147233	-0.03841	0.09112	-0.045465	0.09112	-0.045465	0.633559	0.380453
94	-0.147195	-0.038373	0.091047	-0.045089	0.091047	-0.045089	0.631567	0.376409
95	-0.14734	-0.038358	0.090383	-0.045921	0.090383	-0.045921	0.643635	0.379459
96	-0.147311	-0.03851	0.091439	-0.046331	0.091439	-0.046331	0.63685	0.390792
97	-0.146995	-0.038704	0.093788	-0.045129	0.093788	-0.045129	0.60584	0.397093
98	-0.147416	-0.038312	0.089792	-0.046213	0.089792	-0.046213	0.651088	0.378003
99	-0.147358	-0.038175	0.089169	-0.045289	0.089169	-0.045289	0.650475	0.365251
100	-0.146761	-0.038881	0.095649	-0.04437	0.095649	-0.04437	0.58182	0.404452

	Alien - Original							
	S11		S12		S21		S22	
	Real	Imaginary	Real	Imaginary	Real	Imaginary	Real	Imaginary
1	-0.142292	-0.075906	0.039914	0.08125	0.039914	0.08125	0.591197	0.709788
2	-0.14224	-0.076264	0.039475	0.077559	0.039475	0.077559	0.617415	0.652383
3	-0.142206	-0.076148	0.040147	0.078615	0.040147	0.078615	0.617492	0.673475
4	-0.142666	-0.075876	0.036364	0.082404	0.036364	0.082404	0.52725	0.69643
5	-0.142627	-0.075738	0.037037	0.083631	0.037037	0.083631	0.527096	0.721469
6	-0.142321	-0.076069	0.039219	0.079709	0.039219	0.079709	0.59436	0.681067
7	-0.142257	-0.075826	0.040457	0.081959	0.040457	0.081959	0.59326	0.724864
8	-0.142288	-0.075941	0.039868	0.080886	0.039868	0.080886	0.593627	0.704024
9	-0.142295	-0.075772	0.040199	0.082588	0.040199	0.082588	0.584216	0.732083
10	-0.142033	-0.076498	0.040822	0.074563	0.040822	0.074563	0.663474	0.623373
11	-0.142524	-0.075563	0.038371	0.085118	0.038371	0.085118	0.535611	0.755765
12	-0.142587	-0.075547	0.037794	0.085385	0.037794	0.085385	0.524423	0.755275
13	-0.142433	-0.075719	0.038947	0.083411	0.038947	0.083411	0.558478	0.734131
14	-0.14216	-0.076012	0.040967	0.079859	0.040967	0.079859	0.618444	0.698471
15	-0.142424	-0.075669	0.039143	0.083884	0.039143	0.083884	0.557577	0.742979
16	-0.1423	-0.07572	0.040264	0.083117	0.040264	0.083117	0.580844	0.740531
17	-0.142399	-0.075863	0.038964	0.081923	0.038964	0.081923	0.571282	0.711726
18	-0.142357	-0.075747	0.039637	0.082967	0.039637	0.082967	0.572645	0.733117
19	-0.142564	-0.075488	0.038125	0.085913	0.038125	0.085913	0.525399	0.766234
20	-0.142615	-0.075476	0.037649	0.086128	0.037649	0.086128	0.516178	0.765852
21	-0.142461	-0.076026	0.037961	0.080488	0.037961	0.080488	0.568791	0.681384
22	-0.142163	-0.076163	0.040539	0.078348	0.040539	0.078348	0.625446	0.673126
23	-0.142361	-0.075793	0.03949	0.082522	0.03949	0.082522	0.574125	0.725198
24	-0.142903	-0.075938	0.034034	0.082353	0.034034	0.082353	0.490752	0.674478
25	-0.142228	-0.076205	0.039765	0.078107	0.039765	0.078107	0.616578	0.662811
26	-0.142492	-0.07592	0.03792	0.081585	0.03792	0.081585	0.558431	0.697558
27	-0.142554	-0.075574	0.038061	0.08506	0.038061	0.08506	0.531244	0.752343
28	-0.142471	-0.075667	0.038683	0.083993	0.038683	0.083993	0.549617	0.740871
29	-0.142377	-0.075985	0.038887	0.080671	0.038887	0.080671	0.580984	0.692338
30	-0.142344	-0.075821	0.039602	0.082207	0.039602	0.082207	0.57845	0.721402
31	-0.142657	-0.075432	0.037327	0.086624	0.037327	0.086624	0.507122	0.771184
32	-0.14252	-0.075569	0.0384	0.085048	0.0384	0.085048	0.536631	0.754907
33	-0.142355	-0.075702	0.039756	0.08341	0.039756	0.08341	0.570776	0.740795
34	-0.142194	-0.075895	0.040917	0.081119	0.040917	0.081119	0.607049	0.716344
35	-0.142192	-0.07604	0.040574	0.079658	0.040574	0.079658	0.614509	0.692193
36	-0.142501	-0.075604	0.038518	0.08467	0.038518	0.08467	0.541518	0.749986
37	-0.142356	-0.075949	0.039184	0.080978	0.039184	0.080978	0.582708	0.699485
38	-0.142074	-0.076134	0.041516	0.07839	0.041516	0.07839	0.638892	0.68226
39	-0.142092	-0.076198	0.041147	0.077794	0.041147	0.077794	0.638897	0.670666
40	-0.14255	-0.075539	0.038167	0.085393	0.038167	0.085393	0.530202	0.758412
41	-0.142326	-0.075952	0.039467	0.080877	0.039467	0.080877	0.587789	0.70044
42	-0.142124	-0.076131	0.041011	0.078561	0.041011	0.078561	0.63027	0.680298
43	-0.142156	-0.076248	0.04036	0.077478	0.04036	0.077478	0.630655	0.659239
44	-0.142108	-0.076031	0.041443	0.079535	0.041443	0.079535	0.628048	0.697876
45	-0.142274	-0.075741	0.040475	0.082845	0.040475	0.082845	0.586217	0.738188
46	-0.142272	-0.075824	0.040307	0.08201	0.040307	0.08201	0.590618	0.724372
47	-0.14232	-0.075972	0.039481	0.080666	0.039481	0.080666	0.589819	0.697429
48	-0.142187	-0.076357	0.039723	0.076481	0.039723	0.076481	0.630781	0.639493
49	-0.142149	-0.076264	0.040381	0.077291	0.040381	0.077291	0.632616	0.656806
50	-0.142521	-0.075848	0.037815	0.082349	0.037815	0.082349	0.550165	0.70829
51	-0.142641	-0.075636	0.037101	0.084638	0.037101	0.084638	0.51962	0.737837
52	-0.142434	-0.075918	0.03849	0.08147	0.03849	0.08147	0.56805	0.700802
53	-0.142372	-0.075711	0.039564	0.083353	0.039564	0.083353	0.568341	0.738348
54	-0.142269	-0.075802	0.040384	0.082227	0.040384	0.082227	0.589947	0.728233
55	-0.142442	-0.075991	0.038235	0.080774	0.038235	0.080774	0.570338	0.688111
56	-0.142819	-0.075511	0.035647	0.086148	0.035647	0.086148	0.483884	0.750032
57	-0.142236	-0.075918	0.040441	0.080996	0.040441	0.080996	0.601124	0.710527
58	-0.142351	-0.07586	0.039442	0.081838	0.039442	0.081838	0.579178	0.714529
59	-0.142239	-0.07595	0.040331	0.080678	0.040331	0.080678	0.602209	0.704938
60	-0.142743	-0.075494	0.036395	0.086178	0.036395	0.086178	0.495741	0.756586
61	-0.142727	-0.075592	0.036367	0.08522	0.036367	0.08522	0.503136	0.740978
62	-0.142455	-0.075652	0.038876	0.084108	0.038876	0.084108	0.551644	0.744232
63	-0.142457	-0.075636	0.03889	0.084269	0.03889	0.084269	0.550549	0.746817
64	-0.142357	-0.076177	0.038571	0.078748	0.038571	0.078748	0.593561	0.661218
65	-0.142274	-0.075968	0.039944	0.080581	0.039944	0.080581	0.597372	0.700201
66	-0.142694	-0.075567	0.036728	0.085396	0.036728	0.085396	0.507446	0.746769
67	-0.142765	-0.075583	0.036021	0.085375	0.036021	0.085375	0.496306	0.740611
68	-0.1424	-0.075754	0.039201	0.082992	0.039201	0.082992	0.565829	0.729876
69	-0.142271	-0.075649	0.040705	0.083757	0.040705	0.083757	0.582279	0.753707
70	-0.142231	-0.075944	0.040425	0.08072	0.040425	0.08072	0.603221	0.706343
71	-0.142373	-0.076018	0.038841	0.080346	0.038841	0.080346	0.583158	0.6871
72	-0.142169	-0.07599	0.040939	0.080099	0.040939	0.080099	0.615991	0.701688
73	-0.142681	-0.075555	0.036873	0.085481	0.036873	0.085481	0.509075	0.749313
74	-0.142252	-0.075834	0.040481	0.081871	0.040481	0.081871	0.594361	0.723753
75	-0.142536	-0.075559	0.038267	0.085171	0.038267	0.085171	0.533567	0.755747
76	-0.142461	-0.075729	0.038651	0.083368	0.038651	0.083368	0.554302	0.731013
77	-0.142461	-0.07573	0.038651	0.083363	0.038651	0.083363	0.554347	0.730939
78	-0.142462	-0.07573	0.038641	0.083358	0.038641	0.083358	0.554244	0.730776
79	-0.142363	-0.075853	0.03934	0.081937	0.03934	0.081937	0.576808	0.715137
80	-0.142332	-0.075865	0.039618	0.081742	0.039618	0.081742	0.582624	0.714585
81	-0.142393	-0.076046	0.038577	0.080122	0.038577	0.080122	0.581243	0.681438
82	-0.142481	-0.075569	0.038784	0.084975	0.038784	0.084975	0.543173	0.756869
83	-0.142222	-0.076147	0.039992	0.07867	0.039992	0.07867	0.614788	0.672884
84	-0.142536	-0.075516	0.038346	0.08559	0.038346	0.08559	0.531431	0.762942
85	-0.142569	-0.075493	0.038065	0.085874	0.038065	0.085874	0.524754	0.765146
86	-0.14226	-0.075922	0.040192	0.081007	0.040192	0.081007	0.597365	0.708576
87	-0.14234	-0.075931	0.039375	0.081115	0.039375	0.081115	0.584365	0.703173
88	-0.14231	-0.075933	0.039672	0.081027	0.039672	0.081027	0.589521	0.704423
89	-0.142271	-0.076178	0.039415	0.078497	0.039415	0.078497	0.608041	0.665242
90	-0.142379	-0.075837	0.039213	0.082128	0.039213	0.082128	0.573282	0.716937
91	-0.142187	-0.076072	0.040539	0.07933	0.040539	0.07933	0.616839	0.687156
92	-0.142201	-0.075991	0.040614	0.080175	0.040614	0.080175	0.610637	0.700024
93	-0.142533	-0.075916	0.037538	0.081721	0.037538	0.081721	0.551428	0.696275
94	-0.142242	-0.076092	0.039939	0.079272	0.039939	0.079272	0.608692	0.681084
95	-0.14242	-0.075693	0.039126	0.083637	0.039126	0.083637	0.559353	0.739065
96	-0.142291	-0.075712	0.040367	0.083178	0.040367	0.083178	0.581882	0.742287
97	-0.142554	-0.075788	0.037629	0.083001	0.037629	0.083001	0.541693	0.71672
98	-0.142262	-0.075941	0.040127	0.080823	0.040127	0.080823	0.597978	0.70532
99	-0.142629	-0.075529	0.03742	0.085638	0.03742	0.085638	0.516466	0.756251
100	-0.142466	-0.075669	0.038732	0.083968	0.038732	0.083968	0.550582	0.740891

	Alien - Printed							
	S11		S12		S21		S22	
	Real	Imaginary	Real	Imaginary	Real	Imaginary	Real	Imaginary
1	-0.142346	-0.075748	0.039739	0.082939	0.039739	0.082939	0.574405	0.733536
2	-0.142445	-0.075741	0.038787	0.083213	0.038787	0.083213	0.557683	0.729781
3	-0.142273	-0.075894	0.040135	0.081317	0.040135	0.081317	0.5939	0.712658
4	-0.14244	-0.075818	0.038662	0.082452	0.038662	0.082452	0.562198	0.717142
5	-0.142381	-0.075688	0.039524	0.083607	0.039524	0.083607	0.565641	0.741882
6	-0.142663	-0.07542	0.037289	0.086745	0.037289	0.086745	0.50556	0.772809
7	-0.142619	-0.075468	0.037624	0.086206	0.037624	0.086206	0.515156	0.76689
8	-0.142341	-0.075722	0.039847	0.083183	0.039847	0.083183	0.574019	0.738106
9	-0.142219	-0.075964	0.040498	0.080488	0.040498	0.080488	0.606268	0.703575
10	-0.142536	-0.075765	0.037851	0.083184	0.037851	0.083184	0.54356	0.721441
11	-0.14233	-0.075674	0.040064	0.08363	0.040064	0.08363	0.573637	0.746632
12	-0.142287	-0.075926	0.039914	0.081036	0.039914	0.081036	0.593021	0.706631
13	-0.142377	-0.075759	0.039414	0.082898	0.039414	0.082898	0.569846	0.730223
14	-0.142693	-0.0756	0.03668	0.085073	0.03668	0.085073	0.509348	0.741232
15	-0.142683	-0.075571	0.036822	0.085333	0.036822	0.085333	0.509467	0.746537
16	-0.142214	-0.075948	0.040594	0.080637	0.040594	0.080637	0.606409	0.706571
17	-0.142314	-0.075822	0.039895	0.082126	0.039895	0.082126	0.583506	0.722645
18	-0.142284	-0.075829	0.040176	0.081992	0.040176	0.081992	0.588826	0.723011
19	-0.142199	-0.076034	0.04052	0.079735	0.04052	0.079735	0.613049	0.692837
20	-0.142389	-0.075795	0.039214	0.082569	0.039214	0.082569	0.569575	0.72358
21	-0.14245	-0.075867	0.038453	0.081999	0.038453	0.081999	0.562918	0.708477
22	-0.142795	-0.075742	0.03544	0.083932	0.03544	0.083932	0.499206	0.712501
23	-0.142339	-0.075851	0.03958	0.081896	0.03958	0.081896	0.580749	0.716561
24	-0.142178	-0.076128	0.040478	0.078745	0.040478	0.078745	0.621077	0.678253
25	-0.142615	-0.075819	0.036976	0.082835	0.036976	0.082835	0.533009	0.70852
26	-0.142156	-0.075928	0.04122	0.080693	0.04122	0.080693	0.615039	0.712682
27	-0.142455	-0.075621	0.03893	0.084413	0.03893	0.084413	0.549988	0.74937
28	-0.142392	-0.075708	0.039372	0.083432	0.039372	0.083432	0.564773	0.737977
29	-0.142506	-0.075728	0.038222	0.08347	0.038222	0.08347	0.546864	0.728996
30	-0.141955	-0.076336	0.042146	0.075982	0.042146	0.075982	0.668607	0.654431
31	-0.142357	-0.075865	0.039369	0.081806	0.039369	0.081806	0.578354	0.713416
32	-0.142353	-0.075824	0.039498	0.082196	0.039498	0.082196	0.576984	0.720359
33	-0.14248	-0.075723	0.038477	0.083465	0.038477	0.083465	0.550821	0.731051
34	-0.142425	-0.075694	0.039079	0.08364	0.039079	0.08364	0.558594	0.738729
35	-0.142341	-0.075997	0.039206	0.080464	0.039206	0.080464	0.587529	0.692059
36	-0.1422	-0.076097	0.040349	0.079109	0.040349	0.079109	0.616038	0.682335
37	-0.142375	-0.075703	0.039556	0.083444	0.039556	0.083444	0.567469	0.73966
38	-0.142275	-0.075887	0.040131	0.081391	0.040131	0.081391	0.593209	0.71372
39	-0.142272	-0.075889	0.040154	0.08137	0.040154	0.08137	0.593723	0.713597
40	-0.142273	-0.075888	0.040147	0.081381	0.040147	0.081381	0.59352	0.713708
41	-0.142357	-0.075731	0.039667	0.083122	0.039667	0.083122	0.571801	0.735714
42	-0.142424	-0.075733	0.039003	0.08325	0.039003	0.08325	0.560669	0.732144
43	-0.142246	-0.076075	0.039941	0.079454	0.039941	0.079454	0.607131	0.68374
44	-0.142401	-0.075873	0.038918	0.081827	0.038918	0.081827	0.571415	0.709883
45	-0.142493	-0.075671	0.038468	0.084004	0.038468	0.084004	0.546207	0.739277
46	-0.142332	-0.075988	0.039322	0.080535	0.039322	0.080535	0.588616	0.694115
47	-0.142399	-0.075784	0.039138	0.082698	0.039138	0.082698	0.567343	0.724889
48	-0.142235	-0.075967	0.040334	0.080501	0.040334	0.080501	0.603762	0.702364
49	-0.142635	-0.075782	0.036863	0.083233	0.036863	0.083233	0.527785	0.713742
50	-0.142511	-0.075846	0.037912	0.082341	0.037912	0.082341	0.551718	0.709011
51	-0.142309	-0.075929	0.039695	0.081061	0.039695	0.081061	0.589577	0.705131
52	-0.142169	-0.076222	0.040309	0.077774	0.040309	0.077774	0.627278	0.662957
53	-0.142323	-0.075807	0.039837	0.0823	0.039837	0.0823	0.581188	0.72477
54	-0.14217	-0.075908	0.04113	0.080927	0.04113	0.080927	0.611765	0.715326
55	-0.142296	-0.076256	0.038953	0.077807	0.038953	0.077807	0.607697	0.651129
56	-0.142174	-0.075989	0.040885	0.080126	0.040885	0.080126	0.614985	0.701631
57	-0.142504	-0.075749	0.038191	0.083263	0.038191	0.083263	0.548135	0.725541
58	-0.142473	-0.075635	0.038729	0.084309	0.038729	0.084309	0.547744	0.746122
59	-0.14216	-0.076354	0.040008	0.076422	0.040008	0.076422	0.635293	0.641297
60	-0.142361	-0.075749	0.039588	0.082958	0.039588	0.082958	0.571971	0.73258
61	-0.142331	-0.075786	0.039807	0.082529	0.039807	0.082529	0.578831	0.727943
62	-0.142255	-0.076076	0.039856	0.079461	0.039856	0.079461	0.605826	0.683085
63	-0.142359	-0.076174	0.038565	0.078785	0.038565	0.078785	0.593136	0.661691
64	-0.142297	-0.075902	0.039876	0.081295	0.039876	0.081295	0.590247	0.710131
65	-0.14252	-0.075502	0.038529	0.085699	0.038529	0.085699	0.533436	0.766091
66	-0.142395	-0.075714	0.039332	0.08338	0.039332	0.08338	0.564605	0.736847
67	-0.142109	-0.076141	0.041141	0.078424	0.041141	0.078424	0.6333	0.679483
68	-0.142825	-0.075407	0.035761	0.087138	0.035761	0.087138	0.477791	0.767075
69	-0.142194	-0.075999	0.040657	0.080072	0.040657	0.080072	0.612142	0.698886
70	-0.142367	-0.076027	0.038878	0.080235	0.038878	0.080235	0.584686	0.685782
71	-0.142181	-0.075891	0.041055	0.081127	0.041055	0.081127	0.608998	0.717607
72	-0.142196	-0.07599	0.040663	0.080175	0.040663	0.080175	0.611341	0.700438
73	-0.142394	-0.075683	0.039412	0.083679	0.039412	0.083679	0.563353	0.742057
74	-0.142432	-0.075634	0.039135	0.084236	0.039135	0.084236	0.554578	0.748314
75	-0.14211	-0.076376	0.040437	0.076054	0.040437	0.076054	0.644591	0.640114
76	-0.142379	-0.07572	0.03948	0.08328	0.03948	0.08328	0.567673	0.73656
77	-0.142354	-0.076035	0.03898	0.080131	0.03898	0.080131	0.58711	0.685159
78	-0.142273	-0.076316	0.038998	0.077145	0.038998	0.077145	0.614468	0.642119
79	-0.142491	-0.076024	0.037677	0.080581	0.037677	0.080581	0.5637	0.680227
80	-0.142387	-0.075873	0.039055	0.081799	0.039055	0.081799	0.573709	0.710635
81	-0.142246	-0.07617	0.039687	0.078514	0.039687	0.078514	0.611801	0.667934
82	-0.14198	-0.076154	0.042416	0.077926	0.042416	0.077926	0.655477	0.683496
83	-0.142432	-0.075769	0.038853	0.082915	0.038853	0.082915	0.561183	0.725795
84	-0.142093	-0.075991	0.041698	0.079896	0.041698	0.079896	0.628631	0.7052
85	-0.14216	-0.076021	0.040947	0.079768	0.040947	0.079768	0.618937	0.696996
86	-0.142288	-0.075902	0.039965	0.08128	0.039965	0.08128	0.591696	0.710677
87	-0.142488	-0.075626	0.038605	0.084433	0.038605	0.084433	0.544804	0.747032
88	-0.142639	-0.075626	0.037145	0.084727	0.037145	0.084727	0.519585	0.73961
89	-0.142111	-0.076059	0.041345	0.079249	0.041345	0.079249	0.629078	0.692953
90	-0.142401	-0.075942	0.038761	0.081157	0.038761	0.081157	0.574846	0.698469
91	-0.142421	-0.076114	0.038129	0.079535	0.038129	0.079535	0.579903	0.668717
92	-0.142543	-0.075751	0.03781	0.08333	0.03781	0.08333	0.541686	0.723356
93	-0.142534	-0.075833	0.037716	0.082524	0.037716	0.082524	0.547143	0.710125
94	-0.142548	-0.075609	0.038055	0.084711	0.038055	0.084711	0.533985	0.74684
95	-0.142073	-0.076117	0.041575	0.07856	0.041575	0.07856	0.638259	0.685159
96	-0.142062	-0.076194	0.041471	0.077748	0.041471	0.077748	0.64383	0.672851
97	-0.142205	-0.075903	0.040786	0.081064	0.040786	0.081064	0.605601	0.71443
98	-0.142391	-0.075845	0.039082	0.082084	0.039082	0.082084	0.571688	0.715145
99	-0.142465	-0.075618	0.038845	0.084466	0.038845	0.084466	0.548239	0.749495
100	-0.142474	-0.075831	0.038304	0.08241	0.038304	0.08241	0.557112	0.713447

	TI - Original							
	S11		S12		S21		S22	
	Real	Imaginary	Real	Imaginary	Real	Imaginary	Real	Imaginary
1	-0.149901	-0.073629	0.047887	0.04977	0.047887	0.04977	0.81287	0.523541
2	-0.149934	-0.073389	0.048154	0.053074	0.048154	0.053074	0.777554	0.563393
3	-0.149933	-0.073372	0.048225	0.053301	0.048225	0.053301	0.775725	0.566845
4	-0.149963	-0.073527	0.047379	0.051342	0.047379	0.051342	0.789109	0.534761
5	-0.149917	-0.073552	0.047906	0.050863	0.047906	0.050863	0.800494	0.53563
6	-0.15004	-0.073499	0.046452	0.051952	0.046452	0.051952	0.771586	0.530519
7	-0.149981	-0.073372	0.047597	0.053435	0.047597	0.053435	0.766869	0.561009
8	-0.150027	-0.073648	0.046115	0.049946	0.046115	0.049946	0.791926	0.504731
9	-0.1499	-0.073643	0.047854	0.049582	0.047854	0.049582	0.814666	0.521149
10	-0.149918	-0.073426	0.048273	0.052551	0.048273	0.052551	0.785022	0.558783
11	-0.149949	-0.073511	0.047603	0.051517	0.047603	0.051517	0.789532	0.539319
12	-0.14991	-0.073446	0.048316	0.052263	0.048316	0.052263	0.78885	0.556011
13	-0.149942	-0.073626	0.047329	0.049946	0.047329	0.049946	0.80486	0.518999
14	-0.149935	-0.073452	0.047962	0.052252	0.047962	0.052252	0.784958	0.551768
15	-0.14993	-0.073604	0.047574	0.050208	0.047574	0.050208	0.804463	0.524649
16	-0.149997	-0.073665	0.046468	0.049613	0.046468	0.049613	0.799597	0.505375
17	-0.150003	-0.073306	0.047488	0.054341	0.047488	0.054341	0.754823	0.570296
18	-0.150003	-0.073403	0.047221	0.053094	0.047221	0.053094	0.766603	0.552604
19	-0.149897	-0.073523	0.04827	0.051201	0.04827	0.051201	0.8006	0.543558
20	-0.150014	-0.073561	0.046591	0.051059	0.046591	0.051059	0.783789	0.522343
21	-0.149997	-0.073575	0.046769	0.050818	0.046769	0.050818	0.788601	0.521836
22	-0.149939	-0.073315	0.048291	0.054063	0.048291	0.054063	0.767566	0.5765
23	-0.149892	-0.073505	0.048391	0.051425	0.048391	0.051425	0.799372	0.547456
24	-0.149961	-0.073523	0.047413	0.051395	0.047413	0.051395	0.788857	0.53575
25	-0.149899	-0.073359	0.048699	0.053383	0.048699	0.053383	0.780265	0.573315
26	-0.149912	-0.073674	0.047578	0.049194	0.047578	0.049194	0.81619	0.51386
27	-0.149934	-0.073706	0.047181	0.04883	0.047181	0.04883	0.816202	0.505465
28	-0.149911	-0.073663	0.047634	0.049342	0.047634	0.049342	0.81509	0.516075
29	-0.149945	-0.073392	0.04801	0.053074	0.04801	0.053074	0.775898	0.561708
30	-0.149963	-0.073389	0.047783	0.053157	0.047783	0.053157	0.772299	0.559986
31	-0.149953	-0.073534	0.04749	0.051218	0.04749	0.051218	0.791787	0.534697
32	-0.149899	-0.073363	0.04869	0.053325	0.04869	0.053325	0.78083	0.572529
33	-0.149897	-0.073399	0.048617	0.052847	0.048617	0.052847	0.785525	0.566159
34	-0.149941	-0.073597	0.047441	0.050343	0.047441	0.050343	0.801458	0.52457
35	-0.149927	-0.073435	0.048126	0.052449	0.048126	0.052449	0.784523	0.555911
36	-0.149948	-0.073429	0.047858	0.05259	0.047858	0.05259	0.779822	0.554377
37	-0.149937	-0.073643	0.047341	0.049704	0.047341	0.049704	0.807796	0.516551
38	-0.149921	-0.073532	0.047922	0.05115	0.047922	0.05115	0.797345	0.538982
39	-0.149953	-0.073529	0.047498	0.051285	0.047498	0.051285	0.79108	0.535524
40	-0.149904	-0.073703	0.047593	0.048768	0.047593	0.048768	0.821215	0.509543
41	-0.149884	-0.073554	0.048353	0.05073	0.048353	0.05073	0.806928	0.539316
42	-0.149877	-0.073502	0.048597	0.051416	0.048597	0.051416	0.801783	0.549714
43	-0.149911	-0.073571	0.047925	0.050589	0.047925	0.050589	0.803865	0.532853
44	-0.149914	-0.073737	0.047347	0.048331	0.047347	0.048331	0.823648	0.502175
45	-0.14989	-0.073419	0.04865	0.052558	0.04865	0.052558	0.789235	0.563222
46	-0.14991	-0.073599	0.047849	0.050206	0.047849	0.050206	0.807454	0.527806
47	-0.149909	-0.07358	0.047934	0.050457	0.047934	0.050457	0.805485	0.531519
48	-0.149983	-0.073558	0.047005	0.050998	0.047005	0.050998	0.789045	0.526583
49	-0.149916	-0.073587	0.047816	0.050393	0.047816	0.050393	0.804942	0.529457
50	-0.14989	-0.073645	0.047976	0.049519	0.047976	0.049519	0.816706	0.521866
51	-0.149924	-0.073486	0.04801	0.051773	0.04801	0.051773	0.791081	0.54693
52	-0.149963	-0.073363	0.047856	0.053499	0.047856	0.053499	0.769118	0.564804
53	-0.149881	-0.073487	0.048589	0.051632	0.048589	0.051632	0.79921	0.552037
54	-0.149977	-0.073691	0.046639	0.049186	0.046639	0.049186	0.806394	0.502905
55	-0.149912	-0.073407	0.048403	0.052779	0.048403	0.052779	0.783845	0.562898
56	-0.149912	-0.073447	0.048287	0.052254	0.048287	0.052254	0.788619	0.555577
57	-0.14988	-0.073695	0.047961	0.048799	0.047961	0.048799	0.824747	0.51406
58	-0.14997	-0.073638	0.046922	0.049873	0.046922	0.049873	0.801357	0.513462
59	-0.149956	-0.073438	0.047731	0.052503	0.047731	0.052503	0.779409	0.551909
60	-0.149926	-0.073379	0.048296	0.053187	0.048296	0.053187	0.777868	0.566345
61	-0.149966	-0.073495	0.047435	0.051781	0.047435	0.051781	0.784561	0.540302
62	-0.149909	-0.073391	0.048484	0.052977	0.048484	0.052977	0.782475	0.566123
63	-0.149883	-0.073495	0.048541	0.051528	0.048541	0.051528	0.799867	0.550328
64	-0.149869	-0.073627	0.048333	0.049699	0.048333	0.049699	0.818479	0.527873
65	-0.149877	-0.073591	0.048331	0.050215	0.048331	0.050215	0.812582	0.533424
66	-0.149948	-0.073536	0.047547	0.051178	0.047547	0.051178	0.792869	0.534921
67	-0.149884	-0.073541	0.048385	0.050909	0.048385	0.050909	0.805236	0.54166
68	-0.149967	-0.073608	0.047065	0.050271	0.047065	0.050271	0.798232	0.5194
69	-0.1499	-0.073539	0.048184	0.050985	0.048184	0.050985	0.802144	0.540179
70	-0.149898	-0.073564	0.04813	0.050651	0.04813	0.050651	0.805393	0.535892
71	-0.149908	-0.073477	0.04826	0.05184	0.04826	0.05184	0.793119	0.550589
72	-0.149931	-0.073461	0.047997	0.052126	0.047997	0.052126	0.786829	0.550748
73	-0.149912	-0.073485	0.04818	0.051741	0.04818	0.051741	0.793365	0.548551
74	-0.149884	-0.073553	0.048345	0.050749	0.048345	0.050749	0.806631	0.539429
75	-0.149858	-0.073418	0.049081	0.052494	0.049081	0.052494	0.794897	0.56745
76	-0.149954	-0.073439	0.047749	0.052475	0.047749	0.052475	0.779941	0.551805
77	-0.149874	-0.073524	0.048572	0.051119	0.048572	0.051119	0.804896	0.546129
78	-0.149873	-0.073504	0.048645	0.05138	0.048645	0.05138	0.802716	0.549862
79	-0.149921	-0.073598	0.047717	0.050259	0.047717	0.050259	0.805416	0.526863
80	-0.149908	-0.073668	0.047661	0.04927	0.047661	0.04927	0.816204	0.515616
81	-0.149968	-0.073735	0.046608	0.048554	0.046608	0.048554	0.813436	0.495967
82	-0.149949	-0.07359	0.04736	0.050452	0.04736	0.050452	0.799307	0.524813
83	-0.149952	-0.07358	0.047353	0.050597	0.047353	0.050597	0.797547	0.526297
84	-0.14991	-0.073732	0.047419	0.048389	0.047419	0.048389	0.823731	0.503602
85	-0.14989	-0.073594	0.048144	0.050221	0.048144	0.050221	0.810488	0.531356
86	-0.149959	-0.073564	0.047306	0.050839	0.047306	0.050839	0.7942	0.528382
87	-0.149911	-0.073468	0.048239	0.05197	0.048239	0.05197	0.791363	0.551801
88	-0.149891	-0.073635	0.048	0.049654	0.048	0.049654	0.815417	0.523582
89	-0.14993	-0.073734	0.047127	0.048441	0.047127	0.048441	0.820109	0.500804
90	-0.149887	-0.073577	0.048243	0.050439	0.048243	0.050439	0.80906	0.534876
91	-0.14987	-0.073551	0.04854	0.050732	0.04854	0.050732	0.808966	0.541474
92	-0.149928	-0.073642	0.04748	0.049691	0.04748	0.049691	0.809437	0.518013
93	-0.149898	-0.073673	0.047782	0.049167	0.047782	0.049167	0.818658	0.515907
94	-0.149904	-0.073496	0.048249	0.051577	0.048249	0.051577	0.796036	0.547509
95	-0.149927	-0.073525	0.047861	0.051263	0.047861	0.051263	0.795355	0.539524
96	-0.149915	-0.073645	0.047639	0.049597	0.047639	0.049597	0.812213	0.518846
97	-0.150054	-0.073662	0.045701	0.049848	0.045701	0.049848	0.788735	0.498756
98	-0.149946	-0.073606	0.047349	0.050236	0.047349	0.050236	0.801708	0.522343
99	-0.149945	-0.073488	0.047737	0.051805	0.047737	0.051805	0.787653	0.544107
100	-0.149961	-0.073681	0.046889	0.049267	0.046889	0.049267	0.808075	0.506666

	TI - Printed							
	S11		S12		S21		S22	
	Real	Imaginary	Real	Imaginary	Real	Imaginary	Real	Imaginary
1	-0.149904	-0.073384	0.048994	0.052898	0.048994	0.052898	0.788367	0.5751
2	-0.149928	-0.07342	0.048582	0.052477	0.048582	0.052477	0.788465	0.565468
3	-0.149887	-0.073328	0.049361	0.053591	0.049361	0.053591	0.7847	0.587436
4	-0.149964	-0.073487	0.047914	0.051695	0.047914	0.051695	0.789955	0.548795
5	-0.149955	-0.073413	0.048246	0.052638	0.048246	0.052638	0.782721	0.563422
6	-0.150044	-0.07349	0.046844	0.051883	0.046844	0.051883	0.775707	0.538274
7	-0.149916	-0.073438	0.048696	0.052199	0.048696	0.052199	0.792986	0.563592
8	-0.149911	-0.073374	0.048928	0.053042	0.048928	0.053042	0.785941	0.576008
9	-0.149954	-0.073429	0.048207	0.052434	0.048207	0.052434	0.784653	0.560626
10	-0.149991	-0.073334	0.047984	0.053781	0.047984	0.053781	0.766254	0.573652
11	-0.149958	-0.073502	0.047953	0.051466	0.047953	0.051466	0.793062	0.546678
12	-0.149959	-0.073469	0.048033	0.051908	0.048033	0.051908	0.788819	0.552595
13	-0.149907	-0.073523	0.048579	0.051039	0.048579	0.051039	0.805006	0.549145
14	-0.149945	-0.073348	0.048544	0.053473	0.048544	0.053473	0.776449	0.576598
15	-0.149937	-0.07328	0.048822	0.054347	0.048822	0.054347	0.769558	0.590186
16	-0.149934	-0.073577	0.048052	0.050392	0.048052	0.050392	0.806609	0.535913
17	-0.149967	-0.073504	0.047822	0.051471	0.047822	0.051471	0.791536	0.545214
18	-0.149961	-0.073336	0.04837	0.053678	0.04837	0.053678	0.772018	0.576974
19	-0.14993	-0.073567	0.048129	0.050506	0.048129	0.050506	0.806145	0.538053
20	-0.149923	-0.073501	0.048422	0.051388	0.048422	0.051388	0.79923	0.551241
21	-0.149966	-0.073444	0.048018	0.05226	0.048018	0.05226	0.784517	0.556417
22	-0.149976	-0.073371	0.048089	0.053258	0.048089	0.053258	0.773651	0.568758
23	-0.149984	-0.073598	0.047301	0.050257	0.047301	0.050257	0.799979	0.525715
24	-0.149942	-0.073527	0.048085	0.051087	0.048085	0.051087	0.798937	0.543977
25	-0.149965	-0.073484	0.047911	0.051727	0.047911	0.051727	0.789543	0.549121
26	-0.14999	-0.073428	0.047735	0.052543	0.047735	0.052543	0.777976	0.556335
27	-0.149918	-0.073529	0.048409	0.050984	0.048409	0.050984	0.80374	0.546562
28	-0.150029	-0.073473	0.0471	0.052063	0.0471	0.052063	0.776433	0.543353
29	-0.14995	-0.073436	0.048244	0.052321	0.048244	0.052321	0.786389	0.559757
30	-0.149921	-0.073486	0.048493	0.051572	0.048493	0.051572	0.797916	0.55413
31	-0.149963	-0.073567	0.047688	0.050616	0.047688	0.050616	0.800014	0.534154
32	-0.149935	-0.073368	0.048632	0.053187	0.048632	0.053187	0.780804	0.574269
33	-0.149933	-0.073353	0.048689	0.053382	0.048689	0.053382	0.779207	0.577209
34	-0.149976	-0.073455	0.047851	0.052146	0.047851	0.052146	0.783952	0.553167
35	-0.14995	-0.073578	0.047836	0.050429	0.047836	0.050429	0.803811	0.533815
36	-0.149927	-0.073307	0.048889	0.053971	0.048889	0.053971	0.774723	0.586486
37	-0.149977	-0.073324	0.048195	0.053865	0.048195	0.053865	0.76775	0.577115
38	-0.149924	-0.073377	0.04875	0.053041	0.04875	0.053041	0.78387	0.573943
39	-0.14995	-0.073543	0.047939	0.050892	0.047939	0.050892	0.799579	0.540125
40	-0.149956	-0.073561	0.047806	0.050676	0.047806	0.050676	0.800619	0.536183
41	-0.149952	-0.073433	0.04823	0.052373	0.04823	0.052373	0.785628	0.560184
42	-0.149993	-0.073478	0.047552	0.051891	0.047552	0.051891	0.783572	0.54676
43	-0.149961	-0.073478	0.047987	0.051803	0.047987	0.051803	0.789517	0.550861
44	-0.150007	-0.073522	0.047238	0.051357	0.047238	0.051357	0.786359	0.537078
45	-0.14995	-0.073583	0.047812	0.050359	0.047812	0.050359	0.804357	0.532772
46	-0.149976	-0.073477	0.047789	0.05185	0.047789	0.05185	0.786729	0.549079
47	-0.149939	-0.073511	0.048181	0.051294	0.048181	0.051294	0.797619	0.547401
48	-0.149921	-0.073452	0.048595	0.052037	0.048595	0.052037	0.793688	0.560581
49	-0.149934	-0.073541	0.048152	0.050875	0.048152	0.050875	0.802141	0.542388
50	-0.149987	-0.073508	0.047541	0.051474	0.047541	0.051474	0.788358	0.541944
51	-0.149949	-0.073467	0.048166	0.051915	0.048166	0.051915	0.790237	0.554232
52	-0.149921	-0.07349	0.048485	0.051523	0.048485	0.051523	0.798381	0.553482
53	-0.14998	-0.073467	0.047761	0.051999	0.047761	0.051999	0.784653	0.55044
54	-0.149947	-0.07338	0.048441	0.053054	0.048441	0.053054	0.780135	0.5705
55	-0.149921	-0.073427	0.04865	0.052365	0.04865	0.052365	0.79054	0.564979
56	-0.149926	-0.073478	0.048447	0.051704	0.048447	0.051704	0.795862	0.555091
57	-0.149961	-0.073456	0.048039	0.052089	0.048039	0.052089	0.786764	0.554717
58	-0.149982	-0.073334	0.048104	0.053758	0.048104	0.053758	0.767938	0.574802
59	-0.14996	-0.073567	0.047728	0.050609	0.047728	0.050609	0.800532	0.534538
60	-0.149962	-0.073513	0.047865	0.051341	0.047865	0.051341	0.793524	0.544253
61	-0.149922	-0.073441	0.048609	0.052183	0.048609	0.052183	0.792171	0.562421
62	-0.150008	-0.073417	0.047531	0.052744	0.047531	0.052744	0.773251	0.556231
63	-0.149956	-0.073394	0.048279	0.052901	0.048279	0.052901	0.780029	0.566835
64	-0.149918	-0.073471	0.048576	0.051774	0.048576	0.051774	0.796517	0.557378
65	-0.149937	-0.073559	0.048067	0.05064	0.048067	0.05064	0.803904	0.538808
66	-0.149995	-0.073365	0.047846	0.05339	0.047846	0.05339	0.769257	0.567442
67	-0.149922	-0.073442	0.0486	0.052174	0.0486	0.052174	0.792168	0.562209
68	-0.149933	-0.073502	0.048287	0.051392	0.048287	0.051392	0.797667	0.549733
69	-0.149954	-0.073542	0.047892	0.050924	0.047892	0.050924	0.798678	0.539929
70	-0.149956	-0.073366	0.048362	0.053264	0.048362	0.053264	0.776756	0.572035
71	-0.14995	-0.073304	0.0486	0.054061	0.0486	0.054061	0.770257	0.584188
72	-0.149924	-0.073495	0.048422	0.051461	0.048422	0.051461	0.79839	0.552058
73	-0.14994	-0.073604	0.047878	0.050044	0.047878	0.050044	0.808719	0.530087
74	-0.149923	-0.073442	0.048589	0.052171	0.048589	0.052171	0.792081	0.562041
75	-0.149933	-0.073288	0.048853	0.054231	0.048853	0.054231	0.771286	0.589157
76	-0.149961	-0.073377	0.048262	0.053141	0.048262	0.053141	0.777023	0.569425
77	-0.149964	-0.073369	0.048251	0.053254	0.048251	0.053254	0.775579	0.570606
78	-0.149956	-0.073287	0.048558	0.054304	0.048558	0.054304	0.766909	0.586589
79	-0.149934	-0.073462	0.048392	0.051928	0.048392	0.051928	0.792643	0.556996
80	-0.149932	-0.073457	0.048425	0.052002	0.048425	0.052002	0.79217	0.558218
81	-0.150048	-0.073431	0.04697	0.052669	0.04697	0.052669	0.767707	0.548681
82	-0.150092	-0.073325	0.046708	0.054171	0.046708	0.054171	0.746554	0.562958
83	-0.149948	-0.073497	0.048106	0.05151	0.048106	0.05151	0.79427	0.548956
84	-0.149966	-0.073433	0.04804	0.052416	0.04804	0.052416	0.78295	0.558454
85	-0.149985	-0.073491	0.047624	0.051703	0.047624	0.051703	0.786596	0.545486
86	-0.149942	-0.07338	0.048499	0.05305	0.048499	0.05305	0.780857	0.571129
87	-0.149963	-0.073487	0.047932	0.05168	0.047932	0.05168	0.790324	0.548839
88	-0.150023	-0.073476	0.04716	0.052009	0.04716	0.052009	0.777751	0.54345
89	-0.149946	-0.073413	0.04837	0.052622	0.04837	0.052622	0.78434	0.564674
90	-0.149966	-0.073466	0.047951	0.051968	0.047951	0.051968	0.787184	0.552317
91	-0.149913	-0.07366	0.048071	0.049181	0.048071	0.049181	0.820699	0.52299
92	-0.149928	-0.073508	0.048336	0.051296	0.048336	0.051296	0.799324	0.549213
93	-0.149927	-0.073356	0.048761	0.053326	0.048761	0.053326	0.780696	0.577397
94	-0.149955	-0.073503	0.047991	0.051452	0.047991	0.051452	0.79366	0.546965
95	-0.1499	-0.073503	0.048726	0.051286	0.048726	0.051286	0.803813	0.553592
96	-0.149955	-0.073501	0.047998	0.051474	0.047998	0.051474	0.79347	0.547286
97	-0.149969	-0.073395	0.048109	0.052923	0.048109	0.052923	0.777814	0.565099
98	-0.15002	-0.073409	0.047395	0.052875	0.047395	0.052875	0.770124	0.55612
99	-0.149914	-0.073661	0.048062	0.049182	0.048062	0.049182	0.820599	0.522906
100	-0.14994	-0.073425	0.048407	0.052439	0.048407	0.052439	0.786881	0.563004

	Rafsec - Original							
	S11		S12		S21		S22	
	Real	Imaginary	Real	Imaginary	Real	Imaginary	Real	Imaginary
1	-0.160571	-0.047053	0.067701	0.012767	0.067701	0.012767	0.808202	0.508163
2	-0.160389	-0.046881	0.069126	0.015839	0.069126	0.015839	0.762315	0.536501
3	-0.160425	-0.046899	0.068766	0.015431	0.068766	0.015431	0.768182	0.529863
4	-0.160681	-0.046804	0.065131	0.015444	0.065131	0.015444	0.762674	0.471424
5	-0.160622	-0.046899	0.066301	0.014494	0.066301	0.014494	0.779101	0.488966
6	-0.160473	-0.046954	0.068448	0.014511	0.068448	0.014511	0.782282	0.523007
7	-0.160335	-0.046794	0.069345	0.017145	0.069345	0.017145	0.741358	0.542807
8	-0.160848	-0.047079	0.064153	0.011065	0.064153	0.011065	0.829104	0.452228
9	-0.160442	-0.046716	0.067694	0.017579	0.067694	0.017579	0.731004	0.516158
10	-0.160643	-0.046892	0.06601	0.014494	0.06601	0.014494	0.77874	0.484364
11	-0.160624	-0.046799	0.065829	0.015753	0.065829	0.015753	0.75843	0.482977
12	-0.160543	-0.046998	0.067786	0.013611	0.067786	0.013611	0.795263	0.510952
13	-0.16067	-0.047071	0.066503	0.012037	0.066503	0.012037	0.817445	0.488651
14	-0.160615	-0.047029	0.06702	0.012854	0.06702	0.012854	0.805727	0.497808
15	-0.160741	-0.046941	0.064949	0.013412	0.064949	0.013412	0.794444	0.466579
16	-0.160614	-0.047031	0.067037	0.012834	0.067037	0.012834	0.806067	0.498039
17	-0.160726	-0.04687	0.064841	0.01441	0.064841	0.01441	0.778797	0.46586
18	-0.160538	-0.046968	0.0677	0.014011	0.0677	0.014011	0.788834	0.510289
19	-0.160339	-0.04684	0.069524	0.016573	0.069524	0.016573	0.75117	0.544543
20	-0.16048	-0.04699	0.068544	0.01403	0.068544	0.01403	0.790074	0.523599
21	-0.160425	-0.046805	0.068312	0.016587	0.068312	0.016587	0.748508	0.524661
22	-0.160595	-0.046872	0.066527	0.014968	0.066527	0.014968	0.771889	0.493191
23	-0.1605	-0.046885	0.067776	0.015251	0.067776	0.015251	0.769276	0.513608
24	-0.160617	-0.046935	0.066535	0.01406	0.066535	0.01406	0.786261	0.492062
25	-0.160405	-0.046861	0.068827	0.015994	0.068827	0.015994	0.759183	0.531943
26	-0.160449	-0.046983	0.068893	0.014276	0.068893	0.014276	0.786878	0.529591
27	-0.160677	-0.046873	0.065485	0.014587	0.065485	0.014587	0.77665	0.476184
28	-0.160626	-0.047005	0.066752	0.013114	0.066752	0.013114	0.801313	0.494072
29	-0.160611	-0.046941	0.066645	0.014019	0.066645	0.014019	0.78706	0.493729
30	-0.160613	-0.04703	0.067043	0.01286	0.067043	0.01286	0.805679	0.498173
31	-0.16068	-0.047084	0.066436	0.011811	0.066436	0.011811	0.820769	0.4873
32	-0.16069	-0.047027	0.066021	0.012523	0.066021	0.012523	0.809349	0.482004
33	-0.160629	-0.046803	0.065783	0.015682	0.065783	0.015682	0.759515	0.482152
34	-0.160791	-0.047015	0.064619	0.012206	0.064619	0.012206	0.812532	0.460334
35	-0.160524	-0.046796	0.067067	0.016241	0.067067	0.016241	0.752116	0.503696
36	-0.160618	-0.047034	0.066995	0.012781	0.066995	0.012781	0.806819	0.497307
37	-0.16055	-0.046967	0.067542	0.013972	0.067542	0.013972	0.789187	0.507741
38	-0.160679	-0.04694	0.06576	0.013701	0.06576	0.013701	0.790859	0.479482

	Rafsec - Printed							
	S11		S12		S21		S22	
	Real	Imaginary	Real	Imaginary	Real	Imaginary	Real	Imaginary
1	-0.160489	-0.046982	0.068389	0.014091	0.068389	0.014091	0.788809	0.521273
2	-0.160637	-0.047031	0.066742	0.012725	0.066742	0.012725	0.807293	0.49333
3	-0.160357	-0.046843	0.069325	0.016458	0.069325	0.016458	0.752638	0.541034
4	-0.160449	-0.046863	0.068301	0.015763	0.068301	0.015763	0.761944	0.522973
5	-0.160505	-0.046777	0.067205	0.016556	0.067205	0.016556	0.747168	0.506424
6	-0.160645	-0.046857	0.065825	0.014932	0.065825	0.014932	0.771575	0.481954
7	-0.160602	-0.04705	0.067291	0.012644	0.067291	0.012644	0.80941	0.501638
8	-0.160703	-0.047076	0.066091	0.011813	0.066091	0.011813	0.820229	0.482094
9	-0.160517	-0.046949	0.067877	0.014366	0.067877	0.014366	0.78355	0.51369
10	-0.160631	-0.046827	0.065874	0.015372	0.065874	0.015372	0.764596	0.483263
11	-0.160444	-0.046645	0.067359	0.018414	0.067359	0.018414	0.716393	0.511842
12	-0.160725	-0.046806	0.064582	0.015233	0.064582	0.015233	0.765563	0.462476
13	-0.160888	-0.04685	0.062617	0.014009	0.062617	0.014009	0.783666	0.431001
14	-0.160526	-0.046934	0.067685	0.014511	0.067685	0.014511	0.780913	0.510906
15	-0.160767	-0.046716	0.063683	0.016224	0.063683	0.016224	0.749105	0.448671
16	-0.160869	-0.047001	0.06351	0.012051	0.06351	0.012051	0.813881	0.443517
17	-0.160803	-0.047034	0.064548	0.011889	0.064548	0.011889	0.817226	0.458944
18	-0.160476	-0.046959	0.068435	0.014437	0.068435	0.014437	0.783433	0.522659
19	-0.160758	-0.046984	0.064925	0.012768	0.064925	0.012768	0.8043	0.465549
20	-0.160699	-0.047086	0.066193	0.01169	0.066193	0.01169	0.822237	0.483457
21	-0.160583	-0.047045	0.067511	0.012807	0.067511	0.012807	0.807268	0.505293
22	-0.160753	-0.046998	0.065057	0.012604	0.065057	0.012604	0.806951	0.467386
23	-0.160693	-0.046988	0.065797	0.013021	0.065797	0.013021	0.801432	0.479219
24	-0.160764	-0.046975	0.064803	0.012858	0.064803	0.012858	0.802805	0.463786
25	-0.160476	-0.04696	0.068436	0.014427	0.068436	0.014427	0.783598	0.522657
26	-0.160715	-0.047156	0.066332	0.010675	0.066332	0.010675	0.837625	0.484033
27	-0.16066	-0.047044	0.066499	0.012433	0.066499	0.012433	0.811409	0.489178
28	-0.160665	-0.047065	0.066542	0.012146	0.066542	0.012146	0.815835	0.489402
29	-0.160594	-0.047061	0.067454	0.012549	0.067454	0.012549	0.811128	0.50398
30	-0.160531	-0.046901	0.067471	0.014892	0.067471	0.014892	0.774507	0.508122
31	-0.160494	-0.046939	0.068108	0.0146	0.068108	0.0146	0.780245	0.517765
32	-0.160648	-0.047066	0.066774	0.012209	0.066774	0.012209	0.815237	0.493039
33	-0.160785	-0.046863	0.06404	0.014248	0.06404	0.014248	0.78068	0.453192
34	-0.160702	-0.046878	0.065188	0.014413	0.065188	0.014413	0.77908	0.471324
35	-0.160698	-0.046869	0.065205	0.014538	0.065205	0.014538	0.777133	0.471713
36	-0.160661	-0.046956	0.066068	0.01358	0.066068	0.01358	0.793131	0.484118
37	-0.160641	-0.046487	0.064402	0.019499	0.064402	0.019499	0.694636	0.462271
38	-0.16054	-0.046979	0.067727	0.013864	0.067727	0.013864	0.791192	0.510467

APPENDIX H

THE EXTRACTED RESIDUAL TWO-PORT NETWORK FOR ALL TESTED TAGS

	AD220 - Original							
	S11		S12		S21		S22	
	Real	Imaginary	Real	Imaginary	Real	Imaginary	Real	Imaginary
1	0.030428	-0.011808	0.999607	0.000359	0.999607	0.000359	-0.030428	0.011808
2	-0.001446	-0.002823	1.000003	-4.08E-06	1.000003	-4.08E-06	0.001446	0.002823
3	0.014551	-0.013764	0.999989	0.0002	0.999989	0.0002	-0.014551	0.013764
4	0.025626	0.009577	0.999718	-0.000246	0.999718	-0.000246	-0.025626	-0.009577
5	0.010469	-0.001322	0.999946	1.38E-05	0.999946	1.38E-05	-0.010469	0.001322
6	0.03136	-0.002757	0.999512	8.65E-05	0.999512	8.65E-05	-0.03136	0.002757
7	0.039288	0.002128	0.99923	-8.37E-05	0.99923	-8.37E-05	-0.039288	-0.002128
8	0.048171	-0.003758	0.998846	0.000181	0.998846	0.000181	-0.048171	0.003758
9	-0.030391	-0.012906	0.999621	-0.000392	0.999621	-0.000392	0.030391	0.012906
10	-0.012644	-0.011091	0.999982	-0.00014	0.999982	-0.00014	0.012644	0.011091
11	-0.003079	-0.016818	1.000137	-5.18E-05	1.000137	-5.18E-05	0.003079	0.016818
12	0.010789	-0.014104	1.000041	0.000152	1.000041	0.000152	-0.010789	0.014104
13	0.006415	-0.019944	1.000178	0.000128	1.000178	0.000128	-0.006415	0.019944
14	0.019167	-0.018797	0.999993	0.00036	0.999993	0.00036	-0.019167	0.018797
15	-0.017481	0.001851	0.999849	3.24E-05	0.999849	3.24E-05	0.017481	-0.001851
16	0.039673	-0.001446	0.999214	5.74E-05	0.999214	5.74E-05	-0.039673	0.001446
17	0.017819	-0.015889	0.999967	0.000283	0.999967	0.000283	-0.017819	0.015889
18	0.01998	0.00356	0.999807	-7.11E-05	0.999807	-7.11E-05	-0.01998	-0.00356
19	0.001699	1.37E-05	0.999999	-2.32E-08	0.999999	-2.32E-08	-0.001699	-1.37E-05
20	-0.006095	-0.001563	0.999983	-9.53E-06	0.999983	-9.53E-06	0.006095	0.001563
21	-0.003281	-0.012536	1.000073	-4.11E-05	1.000073	-4.11E-05	0.003281	0.012536
22	0.016045	-0.014775	0.99998	0.000237	0.99998	0.000237	-0.016045	0.014775
23	0.004322	-0.004475	1.000001	1.93E-05	1.000001	1.93E-05	-0.004322	0.004475
24	-0.007583	-0.010313	1.000024	-7.82E-05	1.000024	-7.82E-05	0.007583	0.010313
25	-0.014231	-0.002956	0.999903	-4.21E-05	0.999903	-4.21E-05	0.014231	0.002956
26	-0.013275	-0.009851	0.99996	-0.000131	0.99996	-0.000131	0.013275	0.009851
27	0.001881	-0.017007	1.000143	3.2E-05	1.000143	3.2E-05	-0.001881	0.017007
28	0.022692	-0.00677	0.999765	0.000154	0.999765	0.000154	-0.022692	0.00677
29	0.025315	-0.005095	0.999693	0.000129	0.999693	0.000129	-0.025315	0.005095
30	0.019687	0.017202	0.999954	-0.000339	0.999954	-0.000339	-0.019687	-0.017202
31	0.043959	-0.015937	0.999161	0.000701	0.999161	0.000701	-0.043959	0.015937
32	0.032848	0.004845	0.999472	-0.000159	0.999472	-0.000159	-0.032848	-0.004845
33	0.017801	-0.004103	0.99985	7.3E-05	0.99985	7.3E-05	-0.017801	0.004103
34	0.007522	0.004847	0.999983	-3.65E-05	0.999983	-3.65E-05	-0.007522	-0.004847
35	0.033238	0.010559	0.999503	-0.000351	0.999503	-0.000351	-0.033238	-0.010559
36	0.022183	-0.002709	0.999758	6.01E-05	0.999758	6.01E-05	-0.022183	0.002709
37	-0.04771	-0.009133	0.998903	-0.000436	0.998903	-0.000436	0.04771	0.009133
38	-0.009633	-0.009797	1.000002	-9.44E-05	1.000002	-9.44E-05	0.009633	0.009797
39	-0.000861	-0.001386	1.000001	-1.19E-06	1.000001	-1.19E-06	0.000861	0.001386
40	-0.0255	-0.014266	0.999777	-0.000364	0.999777	-0.000364	0.0255	0.014266
41	0.002162	-0.008122	1.000031	1.76E-05	1.000031	1.76E-05	-0.002162	0.008122
42	0.027534	0.020274	0.999827	-0.000558	0.999827	-0.000558	-0.027534	-0.020274
43	0.024204	-0.005766	0.999724	0.00014	0.999724	0.00014	-0.024204	0.005766
44	0.007472	-0.001218	0.999973	9.1E-06	0.999973	9.1E-06	-0.007472	0.001218
45	0.017398	-0.012531	0.999927	0.000218	0.999927	0.000218	-0.017398	0.012531
46	0.009677	-0.007831	0.999984	7.58E-05	0.999984	7.58E-05	-0.009677	0.007831
47	0.023239	0.0117	0.999798	-0.000272	0.999798	-0.000272	-0.023239	-0.0117
48	0.024846	0.00025	0.999691	-6.22E-06	0.999691	-6.22E-06	-0.024846	-0.00025
49	-0.096397	-0.003126	0.995348	-0.000303	0.995348	-0.000303	0.096397	0.003126
50	0.044095	-8.71E-05	0.999027	3.84E-06	0.999027	3.84E-06	-0.044095	8.71E-05
51	0.036392	0.021839	0.999577	-0.000795	0.999577	-0.000795	-0.036392	-0.021839
52	0.037842	-8.38E-05	0.999284	3.17E-06	0.999284	3.17E-06	-0.037842	8.38E-05
53	0.037912	-0.00442	0.999291	0.000168	0.999291	0.000168	-0.037912	0.00442
54	-0.020831	0.007705	0.999813	0.000161	0.999813	0.000161	0.020831	-0.007705
55	0.01225	0.003285	0.99993	-4.02E-05	0.99993	-4.02E-05	-0.01225	-0.003285
56	-0.034849	-0.00503	0.999405	-0.000175	0.999405	-0.000175	0.034849	0.00503
57	0.019871	-0.000235	0.999803	4.68E-06	0.999803	4.68E-06	-0.019871	0.000235
58	-0.008149	0.010854	1.000026	8.85E-05	1.000026	8.85E-05	0.008149	-0.010854
59	-0.006496	0.008774	1.000017	5.7E-05	1.000017	5.7E-05	0.006496	-0.008774
60	-0.08858	-0.002629	0.996073	-0.000234	0.996073	-0.000234	0.08858	0.002629
61	0.000402	-0.001465	1.000001	5.89E-07	1.000001	5.89E-07	-0.000402	0.001465
62	-0.035331	-0.00289	0.99938	-0.000102	0.99938	-0.000102	0.035331	0.00289
63	-0.011982	8.78E-05	0.999928	1.05E-06	0.999928	1.05E-06	0.011982	-8.78E-05
64	0.025237	0.005709	0.999698	-0.000144	0.999698	-0.000144	-0.025237	-0.005709
65	-0.026785	0.004789	0.999653	0.000128	0.999653	0.000128	0.026785	-0.004789
66	0.008504	-0.001983	0.999966	1.69E-05	0.999966	1.69E-05	-0.008504	0.001983
67	0.034975	-0.006641	0.99941	0.000232	0.99941	0.000232	-0.034975	0.006641
68	0.039837	-0.003892	0.999214	0.000155	0.999214	0.000155	-0.039837	0.003892
69	-0.044033	-0.001499	0.999031	-6.61E-05	0.999031	-6.61E-05	0.044033	0.001499
70	-0.037134	0.009867	0.999359	0.000367	0.999359	0.000367	0.037134	-0.009867
71	0.007938	0.041388	1.000825	-0.000328	1.000825	-0.000328	-0.007938	-0.041388
72	-0.07919	0.019479	0.997051	0.001547	0.997051	0.001547	0.07919	-0.019479
73	0.015858	0.013752	0.999969	-0.000218	0.999969	-0.000218	-0.015858	-0.013752
74	0.000608	0.005921	1.000017	-3.6E-06	1.000017	-3.6E-06	-0.000608	-0.005921
75	-0.036188	0.006421	0.999366	0.000233	0.999366	0.000233	0.036188	-0.006421
76	-0.02032	0.002858	0.999798	5.81E-05	0.999798	5.81E-05	0.02032	-0.002858
77	0.021255	-0.005445	0.999789	0.000116	0.999789	0.000116	-0.021255	0.005445
78	0.009905	0.009595	0.999997	-9.5E-05	0.999997	-9.5E-05	-0.009905	-0.009595
79	-0.032756	0.019942	0.999663	0.000653	0.999663	0.000653	0.032756	-0.019942
80	-0.008233	0.002866	0.99997	2.36E-05	0.99997	2.36E-05	0.008233	-0.002866
81	-0.000675	0.001003	1	6.78E-07	1	6.78E-07	0.000675	-0.001003
82	-0.043489	-0.002001	0.999056	-8.71E-05	0.999056	-8.71E-05	0.043489	0.002001
83	-0.053122	0.015292	0.998705	0.000813	0.998705	0.000813	0.053122	-0.015292
84	0.013562	0.006706	0.999931	-9.1E-05	0.999931	-9.1E-05	-0.013562	-0.006706
85	0.007881	-0.001387	0.99997	1.09E-05	0.99997	1.09E-05	-0.007881	0.001387
86	0.03057	6.66E-05	0.999533	-2.04E-06	0.999533	-2.04E-06	-0.03057	-6.66E-05
87	-0.066267	0.000288	0.997802	1.91E-05	0.997802	1.91E-05	0.066267	-0.000288
88	0.003682	0.003168	0.999998	-1.17E-05	0.999998	-1.17E-05	-0.003682	-0.003168
89	0.002641	0.007215	1.000023	-1.91E-05	1.000023	-1.91E-05	-0.002641	-0.007215
90	-0.040902	0.000812	0.999164	3.32E-05	0.999164	3.32E-05	0.040902	-0.000812
91	0.002165	0.000485	0.999998	-1.05E-06	0.999998	-1.05E-06	-0.002165	-0.000485
92	-0.009307	0.014579	1.000063	0.000136	1.000063	0.000136	0.009307	-0.014579
93	-0.003632	0.001555	0.999995	5.65E-06	0.999995	5.65E-06	0.003632	-0.001555
94	-0.000738	0.012035	1.000072	8.88E-06	1.000072	8.88E-06	0.000738	-0.012035
95	0.022303	0.00118	0.999752	-2.63E-05	0.999752	-2.63E-05	-0.022303	-0.00118
96	-0.038379	0.006315	0.999283	0.000243	0.999283	0.000243	0.038379	-0.006315
97	0.005735	5.71E-05	0.999984	-3.28E-07	0.999984	-3.28E-07	-0.005735	-5.71E-05
98	-0.035517	-0.00458	0.99938	-0.000163	0.99938	-0.000163	0.035517	0.00458
99	0.004787	0.001151	0.999989	-5.51E-06	0.999989	-5.51E-06	-0.004787	-0.001151
100	0.003427	0.014407	1.000098	-4.94E-05	1.000098	-4.94E-05	-0.003427	-0.014407

	AD220 - Printed							
	S11		S12		S21		S22	
	Real	Imaginary	Real	Imaginary	Real	Imaginary	Real	Imaginary
1	-0.058469	-0.004938	0.998301	-0.000289	0.998301	-0.000289	0.058469	0.004938
2	-0.015361	-0.016084	1.000011	-0.000247	1.000011	-0.000247	0.015361	0.016084
3	0.044324	-0.00884	0.999056	0.000392	0.999056	0.000392	-0.044324	0.00884
4	0.030391	-0.010656	0.999595	0.000324	0.999595	0.000324	-0.030391	0.010656
5	0.045069	-0.009602	0.99903	0.000433	0.99903	0.000433	-0.045069	0.009602
6	-0.028309	-0.011774	0.999669	-0.000333	0.999669	-0.000333	0.028309	0.011774
7	0.015431	-0.001827	0.999883	2.82E-05	0.999883	2.82E-05	-0.015431	0.001827
8	-0.004846	-0.003937	0.999996	-1.91E-05	0.999996	-1.91E-05	0.004846	0.003937
9	-0.003564	-0.005369	1.000008	-1.91E-05	1.000008	-1.91E-05	0.003564	0.005369
10	-0.072627	-0.011504	0.997426	-0.000838	0.997426	-0.000838	0.072627	0.011504
11	-0.021785	-0.010385	0.999817	-0.000226	0.999817	-0.000226	0.021785	0.010385
12	-0.012915	-0.002471	0.99992	-3.19E-05	0.99992	-3.19E-05	0.012915	0.002471
13	0.011875	0.00906	0.999971	-0.000108	0.999971	-0.000108	-0.011875	-0.00906
14	0.015103	0.007339	0.999913	-0.000111	0.999913	-0.000111	-0.015103	-0.007339
15	0.033644	-0.003087	0.999439	0.000104	0.999439	0.000104	-0.033644	0.003087
16	0.008736	0.018248	1.000128	-0.000159	1.000128	-0.000159	-0.008736	-0.018248
17	-0.036667	-0.010054	0.999378	-0.000369	0.999378	-0.000369	0.036667	0.010054
18	-0.054632	-0.005001	0.998519	-0.000274	0.998519	-0.000274	0.054632	0.005001
19	-0.024854	-0.013757	0.999786	-0.000342	0.999786	-0.000342	0.024854	0.013757
20	-0.033713	-0.010854	0.999491	-0.000366	0.999491	-0.000366	0.033713	0.010854
21	-0.01296	-0.004547	0.999926	-5.89E-05	0.999926	-5.89E-05	0.01296	0.004547
22	0.047297	0.0046	0.998891	-0.000218	0.998891	-0.000218	-0.047297	-0.0046
23	-0.049508	-0.004319	0.998783	-0.000214	0.998783	-0.000214	0.049508	0.004319
24	0.016992	0.007929	0.999887	-0.000135	0.999887	-0.000135	-0.016992	-0.007929
25	-0.030892	-0.001507	0.999524	-4.66E-05	0.999524	-4.66E-05	0.030892	0.001507
26	0.031836	0.007726	0.999523	-0.000246	0.999523	-0.000246	-0.031836	-0.007726
27	-0.032492	0.018019	0.999635	0.000586	0.999635	0.000586	0.032492	-0.018019
28	0.026696	0.026602	0.999998	-0.00071	0.999998	-0.00071	-0.026696	-0.026602
29	-0.031643	0.007056	0.999524	0.000223	0.999524	0.000223	0.031643	-0.007056
30	0.006717	0.01794	1.000138	-0.00012	1.000138	-0.00012	-0.006717	-0.01794
31	0.029624	0.016585	0.999699	-0.000491	0.999699	-0.000491	-0.029624	-0.016585
32	0.013678	-0.002181	0.999909	2.98E-05	0.999909	2.98E-05	-0.013678	0.002181
33	-0.063678	-0.014324	0.998074	-0.000914	0.998074	-0.000914	0.063678	0.014324
34	0.035857	0.008687	0.999395	-0.000312	0.999395	-0.000312	-0.035857	-0.008687
35	-0.015467	-0.003407	0.999886	-5.27E-05	0.999886	-5.27E-05	0.015467	0.003407
36	-0.023117	-0.009635	0.999779	-0.000223	0.999779	-0.000223	0.023117	0.009635
37	-0.077811	-0.007221	0.996994	-0.000564	0.996994	-0.000564	0.077811	0.007221
38	-0.058127	-0.015061	0.998423	-0.000877	0.998423	-0.000877	0.058127	0.015061
39	0.012675	-0.009852	0.999968	0.000125	0.999968	0.000125	-0.012675	0.009852
40	0.007522	-0.012086	1.000045	9.09E-05	1.000045	9.09E-05	-0.007522	0.012086
41	-0.054121	-0.010657	0.998591	-0.000578	0.998591	-0.000578	0.054121	0.010657
42	0.036971	-0.005349	0.999331	0.000198	0.999331	0.000198	-0.036971	0.005349
43	0.030227	-0.002342	0.999546	7.08E-05	0.999546	7.08E-05	-0.030227	0.002342
44	0.060642	0.015659	0.998283	-0.000951	0.998283	-0.000951	-0.060642	-0.015659
45	0.008006	0.006314	0.999988	-5.06E-05	0.999988	-5.06E-05	-0.008006	-0.006314
46	0.004645	0.022672	1.000246	-0.000105	1.000246	-0.000105	-0.004645	-0.022672
47	-0.032235	-0.013198	0.999568	-0.000426	0.999568	-0.000426	0.032235	0.013198
48	0.034597	-0.000141	0.999401	4.89E-06	0.999401	4.89E-06	-0.034597	0.000141
49	-0.051972	-0.013541	0.998741	-0.000705	0.998741	-0.000705	0.051972	0.013541
50	0.043523	0.003997	0.99906	-0.000174	0.99906	-0.000174	-0.043523	-0.003997
51	-0.017973	0.013028	0.999923	0.000234	0.999923	0.000234	0.017973	-0.013028
52	0.032022	0.003565	0.999494	-0.000114	0.999494	-0.000114	-0.032022	-0.003565
53	-0.023053	-0.011687	0.999803	-0.000269	0.999803	-0.000269	0.023053	0.011687
54	0.057181	0.013277	0.998452	-0.00076	0.998452	-0.00076	-0.057181	-0.013277
55	0.045261	0.010671	0.999032	-0.000483	0.999032	-0.000483	-0.045261	-0.010671
56	0.052086	0.031025	0.999126	-0.001617	0.999126	-0.001617	-0.052086	-0.031025
57	0.03407	-0.001342	0.99942	4.57E-05	0.99942	4.57E-05	-0.03407	0.001342
58	0.021323	0.015488	0.999893	-0.00033	0.999893	-0.00033	-0.021323	-0.015488
59	0.029676	-0.005749	0.999576	0.000171	0.999576	0.000171	-0.029676	0.005749
60	-0.002531	-0.007746	1.000027	-1.96E-05	1.000027	-1.96E-05	0.002531	0.007746
61	0.012012	-0.003922	0.999936	4.71E-05	0.999936	4.71E-05	-0.012012	0.003922
62	-0.055066	-0.015985	0.998611	-0.000881	0.998611	-0.000881	0.055066	0.015985
63	-0.010852	-0.010408	0.999995	-0.000113	0.999995	-0.000113	0.010852	0.010408
64	0.005714	0.02545	1.000307	-0.000145	1.000307	-0.000145	-0.005714	-0.02545
65	0.027405	0.013538	0.999716	-0.000371	0.999716	-0.000371	-0.027405	-0.013538
66	0.035021	-0.001478	0.999388	5.18E-05	0.999388	5.18E-05	-0.035021	0.001478
67	0.005818	0.000535	0.999983	-3.12E-06	0.999983	-3.12E-06	-0.005818	-0.000535
68	0.049497	0.038857	0.999532	-0.001924	0.999532	-0.001924	-0.049497	-0.038857
69	-0.083789	-0.013922	0.996581	-0.00117	0.996581	-0.00117	0.083789	0.013922
70	-0.029751	-0.012748	0.999639	-0.000379	0.999639	-0.000379	0.029751	0.012748
71	0.026573	0.005317	0.999661	-0.000141	0.999661	-0.000141	-0.026573	-0.005317
72	0.018164	-0.001557	0.999836	2.83E-05	0.999836	2.83E-05	-0.018164	0.001557
73	-0.015711	-0.005625	0.999892	-8.84E-05	0.999892	-8.84E-05	0.015711	0.005625
74	0.03563	-0.000201	0.999365	7.17E-06	0.999365	7.17E-06	-0.03563	0.000201
75	-0.027082	-0.015463	0.999753	-0.000419	0.999753	-0.000419	0.027082	0.015463
76	-0.013725	-0.004207	0.999915	-5.78E-05	0.999915	-5.78E-05	0.013725	0.004207
77	0.016558	0.004289	0.999872	-7.1E-05	0.999872	-7.1E-05	-0.016558	-0.004289
78	0.054949	0.012154	0.998563	-0.000669	0.998563	-0.000669	-0.054949	-0.012154
79	-0.029837	-0.002915	0.999559	-8.7E-05	0.999559	-8.7E-05	0.029837	0.002915
80	0.034438	0.004103	0.999415	-0.000141	0.999415	-0.000141	-0.034438	-0.004103
81	0.063277	0.023019	0.998263	-0.001459	0.998263	-0.001459	-0.063277	-0.023019
82	0.011953	0.005924	0.999946	-7.08E-05	0.999946	-7.08E-05	-0.011953	-0.005924
83	0.000568	0.003383	1.000006	-1.92E-06	1.000006	-1.92E-06	-0.000568	-0.003383
84	0.051394	0.01791	0.998839	-0.000922	0.998839	-0.000922	-0.051394	-0.01791
85	-0.037334	-0.007018	0.999328	-0.000262	0.999328	-0.000262	0.037334	0.007018
86	0.062343	0.011689	0.998124	-0.00073	0.998124	-0.00073	-0.062343	-0.011689
87	-0.000609	-0.00131	1.000001	-7.97E-07	1.000001	-7.97E-07	0.000609	0.00131
88	0.032691	0.010642	0.999522	-0.000348	0.999522	-0.000348	-0.032691	-0.010642
89	0.00289	-0.005799	1.000013	1.68E-05	1.000013	1.68E-05	-0.00289	0.005799
90	-0.071229	0.007593	0.997489	0.000542	0.997489	0.000542	0.071229	-0.007593
91	0.043803	0.008673	0.999078	-0.00038	0.999078	-0.00038	-0.043803	-0.008673
92	0.011349	-0.006993	0.99996	7.94E-05	0.99996	7.94E-05	-0.011349	0.006993
93	-0.016644	-0.002123	0.999864	-3.53E-05	0.999864	-3.53E-05	0.016644	0.002123
94	-0.017227	0.002942	0.999856	5.07E-05	0.999856	5.07E-05	0.017227	-0.002942
95	-0.026799	-0.007461	0.999669	-0.0002	0.999669	-0.0002	0.026799	0.007461
96	-0.013363	-0.013836	1.000006	-0.000185	1.000006	-0.000185	0.013363	0.013836
97	0.01904	-0.001396	0.99982	2.66E-05	0.99982	2.66E-05	-0.01904	0.001396
98	-0.034783	-0.010852	0.999454	-0.000378	0.999454	-0.000378	0.034783	0.010852
99	-0.042462	0.001769	0.9991	7.52E-05	0.9991	7.52E-05	0.042462	-0.001769
100	0.045065	0.004837	0.998996	-0.000218	0.998996	-0.000218	-0.045065	-0.004837

	Alien - Original							
	S11		S12		S21		S22	
	Real	Imaginary	Real	Imaginary	Real	Imaginary	Real	Imaginary
1	-0.011357	-0.003982	0.999943	-4.52E-05	0.999943	-4.52E-05	0.011357	0.003982
2	-0.051704	0.017989	0.998825	0.000931	0.998825	0.000931	0.051704	-0.017989
3	-0.042109	0.00552	0.999128	0.000233	0.999128	0.000233	0.042109	-0.00552
4	0.020933	0.028797	1.000196	-0.000603	1.000196	-0.000603	-0.020933	-0.028797
5	0.030099	0.013949	0.999644	-0.00042	0.999644	-0.00042	-0.030099	-0.013949
6	-0.025252	0.011261	0.999745	0.000284	0.999745	0.000284	0.025252	-0.011261
7	-0.006346	-0.013277	1.000068	-8.42E-05	1.000068	-8.42E-05	0.006346	0.013277
8	-0.015126	-0.001713	0.999887	-2.59E-05	0.999887	-2.59E-05	0.015126	0.001713
9	0.001562	-0.013647	1.000092	2.13E-05	1.000092	2.13E-05	-0.001562	0.013647
10	-0.093384	0.01266	0.995711	0.001187	0.995711	0.001187	0.093384	-0.01266
11	0.037393	-0.008638	0.999338	0.000323	0.999338	0.000323	-0.037393	0.008638
12	0.043471	-0.00448	0.999065	0.000195	0.999065	0.000195	-0.043471	0.00448
13	0.016725	-0.004845	0.999872	8.1E-05	0.999872	8.1E-05	-0.016725	0.004845
14	-0.031538	-0.009178	0.999545	-0.00029	0.999545	-0.00029	0.031538	0.009178
15	0.020541	-0.009463	0.999834	0.000194	0.999834	0.000194	-0.020541	0.009463
16	0.006742	-0.016977	1.000121	0.000114	1.000121	0.000114	-0.006742	0.016977
17	0.000791	0.002957	1.000004	-2.34E-06	1.000004	-2.34E-06	-0.000791	-0.002957
18	0.008396	-0.009687	1.000012	8.13E-05	1.000012	8.13E-05	-0.008396	0.009687
19	0.046671	-0.010912	0.99897	0.00051	0.99897	0.00051	-0.046671	0.010912
20	0.051652	-0.007596	0.998694	0.000393	0.998694	0.000393	-0.051652	0.007596
21	-0.00994	0.02177	1.000188	0.000216	1.000188	0.000216	0.00994	-0.02177
22	-0.046872	0.002109	0.998903	9.89E-05	0.998903	9.89E-05	0.046872	-0.002109
23	0.004481	-0.005826	1.000007	2.61E-05	1.000007	2.61E-05	-0.004481	0.005826
24	0.035798	0.055434	1.000897	-0.001983	1.000897	-0.001983	-0.035798	-0.055434
25	-0.046413	0.012179	0.998997	0.000566	0.998997	0.000566	0.046413	-0.012179
26	0.0027	0.01628	1.000129	-4.39E-05	1.000129	-4.39E-05	-0.0027	-0.01628
27	0.038633	-0.005198	0.999267	0.000201	0.999267	0.000201	-0.038633	0.005198
28	0.024215	-0.005341	0.999721	0.000129	0.999721	0.000129	-0.024215	0.005341
29	-0.012669	0.010278	0.999973	0.00013	0.999973	0.00013	0.012669	-0.010278
30	0.000547	-0.005393	1.000014	2.95E-06	1.000014	2.95E-06	-0.000547	0.005393
31	0.058438	-0.007574	0.99832	0.000443	0.99832	0.000443	-0.058438	0.007574
32	0.036524	-0.008519	0.999369	0.000311	0.999369	0.000311	-0.036524	0.008519
33	0.012391	-0.013233	1.000011	0.000164	1.000011	0.000164	-0.012391	0.013233
34	-0.017511	-0.014255	0.999948	-0.00025	0.999948	-0.00025	0.017511	0.014255
35	-0.032069	-0.003908	0.999493	-0.000125	0.999493	-0.000125	0.032069	0.003908
36	0.032054	-0.007511	0.999514	0.000241	0.999514	0.000241	-0.032054	0.007511
37	-0.010732	0.00541	0.999957	5.81E-05	0.999957	5.81E-05	0.010732	-0.00541
38	-0.050326	-0.00928	0.998776	-0.000468	0.998776	-0.000468	0.050326	0.00928
39	-0.055732	-0.002714	0.998449	-0.000151	0.998449	-0.000151	0.055732	0.002714
40	0.041325	-0.008225	0.99918	0.00034	0.99918	0.00034	-0.041325	0.008225
41	-0.01327	0.002764	0.999916	3.67E-05	0.999916	3.67E-05	0.01327	-0.002764
42	-0.046355	-0.004205	0.998934	-0.000195	0.998934	-0.000195	0.046355	0.004205
43	-0.056336	0.007758	0.998442	0.000438	0.998442	0.000438	0.056336	-0.007758
44	-0.03717	-0.01309	0.999395	-0.000487	0.999395	-0.000487	0.03717	0.01309
45	0.002875	-0.017801	1.000154	5.12E-05	1.000154	5.12E-05	-0.002875	0.017801
46	-0.005078	-0.011933	1.000058	-6.06E-05	1.000058	-6.06E-05	0.005078	0.011933
47	-0.015691	0.003656	0.999884	5.74E-05	0.999884	5.74E-05	0.015691	-0.003656
48	-0.065805	0.019401	0.998022	0.001279	0.998022	0.001279	0.065805	-0.019401
49	-0.05863	0.008258	0.998314	0.000485	0.998314	0.000485	0.05863	-0.008258
50	0.011716	0.013154	1.000018	-0.000154	1.000018	-0.000154	-0.011716	-0.013154
51	0.040193	0.007079	0.999217	-0.000285	0.999217	-0.000285	-0.040193	-0.007079
52	-0.001674	0.010571	1.000054	1.77E-05	1.000054	1.77E-05	0.001674	-0.010571
53	0.012806	-0.010945	0.999978	0.00014	0.999978	0.00014	-0.012806	0.010945
54	-0.003148	-0.013804	1.00009	-4.34E-05	1.00009	-4.34E-05	0.003148	0.013804
55	-0.008125	0.017126	1.000114	0.000139	1.000114	0.000139	0.008125	-0.017126
56	0.064831	0.011841	0.997967	-0.000769	0.997967	-0.000769	-0.064831	-0.011841
57	-0.016649	-0.008523	0.999898	-0.000142	0.999898	-0.000142	0.016649	0.008523
58	-0.002607	-0.00179	0.999998	-4.67E-06	0.999998	-4.67E-06	0.002607	0.00179
59	-0.019612	-0.005833	0.999825	-0.000114	0.999825	-0.000114	0.019612	0.005833
60	0.060114	0.004311	0.998201	-0.00026	0.998201	-0.00026	-0.060114	-0.004311
61	0.05077	0.010853	0.99877	-0.000552	0.99877	-0.000552	-0.05077	-0.010853
62	0.024314	-0.007968	0.999736	0.000194	0.999736	0.000194	-0.024314	0.007968
63	0.025872	-0.009009	0.999706	0.000233	0.999706	0.000233	-0.025872	0.009009
64	-0.033383	0.02343	0.999718	0.000782	0.999718	0.000782	0.033383	-0.02343
65	-0.018864	-0.001101	0.999823	-2.08E-05	0.999823	-2.08E-05	0.018864	0.001101
66	0.050215	0.006084	0.998757	-0.000306	0.998757	-0.000306	-0.050215	-0.006084
67	0.05461	0.013317	0.998597	-0.000728	0.998597	-0.000728	-0.05461	-0.013317
68	0.010967	-0.005242	0.999954	5.75E-05	0.999954	5.75E-05	-0.010967	0.005242
69	0.011069	-0.024699	1.000244	0.000273	1.000244	0.000273	-0.011069	0.024699
70	-0.019589	-0.007053	0.999833	-0.000138	0.999833	-0.000138	0.019589	0.007053
71	-0.016116	0.01245	0.999948	0.000201	0.999948	0.000201	0.016116	-0.01245
72	-0.028759	-0.009912	0.999636	-0.000285	0.999636	-0.000285	0.028759	0.009912
73	0.050133	0.004087	0.998751	-0.000205	0.998751	-0.000205	-0.050133	-0.004087
74	-0.007409	-0.013109	1.000058	-9.71E-05	1.000058	-9.71E-05	0.007409	0.013109
75	0.038525	-0.007912	0.999289	0.000305	0.999289	0.000305	-0.038525	0.007912
76	0.017914	-0.001514	0.999841	2.71E-05	0.999841	2.71E-05	-0.017914	0.001514
77	0.017861	-0.001489	0.999842	2.66E-05	0.999842	2.66E-05	-0.017861	0.001489
78	0.017858	-0.001358	0.999841	2.43E-05	0.999841	2.43E-05	-0.017858	0.001358
79	-0.001015	-0.001189	1	-1.21E-06	1	-1.21E-06	0.001015	0.001189
80	-0.004541	-0.003207	0.999995	-1.46E-05	0.999995	-1.46E-05	0.004541	0.003207
81	-0.017349	0.016595	0.999987	0.000288	0.999987	0.000288	0.017349	-0.016595
82	0.033591	-0.011925	0.999507	0.000401	0.999507	0.000401	-0.033591	0.011925
83	-0.040801	0.007082	0.999192	0.000289	0.999192	0.000289	0.040801	-0.007082
84	0.042211	-0.011161	0.999171	0.000472	0.999171	0.000472	-0.042211	0.011161
85	0.046658	-0.010092	0.998962	0.000471	0.998962	0.000471	-0.046658	0.010092
86	-0.015348	-0.005853	0.999899	-8.98E-05	0.999899	-8.98E-05	0.015348	0.005853
87	-0.010175	0.002602	0.999952	2.65E-05	0.999952	2.65E-05	0.010175	-0.002602
88	-0.012617	-0.000237	0.99992	-2.99E-06	0.99992	-2.99E-06	0.012617	0.000237
89	-0.040264	0.014603	0.999296	0.000588	0.999296	0.000588	0.040264	-0.014603
90	0.001708	-0.000815	0.999999	1.39E-06	0.999999	1.39E-06	-0.001708	0.000815
91	-0.035616	-0.002066	0.999368	-7.36E-05	0.999368	-7.36E-05	0.035616	0.002066
92	-0.026469	-0.006657	0.999672	-0.000176	0.999672	-0.000176	0.026469	0.006657
93	0.006356	0.01977	1.000175	-0.000126	1.000175	-0.000126	-0.006356	-0.01977
94	-0.033611	0.005025	0.999448	0.000169	0.999448	0.000169	0.033611	-0.005025
95	0.018088	-0.007942	0.999868	0.000144	0.999868	0.000144	-0.018088	0.007942
96	0.006858	-0.018344	1.000145	0.000126	1.000145	0.000126	-0.006858	0.018344
97	0.01984	0.011408	0.999868	-0.000226	0.999868	-0.000226	-0.01984	-0.011408
98	-0.017057	-0.004268	0.999864	-7.28E-05	0.999864	-7.28E-05	0.017057	0.004268
99	0.048273	-0.002323	0.998837	0.000112	0.998837	0.000112	-0.048273	0.002323
100	0.023681	-0.005707	0.999736	0.000135	0.999736	0.000135	-0.023681	0.005707

	Alien - Printed							
	S11		S12		S21		S22	
	Real	Imaginary	Real	Imaginary	Real	Imaginary	Real	Imaginary
1	0.011866	-0.009466	0.999974	0.000112	0.999974	0.000112	-0.011866	0.009466
2	0.019821	-0.00095	0.999804	1.88E-05	0.999804	1.88E-05	-0.019821	0.00095
3	-0.007412	-0.005581	0.999988	-4.14E-05	0.999988	-4.14E-05	0.007412	0.005581
4	0.012417	0.004536	0.999933	-5.63E-05	0.999933	-5.63E-05	-0.012417	-0.004536
5	0.019936	-0.010741	0.999859	0.000214	0.999859	0.000214	-0.019936	0.010741
6	0.064103	-0.006832	0.997967	0.000439	0.997967	0.000439	-0.064103	0.006832
7	0.056841	-0.006695	0.998406	0.000381	0.998406	0.000381	-0.056841	0.006695
8	0.013851	-0.011853	0.999974	0.000164	0.999974	0.000164	-0.013851	0.011853
9	-0.018194	-0.005651	0.99985	-0.000103	0.99985	-0.000103	0.018194	0.005651
10	0.024791	0.009108	0.999734	-0.000226	0.999734	-0.000226	-0.024791	-0.009108
11	0.017337	-0.016399	0.999984	0.000284	0.999984	0.000284	-0.017337	0.016399
12	-0.009409	-0.001807	0.999957	-1.7E-05	0.999957	-1.7E-05	0.009409	0.001807
13	0.013131	-0.005847	0.999931	7.68E-05	0.999931	7.68E-05	-0.013131	0.005847
14	0.051547	0.00976	0.998718	-0.000504	0.998718	-0.000504	-0.051547	-0.00976
15	0.053259	0.006674	0.998603	-0.000356	0.998603	-0.000356	-0.053259	-0.006674
16	-0.016997	-0.007397	0.999883	-0.000126	0.999883	-0.000126	0.016997	0.007397
17	0.002488	-0.00697	1.000021	1.73E-05	1.000021	1.73E-05	-0.002488	0.00697
18	-0.00034	-0.009313	1.000043	-3.17E-06	1.000043	-3.17E-06	0.00034	0.009313
19	-0.026672	-0.002499	0.999647	-6.67E-05	0.999647	-6.67E-05	0.026672	0.002499
20	0.010707	-0.001997	0.999945	2.14E-05	0.999945	2.14E-05	-0.010707	0.001997
21	0.008634	0.009261	1.000006	-8E-05	1.000006	-8E-05	-0.008634	-0.009261
22	0.047828	0.030109	0.99931	-0.001441	0.99931	-0.001441	-0.047828	-0.030109
23	0.001605	-0.002436	1.000002	3.91E-06	1.000002	3.91E-06	-0.001605	0.002436
24	-0.037744	0.002276	0.99929	8.6E-05	0.99929	8.6E-05	0.037744	-0.002276
25	0.026211	0.02057	0.999868	-0.000539	0.999868	-0.000539	-0.026211	-0.02057
26	-0.019198	-0.014484	0.999921	-0.000278	0.999921	-0.000278	0.019198	0.014484
27	0.0314	-0.009085	0.999548	0.000285	0.999548	0.000285	-0.0314	0.009085
28	0.018938	-0.008241	0.999855	0.000156	0.999855	0.000156	-0.018938	0.008241
29	0.025686	0.00354	0.999676	-9.1E-05	0.999676	-9.1E-05	-0.025686	-0.00354
30	-0.076227	-0.006801	0.997114	-0.00052	0.997114	-0.00052	0.076227	0.006801
31	0.001706	0.000311	0.999999	-5.31E-07	0.999999	-5.31E-07	-0.001706	-0.000311
32	0.005249	-0.003085	0.999991	1.62E-05	0.999991	1.62E-05	-0.005249	0.003085
33	0.024192	0.0009	0.999708	-2.18E-05	0.999708	-2.18E-05	-0.024192	-0.0009
34	0.022674	-0.006332	0.999763	0.000144	0.999763	0.000144	-0.022674	0.006332
35	-0.012318	0.008862	0.999963	0.000109	0.999963	0.000109	0.012318	-0.008862
36	-0.033015	0.002187	0.999457	7.23E-05	0.999457	7.23E-05	0.033015	-0.002187
37	0.018078	-0.010203	0.999889	0.000184	0.999889	0.000184	-0.018078	0.010203
38	-0.006585	-0.005894	0.999996	-3.88E-05	0.999996	-3.88E-05	0.006585	0.005894
39	-0.006925	-0.006037	0.999994	-4.18E-05	0.999994	-4.18E-05	0.006925	0.006037
40	-0.006765	-0.006015	0.999995	-4.07E-05	0.999995	-4.07E-05	0.006765	0.006015
41	0.014159	-0.00967	0.999947	0.000137	0.999947	0.000137	-0.014159	0.00967
42	0.019027	-0.003415	0.999825	6.5E-05	0.999825	6.5E-05	-0.019027	0.003415
43	-0.027256	0.005308	0.999643	0.000145	0.999643	0.000145	0.027256	-0.005308
44	0.004273	0.005101	1.000004	-2.18E-05	1.000004	-2.18E-05	-0.004273	-0.005101
45	0.029837	-0.002058	0.999557	6.14E-05	0.999557	6.14E-05	-0.029837	0.002058
46	-0.01209	0.007212	0.999953	8.72E-05	0.999953	8.72E-05	0.01209	-0.007212
47	0.012479	-0.001873	0.999924	2.34E-05	0.999924	2.34E-05	-0.012479	0.001873
48	-0.017294	-0.003899	0.999858	-6.74E-05	0.999858	-6.74E-05	0.017294	0.003899
49	0.031205	0.019378	0.999701	-0.000605	0.999701	-0.000605	-0.031205	-0.019378
50	0.01537	0.013276	0.99997	-0.000204	0.99997	-0.000204	-0.01537	-0.013276
51	-0.008068	0.000473	0.999968	3.81E-06	0.999968	3.81E-06	0.008068	-0.000473
52	-0.048348	0.008302	0.998865	0.000402	0.998865	0.000402	0.048348	-0.008302
53	0.004634	-0.007236	1.000015	3.35E-05	1.000015	3.35E-05	-0.004634	0.007236
54	-0.016261	-0.014549	0.999974	-0.000237	0.999974	-0.000237	0.016261	0.014549
55	-0.042155	0.024353	0.999408	0.001027	0.999408	0.001027	0.042155	-0.024353
56	-0.023933	-0.008309	0.999748	-0.000199	0.999748	-0.000199	0.023933	0.008309
57	0.023676	0.005047	0.999732	-0.00012	0.999732	-0.00012	-0.023676	-0.005047
58	0.031468	-0.00646	0.999526	0.000203	0.999526	0.000203	-0.031468	0.00646
59	-0.063365	0.017283	0.998141	0.001097	0.998141	0.001097	0.063365	-0.017283
60	0.012853	-0.007989	0.999949	0.000103	0.999949	0.000103	-0.012853	0.007989
61	0.007209	-0.008078	1.000007	5.82E-05	1.000007	5.82E-05	-0.007209	0.008078
62	-0.026786	0.006258	0.999661	0.000168	0.999661	0.000168	0.026786	-0.006258
63	-0.028632	0.024474	0.99989	0.000701	0.99989	0.000701	0.028632	-0.024474
64	-0.006389	-0.002649	0.999983	-1.69E-05	0.999983	-1.69E-05	0.006389	0.002649
65	0.046474	-0.012449	0.998997	0.000579	0.998997	0.000579	-0.046474	0.012449
66	0.018604	-0.007547	0.999855	0.00014	0.999855	0.00014	-0.018604	0.007547
67	-0.044169	-0.003998	0.999032	-0.000177	0.999032	-0.000177	0.044169	0.003998
68	0.077863	0.005103	0.996977	-0.000399	0.996977	-0.000399	-0.077863	-0.005103
69	-0.023524	-0.005531	0.999739	-0.00013	0.999739	-0.00013	0.023524	0.005531
70	-0.013278	0.013726	1.000006	0.000182	1.000006	0.000182	0.013278	-0.013726
71	-0.013768	-0.014638	1.000012	-0.000202	1.000012	-0.000202	0.013768	0.014638
72	-0.022401	-0.00606	0.999767	-0.000136	0.999767	-0.000136	0.022401	0.00606
73	0.021271	-0.009975	0.999824	0.000212	0.999824	0.000212	-0.021271	0.009975
74	0.028467	-0.010179	0.999647	0.00029	0.999647	0.00029	-0.028467	0.010179
75	-0.069469	0.013441	0.997675	0.000936	0.997675	0.000936	0.069469	-0.013441
76	0.016782	-0.008556	0.999896	0.000144	0.999896	0.000144	-0.016782	0.008556
77	-0.014966	0.013075	0.999974	0.000196	0.999974	0.000196	0.014966	-0.013075
78	-0.050421	0.026696	0.999086	0.001347	0.999086	0.001347	0.050421	-0.026696
79	-0.003056	0.025672	1.000325	7.84E-05	1.000325	7.84E-05	0.003056	-0.025672
80	0.003253	0.003757	1.000002	-1.22E-05	1.000002	-1.22E-05	-0.003253	-0.003757
81	-0.036994	0.012464	0.999393	0.000461	0.999393	0.000461	0.036994	-0.012464
82	-0.054702	-0.01661	0.998641	-0.00091	0.998641	-0.00091	0.054702	0.01661
83	0.016322	-1.76E-05	0.999867	2.87E-07	0.999867	2.87E-07	-0.016322	1.76E-05
84	-0.029955	-0.016273	0.999684	-0.000488	0.999684	-0.000488	0.029955	0.016273
85	-0.028177	-0.007432	0.999631	-0.000209	0.999631	-0.000209	0.028177	0.007432
86	-0.006985	-0.003554	0.999982	-2.48E-05	0.999982	-2.48E-05	0.006985	0.003554
87	0.033441	-0.005904	0.999458	0.000198	0.999458	0.000198	-0.033441	0.005904
88	0.045107	0.007205	0.999008	-0.000325	0.999008	-0.000325	-0.045107	-0.007205
89	-0.035664	-0.009671	0.999411	-0.000345	0.999411	-0.000345	0.035664	0.009671
90	-0.00229	0.010342	1.000051	2.37E-05	1.000051	2.37E-05	0.00229	-0.010342
91	-0.017607	0.025923	1.000181	0.000456	1.000181	0.000456	0.017607	-0.025923
92	0.026583	0.008692	0.999684	-0.000231	0.999684	-0.000231	-0.026583	-0.008692
93	0.018473	0.01436	0.999933	-0.000265	0.999933	-0.000265	-0.018473	-0.01436
94	0.039443	-0.001932	0.999224	7.63E-05	0.999224	7.63E-05	-0.039443	0.001932
95	-0.044352	-0.009483	0.999061	-0.000421	0.999061	-0.000421	0.044352	0.009483
96	-0.053232	-0.005147	0.998595	-0.000274	0.998595	-0.000274	0.053232	0.005147
97	-0.013223	-0.011447	0.999978	-0.000151	0.999978	-0.000151	0.013223	0.011447
98	0.006198	0.001974	0.999983	-1.22E-05	0.999983	-1.22E-05	-0.006198	-0.001974
99	0.032417	-0.00852	0.999511	0.000276	0.999511	0.000276	-0.032417	0.00852
100	0.013928	0.008627	0.99994	-0.00012	0.99994	-0.00012	-0.013928	-0.008627

	TI - Original							
	S11		S12		S21		S22	
	Real	Imaginary	Real	Imaginary	Real	Imaginary	Real	Imaginary
1	-0.017762	-0.004714	0.999853	-8.37E-05	0.999853	-8.37E-05	0.017762	0.004714
2	0.031	-0.001227	0.99952	3.81E-05	0.99952	3.81E-05	-0.031	0.001227
3	0.034378	-0.001902	0.999411	6.54E-05	0.999411	6.54E-05	-0.034378	0.001902
4	0.00415	0.006812	1.000015	-2.83E-05	1.000015	-2.83E-05	-0.00415	-0.006812
5	-0.001677	-0.002086	1.000001	-3.5E-06	1.000001	-3.5E-06	0.001677	0.002086
6	0.011392	0.022016	1.000177	-0.000251	1.000177	-0.000251	-0.011392	-0.022016
7	0.035415	0.007405	0.9994	-0.000262	0.9994	-0.000262	-0.035415	-0.007405
8	-0.020134	0.022442	1.000049	0.000452	1.000049	0.000452	0.020134	-0.022442
9	-0.020618	-0.004774	0.999799	-9.85E-05	0.999799	-9.85E-05	0.020618	0.004774
10	0.023651	-0.003836	0.999728	9.08E-05	0.999728	9.08E-05	-0.023651	0.003836
11	0.007234	0.003892	0.999981	-2.82E-05	0.999981	-2.82E-05	-0.007234	-0.003892
12	0.019583	-0.004992	0.999821	9.78E-05	0.999821	9.78E-05	-0.019583	0.004992
13	-0.016741	0.004034	0.999868	6.75E-05	0.999868	6.75E-05	0.016741	-0.004034
14	0.018753	0.000125	0.999824	-2.35E-06	0.999824	-2.35E-06	-0.018753	-0.000125
15	-0.012184	0.001117	0.999926	1.36E-05	0.999926	1.36E-05	0.012184	-0.001117
16	-0.024246	0.016081	0.999835	0.00039	0.999835	0.00039	0.024246	-0.016081
17	0.048512	0.010094	0.998874	-0.00049	0.998874	-0.00049	-0.048512	-0.010094
18	0.029839	0.012438	0.999632	-0.000371	0.999632	-0.000371	-0.029839	-0.012438
19	0.004122	-0.006573	1.000013	2.71E-05	1.000013	2.71E-05	-0.004122	0.006573
20	-0.001887	0.018012	1.00016	3.4E-05	1.00016	3.4E-05	0.001887	-0.018012
21	-0.005122	0.014727	1.000095	7.54E-05	1.000095	7.54E-05	0.005122	-0.014727
22	0.04539	-0.001796	0.998971	8.16E-05	0.998971	8.16E-05	-0.04539	0.001796
23	0.007647	-0.007822	1.000001	5.98E-05	1.000001	5.98E-05	-0.007647	0.007822
24	0.005018	0.006427	1.000008	-3.23E-05	1.000008	-3.23E-05	-0.005018	-0.006427
25	0.036272	-0.008548	0.999379	0.00031	0.999379	0.00031	-0.036272	0.008548
26	-0.027186	-0.001885	0.999632	-5.13E-05	0.999632	-5.13E-05	0.027186	0.001885
27	-0.033875	0.002871	0.99943	9.73E-05	0.99943	9.73E-05	0.033875	-0.002871
28	-0.024823	-0.002265	0.999694	-5.62E-05	0.999694	-5.62E-05	0.024823	0.002265
29	0.030771	0.000852	0.999527	-2.62E-05	0.999527	-2.62E-05	-0.030771	-0.000852
30	0.031623	0.004291	0.999509	-0.000136	0.999509	-0.000136	-0.031623	-0.004291
31	0.002566	0.004883	1.000009	-1.25E-05	1.000009	-1.25E-05	-0.002566	-0.004883
32	0.035431	-0.008504	0.999408	0.000301	0.999408	0.000301	-0.035431	0.008504
33	0.028503	-0.008246	0.999628	0.000235	0.999628	0.000235	-0.028503	0.008246
34	-0.010533	0.003448	0.99995	3.63E-05	0.99995	3.63E-05	0.010533	-0.003448
35	0.021917	-0.001888	0.999762	4.14E-05	0.999762	4.14E-05	-0.021917	0.001888
36	0.023482	0.002266	0.999727	-5.32E-05	0.999727	-5.32E-05	-0.023482	-0.002266
37	-0.020315	0.003164	0.999799	6.43E-05	0.999799	6.43E-05	0.020315	-0.003164
38	0.002569	-0.001635	0.999998	4.2E-06	0.999998	4.2E-06	-0.002569	0.001635
39	0.003578	0.004929	1.000006	-1.76E-05	1.000006	-1.76E-05	-0.003578	-0.004929
40	-0.033446	-0.003458	0.999447	-0.000116	0.999447	-0.000116	0.033446	0.003458
41	-0.002498	-0.008922	1.000037	-2.23E-05	1.000037	-2.23E-05	0.002498	0.008922
42	0.007972	-0.010811	1.000027	8.62E-05	1.000027	8.62E-05	-0.007972	0.010811
43	-0.00564	-0.00305	0.999989	-1.72E-05	0.999989	-1.72E-05	0.00564	0.00305
44	-0.040769	-0.001275	0.999169	-5.2E-05	0.999169	-5.2E-05	0.040769	0.001275
45	0.024438	-0.009221	0.999744	0.000225	0.999744	0.000225	-0.024438	0.009221
46	-0.011465	-0.002941	0.999939	-3.37E-05	0.999939	-3.37E-05	0.011465	0.002941
47	-0.007549	-0.003525	0.999978	-2.66E-05	0.999978	-2.66E-05	0.007549	0.003525
48	-0.001844	0.011606	1.000066	2.14E-05	1.000066	2.14E-05	0.001844	-0.011606
49	-0.008803	-0.00196	0.999963	-1.73E-05	0.999963	-1.73E-05	0.008803	0.00196
50	-0.021193	-0.006761	0.999798	-0.000143	0.999798	-0.000143	0.021193	0.006761
51	0.011866	-0.001529	0.999931	1.81E-05	0.999931	1.81E-05	-0.011866	0.001529
52	0.036702	0.003723	0.999333	-0.000137	0.999333	-0.000137	-0.036702	-0.003723
53	0.011058	-0.010211	0.999991	0.000113	0.999991	0.000113	-0.011058	0.010211
54	-0.030221	0.012185	0.999618	0.000368	0.999618	0.000368	0.030221	-0.012185
55	0.027168	-0.005293	0.999645	0.000144	0.999645	0.000144	-0.027168	0.005293
56	0.019404	-0.004588	0.999822	8.9E-05	0.999822	8.9E-05	-0.019404	0.004588
57	-0.031794	-0.008794	0.999533	-0.00028	0.999533	-0.00028	0.031794	0.008794
58	-0.018989	0.009941	0.999869	0.000189	0.999869	0.000189	0.018989	-0.009941
59	0.021989	0.003954	0.999766	-8.7E-05	0.999766	-8.7E-05	-0.021989	-0.003954
60	0.032846	-0.003085	0.999465	0.000101	0.999465	0.000101	-0.032846	0.003085
61	0.010792	0.006929	0.999966	-7.48E-05	0.999966	-7.48E-05	-0.010792	-0.006929
62	0.030149	-0.006122	0.999564	0.000185	0.999564	0.000185	-0.030149	0.006122
63	0.009463	-0.009754	1.000003	9.23E-05	1.000003	9.23E-05	-0.009463	0.009754
64	-0.017505	-0.011438	0.999912	-0.0002	0.999912	-0.0002	0.017505	0.011438
65	-0.01003	-0.009951	0.999999	-9.98E-05	0.999999	-9.98E-05	0.01003	0.009951
66	0.002111	0.003959	1.000006	-8.36E-06	1.000006	-8.36E-06	-0.002111	-0.003959
67	0.000173	-0.008949	1.00004	1.55E-06	1.00004	1.55E-06	-0.000173	0.008949
68	-0.012608	0.008881	0.99996	0.000112	0.99996	0.000112	0.012608	-0.008881
69	0.000779	-0.005844	1.000017	4.55E-06	1.000017	4.55E-06	-0.000779	0.005844
70	-0.004211	-0.005888	1.000008	-2.48E-05	1.000008	-2.48E-05	0.004211	0.005888
71	0.01336	-0.005031	0.999923	6.72E-05	0.999923	6.72E-05	-0.01336	0.005031
72	0.016979	-0.000628	0.999856	1.07E-05	0.999856	1.07E-05	-0.016979	0.000628
73	0.011758	-0.004078	0.999939	4.8E-05	0.999939	4.8E-05	-0.011758	0.004078
74	-0.002251	-0.008762	1.000036	-1.97E-05	1.000036	-1.97E-05	0.002251	0.008762
75	0.024338	-0.01546	0.999823	0.000376	0.999823	0.000376	-0.024338	0.01546
76	0.021613	0.00364	0.999773	-7.87E-05	0.999773	-7.87E-05	-0.021613	-0.00364
77	0.003658	-0.011138	1.000055	4.07E-05	1.000055	4.07E-05	-0.003658	0.011138
78	0.007574	-0.011571	1.000038	8.76E-05	1.000038	8.76E-05	-0.007574	0.011571
79	-0.011037	-0.00086	0.999939	-9.49E-06	0.999939	-9.49E-06	0.011037	0.00086
80	-0.025809	-0.002884	0.999671	-7.45E-05	0.999671	-7.45E-05	0.025809	0.002884
81	-0.039936	0.01061	0.999259	0.000424	0.999259	0.000424	0.039936	-0.01061
82	-0.009118	0.004939	0.999971	4.5E-05	0.999971	4.5E-05	0.009118	-0.004939
83	-0.006988	0.005415	0.99999	3.78E-05	0.99999	3.78E-05	0.006988	-0.005415
84	-0.039654	-0.002148	0.999216	-8.53E-05	0.999216	-8.53E-05	0.039654	0.002148
85	-0.010451	-0.007223	0.999971	-7.55E-05	0.999971	-7.55E-05	0.010451	0.007223
86	-0.003499	0.006723	1.000016	2.35E-05	1.000016	2.35E-05	0.003499	-0.006723
87	0.015201	-0.004445	0.999894	6.76E-05	0.999894	6.76E-05	-0.015201	0.004445
88	-0.019145	-0.006709	0.999839	-0.000128	0.999839	-0.000128	0.019145	0.006709
89	-0.039873	0.002384	0.999208	9.51E-05	0.999208	9.51E-05	0.039873	-0.002384
90	-0.006999	-0.008082	1.000008	-5.66E-05	1.000008	-5.66E-05	0.006999	0.008082
91	-0.002002	-0.011619	1.000066	-2.33E-05	1.000066	-2.33E-05	0.002002	0.011619
92	-0.020114	0.001056	0.999798	2.12E-05	0.999798	2.12E-05	0.020114	-0.001056
93	-0.026953	-0.004981	0.999649	-0.000134	0.999649	-0.000134	0.026953	0.004981
94	0.009525	-0.005429	0.999969	5.17E-05	0.999969	5.17E-05	-0.009525	0.005429
95	0.004085	-0.000477	0.999992	1.95E-06	0.999992	1.95E-06	-0.004085	0.000477
96	-0.021037	-0.001574	0.99978	-3.31E-05	0.99978	-3.31E-05	0.021037	0.001574
97	-0.022819	0.028581	1.000148	0.000652	1.000148	0.000652	0.022819	-0.028581
98	-0.012371	0.004533	0.999934	5.61E-05	0.999934	5.61E-05	0.012371	-0.004533
99	0.011766	0.002528	0.999934	-2.98E-05	0.999934	-2.98E-05	-0.011766	-0.002528
100	-0.028224	0.008649	0.999639	0.000244	0.999639	0.000244	0.028224	-0.008649

	TI - Printed							
	S11		S12		S21		S22	
	Real	Imaginary	Real	Imaginary	Real	Imaginary	Real	Imaginary
1	0.013323	-0.010549	0.999967	0.000141	0.999967	0.000141	-0.013323	0.010549
2	0.006625	-0.00542	0.999993	3.59E-05	0.999993	3.59E-05	-0.006625	0.00542
3	0.023606	-0.014622	0.999828	0.000345	0.999828	0.000345	-0.023606	0.014622
4	-0.005965	0.002729	0.999986	1.63E-05	0.999986	1.63E-05	0.005965	-0.002729
5	0.008357	-0.000313	0.999965	2.62E-06	0.999965	2.62E-06	-0.008357	0.000313
6	-0.005317	0.018952	1.000165	0.000101	1.000165	0.000101	0.005317	-0.018952
7	0.002862	-0.00756	1.000024	2.16E-05	1.000024	2.16E-05	-0.002862	0.00756
8	0.015242	-0.00938	0.999928	0.000143	0.999928	0.000143	-0.015242	0.00938
9	0.005346	-0.000108	0.999986	5.78E-07	0.999986	5.78E-07	-0.005346	0.000108
10	0.02446	0.005152	0.999714	-0.000126	0.999714	-0.000126	-0.02446	-0.005152
11	-0.009223	0.001677	0.999959	1.55E-05	0.999959	1.55E-05	0.009223	-0.001677
12	-0.002619	0.001419	0.999998	3.72E-06	0.999998	3.72E-06	0.002619	-0.001419
13	-0.013991	-0.008358	0.999937	-0.000117	0.999937	-0.000117	0.013991	0.008358
14	0.020782	-0.003283	0.999789	6.82E-05	0.999789	6.82E-05	-0.020782	0.003283
15	0.033501	-0.006118	0.999457	0.000205	0.999457	0.000205	-0.033501	0.006118
16	-0.024663	-0.002316	0.999699	-5.71E-05	0.999699	-5.71E-05	0.024663	0.002316
17	-0.009427	0.003598	0.999962	3.39E-05	0.999962	3.39E-05	0.009427	-0.003598
18	0.023466	-0.000527	0.999725	1.24E-05	0.999725	1.24E-05	-0.023466	0.000527
19	-0.022807	-0.003149	0.999745	-7.18E-05	0.999745	-7.18E-05	0.022807	0.003149
20	-0.00933	-0.005298	0.999971	-4.94E-05	0.999971	-4.94E-05	0.00933	0.005298
21	0.002478	0.002326	1	-5.76E-06	1	-5.76E-06	-0.002478	-0.002326
22	0.017044	0.002931	0.999859	-5E-05	0.999859	-5E-05	-0.017044	-0.002931
23	-0.028615	0.008402	0.999626	0.000241	0.999626	0.000241	0.028615	-0.008402
24	-0.014451	-0.001092	0.999896	-1.58E-05	0.999896	-1.58E-05	0.014451	0.001092
25	-0.005501	0.002842	0.999989	1.56E-05	0.999989	1.56E-05	0.005501	-0.002842
26	0.006096	0.006941	1.000006	-4.23E-05	1.000006	-4.23E-05	-0.006096	-0.006941
27	-0.015196	-0.006029	0.999903	-9.16E-05	0.999903	-9.16E-05	0.015196	0.006029
28	-0.00213	0.015468	1.000117	3.29E-05	1.000117	3.29E-05	0.00213	-0.015468
29	0.00378	-0.00084	0.999993	3.18E-06	0.999993	3.18E-06	-0.00378	0.00084
30	-0.006532	-0.005926	0.999996	-3.87E-05	0.999996	-3.87E-05	0.006532	0.005926
31	-0.022303	0.003592	0.999758	8.01E-05	0.999758	8.01E-05	0.022303	-0.003592
32	0.016837	-0.004949	0.999871	8.33E-05	0.999871	8.33E-05	-0.016837	0.004949
33	0.019691	-0.005469	0.999821	0.000108	0.999821	0.000108	-0.019691	0.005469
34	0.000508	0.004544	1.00001	-2.31E-06	1.00001	-2.31E-06	-0.000508	-0.004544
35	-0.024683	0.000945	0.999696	2.33E-05	0.999696	2.33E-05	0.024683	-0.000945
36	0.028293	-0.007501	0.999628	0.000212	0.999628	0.000212	-0.028293	0.007501
37	0.02592	0.002229	0.999666	-5.78E-05	0.999666	-5.78E-05	-0.02592	-0.002229
38	0.014952	-0.006857	0.999912	0.000103	0.999912	0.000103	-0.014952	0.006857
39	-0.017636	0.000575	0.999845	1.01E-05	0.999845	1.01E-05	0.017636	-0.000575
40	-0.021133	0.002004	0.999779	4.24E-05	0.999779	4.24E-05	0.021133	-0.002004
41	0.004499	-0.000544	0.99999	2.45E-06	0.99999	2.45E-06	-0.004499	0.000544
42	-0.003816	0.008437	1.000028	3.22E-05	1.000028	3.22E-05	0.003816	-0.008437
43	-0.004243	0.001888	0.999993	8.01E-06	0.999993	8.01E-06	0.004243	-0.001888
44	-0.012378	0.011977	0.999995	0.000148	0.999995	0.000148	0.012378	-0.011977
45	-0.02577	0.001118	0.999669	2.88E-05	0.999669	2.88E-05	0.02577	-0.001118
46	-0.003951	0.004874	1.000004	1.93E-05	1.000004	1.93E-05	0.003951	-0.004874
47	-0.011228	-0.002024	0.999939	-2.27E-05	0.999939	-2.27E-05	0.011228	0.002024
48	0.000361	-0.006423	1.000021	2.32E-06	1.000021	2.32E-06	-0.000361	0.006423
49	-0.017387	-0.002567	0.999852	-4.46E-05	0.999852	-4.46E-05	0.017387	0.002567
50	-0.009995	0.007742	0.99998	7.74E-05	0.99998	7.74E-05	0.009995	-0.007742
51	-0.002243	-0.000497	0.999998	-1.12E-06	0.999998	-1.12E-06	0.002243	0.000497
52	-0.007251	-0.005907	0.999991	-4.28E-05	0.999991	-4.28E-05	0.007251	0.005907
53	-0.001814	0.005583	1.000014	1.01E-05	1.000014	1.01E-05	0.001814	-0.005583
54	0.014641	-0.002436	0.999896	3.57E-05	0.999896	3.57E-05	-0.014641	0.002436
55	0.005157	-0.006599	1.000008	3.4E-05	1.000008	3.4E-05	-0.005157	0.006599
56	-0.004723	-0.004978	1.000001	-2.35E-05	1.000001	-2.35E-05	0.004723	0.004978
57	2.85E-05	0.001693	1.000001	-4.82E-08	1.000001	-4.82E-08	-2.85E-05	-0.001693
58	0.024282	0.003391	0.999711	-8.24E-05	0.999711	-8.24E-05	-0.024282	-0.003391
59	-0.022308	0.002991	0.999756	6.67E-05	0.999756	6.67E-05	0.022308	-0.002991
60	-0.011236	0.002698	0.999941	3.03E-05	0.999941	3.03E-05	0.011236	-0.002698
61	0.002481	-0.006353	1.000017	1.58E-05	1.000017	1.58E-05	-0.002481	0.006353
62	0.008709	0.010273	1.000015	-8.95E-05	1.000015	-8.95E-05	-0.008709	-0.010273
63	0.012195	-0.000346	0.999926	4.22E-06	0.999926	4.22E-06	-0.012195	0.000346
64	-0.003448	-0.00669	1.000016	-2.31E-05	1.000016	-2.31E-05	0.003448	0.00669
65	-0.021008	-0.001896	0.999781	-3.98E-05	0.999781	-3.98E-05	0.021008	0.001896
66	0.01862	0.006635	0.999849	-0.000124	0.999849	-0.000124	-0.01862	-0.006635
67	0.002334	-0.006236	1.000017	1.46E-05	1.000017	1.46E-05	-0.002334	0.006236
68	-0.009564	-0.003342	0.99996	-3.2E-05	0.99996	-3.2E-05	0.009564	0.003342
69	-0.017278	0.001347	0.999852	2.33E-05	0.999852	2.33E-05	0.017278	-0.001347
70	0.017541	-0.000986	0.999847	1.73E-05	0.999847	1.73E-05	-0.017541	0.000986
71	0.029203	-0.003317	0.999579	9.69E-05	0.999579	9.69E-05	-0.029203	0.003317
72	-0.008282	-0.005137	0.999979	-4.25E-05	0.999979	-4.25E-05	0.008282	0.005137
73	-0.030226	-0.000682	0.999543	-2.06E-05	0.999543	-2.06E-05	0.030226	0.000682
74	0.002262	-0.006083	1.000016	1.38E-05	1.000016	1.38E-05	-0.002262	0.006083
75	0.031897	-0.006687	0.999514	0.000213	0.999514	0.000213	-0.031897	0.006687
76	0.015624	0.000274	0.999878	-4.28E-06	0.999878	-4.28E-06	-0.015624	-0.000274
77	0.017224	0.000599	0.999852	-1.03E-05	0.999852	-1.03E-05	-0.017224	-0.000599
78	0.032601	-0.00244	0.999471	7.96E-05	0.999471	7.96E-05	-0.032601	0.00244
79	-0.001607	-0.003728	1.000006	-5.99E-06	1.000006	-5.99E-06	0.001607	0.003728
80	-0.000482	-0.004062	1.000008	-1.96E-06	1.000008	-1.96E-06	0.000482	0.004062
81	0.006694	0.018472	1.000148	-0.000124	1.000148	-0.000124	-0.006694	-0.018472
82	0.02877	0.024301	0.999882	-0.000699	0.999882	-0.000699	-0.02877	-0.024301
83	-0.008252	-0.000461	0.999966	-3.81E-06	0.999966	-3.81E-06	0.008252	0.000461
84	0.004778	0.002287	0.999991	-1.09E-05	0.999991	-1.09E-05	-0.004778	-0.002287
85	-0.006444	0.007	1.000004	4.51E-05	1.000004	4.51E-05	0.006444	-0.007
86	0.014675	-0.003272	0.999898	4.8E-05	0.999898	4.8E-05	-0.014675	0.003272
87	-0.00614	0.00244	0.999984	1.5E-05	0.999984	1.5E-05	0.00614	-0.00244
88	-0.002826	0.014476	1.000101	4.09E-05	1.000101	4.09E-05	0.002826	-0.014476
89	0.008331	-0.002124	0.999968	1.77E-05	0.999968	1.77E-05	-0.008331	0.002124
90	-0.001904	0.002735	1.000002	5.21E-06	1.000002	5.21E-06	0.001904	-0.002735
91	-0.042292	-0.005998	0.999123	-0.000254	0.999123	-0.000254	0.042292	0.005998
92	-0.01085	-0.004256	0.99995	-4.62E-05	0.99995	-4.62E-05	0.01085	0.004256
93	0.01901	-0.006574	0.999841	0.000125	0.999841	0.000125	-0.01901	0.006574
94	-0.009349	0.001085	0.999957	1.01E-05	0.999957	1.01E-05	0.009349	-0.001085
95	-0.010111	-0.009888	0.999998	-1E-04	0.999998	-1E-04	0.010111	0.009888
96	-0.009011	0.001043	0.99996	9.4E-06	0.99996	9.4E-06	0.009011	-0.001043
97	0.012234	0.002135	0.999927	-2.61E-05	0.999927	-2.61E-05	-0.012234	-0.002135
98	0.010424	0.01249	1.000024	-0.00013	1.000024	-0.00013	-0.010424	-0.01249
99	-0.042302	-0.005874	0.999122	-0.000249	0.999122	-0.000249	0.042302	0.005874
100	0.005776	-0.002971	0.999988	1.72E-05	0.999988	1.72E-05	-0.005776	0.002971

	Rafsec - Original							
	S11		S12		S21		S22	
	Real	Imaginary	Real	Imaginary	Real	Imaginary	Real	Imaginary
1	-0.160571	-0.047053	0.067701	0.012767	0.067701	0.012767	0.808202	0.508163
2	-0.160389	-0.046881	0.069126	0.015839	0.069126	0.015839	0.762315	0.536501
3	-0.160425	-0.046899	0.068766	0.015431	0.068766	0.015431	0.768182	0.529863
4	-0.160681	-0.046804	0.065131	0.015444	0.065131	0.015444	0.762674	0.471424
5	-0.160622	-0.046899	0.066301	0.014494	0.066301	0.014494	0.779101	0.488966
6	-0.160473	-0.046954	0.068448	0.014511	0.068448	0.014511	0.782282	0.523007
7	-0.160335	-0.046794	0.069345	0.017145	0.069345	0.017145	0.741358	0.542807
8	-0.160848	-0.047079	0.064153	0.011065	0.064153	0.011065	0.829104	0.452228
9	-0.160442	-0.046716	0.067694	0.017579	0.067694	0.017579	0.731004	0.516158
10	-0.160643	-0.046892	0.06601	0.014494	0.06601	0.014494	0.77874	0.484364
11	-0.160624	-0.046799	0.065829	0.015753	0.065829	0.015753	0.75843	0.482977
12	-0.160543	-0.046998	0.067786	0.013611	0.067786	0.013611	0.795263	0.510952
13	-0.16067	-0.047071	0.066503	0.012037	0.066503	0.012037	0.817445	0.488651
14	-0.160615	-0.047029	0.06702	0.012854	0.06702	0.012854	0.805727	0.497808
15	-0.160741	-0.046941	0.064949	0.013412	0.064949	0.013412	0.794444	0.466579
16	-0.160614	-0.047031	0.067037	0.012834	0.067037	0.012834	0.806067	0.498039
17	-0.160726	-0.04687	0.064841	0.01441	0.064841	0.01441	0.778797	0.46586
18	-0.160538	-0.046968	0.0677	0.014011	0.0677	0.014011	0.788834	0.510289
19	-0.160339	-0.04684	0.069524	0.016573	0.069524	0.016573	0.75117	0.544543
20	-0.16048	-0.04699	0.068544	0.01403	0.068544	0.01403	0.790074	0.523599
21	-0.160425	-0.046805	0.068312	0.016587	0.068312	0.016587	0.748508	0.524661
22	-0.160595	-0.046872	0.066527	0.014968	0.066527	0.014968	0.771889	0.493191
23	-0.1605	-0.046885	0.067776	0.015251	0.067776	0.015251	0.769276	0.513608
24	-0.160617	-0.046935	0.066535	0.01406	0.066535	0.01406	0.786261	0.492062
25	-0.160405	-0.046861	0.068827	0.015994	0.068827	0.015994	0.759183	0.531943
26	-0.160449	-0.046983	0.068893	0.014276	0.068893	0.014276	0.786878	0.529591
27	-0.160677	-0.046873	0.065485	0.014587	0.065485	0.014587	0.77665	0.476184
28	-0.160626	-0.047005	0.066752	0.013114	0.066752	0.013114	0.801313	0.494072
29	-0.160611	-0.046941	0.066645	0.014019	0.066645	0.014019	0.78706	0.493729
30	-0.160613	-0.04703	0.067043	0.01286	0.067043	0.01286	0.805679	0.498173
31	-0.16068	-0.047084	0.066436	0.011811	0.066436	0.011811	0.820769	0.4873
32	-0.16069	-0.047027	0.066021	0.012523	0.066021	0.012523	0.809349	0.482004
33	-0.160629	-0.046803	0.065783	0.015682	0.065783	0.015682	0.759515	0.482152
34	-0.160791	-0.047015	0.064619	0.012206	0.064619	0.012206	0.812532	0.460334
35	-0.160524	-0.046796	0.067067	0.016241	0.067067	0.016241	0.752116	0.503696
36	-0.160618	-0.047034	0.066995	0.012781	0.066995	0.012781	0.806819	0.497307
37	-0.16055	-0.046967	0.067542	0.013972	0.067542	0.013972	0.789187	0.507741
38	-0.160679	-0.04694	0.06576	0.013701	0.06576	0.013701	0.790859	0.479482

	Rafsec - Printed							
	S11		S12		S21		S22	
	Real	Imaginary	Real	Imaginary	Real	Imaginary	Real	Imaginary
1	0.024249	-0.020927	0.999925	0.000508	0.999925	0.000508	-0.024249	0.020927
2	-0.008531	-0.018664	1.000138	-0.000159	1.000138	-0.000159	0.008531	0.018664
3	0.060072	-0.006895	0.998218	0.000415	0.998218	0.000415	-0.060072	0.006895
4	0.041762	-0.002304	0.99913	9.63E-05	0.99913	9.63E-05	-0.041762	0.002304
5	0.039411	0.01881	0.9994	-0.000742	0.9994	-0.000742	-0.039411	-0.01881
6	0.005063	0.016865	1.000129	-8.54E-05	1.000129	-8.54E-05	-0.005063	-0.016865
7	-0.003105	-0.025308	1.000315	-7.86E-05	1.000315	-7.86E-05	0.003105	0.025308
8	-0.025559	-0.022606	0.999929	-0.000578	0.999929	-0.000578	0.025559	0.022606
9	0.021704	-0.01244	0.999842	0.00027	0.999842	0.00027	-0.021704	0.01244
10	0.010733	0.021362	1.000171	-0.000229	1.000171	-0.000229	-0.010733	-0.021362
11	0.063793	0.036326	0.998627	-0.002321	0.998627	-0.002321	-0.063793	-0.036326
12	-0.0061	0.034877	1.000589	0.000213	1.000589	0.000213	0.0061	-0.034877
13	-0.045083	0.042364	0.999883	0.00191	0.999883	0.00191	0.045083	-0.042364
14	0.021218	-0.008758	0.999813	0.000186	0.999813	0.000186	-0.021218	0.008758
15	-0.005072	0.057825	1.001658	0.000293	1.001658	0.000293	0.005072	-0.057825
16	-0.055018	0.007112	0.998511	0.000392	0.998511	0.000392	0.055018	-0.007112
17	-0.043558	-0.005805	0.999068	-0.000253	0.999068	-0.000253	0.043558	0.005805
18	0.02847	-0.017742	0.999752	0.000505	0.999752	0.000505	-0.02847	0.017742
19	-0.029641	0.001085	0.999561	3.22E-05	0.999561	3.22E-05	0.029641	-0.001085
20	-0.025605	-0.025108	0.999988	-0.000643	0.999988	-0.000643	0.025605	0.025108
21	0.001064	-0.025748	1.000331	2.74E-05	1.000331	2.74E-05	-0.001064	0.025748
22	-0.029784	-0.002331	0.999559	-6.95E-05	0.999559	-6.95E-05	0.029784	0.002331
23	-0.016431	-0.005213	0.999879	-8.57E-05	0.999879	-8.57E-05	0.016431	0.005213
24	-0.030167	0.003486	0.999551	0.000105	0.999551	0.000105	0.030167	-0.003486
25	0.02837	-0.017864	0.999757	0.000507	0.999757	0.000507	-0.02837	0.017864
26	-0.034046	-0.038542	1.000164	-0.001312	1.000164	-0.001312	0.034046	0.038542
27	-0.014388	-0.01952	1.000087	-0.000281	1.000087	-0.000281	0.014388	0.01952
28	-0.016849	-0.023297	1.00013	-0.000392	1.00013	-0.000392	0.016849	0.023297
29	-0.002238	-0.028053	1.000391	-6.28E-05	1.000391	-6.28E-05	0.002238	0.028053
30	0.023097	-0.002232	0.999736	5.16E-05	0.999736	5.16E-05	-0.023097	0.002232
31	0.026752	-0.012439	0.99972	0.000333	0.99972	0.000333	-0.026752	0.012439
32	-0.013503	-0.024959	1.00022	-0.000337	1.00022	-0.000337	0.013503	0.024959
33	-0.024179	0.02912	1.000132	0.000704	1.000132	0.000704	0.024179	-0.02912
34	-0.008323	0.018045	1.000128	0.00015	1.000128	0.00015	0.008323	-0.018045
35	-0.006705	0.019339	1.000165	0.00013	1.000165	0.00013	0.006705	-0.019339
36	-0.007218	-0.001561	0.999975	-1.13E-05	0.999975	-1.13E-05	0.007218	0.001561
37	0.046506	0.087141	1.00272	-0.004042	1.00272	-0.004042	-0.046506	-0.087141
38	0.014643	-0.016294	1.000026	0.000239	1.000026	0.000239	-0.014643	0.016294

APPENDIX I

THE SOURCE CODE FOR THE SOFTWARE TOOL

```
'************************************************
'* RFID Tag Tester  Software programm
'* (c) 2007, Leonid Mats
'* mailto: leomats@gmail.com
'*
'*
'* This program is a part of the dissertation
*
'* 02/15/2007
'* MS Visual Basic Version 6.0
'*
'* The software tool controls Agilen Vector Networ Analyser
'* HP8753 in order to measure S-parameter for N number of
'* tags.  The tool computes the variations in the input
'*impedance of the antenna in the RFID tag
'************************************************
Option Explicit

' Maximum number of tags
Const items As Integer = 1000

' Connection Identifier
Const VNAINSTR As String = "GPIB0::16::INSTR"

' Automation server variable
Dim VNA As New AgtServer8714

' Declaration of data type for complex numbers
Private Type Complex
   X As Double  ' Real part of number in rectangular form, or
   'magnitude of number in polar form
   Y As Double     ' Imaginary part of number in rectangular
form, or  angle associated with number in polar form
End Type

' Declaration of data type for complex non-linear numbers
Private Type NLComplexNode
   sIn As Complex
   pwr As Double   ' Power level
End Type

'Declaration of total number of power levels
Const PWRLevels As Integer = 40

' Declaration of data type for complex non-linear numbers
Private Type NLComplex
   sIn As Complex
   pwr As Double   ' Power level
   Data(PWRLevels) As NLComplexNode
End Type

' Declaration of the PI transformation network
Private Type pi
   Cl As Double
   Cs As Double
   L As Double
End Type

' Declaration of the Y type parameters
Private Type Y
   y11 As Complex
   Y22 As Complex
   y12 As Complex
   Y21 As Complex
End Type

' Declaration of the S type parameters
Private Type S
   s11 As Complex
   s22 As Complex
   s12 As Complex
   s21 As Complex
End Type

' Declaration the two port data
Dim twoPort(items) As S
Dim twoPortMean As S
Dim twoPortSD As S

' Declaration of the control variables
Dim Gpower As Double
Dim opt As Integer
Dim count1 As Integer
Const RunMean As Boolean = True
Const RunSweep As Boolean = False
Dim lstBoxSelIndex As Integer

' Declaration of the Z type parameters open/short/load
Dim zOUTo(items) As Complex
Dim zOUTs(items) As Complex
Dim zOUTl(items) As Complex

' Date and Time stamp for each measurement
Dim dts(3, items) As String

' zIn(0) - open zIn(1) - short zIn(2) - load zIn(3) - calculated
Dim zIn(3, items) As Complex

' ssIn(0) - open ssIn(1) - short ssIn(2) - load ssIn(3) -
calculated
Dim ssIn(3, items) As Complex

' 0 - HFSS 1 - SONNET 2 - IMPINJ OPT1 3 - IMPINJ OPT2
Dim simZin(3) As Complex

' zIn_Count(0) - open zIn_Count(1) - short zIn_Count(2) -
load zIn_Coount(3) - calculated
Dim zIn_Count(3) As Integer

' sIn_Count(0) - open sIn_Count(1) - short sIn_Count(2) -
load sIn_Coount(3) - calculated
Dim sIn_Count(3) As Integer

' Non-lienar S-parameters
Dim sInNL(items) As NLComplex

' Frequencies
Dim f(items) As Integer

' zIn_Mean(0) - open zIn_Mean(1) - short zIn_Mean(2) -
load
Dim zIn_Mean(3) As Complex
Dim zIn_SD(3) As Complex

' sIn_Mean(0) - open sIn_Mean(1) - short sIn_Mean(2) - load
Dim sIn_Mean(3) As Complex
Dim sIn_SD(3) As Complex

' Declaration of the initialization flag
Dim initFlag As Boolean

' Virtual Instrument Handler (VNA)
Dim vi        As Long
Dim err_status As Long
Dim nwa       As String

' Declaration of the Z load impidance
Dim ZL As Complex

' Declaration of the maximum value variables
```

```
Dim maxFreq, minFreq, stepFreq As Integer
Dim maxPwr, minPwr, stepPwr As Double
Dim freqSweepFlag As Boolean
Dim strFilePath As String

' The subroutine that calculates the tag's impedance
Private Sub cmdCalc_Click()

Screen.MousePointer = vbHourglass

' First calculate Zin
Call calculateZin
DoEvents

' Generate histograms for the measured results
Call generateHistogram
DoEvents

' Calculate the two port network
Call getTwoPort
DoEvents

' Get the mean of the S parameters
Call getMeanS
DoEvents

' Get the standard deviation of the S parameters
Call getSDS
DoEvents

'Generate the L-matched network
Call getMatchLowL

Screen.MousePointer = vbDefault

End Sub

' Load the chart data with the test results
Private Sub loadMSChart(index As Integer)

Dim I As Integer

If zIn_Count(index) = 0 Then
   Exit Sub
End If

ReDim GraphRe(zIn_Count(index) - 1, 1 To 2) As Double
ReDim GraphIm(zIn_Count(index) - 1, 1 To 2) As Double

Dim re, im As Integer


Select Case index
Case 0
   ' Code for first action here.
   re = 0
   im = 1
Case 1
   ' Code for second action here.
   re = 2
   im = 3
Case 2
   ' Code for third action here.
   re = 4
   im = 5
End Select


For I = 0 To zIn_Count(index) - 1
   GraphRe(I, 1) = I  'X-axis
   GraphRe(I, 2) = zIn(index, I).X 'Y-axis
Next

'Reset the chart back to default to avoid surprises
MSChart3(re).ToDefaults
MSChart3(re).chartType = VtChChartType2dXY  ' set to X
Y Scatter chart
MSChart3(re) = GraphRe ' populate chart's data grid using
Graph array
DoEvents
MSChart3(re).Plot.UniformAxis = False


For I = 0 To zIn_Count(index) - 1
   GraphIm(I, 1) = I  'X-axis
   GraphIm(I, 2) = zIn(index, I).Y 'Y-axis
Next

'Reset the chart back to default to avoid surprises
MSChart3(im).ToDefaults
MSChart3(im).chartType = VtChChartType2dXY  ' set to X
Y Scatter chart
MSChart3(im) = GraphIm ' populate chart's data grid using
Graph array
DoEvents
MSChart3(im).Plot.UniformAxis = False

End Sub

' Get the data from the VNA
Private Sub getVNAData()
Dim value1, value2, stimulus As Double
Dim I As Integer

' Get VNA Data - S11
If lstBoxSelIndex = -1 Then
   Call GetS11(opt, sIn_Count(opt))
   sIn_Count(opt) = sIn_Count(opt) + 1
Else
   Call GetS11(opt, lstBoxSelIndex)
End If

' Initilize VNA
Call initVNA

' Read active marker values
err_status = hp875x_markerQuery(vi, value1, value2,
stimulus, hp875x_MKR_VALUE_STIM_Q, hp875x_CH1)
Call checkErr(vi, err_status)

' Turn-off power
err_status = hp875x_sourcePowerCouple(vi,
hp875x_SRC_PWR_OFF, hp875x_POWER_CPLD)
Call checkErr(vi, err_status)

' Close VNA
err_status = hp875x_close(vi)
Call checkErr(vi, err_status)

' Load Data into open/short/load list boxes
If lstBoxSelIndex = -1 Then

   zIn(opt, zIn_Count(opt)).X = value1
   zIn(opt, zIn_Count(opt)).Y = value2

   dts(opt, zIn_Count(opt)) = Time

   zIn_Count(opt) = zIn_Count(opt) + 1
Else
   zIn(opt, lstBoxSelIndex).X = value1
```

```
zIn(opt, lstBoxSelIndex).Y = value2

   dts(opt, lstBoxSelIndex) = Time

   lstBoxSelIndex = -1
End If

If (opt = 2) Then f(zIn_Count(opt)) = Val(freq.Text)

' Print marker values
lstBox(opt).Clear
For I = 0 To zIn_Count(opt) - 1
   If opt <> 2 Then
      lstBox(opt).AddItem CStr(lstBox(opt).ListCount + 1)
& ":" & vbTab & cFormat2(zIn(opt, I).X, zIn(opt, I).Y)
   Else
      lstBox(opt).AddItem CStr(lstBox(opt).ListCount + 1)
& ":" & vbTab & cFormat2(zIn(opt, I).X, zIn(opt, I).Y) &
vbTab & sInNL(I).pwr
   End If

Next I
lstBox(opt).Refresh

Screen.MousePointer = vbDefault

End Sub

' Initilization routine for the VNA
Private Sub initVNA()

Dim reply As Integer
Dim freq1, freq2, freq_span As Double

' Assign GPIB address
nwa = VNAINSTR

' Initialize the network analyzer
Call initialize(nwa, VI_FALSE, VI_TRUE, vi)

' Set the timeout to 5000 msec (5 sec)
err_status = hp875x_timeOut(vi, 5000)
Call checkErr(vi, err_status)

' Use Channel 1
err_status = hp875x_channelSelect(vi, hp875x_CH1)
Call checkErr(vi, err_status)

' Smith Chart display
err_status = hp875x_displaySelect(vi, hp875x_CH1,
hp875x_DISP_DATA, hp875x_DISP_SMIC)
Call checkErr(vi, err_status)

' Power range
err_status = hp875x_powerRange(vi,
hp875x_PWR_RANGE_AUTO, hp875x_SET,
hp875x_CH1)
Call checkErr(vi, err_status)

' Set power level
If opt <> 2 Then
   Gpower = 5
End If
err_status = hp875x_powerSet(vi, Gpower,
hp875x_PWR_LEVEL, hp875x_CH1)
Call checkErr(vi, err_status)

' Sweep
err_status = hp875x_freqSweepType(vi,
hp875x_SWP_LINF)
Call checkErr(vi, err_status)


freq1 = Val(freq.Text) * 1000000# ' Convert to real value in
Hz
freq2 = Val("928") * 1000000# ' Convert to real value in Hz
freq_span = Val("0") * 1000000# ' Convert to real value in
Hz

err_status = hp875x_freqStimulus(vi,
hp875x_STIM_CENT_SPAN, freq1, freq_span,
hp875x_PNTS_03)
Call checkErr(vi, err_status)

' Continuous sweep
err_status = hp875x_trigger(vi, hp875x_TRIG_CONT,
hp875x_CH1)
Call checkErr(vi, err_status)

' Turn on marker 1
err_status = hp875x_markerSet(vi, hp875x_ON,
hp875x_MKR_1)
Call checkErr(vi, err_status)

' Sets the CW frequency to the frequency of the specified
marker
err_status = hp875x_markerSet(vi,
hp875x_MKR_CW_TO_MKR)
Call checkErr(vi, err_status)

' CW Sweep
err_status = hp875x_freqSweepType(vi,
hp875x_SWP_CWTIME)
Call checkErr(vi, err_status)

'
err_status = hp875x_average(vi, hp875x_CH1,
hp875x_AVG_FACTOR_MIN,
hp875x_SMOOTH_APERTURE_MIN, hp875x_IF_BW_10)
Call checkErr(vi, err_status)


err_status = hp875x_sourcePowerCouple(vi,
hp875x_SRC_PWR_ON, hp875x_POWER_CPLD)
Call checkErr(vi, err_status)


' Single sweep
err_status = hp875x_takeSweep(vi, 1)
Call checkErr(vi, err_status)

' Discrete marker mode
err_status = hp875x_markerSet(vi,
hp875x_MKR_DISCRETE)
Call checkErr(vi, err_status)

' Wait for the analyzer to finish
err_status = hp875x_opc_Q(vi, "WAIT", reply)
Call checkErr(vi, err_status)

End Sub

' Function for measuring the absolute minimum operating P
Private Function cGetNonLinearS11(index As Integer) As
Complex

Dim I, j, k As Integer
Dim Data() As Complex
Dim dataPolar() As Complex
Dim var() As Complex
```

```
Dim maxPwrPoints As Integer

Dim re1, re2, im1, im2 As Double
Dim im, re As Double

Dim tmp As Double

Dim remaxPer, repwr As Double
Dim immaxPer, impwr As Double

Dim pwr As Double

Dim remaxIndex As Integer
Dim immaxIndex As Integer

Dim maxIndex As Integer

Dim pwr1, pwr2, rek, imk As Double
Dim value1, value2, stimulus As Double

'dBm
minPwr = Val(txtPwr(0).Text)
maxPwr = Val(txtPwr(1).Text)
stepPwr = Val(txtPwr(2).Text)

maxPwrPoints = (maxPwr - minPwr) / stepPwr

ReDim GraphRe(maxPwrPoints - 1, 1 To 2) As Double
ReDim GraphIm(maxPwrPoints - 1, 1 To 2) As Double

ReDim Data(maxPwrPoints)
ReDim dataPolar(maxPwrPoints)
ReDim var(maxPwrPoints)

Gpower = minPwr ' Global power level for VNA
j = 0
' Sweep output power level of the VNA
Do While Gpower <= maxPwr

   dataPolar(j) = cGetS11()

   Data(j) = cRect(dataPolar(j))


   ' store data
   sInNL(index).Data(j).sIn = dataPolar(j)
   sInNL(index).Data(j).pwr = Gpower

   framePWR.Caption = "Power " + CStr(Gpower)

   j = j + 1

   Gpower = Gpower + stepPwr
Loop

‘ Calculate first derivative
For j = 1 To maxPwrPoints

   re1 = Data(j).X
   re2 = Data(j - 1).X

   im1 = Data(j).Y
   im2 = Data(j - 1).Y

   pwr1 = minPwr + j * stepPwr
   pwr2 = minPwr + (j - 1) * stepPwr

   rek = (re1 - re2) / (pwr1 - pwr2)
   imk = (im1 - im2) / (pwr1 - pwr2)

   If im2 <> 0 Then
      im = im1 / im2
   Else
      im = 0
   End If

   If re2 <> 0 Then
      re = re1 / re2
   Else
      re = 0
   End If


   im = im - 1
   re = re - 1

   im = im * 100
   re = re * 100

   var(j).X = re
   var(j).Y = im

Next j

, plot the calculated values
For I = 0 To maxPwrPoints - 1
   GraphRe(I, 1) = minPwr + (I + 1) * stepPwr 'X-axis
   GraphRe(I, 2) = var(I + 1).X
Next I

MSChartNLRe.ToDefaults
MSChartNLRe.chartType = VtChChartType2dXY  ' set to
X Y Scatter chart
'MSChartNLRe.ColumnCount = maxPwrPoints
MSChartNLRe.ChartData = GraphRe
DoEvents
MSChartNLRe.Plot.UniformAxis = False

For I = 0 To maxPwrPoints - 1
   GraphIm(I, 1) = minPwr + (I + 1) * stepPwr 'X-axis
   GraphIm(I, 2) = var(I + 1).Y
Next I
MSChartNLIm.ToDefaults
MSChartNLIm.chartType = VtChChartType2dXY  ' set to
X Y Scatter chart
'MSChartNLIm.ColumnCount = maxPwrPoints
MSChartNLIm.ChartData = GraphIm
DoEvents
MSChartNLIm.Plot.UniformAxis = False


‘ calculate second derivative
remaxPer = 0
repwr = 0
remaxIndex = 0

For j = 2 To maxPwrPoints - 1
   tmp = Abs(var(j - 1).X - var(j).X)
   If var(j - 1).X * var(j).X < 0 And remaxPer < tmp And
remaxIndex + 1 <> j Then
      remaxPer = tmp
      repwr = minPwr + j * stepPwr
      remaxIndex = j
   End If
Next j

immaxPer = 0
impwr = 0
immaxIndex = 0
```

```
For j = 2 To maxPwrPoints - 1
   tmp = Abs(var(j - 1).Y - var(j).Y)
   If var(j - 1).Y * var(j).Y < 0 And immaxPer < tmp And
immaxIndex + 1 <> j Then
      immaxPer = tmp
      impwr = minPwr + j * stepPwr
      immaxIndex = j
   End If
Next j

If repwr <= impwr And repwr <> 0 Then
   pwr = repwr
   maxIndex = remaxIndex
Else
   pwr = impwr
   maxIndex = immaxIndex
End If

cFormat(dataPolar(maxIndex))

sInNL(index).sIn = dataPolar(maxIndex)
sInNL(index).pwr = pwr

Gpower = pwr

framePWR.Caption = "Power"

cGetNonLinearS11 = dataPolar(maxIndex)
End Function

‘ Load Data from files
Private Sub LoadData()

Dim strFile1, strFile2, strFile3 As String
Dim I, j As Integer
Dim strNew As String
Dim value() As String
Dim fl As Integer
Dim tmp As Complex

Screen.MousePointer = vbHourglass

Call updateFilePath


For I = 0 To 3
   lstBox(I).Clear
   zIn_Count(I) = 0
   sIn_Count(I) = 0
Next I

Call updateFilePath

strFile1 = strFilePath + "\" + "s11_2_NL.txt"

If FileExists(strFile1) = True Then

   Open strFile1 For Input As #1 'open data file
   I = 0
   Do While Not EOF(1)
      DoEvents

      Line Input #1, strNew
      If strNew <> "" Then
         value = Split(strNew, vbTab)
         sInNL(I).pwr = Val(value(0))
         tmp.X = Val(value(1))
         tmp.Y = Val(value(2))
         sInNL(I).sIn = tmp
         For j = 3 To UBound(value) Step 3
            sInNL(I).Data(j / 3 - 1).pwr = Val(value(j))
            tmp.X = Val(value(j + 1))
            tmp.Y = Val(value(j + 2))
            sInNL(I).Data(j / 3 - 1).sIn = tmp
         Next j
         I = I + 1
      End If
   Loop
   Close #1
End If



fl = 860

For I = 0 To 2
   'strFile = strFilePath + "\" + Format(Now, "ddmmmyyyy")
+ CStr(i) + ".txt"
   strFile1 = strFilePath + "\" + "data" + CStr(I) + ".txt"
   strFile2 = strFilePath + "\" + "s11_" + CStr(I) + ".txt"
   strFile3 = strFilePath + "\" + "dts_" + CStr(I) + ".txt"

   If FileExists(strFile1) = True Then

      Open strFile1 For Input As #1 'open data file
      Open strFile2 For Input As #2 'open data file
      Open strFile3 For Input As #3 'open data file
      j = 0
      Do While Not EOF(1)
         DoEvents
         Line Input #1, strNew
         If strNew <> "" Then
            value = Split(strNew)
            'Debug.Print value(0); " "; value(1)
            zIn(I, j).X = value(0)
            zIn(I, j).Y = value(1)

            zIn_Count(I) = zIn_Count(I) + 1

            ' Print marker values
            If I <> 2 Then
               lstBox(I).AddItem j + 1 & ":" & vbTab &
cFormat(zIn(I, j))
            Else
               lstBox(I).AddItem j + 1 & ":" & vbTab &
cFormat(zIn(I, j)) & vbTab & sInNL(j).pwr
            End If
            lstBox(I).Refresh
            j = j + 1
         End If
      Loop

      j = 0
      Do While Not EOF(2)
         Line Input #2, strNew
         If strNew <> "" Then
            value = Split(strNew, vbTab)
            ssIn(I, j).X = value(0)
            ssIn(I, j).Y = value(1)
            j = j + 1

            sIn_Count(I) = sIn_Count(I) + 1
         End If
      Loop

      j = 0
      Do While Not EOF(2)
         Line Input #3, strNew
```

```
        If strNew <> "" Then
          dts(I, j) = strNew
          j = j + 1
        End If
      Loop

      Close #1
      Close #2
      Close #3

   End If
Next I


strFile1 = strFilePath + "\" + "data4.txt"
If FileExists(strFile1) = True Then

   Open strFile1 For Input As #1 'open data file
   j = 0
   Do While Not EOF(1)
      Line Input #1, strNew
      f(j) = Val(strNew)

      j = j + 1
   Loop
   Close #1
End If

Call loadSimZin

DoEvents
Call cmdCalc_Click
Call cmdCalc_Click
DoEvents


Call LoadSmithChart
DoEvents

Screen.MousePointer = vbDefault
End Sub

Private Function rad2deg() As Double


Dim pi As Single, Deg2Rad As Double
pi = Atn(1) * 4 ' 1 represents 45 degrees to ATN, which
returns 45 degrees in radians
' Multiplied by 4 gives us 180 degrees in radians which is Pi
(3.1415926...)
rad2deg = 180# / pi 'factor to multiply degrees by to get
radians

End Function


Private Function cAngle(ByRef cOne As Complex) As
Double
Dim cretval As Double

cretval = Atn(cOne.Y / cOne.X) * rad2deg

cAngle = cretval
End Function

‘ Convert complex value to rectangular format
Private Function cRect(ByRef cOne As Complex) As
Complex
Dim tmp As Complex

tmp.Y = cAngle(cOne)
tmp.X = cMagnitude(cOne)

cRect = tmp
End Function

Private Function cMagnitude(ByRef cOne As Complex)
As Double
Dim cretval As Double

cretval = Sqr((cOne.X) ^ 2 + (cOne.Y) ^ 2)
cMagnitude = cretval
End Function

Private Sub GetS11(opt As Integer, index As Integer)

If opt = 2 Then
   ssIn(opt, index) = cGetNonLinearS11(index)
Else
   ssIn(opt, index) = cGetS11()
End If

cFormat(ssIn(opt, index))

End Sub

‘Calculate S11
Private Function cGetS11() As Complex
Dim freq1 As Variant              'these variants hold the SxP
data
Dim s11data As Variant
Dim dImpedance As Double          'variable to hold
characteristic impedance value

Dim tmp As Complex

Dim value1, value2, stimulus As Double

Call initVNA

' Read active marker values
err_status = hp875x_markerQuery(vi, value1, value2,
stimulus, hp875x_MKR_VALUE_STIM_Q, hp875x_CH1)
Call checkErr(vi, err_status)


If VNA.TestS1PObtainable Then 'get a filename and
description and call the SaveSxPData routine


   VNA.GetS1PData freq1, s11data

   tmp.X = s11data(0)
   tmp.Y = s11data(1)

End If

dImpedance =
VNA.Measure.SenseZ0(Agt_AnalogChannel_1)

cGetS11 = tmp

'Dim ActiveChannel As Agt_AnalogChannels 'global
variable to hold active channel
'ActiveChannel = Agt_AnalogChannel_1

'    Dim vFrequency As Variant          'variant to hold
frequency data returned from instrument
'   Dim vData As Variant               'variant to hold
measurement data returned from instrument
```

```
'The following line demonstrates how to retrieve the data points from the instrument
'   VNA.GetFormattedData ActiveChannel, vFrequency, vData

err_status = hp875x_sourcePowerCouple(vi, hp875x_SRC_PWR_OFF, hp875x_POWER_CPLD)
Call checkErr(vi, err_status)

err_status = hp875x_close(vi)
Call checkErr(vi, err_status)
End Function

'Perform the matrix inverse
Private Function cMatrixInverse(cOne As S) As S
Dim A As Complex
Dim B As Complex
Dim C As Complex
Dim d As Complex

Dim tmp As Complex
Dim pOne As Complex

Dim retVal As S


A = cOne.s11
B = cOne.s12
C = cOne.s21
d = cOne.s22

pOne.X = 1
pOne.Y = 0

tmp = cDivide2(pOne, cSubtract(cMultiply2(A, d), cMultiply2(B, C)))

retVal.s11 = cMultiply2(tmp, d)
retVal.s12 = cMultiply2(tmp, cInvert(B))
retVal.s21 = cMultiply2(tmp, cInvert(C))
retVal.s22 = cMultiply2(tmp, A)
cMatrixInverse = retVal
End Function

' Add two matrices
Private Function cMatrixAdd(cOne As S, cTwo As S) As S
Dim A As Complex
Dim B As Complex
Dim C As Complex
Dim d As Complex
Dim e As Complex
Dim f As Complex
Dim g As Complex
Dim h As Complex
Dim retVal As S


A = cOne.s11
B = cOne.s12
C = cOne.s21
d = cOne.s22

e = cTwo.s11
f = cTwo.s12
g = cTwo.s21
h = cTwo.s22

retVal.s11 = cAdd(A, e)
retVal.s12 = cAdd(B, f)
retVal.s21 = cAdd(C, g)
retVal.s22 = cAdd(d, h)

cMatrixAdd = retVal

End Function

' Multiply two matrices
Private Function cMatrixMultiply(cOne As S, cTwo As S) As S
Dim A As Complex
Dim B As Complex
Dim C As Complex
Dim d As Complex
Dim e As Complex
Dim f As Complex
Dim g As Complex
Dim h As Complex


Dim retVal As S


A = cOne.s11
B = cOne.s12
C = cOne.s21
d = cOne.s22

e = cTwo.s11
f = cTwo.s12
g = cTwo.s21
h = cTwo.s22


retVal.s11 = cAdd(cMultiply2(A, e), cMultiply2(B, g))
retVal.s12 = cAdd(cMultiply2(A, f), cMultiply2(B, h))
retVal.s21 = cAdd(cMultiply2(C, e), cMultiply2(d, g))
retVal.s22 = cAdd(cMultiply2(C, f), cMultiply2(d, h))

cMatrixMultiply = retVal

End Function

'Subtract two matrices
Private Function cMatrixSubtract(cOne As S, cTwo As S) As S
Dim A As Complex
Dim B As Complex
Dim C As Complex
Dim d As Complex
Dim e As Complex
Dim f As Complex
Dim g As Complex
Dim h As Complex


Dim retVal As S


A = cOne.s11
B = cOne.s12
C = cOne.s21
d = cOne.s22

e = cTwo.s11
f = cTwo.s12
g = cTwo.s21
h = cTwo.s22
```

```
retVal.s11 = cSubtract(A, e)
retVal.s12 = cSubtract(B, f)
retVal.s21 = cSubtract(C, g)
retVal.s22 = cSubtract(d, h)

cMatrixSubtract = retVal

End Function

Private Function cS2ABCD(cOne As S) As S
'Convert S-parameters to ABCD-parameters

'Syntax
'abcd_params = s2abcd(s_params, Z0)
'Description
'abcd_params = s2abcd(s_params,z0) converts the scattering
parameters s_params into the ABCD-parameters
abcd_params. The s_params input is a complex 2-by-2-by-m
array, representing m 2-port S-parameters. z0 is the reference
impedance; its default is 50 ohms. abcd_params is a complex
2-by-2-by-m array, representing m 2-port ABCD-parameters.


Dim s00 As Complex
Dim s01 As Complex
Dim s10 As Complex
Dim s11 As Complex
Dim Z0 As Complex
Dim pOne As Complex
Dim pTwo As Complex


Dim retVal As S


s00 = cOne.s11
s01 = cOne.s12
s10 = cOne.s21
s11 = cOne.s22

Z0.X = 50
Z0.Y = 0

pOne.X = 1
pOne.Y = 0

pTwo.X = 2
pTwo.Y = 0


retVal.s11 = cDivide2(cAdd(cMultiply2(cAdd(pOne, s00),
cSubtract(pOne, s11)), cMultiply2(s01, s10)),
cMultiply2(pTwo, s10))
retVal.s12 = cMultiply2(Z0,
cDivide2(cSubtract(cMultiply2(cAdd(pOne, s00),
cAdd(pOne, s11)), cMultiply2(s01, s10)), cMultiply2(pTwo,
s10)))
retVal.s21 = cMultiply2(cDivide2(pOne, Z0),
cDivide2(cSubtract(cMultiply2(cSubtract(pOne, s00),
cSubtract(pOne, s11)), cMultiply2(s01, s10)),
cMultiply2(pTwo, s10)))
retVal.s22 = cDivide2(cAdd(cMultiply2(cSubtract(pOne,
s00), cAdd(pOne, s11)), cMultiply2(s01, s10)),
cMultiply2(pTwo, s10))


cS2ABCD = retVal

End Function

Private Function cABCD2S(cOne As S) As S
'Convert ABCD-parameters to S-parameters

'Syntax
's_params = abcd2h(abcd_params, Z0)
'Description
's_params = abcd2h(abcd_params,z0) converts the ABCD-
parameters abcd_params into the scattering parameters
s_params. The abcd_params input is a complex 2-by-2-by-m
array, representing m 2-port ABCD-parameters. z0 is the
reference impedance; its default is 50 ohms. s_params is a
complex 2-by-2-by-m array, representing m 2-port S-
parameters.



Dim A As Complex
Dim B As Complex
Dim C As Complex
Dim d As Complex

Dim tmp As Complex

Dim Z0 As Complex

Dim pOne As Complex
Dim pTwo As Complex


Dim retVal As S


A = cOne.s11
B = cOne.s12
C = cOne.s21
d = cOne.s22

Z0.X = 50
Z0.Y = 0

pOne.X = 1
pOne.Y = 0

pTwo.X = 2
pTwo.Y = 0

tmp = cDivide2(pOne, cAdd(cAdd(A, cDivide2(B, Z0)),
cAdd(cMultiply2(C, Z0), d)))

retVal.s11 = cMultiply2(tmp, cSubtract(cAdd(A,
cDivide2(B, Z0)), cAdd(cMultiply2(C, Z0), d)))
retVal.s12 = cMultiply2(tmp, cMultiply2(pTwo,
cSubtract(cMultiply2(A, d), cMultiply2(B, C))))
retVal.s21 = cMultiply2(tmp, pTwo)
retVal.s22 = cMultiply2(tmp, cAdd(cSubtract(cDivide2(B,
Z0), A), cSubtract(d, cMultiply2(C, Z0))))


cABCD2S = retVal

End Function

Private Function cS2T(cOne As S) As S
'Convert S-parameters to T-parameters

'Syntax
't_params = s2t(s_params)
'Description
```

```
't_params = s2t(s_params) converts the scattering parameters
s_params into the chain scattering parameters t_params. The
s_params input is a complex 2-by-2-by-m array, representing
m 2-port S-parameters. t_params is a complex 2-by-2-by-m
array, representing m 2-port T-parameters.



Dim s11 As Complex
Dim s12 As Complex
Dim s21 As Complex
Dim s22 As Complex
Dim pOne As Complex
Dim retVal As S


pOne.X = 1
pOne.Y = 0

s11 = cOne.s11
s12 = cOne.s12
s21 = cOne.s21
s22 = cOne.s22


retVal.s11 = cInvert(cDivide2(cSubtract(cMultiply2(s11,
s22), cMultiply2(s12, s21)), s21))
retVal.s12 = cDivide2(s11, s21)
retVal.s21 = cInvert(cDivide2(s22, s21))
retVal.s22 = cDivide2(pOne, s21)

cS2T = retVal

End Function

Private Function cT2S(cOne As S) As S
'Convert T-parameters to S-parameters

'Syntax
's_params = t2s(t_params)
'Description
's_params = t2s(t_params) converts the chain scattering
parameters t_params into the scattering parameters s_params.
The t_params input is a complex 2-by-2-by-m array,
representing m 2-port T-parameters. s_params is a complex
2-by-2-by-m array, representing m 2-port S-parameters.



Dim s11 As Complex
Dim s12 As Complex
Dim s21 As Complex
Dim s22 As Complex

Dim pOne As Complex

Dim retVal As S

pOne.X = 1
pOne.Y = 0

s11 = cOne.s11
s12 = cOne.s12
s21 = cOne.s21
s22 = cOne.s22


retVal.s11 = cDivide2(s12, s22)
retVal.s12 = cDivide2(cSubtract(cMultiply2(s11, s22),
cMultiply2(s12, s21)), s22)
retVal.s21 = cDivide2(pOne, s22)
retVal.s22 = cInvert(cDivide2(s21, s22))

cT2S = retVal

End Function

Private Function cS2Y(cOne As S) As S
'Convert S-parameters to Y-parameters

'Syntax
'y_params = s2y(s_params, Z0)
'Description
'y_params = s2y(s_params'z0) converts the scattering
parameters s_params into the admittance parameters
y_params. The s_params input is a complex n-by-n-by-m
array, representing m n-port S-parameters. z0 is the reference
impedance; its default is 50 ohms. y_params is a complex n-
by-n-by-m array, representing m n-port Y-parameters.

Dim A As Complex
Dim B As Complex
Dim C As Complex
Dim d As Complex

Dim tmp As Complex

Dim Z0 As Complex

Dim nOne As Complex


Dim retVal As S

Dim cTwo As S

cTwo = cS2ABCD(cOne)

A = cTwo.s11
B = cTwo.s12
C = cTwo.s21
d = cTwo.s22

Z0.X = 50
Z0.Y = 0

nOne.X = -1
nOne.Y = 0

retVal.s11 = cDivide2(d, B)
retVal.s12 = cDivide2(cSubtract(cMultiply2(B, C),
cMultiply2(A, d)), B)
retVal.s21 = cDivide2(nOne, B)
retVal.s22 = cDivide2(A, B)

cS2Y = retVal

End Function

Private Sub getTwoPort()

Dim nMeanS As S

Dim nMeanABCD As S
Dim nMeanABCDInv As S

Dim nMeanT As S
Dim nMeanTinv As S
```

```
Dim nABCD1 As S
Dim nABCD2 As S


Dim nT1 As S
Dim nT2 As S

Dim nS1 As S
Dim nS2 As S
Dim nABCDS2 As S

Dim I As Integer
Dim Z0 As Complex

Dim tmp As Complex

Dim s11 As Complex
Dim s12 As Complex
Dim s21 As Complex
Dim s22 As Complex
Dim s12s21 As Complex

Dim pOne As Complex
Dim nOne As Complex

Dim so As Complex
Dim ss As Complex

Dim tmp1, strFile1 As String
Dim strFile2 As String


Dim antZin As Complex


If sIn_Count(2) > 0 Then


   'Dim n As S
   'n.s11.X = 2
   'n.s11.Y = 5
   'n.s12.X = 4
   'n.s12.Y = 7
   'n.s21.X = 8
   'n.s21.Y = 5
   'n.s22.X = 9
   'n.s22.Y = 2



   nMeanS = meanTwoPort()


   nMeanABCD = cS2ABCD(nMeanS)
   nMeanABCDInv = cMatrixInverse(nMeanABCD)

   nMeanT = cS2T(nMeanS)
   nMeanTinv = cMatrixInverse(nMeanT)


   Z0.X = 50
   Z0.Y = 0


   pOne.X = 1
   pOne.Y = 0

   nOne.X = -1
   nOne.Y = 0


   strFile1 = strFilePath + "\" + "twoPort.txt"
   strFile2 = strFilePath + "\" + "twoPortOrg.txt"


   Open strFile1 For Output As #1 'open data file
   Open strFile2 For Output As #2 'open data file

   Print #1, "re(S11)"; vbTab; "im(S11)"; vbTab;
"re(S12)"; vbTab; "im(S12)"; vbTab; "re(S21)"; vbTab;
"im(S21)"; vbTab; "re(S22)"; vbTab; "im(S22)"
   Print #2, "re(S11)"; vbTab; "im(S11)"; vbTab;
"re(S12)"; vbTab; "im(S12)"; vbTab; "re(S21)"; vbTab;
"im(S21)"; vbTab; "re(S22)"; vbTab; "im(S22)"


   For I = 0 To sIn_Count(2) - 1

      antZin = ssIn(3, I)

      s22 = cDivide2(cSubtract(antZin, Z0), cAdd(antZin,
Z0))

      so = sIn_Mean(0)
      ss = sIn_Mean(1)

      s12s21 = solver(pOne, cDivide2(nOne, cSubtract(s22,
pOne)), so, pOne, cDivide2(nOne, cAdd(s22, pOne)), ss)
      s11 = solver(pOne, cDivide2(nOne, cSubtract(s22,
pOne)), so, pOne, cDivide2(nOne, cAdd(s22, pOne)), ss, 2)


      s12 = cSQR(s12s21)


      s21 = s12

      nS1.s11 = s11
      nS1.s12 = s12
      nS1.s21 = s21
      nS1.s22 = s22
      'Call cPrintS(CStr(i), nS1)
      With nS1
         tmp1 = .s11.X & vbTab & .s11.Y
         tmp1 = tmp1 & vbTab & .s12.X & vbTab & .s12.Y
         tmp1 = tmp1 & vbTab & .s21.X & vbTab & .s21.Y
         tmp1 = tmp1 & vbTab & .s22.X & vbTab & .s22.Y
      End With
      Print #2, tmp1

      nABCD1 = cS2ABCD(nS1)
      nABCD2 = cMatrixMultiply(nMeanABCDInv,
nABCD1)
      nABCDS2 = cABCD2S(nABCD2)

      nT1 = cS2T(nS1)
      'Call cPrintS(CStr(i), nT1)
      nT2 = cMatrixMultiply(nMeanTinv, nT1)
      nS2 = cT2S(nT2)


      With nS2
         tmp1 = .s11.X & vbTab & .s11.Y
         tmp1 = tmp1 & vbTab & .s12.X & vbTab & .s12.Y
         tmp1 = tmp1 & vbTab & .s21.X & vbTab & .s21.Y
         tmp1 = tmp1 & vbTab & .s22.X & vbTab & .s22.Y
      End With

      Print #1, tmp1
```

```
twoPort(I) = nS2


   Next I

   Close #1
   Close #2

End If


End Sub

'Determine the mean two port network
Private Function meanTwoPort() As S
Dim n As S
Dim I As Integer
Dim Z0 As Complex

Dim tmp As Complex

Dim s11 As Complex
Dim s12 As Complex
Dim s21 As Complex
Dim s22 As Complex
Dim s12s21 As Complex

Dim pOne As Complex
Dim nOne As Complex

Dim so As Complex
Dim ss As Complex

Z0.X = 50
Z0.Y = 0


pOne.X = 1
pOne.Y = 0

nOne.X = -1
nOne.Y = 0


Dim antZin As Complex


antZin = sIn_Mean(3)

lblMeasured.Caption = cFormat(antZin)

s22 = cDivide2(cSubtract(antZin, Z0), cAdd(antZin, Z0))

so = sIn_Mean(0)
ss = sIn_Mean(1)

s12s21 = solver(pOne, cDivide2(nOne, cSubtract(s22,
pOne)), so, pOne, cDivide2(nOne, cAdd(s22, pOne)), ss)
s11 = solver(pOne, cDivide2(nOne, cSubtract(s22, pOne)),
so, pOne, cDivide2(nOne, cAdd(s22, pOne)), ss, 2)


s12 = cSQR(s12s21)


s21 = s12

n.s11 = s11
n.s12 = s12
n.s21 = s21
n.s22 = s22

meanTwoPort = n

End Function

'Get two port netwok
Private Sub cmdTwoPort_Click()

Call getTwoPort

Call getMeanS
End Sub

Private Sub Command1_Click()
Call getMatchLowL
End Sub

' Terminate the program
Private Sub Form_Terminate()

If VNA.ConnectedStatus Then
   'The following demonstrates a way to disconnect from the
connected instrument
   VNA.Close

End If

End Sub

' Select tag in the list box
Private Sub lstBox_Click(index As Integer)
Dim k As Integer

lstBoxSelIndex = lstBox(index).ListIndex
For k = 0 To 3
   If lstBox(k).ListCount > lstBoxSelIndex Then
      lstBox(k).ListIndex = lstBoxSelIndex
   End If
Next

If lstBoxSelIndex <> -1 Then
   txtX.Text = zIn(2, lstBoxSelIndex).X
   txtY.Text = zIn(2, lstBoxSelIndex).Y
End If

If opt = 2 And MSChartNLRe.Tag <> CStr(lstBoxSelIndex)
And lstBoxSelIndex <> -1 Then
   Dim datapts, pwrpts As Integer
   Dim I, j As Integer
   Dim GraphRe() As Single
   Dim GraphIm() As Single


   MSChartNLRe.Tag = CStr(lstBoxSelIndex)

   I = lstBoxSelIndex

   For j = 0 To UBound(sInNL(I).Data) - 1
      If sInNL(I).Data(j).sIn.X = 0 Then
         pwrpts = j - 1
         Exit For
      End If
   Next j

   'pwrpts = UBound(sInNL(i).Data)


   ReDim GraphRe(0 To pwrpts, 1)
```

```
ReDim GraphIm(0 To pwrpts, 1)


   For j = 0 To pwrpts
      GraphRe(j, 0) = sInNL(I).Data(j).pwr
      GraphRe(j, 1) = sInNL(I).Data(j).sIn.X
      GraphIm(j, 0) = sInNL(I).Data(j).pwr
      GraphIm(j, 1) = sInNL(I).Data(j).sIn.Y
   Next j

   MSChartNLRe.ToDefaults
   MSChartNLRe.chartType = VtChChartType2dXY  ' set
to X Y Scatter chart
   'MSChartNLRe.ColumnCount = 6
   MSChartNLRe.ChartData = GraphRe
   DoEvents
   MSChartNLRe.Plot.UniformAxis = False

   MSChartNLIm.ToDefaults
   MSChartNLIm.chartType = VtChChartType2dXY  ' set
to X Y Scatter chart
   'MSChartNLIm.ColumnCount = pwrpts
   MSChartNLIm.ChartData = GraphIm
   DoEvents
   MSChartNLIm.Plot.UniformAxis = False
End If

End Sub

Private Sub cmdQuit_Click()
' Close the application
Form_Terminate

End
End Sub

‘ Initialization routine for the VNA
Public Sub initialize(ByVal nwa As String, ByVal
id_query As Integer, ByVal do_reset As Integer, vi As
Long)

Dim err_status As Long
Dim err_msg    As String * 256
Dim msg As String

' Note that this function can verify that the instrument
' specified is an hp875x (id_query=VI_TRUE) and can send
' a reset to the instrument (do_reset=VI_TRUE).

err_status = hp875x_init(nwa, id_query, do_reset, vi)

If ((err_status < VI_SUCCESS) Or (vi = VI_NULL)) Then

   msg = "init failed with return code " & err_status

   If (vi <> VI_NULL) Then
      err_status = hp875x_error_message(vi, err_status,
err_msg)
      msg = msg & ",  Error Status: " & err_status

      msg = msg & ",  Error Message: " & err_msg
   End If
   MsgBox msg, vbInformation, frmTagTester.Caption
   End
End If
End Sub

‘  The error reporting subroutine
Sub checkErr(ByVal vi As Long, ByVal err_status As
Long)


Dim inst_err          As Long
Dim err_message       As String * 250
Dim retStatus         As Long

Dim nl

Dim msg As String

DoEvents

nl = Chr(10)

If VI_SUCCESS > err_status Then

   'Send a device clear to ensure communication with 'the
instrument.

   retStatus = hp875x_dcl(vi)

   If (hp875x_INSTR_ERROR_DETECTED = err_status)
Then

      'query the instrument for the error
      retStatus = hp875x_error_query(vi, inst_err,
err_message)

      msg = "CHECK :Instrument Error :" & inst_err & nl &
"Error Message = " & err_message

      MsgBox msg, vbOKOnly, frmTagTester.Caption
   Else
      'get the driver error message
      retStatus = hp875x_error_message(vi, err_status,
err_message)
      msg = "CHECK :Driver Error :" & err_status & nl &
"Error Message = " & err_message

      MsgBox msg, vbInformation, frmTagTester.Caption
   End If

End If
' optionally reset the instrument, close the instrument handle

'retStatus=hp875x_reset(vi)
'retStatus=hp875x_close(vi)

End Sub

Private Function cAdd(ByRef cOne As Complex, ByRef
cTwo As Complex) As Complex

'Returns the sum of two complex numbers
Dim cretval As Complex
'cretval.X = Round(cOne.X, 15) + Round(cTwo.X, 15)

cretval.X = cOne.X + cTwo.X
cretval.Y = cOne.Y + cTwo.Y



cAdd = cretval
End Function

Private Function cDivide(ByRef cOne As Complex, ByRef
cTwo As Complex) As Complex
' Returns the quotient of two complex numbers
Dim cretval As Complex
Dim cTemp1 As Complex
Dim cTemp2 As Complex
```

```
cTemp1.X = cOne.X
cTemp1.Y = cOne.Y

cTemp2.X = cTwo.X
cTemp2.Y = cTwo.Y

Call RectToPolar(cTemp1)
Call RectToPolar(cTemp2)
cretval.X = cTemp1.X / cTemp2.X
cretval.Y = cTemp1.Y - cTemp2.Y
Call PolarToRect(cretval)
cDivide = cretval
End Function

Private Function cDivide2(ByRef cOne As Complex,
ByRef cTwo As Complex) As Complex
Dim cretval As Complex
Dim sum As Double
' create the sum only once
'sum = Real * Real + Imaginary * Imaginary
sum = cTwo.X * cTwo.X + cTwo.Y * cTwo.Y

If sum = 0 Then Exit Function

' evaluate the real and imaginary parts
cretval.X = (cOne.X * cTwo.X + cOne.Y * cTwo.Y) / sum
cretval.Y = (cOne.Y * cTwo.X - cOne.X * cTwo.Y) / sum

cDivide2 = cretval
End Function

Private Function cSQR(ByRef cOne As Complex) As
Complex
Dim cretval As Complex
Dim r As Double


r = cMagnitude(cOne)


' evaluate the real and imaginary parts
cretval.X = Sqr((r + cOne.X) / 2)

cretval.Y = cOne.Y / Sqr(2 * (r + cOne.X))
cSQR = cretval
End Function


Private Function cMultiply(ByRef cOne As Complex,
ByRef cTwo As Complex) As Complex
' Returns the product of two complex numbers
Dim cretval As Complex
Dim cTemp1 As Complex
Dim cTemp2 As Complex
cTemp1 = cOne
cTemp2 = cTwo
Call RectToPolar(cTemp1)
Call RectToPolar(cTemp2)
cretval.X = cTemp1.X * cTemp2.X
cretval.Y = cTemp1.Y + cTemp2.Y
Call PolarToRect(cretval)
cMultiply = cretval
End Function

Private Function cPIMATCH(ByRef ZS As Complex,
ByRef ZL As Complex, ByRef freq1 As Integer, ByRef Q
As Integer) As pi
Dim w As Double
Dim p As Double
Dim Qs, Ql As Double

Dim temp As pi

p = 4# * Atn(1#)

w = 2 * p * freq1 * 1000000#

Qs = -1 * ZS.Y / ZS.X

Ql = -1 * ZL.Y / ZL.X

Rpleft = ZS.X * (1 + Qs ^ 2)
Rpright = ZL.X * (1 + Ql ^ 2)

Cpleft = Qs / (Rpleft * w)
Cpright = Ql / (Rpright * w)

Rv = max(Rpleft, Rpright) / (1 + Q ^ 2)

Qleft = Sqr((Rpleft / Rv) - 1)

Lleft = Qleft * Rv / w

Cleft = Qleft / (w * Rpleft)

Cs = Cleft - Cpleft

Qright = Sqr((Rpright / Rv) - 1)

Lright = Qright * Rv / w

Cright = Qright / (w * Rpright)

Cl = Cright - Cpright

L = Lleft + Lright

temp.L = L * 1000000000#
temp.Cs = Cs * 1000000000000#
temp.Cl = Cl * 1000000000000#

cPIMATCH = temp

End Function

‘ Determine the values of L and C in the L-match network
Private Sub getMatchLowL()

Dim mNetwork As pi

mNetwork = cLowLMatch(sIn_Mean(3), simZin(0), 915, 10)

lblL.Caption = Format(mNetwork.L, "0.00") + "nH"
lblC.Caption = Format(mNetwork.Cl, "0.00") + "pF"


End Sub

Private Sub loadSimZin()
Dim strFile1 As String
Dim I As Integer
Dim strNew As String
Dim value() As String


strFile1 = strFilePath + "\" + "simZin.txt"

If FileExists(strFile1) = True Then
```

```
   Open strFile1 For Input As #1 'open data file
   I = 0
   Do While Not EOF(1)
      Line Input #1, strNew
      If strNew <> "" Then
         value = Split(strNew, vbTab)
         simZin(I).X = Val(value(0))
         simZin(I).Y = Val(value(1))
         I = I + 1
      End If
   Loop
   Close 1
End If

lblSimulated.Caption = cFormat(simZin(0)) 'HFSS


End Sub


Private Function cLowLMatch(ByRef ZLin As Complex,
ByRef ZSin As Complex, ByRef freq1 As Integer, ByRef
Q As Integer) As pi
Dim ZL As Complex
Dim ZS As Complex

ZL.X = ZLin.X
ZL.Y = -1 * ZLin.Y


ZS.X = ZSin.X
ZS.Y = ZSin.Y


'ZS.X = ZLin.X
'ZS.Y = ZLin.Y
'ZL.X = ZSin.X
'ZL.Y = -1 * ZSin.Y


Dim w As Double
Dim p As Double
Dim C As Double
Dim L As Double

Dim QQ As Double
Dim Qs As Double
Dim Ql As Double

Dim Rl As Double
Dim Cl As Double


Dim LT As Double
Dim CT As Double


Dim temp As pi

Dim ls As Double


p = 4# * Atn(1#)

w = 2# * p * freq1 * 1000000#

ls = ZS.Y / w

If ZL.X = 0 Then Exit Function
```

```
Ql = -1 * ZL.Y / ZL.X

Rl = ZL.X * (1 + Ql ^ 2)

Cl = Ql / (w * Rl)



If ZS.X = 0 Then Exit Function

QQ = Sqr((Rl / ZS.X) - 1#)

LT = (QQ * ZS.X) / w

CT = QQ / (w * Rl)

L = LT - ls
C = CT - Cl

temp.L = L * 1000000000#
temp.Cs = 0#
temp.Cl = C * 1000000000000#

cLowLMatch = temp

End Function

Public Function max(v1, v2)
If v1 > v2 Then
   max = v1
Else
   max = v2
End If
End Function


Private Function cGamma(ByRef cOne As Complex,
ByRef cTwo As Complex) As Double


cGamma = cMagnitude(cDivide2(cSubtract(cOne,
cConjugate(cTwo)), cAdd(cOne, cTwo)))


End Function

‘ Generate the Smith chart for the calculated data
Private Function cSmithChartGamma(ByRef cOne As
Complex) As Complex
' Returns the product of two complex numbers
Dim cretval As Complex
Dim Zo As Complex

'Nor
Zo.X = 50
Zo.Y = 0


cSmithChartGamma = cDivide2(cSubtract(cOne, Zo),
cAdd(cOne, Zo))


End Function

Private Function cS2Z(ByRef cOne As S) As S
'Converts the scattering parameters s_params into the
impedance parameters z_params.
'The s_params input is a complex n-by-n-by-m array,
representing m n-port S-parameters.
'z0 is the reference impedance; its default is 50 ohms. '
```

```
'z_params is a complex n-by-n-by-m array, representing m n-port Z-parameters.

Dim one As Complex
Dim two As Complex
Dim Zo As Complex
Dim cretval As S

one.X = 1
one.Y = 0

two.X = 2
two.Y = 0

Zo.X = 50
Zo.Y = 0


With cOne
   cretval.s11 = cMultiply(Zo,
cDivide2(cAdd(cMultiply2(cAdd(one, .s11), cSubtract(one,
.s22)), cMultiply2(.s12, .s21)),
cSubtract(cMultiply2(cSubtract(one, .s11), cSubtract(one,
.s22)), cMultiply2(.s12, .s21))))
   cretval.s12 = cMultiply2(Zo, cDivide2(cMultiply2(two,
.s12), cSubtract(cMultiply2(cSubtract(one, .s11),
cSubtract(one, .s22)), cMultiply2(.s12, .s21))))
   cretval.s21 = cMultiply2(Zo, cDivide2(cMultiply2(two,
.s21), cSubtract(cMultiply2(cSubtract(one, .s11),
cSubtract(one, .s22)), cMultiply2(.s12, .s21))))
   cretval.s22 = cMultiply(Zo,
cDivide2(cSubtract(cMultiply2(cAdd(one, .s11), cAdd(one,
.s22)), cMultiply2(.s12, .s21)),
cSubtract(cMultiply2(cSubtract(one, .s11), cSubtract(one,
.s22)), cMultiply2(.s12, .s21))))

End With


cS2Z = cretval

End Function
Private Function cInvert(ByRef cOne As Complex) As
Complex

cOne.X = -1 * cOne.X
cOne.Y = -1 * cOne.Y

cInvert = cOne

End Function


Private Function cMultiply2(ByRef cOne As Complex,
ByRef cTwo As Complex) As Complex
' Returns the product of two complex numbers
Dim cretval As Complex
cretval.X = (cOne.X * cTwo.X - cOne.Y * cTwo.Y)
cretval.Y = cOne.X * cTwo.Y + cOne.Y * cTwo.X
cMultiply2 = cretval
End Function

Private Function cMultiplyByNum(ByRef cOne As
Complex, ByRef cTwo As Integer) As Complex
' Returns the product of two complex numbers
Dim cretval As Complex
cretval.X = cOne.X * cTwo
cretval.Y = cOne.Y * cTwo
cMultiplyByNum = cretval
End Function


Private Function cSubtract(ByRef cOne As Complex,
ByRef cTwo As Complex) As Complex
' Returns the difference between two complex numbers
Dim cretval As Complex
cretval.X = cOne.X - cTwo.X
cretval.Y = cOne.Y - cTwo.Y
cSubtract = cretval
End Function

Private Function cConjugate(ByRef cOne As Complex)
As Complex
' Returns the difference between two complex numbers
Dim cretval As Complex
cretval.X = cOne.X
cretval.Y = -cOne.Y
cConjugate = cretval
End Function


Private Sub PolarToRect(ByRef cNum As Complex)
' Convert complex number from polar form to rectangular
form
Dim ctemp As Complex
ctemp.X = cNum.X * Cos(cNum.Y)
ctemp.Y = cNum.X * sIn(cNum.Y)
cNum.X = ctemp.X
cNum.Y = ctemp.Y
End Sub

Private Sub cPrint(name As String, ByRef cNum As
Complex)

Debug.Print name; "="; cNum.X; " "; cNum.Y; "j"

End Sub


Private Sub cPrintS(ByRef cName As String, ByRef
cNum As S)

Debug.Print cName; vbTab; cNum.s11.X; vbTab;
cNum.s11.Y; vbTab; cNum.s12.X; vbTab; cNum.s12.Y;
vbTab; cNum.s21.X; vbTab; cNum.s21.Y; vbTab;
cNum.s22.X; vbTab; cNum.s22.Y;

End Sub

Private Sub RectToPolar(ByRef cNum As Complex)
' Convert complex number from rectangular form to polar
form
Dim pi As Double
Dim ctemp As Complex
pi = 4# * Atn(1#)
ctemp.X = Sqr(cNum.X ^ 2 + cNum.Y ^ 2)
If cNum.X = 0 And cNum.Y < 0 Then ctemp.Y = -(pi / 2#)
If cNum.X = 0 And cNum.Y > 0 Then ctemp.Y = pi / 2#
If cNum.X = 0 And cNum.Y = 0 Then ctemp.Y = 0
If cNum.X > 0 Then ctemp.Y = Atn(cNum.Y / cNum.X)
If cNum.X < 0 And cNum.Y = 0 Then
   ctemp.X = Abs(cNum.X)
   ctemp.Y = pi
End If
If cNum.X < 0 And cNum.Y < 0 Then ctemp.Y =
Atn(cNum.Y / cNum.X) - pi
If cNum.X < 0 And cNum.Y > 0 Then ctemp.Y =
Atn(cNum.Y / cNum.X) + pi
cNum.X = ctemp.X
cNum.Y = ctemp.Y
```

```
End Sub

' Format Complex Number for the output
Private Function cFormat(ByRef cNum As Complex) As
String

If (cNum.Y < 0) Then
   cFormat = Format(cNum.X, "0.000") + Format(cNum.Y,
"0.000") + "j"
Else
   cFormat = Format(cNum.X, "0.000") + "+" +
Format(cNum.Y, "0.000") + "j"
End If

End Function

' Format Complex Number for the output
Private Function cFormatExp(ByRef cNum As Complex)
As String

If (cNum.Y < 0) Then
   cFormatExp = Format(cNum.X, "0.000000") + " " +
Format(cNum.Y, "0.000000") + "j"
Else
   cFormatExp = Format(cNum.X, "0.000000") + " " + "+"
+ Format(cNum.Y, "0.000000") + "j"
End If

End Function

' Format Complex Number for the output
Private Function cFormat2(ByRef X As Double, ByRef Y
As Double) As String

Dim C As Complex

C.X = X
C.Y = Y

cFormat2 = cFormat(C)

End Function

' Format Complex Number for the output
Private Function cFormat3(ByRef cNum As Double) As
String


cFormat3 = Format(cNum, "0.000")

End Function

Private Sub generateHistogram()
'CREATE HISTOGRAM INPUT DATA
Dim I As Integer

Dim numHits As Double
Dim numBins As Integer

Dim binX2() As Double
Dim binY2() As Double

numHits = lstBox(2).ListCount
numBins = 17 'numHits ^ (1 / 2)

If numHits >= 2 Then
   ReDim hits(numHits - 1) As Double

   For I = 0 To numHits - 1
      hits(I) = cMagnitude(zIn(3, I))
   Next I

   'PROCESS HISTOGRAM DATA


   If numHits <= 2 Then
      Screen.MousePointer = vbDefault
      Exit Sub
   End If

   binY2 = MakeHistogramData(hits, numBins, binX2,
binY2)

   binY2(0) = 0
   '       MSChart1.ColumnCount = numBins
   MSChart1.ChartData = binY2
   '       MSChart1.RowLabel = "REAL"


   For I = 0 To numHits - 1
      hits(I) = cAngle(zIn(3, I))
   Next I

   binY2 = MakeHistogramData(hits, numBins, binX2,
binY2)

   binY2(0) = 0
   '       MSChart2.ColumnCount = numBins
   MSChart2.ChartData = binY2
'      MSChart2.RowLabel = "IMIGINARY"
End If

For I = 0 To 2
   Call loadMSChart(I)
Next
End Sub

' Calculates the Zin based on the measured data in Z and S
parameters
Private Sub calculateZin()
Dim A(2, 2) As Complex
Dim B(2) As Complex
Dim X(2) As Complex

Dim so As Complex
Dim ss As Complex

Dim d As Complex

Dim I As Integer
Dim m As Integer

' remove old values
lstBox(3).Clear

For I = 0 To zIn_Count(2) - 1
   zOUTo(I).X = 10000000#
   zOUTo(I).Y = 0#

   zOUTs(I).X = 0#
   zOUTs(I).Y = 0#

   If RunSweep Then
      If (f(I) < 902) Then
         zOUTl(I).X = 36#
         zOUTl(I).Y = -117#
      Else
         If (f(I) <= 928) Then
            zOUTl(I).X = 33#
            zOUTl(I).Y = -112#
```

```
        Else
            zOUTl(I).X = 30#
            zOUTl(I).Y = -108#
        End If
    End If
  Else
    zOUTl(I).X = 33#
    zOUTl(I).Y = -112#
  End If
Next I

Call Calc_zIN_Means
Call Calc_zIn_SD

zIn_Count(3) = zIn_Count(2)
sIn_Count(3) = sIn_Count(2)

For m = 0 To zIn_Count(2) - 1

  If (RunMean) Then
    A(1, 1) = cSubtract(zOUTo(m), zOUTl(m))
    A(1, 2) = cSubtract(zIn(2, m), zIn_Mean(0))
    A(2, 1) = cSubtract(zOUTs(m), zOUTl(m))
    A(2, 2) = cSubtract(zIn(2, m), zIn_Mean(1))

  ' First element for open and short
  "a(1, 1) = cSubtract(zOUTo(M), zOUTl(M))
  "a(1, 2) = cSubtract(zIn(2, M), zIn(0, 0))
  "a(2, 1) = cSubtract(zOUTs(M), zOUTl(M))
  "a(2, 2) = cSubtract(zIn(2, M), zIn(1, 0))


  Else

    A(1, 1) = cSubtract(zOUTo(m), zOUTl(m))
    A(1, 2) = cSubtract(zIn(2, m), zIn(0, m))
    A(2, 1) = cSubtract(zOUTs(m), zOUTl(m))
    A(2, 2) = cSubtract(zIn(2, m), zIn(1, m))

  End If


  If (RunMean) Then
    B(1) = cSubtract(cMultiply2(zIn_Mean(0), zOUTo(m)), cMultiply2(zIn(2, m), zOUTl(m)))
    B(2) = cSubtract(cMultiply2(zIn_Mean(1), zOUTs(m)), cMultiply2(zIn(2, m), zOUTl(m)))

  ' First element for open and short
  "b(1) = cSubtract(cMultiply2(zIn(0, 0), zOUTo(M)), cMultiply2(zIn(2, M), zOUTl(M)))
  "b(2) = cSubtract(cMultiply2(zIn(1, 0), zOUTs(M)), cMultiply2(zIn(2, M), zOUTl(M)))


  Else
    B(1) = cSubtract(cMultiply2(zIn(0, m), zOUTo(m)), cMultiply2(zIn(2, m), zOUTl(m)))
    B(2) = cSubtract(cMultiply2(zIn(1, m), zOUTs(m)), cMultiply2(zIn(2, m), zOUTl(m)))
  End If


'##############################################################################
    '      Calculate Zin based on T-model
  zIn(3, m) = solver(A(1, 1), A(1, 2), B(1), A(2, 1), A(2, 2), B(2))

'##############################################################################

  '      Calculate Zin based on S-parameters
  'ssIn(3, M) = cInvert(cMultiply2(cDivide2(cSubtract(ssIn(0, 0), ssIn(2, M)), cSubtract(ssIn(1, 0), ssIn(2, M))), zOUTl(M)))
  ssIn(3, m) = cInvert(cMultiply2(cDivide2(cSubtract(sIn_Mean(0), ssIn(2, m)), cSubtract(sIn_Mean(1), ssIn(2, m))), zOUTl(m)))
  'Call cPrint("calculateZin s11=", ssIn(3, M))


  ' Print Zin values
  '
  ' Phase & Mag
  'lstBox(3).AddItem M + 1 & ":" & vbTab & cFormat3(cMagnitude(X(1))) & " <" & cFormat3(cAngle(X(1)))

  ' Real & Im

  ' Based on S
  lstBox(3).AddItem m + 1 & ":" & vbTab & cFormat(ssIn(3, m))

  lstBox(3).Refresh

' Based on Z
'lstBox(3).AddItem M + 1 & ":" & vbTab & cFormat(zIn(3, M))
'lstBox(3).Refresh

Next m

End Sub

Private Function solver(A As Complex, B As Complex, C As Complex, d As Complex, e As Complex, f As Complex, Optional ctrl As Integer = 1) As Complex
'##############################################################################
'      Calculate Zin based on T-model
'
http://www.analyzemath.com/Calculators/Calculator_syst_eq.html
'      2 by 2 systems of linear equations are of the form
'      a x + b y = c
'      d x + e y = f
'      The calculator uses Cramer's rule
'      x = (c e - f b) / D and y = (a f - d c) / D
'      to solve the system.
'      D is the coefficient determinant given by D = a e - b d.

Dim Dtmp As Complex


'                    a      b   c    d      e      f
'    zIn(3, M) = solver(a(1, 1), a(1, 2), b(1), a(2, 1), a(2, 2), b(2))

'    Debug.Print "a="; cFormat(a)
'    Debug.Print "b="; cFormat(b)
'    Debug.Print "c="; cFormat(c)
'    Debug.Print "d="; cFormat(d)
'    Debug.Print "e="; cFormat(e)
'    Debug.Print "f="; cFormat(f)
```

```
Next m

End Sub

Private Function solver(A As Complex, B As Complex, C As Complex, d As Complex, e As Complex, f As Complex, Optional ctrl As Integer = 1) As Complex
'###############################################################################
'       Calculate Zin based on T-model
'
http://www.analyzemath.com/Calculators/Calculator_syst_eq.html
'       2 by 2 systems of linear equations are of the form
'       a x + b y = c
'       d x + e y = f
'       The calculator uses Cramer's rule
'       x = (c e - f b) / D and y = (a f - d c) / D
'       to solve the system.
'       D is the coefficient determinant given by D = a e - b d.

Dim Dtmp As Complex


'                       a       b   c     d      e      f
'     zIn(3, M) = solver(a(1, 1), a(1, 2), b(1), a(2, 1), a(2, 2), b(2))

'     Debug.Print "a="; cFormat(a)
'     Debug.Print "b="; cFormat(b)
'     Debug.Print "c="; cFormat(c)
'     Debug.Print "d="; cFormat(d)
'     Debug.Print "e="; cFormat(e)
'     Debug.Print "f="; cFormat(f)


'       d = cSubtract(cMultiply2(a(1, 1), a(2, 2)), cMultiply2(a(1, 2), a(2, 1)))

Dtmp = cSubtract(cMultiply2(A, e), cMultiply2(B, d))

'cDivide2(cSubtract(cMultiply2(a(1, 1), b(2)), cMultiply2(a(2, 1), b(1))), D)

If ctrl = 1 Then
   solver = cDivide2(cSubtract(cMultiply2(A, f), cMultiply2(d, C)), Dtmp)
Else
   solver = cDivide2(cSubtract(cMultiply2(C, e), cMultiply2(f, B)), Dtmp)
End If
'###############################################################################
End Function

' Calculates the mean value for Zin
Private Sub Calc_zIN_Means()
Dim I, idx As Integer
Dim re As Double
Dim im As Double

Dim reS As Double
Dim imS As Double

For idx = 0 To 3
   re = 0#
   im = 0#
   reS = 0#
   imS = 0#

   For I = 0 To zIn_Count(idx) - 1
      re = re + zIn(idx, I).X
      im = im + zIn(idx, I).Y
   Next I

   For I = 0 To sIn_Count(idx) - 1
      reS = reS + ssIn(idx, I).X
      imS = imS + ssIn(idx, I).Y

   Next I

   If zIn_Count(idx) > 0 Then
      zIn_Mean(idx).X = re / zIn_Count(idx)
      zIn_Mean(idx).Y = im / zIn_Count(idx)

      sIn_Mean(idx).X = reS / sIn_Count(idx)
      sIn_Mean(idx).Y = imS / sIn_Count(idx)

   '   Debug.Print "Index="; idx; " S11 mean = "; cFormat(sIn_Mean(idx))
   Else
      zIn_Mean(idx).X = 0#
      zIn_Mean(idx).Y = 0#

      sIn_Mean(idx).X = 0#
      sIn_Mean(idx).Y = 0#

   End If

   'lblMean(idx).Caption = cFormat(zIn_Mean(idx))
   lblMean(idx).Caption = cFormat(sIn_Mean(idx))
Next idx
End Sub

' Calculates the mean values of the two port network
Private Sub getMeanS()

Dim I As Integer
Dim j As Integer

Dim re(7) As Double
Dim im(7) As Double

Dim index As Integer

index = sIn_Count(2)

For I = 0 To 7
   re(I) = 0#
   im(I) = 0#
Next I

For I = 0 To index
   re(1) = re(1) + twoPort(I).s11.X
   re(2) = re(2) + twoPort(I).s12.X
   re(3) = re(3) + twoPort(I).s21.X
   re(4) = re(4) + twoPort(I).s22.X

   im(1) = im(1) + twoPort(I).s11.Y
   im(2) = im(2) + twoPort(I).s12.Y
   im(3) = im(3) + twoPort(I).s21.Y
   im(4) = im(4) + twoPort(I).s22.Y
Next I

If index > 0 Then
   With twoPortMean
```

```
      .s11.X = re(1) / index
      .s12.X = re(2) / index
      .s21.X = re(3) / index
      .s22.X = re(4) / index

      .s11.Y = im(1) / index
      .s12.Y = im(2) / index
      .s21.Y = im(3) / index
      .s22.Y = im(4) / index
   End With
Else
   With twoPortMean
      .s11.X = 0#
      .s12.X = 0#
      .s21.X = 0#
      .s22.X = 0#

      .s11.Y = 0#
      .s12.Y = 0#
      .s21.Y = 0#
      .s22.Y = 0#
   End With
End If

With twoPortMean
   lblS(0).Caption = cFormatExp(.s11)
   lblS(1).Caption = cFormatExp(.s12)
   lblS(2).Caption = cFormatExp(.s21)
   lblS(3).Caption = cFormatExp(.s22)
End With
End Sub

' Calculate standard deviation of the measured data
Private Sub getSDS()

Dim I As Integer
Dim j As Integer

Dim re(4) As Double
Dim im(4) As Double

Dim reSum(4) As Double
Dim imSum(4) As Double

Dim index As Integer

index = sIn_Count(2)

For I = 0 To 3
   re(I) = 0#
   im(I) = 0#
   reSum(I) = 0#
   imSum(I) = 0#
Next I

For I = 0 To index
   With twoPort(I)
      reSum(0) = reSum(0) + .s11.X
      reSum(1) = reSum(1) + .s12.X
      reSum(2) = reSum(2) + .s21.X
      reSum(3) = reSum(3) + .s22.X

      re(0) = re(0) + (.s11.X * .s11.X)
      re(1) = re(1) + (.s12.X * .s12.X)
      re(2) = re(2) + (.s21.X * .s21.X)
      re(3) = re(3) + (.s22.X * .s22.X)


      imSum(0) = imSum(0) + .s11.Y
      imSum(1) = imSum(1) + .s12.Y
      imSum(2) = imSum(2) + .s21.Y
      imSum(3) = imSum(3) + .s22.Y

      im(0) = im(0) + (.s11.Y * .s11.Y)
      im(1) = im(1) + (.s12.Y * .s12.Y)
      im(2) = im(2) + (.s21.Y * .s21.Y)
      im(3) = im(3) + (.s22.Y * .s22.Y)
   End With
Next I

If index > 0 Then

   With twoPortSD
      On Error Resume Next
      .s11.X = Sqr((re(0) - (reSum(0) * reSum(0) / index)) /
(index))
      .s12.X = Sqr((re(1) - (reSum(1) * reSum(1) / index)) /
(index))
      .s21.X = Sqr((re(2) - (reSum(2) * reSum(2) / index)) /
(index))

      .s22.X = Sqr((re(3) - (reSum(3) * reSum(3) / index)) /
(index))

      .s11.Y = Sqr((im(0) - (imSum(0) * imSum(0) / index)) /
(index))
      .s12.Y = Sqr((im(1) - (imSum(1) * imSum(1) / index)) /
(index))
      .s21.Y = Sqr((im(2) - (imSum(2) * imSum(2) / index)) /
(index))
      .s22.Y = Sqr((im(3) - (imSum(3) * imSum(3) / index)) /
(index))

      On Error GoTo 0
   End With
Else
   With twoPortSD
      .s11.X = 0#
      .s12.X = 0#
      .s21.X = 0#
      .s22.X = 0#

      .s11.Y = 0#
      .s12.Y = 0#
      .s21.Y = 0#
      .s22.Y = 0#
   End With
End If

With twoPortSD
   lblSDS(0).Caption = cFormatExp(.s11)
   lblSDS(1).Caption = cFormatExp(.s12)
   lblSDS(2).Caption = cFormatExp(.s21)
   lblSDS(3).Caption = cFormatExp(.s22)
End With


End Sub

' Calculates standard deviation of the Zin
Private Sub Calc_zIn_SD()
Dim I, idx As Integer
Dim re As Double
Dim im As Double

Dim reS As Double
Dim imS As Double
```

```
For idx = 0 To 3
   re = 0#
   im = 0#

   reS = 0#
   imS = 0#

   For I = 0 To zIn_Count(idx) - 1
      re = re + Abs(zIn(idx, I).X - zIn_Mean(idx).X)
      im = im + Abs(zIn(idx, I).Y - zIn_Mean(idx).Y)
   Next I

   For I = 0 To sIn_Count(idx) - 1
      reS = reS + Abs(ssIn(idx, I).X - sIn_Mean(idx).X)
      imS = imS + Abs(ssIn(idx, I).Y - sIn_Mean(idx).Y)
   Next I

   If (re < 0#) Then re = 0# 'leo
   If (im < 0#) Then im = 0# 'leo



   If (reS < 0#) Then reS = 0# 'leo
   If (imS < 0#) Then imS = 0# 'leo


   If zIn_Count(idx) > 0 Then
      zIn_SD(idx).X = Sqr(re / zIn_Count(idx))
      zIn_SD(idx).Y = Sqr(im / zIn_Count(idx))

      sIn_SD(idx).X = Sqr(reS / sIn_Count(idx))
      sIn_SD(idx).Y = Sqr(imS / sIn_Count(idx))

   'Debug.Print "Index="; idx; " S11 s.d. = ";
cFormat(sIn_SD(idx))
   Else
      zIn_SD(idx).X = 0#
      zIn_SD(idx).Y = 0#

      sIn_SD(idx).X = 0#
      sIn_SD(idx).Y = 0#

   End If

   'lblSD(idx).Caption = cFormat(zIn_SD(idx))
   lblSD(idx).Caption = cFormat(sIn_SD(idx))
Next idx
End Sub


' Check if file exists
Public Function FileExists(ByVal fname As String) As
Boolean

If fname = "" Or Right(fname, 1) = "\" Then
   FileExists = False: Exit Function
End If

FileExists = (Dir(fname) <> "")
End Function


‘Initialization function upon loading the main screen
Private Sub Form_Load()
Dim I As Integer

For I = 0 To 3
   lstBox(I).Clear
Next I

For I = 860 To 960
   freq.AddItem (CStr(I))
Next I

Dim hits(0) As Double
hits(0) = 0
MSChart1.ChartData = hits
MSChart2.ChartData = hits

SSTab1.Tab = 0
SSTab2.Tab = 0

lstBoxSelIndex = -1

initFlag = True
freqSweepFlag = False

ZL.X = 33#
ZL.Y = -112#

'default value for VNA power level dBm
Gpower = 0

'The following demonstrates how to connect to the
instrument at the given address

On Error Resume Next
VNA.Connect VNAINSTR
On Error GoTo 0

Gpower = 7#


minPwr = Val(txtPwr(0).Text)
maxPwr = Val(txtPwr(1).Text)
stepPwr = Val(txtPwr(2).Text)


frmTagTester.Caption = "Tag Tester - Copyright © 2007
Leonid Mats - All Rights Reserved"

Call LoadSmithChart

Call LoadData

End Sub

Private Sub updateFilePath()
Dim str1() As String
str1 = Split(cmbTagSelect.Text)
strFilePath = App.Path + "\PHD\" + str1(0) + "010107\" +
str1(1)

End Sub

Private Sub lstBox_Scroll(index As Integer)

Call lstBox_Click(index)

End Sub

'Draw Smith Chart Function
Private Sub LoadSmithChart()

Dim theta_min As Single
Dim theta_max As Single
Dim dtheta As Single
Dim theta As Single
```

```
Dim values() As Double
Dim I, k As Integer
Dim num_theta As Integer

Dim radius(5) As Double

Dim degree, pi As Double
Dim originx, originy, r As Single
Dim X, Y, x1, y1, x2, y2, x3, y3, x4, y4, x5, y5 As Double
Dim x6, y6, x7, y7, x8, y8, x9, y9, x10, y10, x11, y11 As
Double
Dim x12, y12, x13, y13, x14, y14, x15, y15, x16, y16, x17,
y17 As Double
Dim x18, y18, x19, y19 As Double

theta_min = 0
pi = 3.14159265
Dim j As Double
ReDim values(0 To 360, 1 To 19 * 2)

j = 0
I = 0

Do While j < 1.9 * pi

   originx = 0
   originy = 0
   r = 1
   degree = I * pi / 180

   'x  = originx + Cos(j) * r
   'y = originy + Sin(j) * r


   r = 2
   x1 = originx + (r / (1 + r)) + (1 / (1 + r)) * Cos(j)
   y1 = originy + (1 / (1 + r)) * sIn(j)
   r = 1
   x2 = originx + (r / (1 + r)) + (1 / (1 + r)) * Cos(j)
   y2 = originy + (1 / (1 + r)) * sIn(j)
   r = 0.5
   x3 = originx + (r / (1 + r)) + (1 / (1 + r)) * Cos(j)
   y3 = originy + (1 / (1 + r)) * sIn(j)
   r = 0.2
   x4 = originx + (r / (1 + r)) + (1 / (1 + r)) * Cos(j)
   y4 = originy + (1 / (1 + r)) * sIn(j)
   r = 0.005
   x5 = originx + (r / (1 + r)) + (1 / (1 + r)) * Cos(j)
   y5 = originy + (1 / (1 + r)) * sIn(j)


   ' circle of imaginary Z
   '0.333 1 1.5 2.5 10

   r = 0.333
   x6 = originx + 1 + Cos(j) * r
   y6 = originy + r + sIn(j) * r

   r = 1
   x7 = originx + 1 + Cos(j) * r
   y7 = originy + r + sIn(j) * r

   r = 1.5
   x8 = originx + 1 + Cos(j) * r
   y8 = originy + r + sIn(j) * r

   r = 2.5
   x9 = originx + 1 + Cos(j) * r
   y9 = originy + r + sIn(j) * r

   r = 10
   x10 = originx + 1 + Cos(j) * r
   y10 = originy + r + sIn(j) * r


   r = -0.333
   x11 = originx + 1 + Cos(j) * r
   y11 = originy + r + sIn(j) * r

   r = -1
   x12 = originx + 1 + Cos(j) * r
   y12 = originy + r + sIn(j) * r

   r = -1.5
   x13 = originx + 1 + Cos(j) * r
   y13 = originy + r + sIn(j) * r

   r = -2.5
   x14 = originx + 1 + Cos(j) * r
   y14 = originy + r + sIn(j) * r

   r = -10
   x16 = originx + 1 + Cos(j) * r
   y16 = originy + r + sIn(j) * r

   x17 = cSmithChartGamma(zIn(3, j)).X
   y17 = cSmithChartGamma(zIn(3, j)).Y

   x18 = cSmithChartGamma(simZin(0)).X
   y18 = cSmithChartGamma(simZin(0)).Y

   x19 = cSmithChartGamma(simZin(2)).X
   y19 = cSmithChartGamma(simZin(2)).Y

   ' circle of real Z

   'values(i, 1) = x
   'values(i, 2) = y

   values(I, 1) = x1
   values(I, 2) = y1
   values(I, 3) = x2
   values(I, 4) = y2
   values(I, 5) = x3
   values(I, 6) = y3
   values(I, 7) = x4
   values(I, 8) = y4
   values(I, 9) = x5
   values(I, 10) = y5
   values(I, 11) = x6
   values(I, 12) = y6
   values(I, 13) = x7
   values(I, 14) = y7
   values(I, 15) = x8
   values(I, 16) = y8
   values(I, 17) = x9
   values(I, 18) = y9
   values(I, 19) = x10
   values(I, 20) = y10
   values(I, 21) = x11
   values(I, 22) = y11
   values(I, 23) = x12
   values(I, 24) = y12
   values(I, 25) = x13
   values(I, 26) = y13
   values(I, 27) = x14
   values(I, 28) = y14
```

```
    values(I, 29) = x15
    values(I, 30) = y15
    values(I, 31) = x16
    values(I, 32) = y16
    values(I, 33) = x17
    values(I, 34) = y17
    values(I, 35) = x18
    values(I, 36) = y18
    values(I, 37) = x19
    values(I, 38) = y19


    I = I + 1
    j = j + (2 * pi / 358)
Loop

For I = 0 To 360
   For j = 1 To 38 Step 2

      If values(I, j) = 0 And values(I, j + 1) = 0 Then
         values(I, j) = values(0, j)
         values(I, j + 1) = values(0, j + 1)
      End If
   Next j
Next I

' Send the data to the chart.
Chart1.chartType = VtChChartType2dXY
DoEvents
Chart1.ChartData = values
DoEvents

With Chart1

   For I = 1 To .Plot.SeriesCollection.count - 5

      With .Plot.SeriesCollection(I)
         '.SeriesMarker.Show = True
         .SeriesMarker.Auto = False
         .DataPoints.Item(-1).marker.Size = 1
         .DataPoints(-1).Brush.FillColor.Set 176, 176, 176
      End With

      .Plot.SeriesCollection(.Plot.SeriesCollection.count -
5).DataPoints(-1).Brush.FillColor.Set 255, 0, 0



      .Plot.SeriesCollection(.Plot.SeriesCollection.count -
3).SeriesMarker.Show = True
      .Plot.SeriesCollection(.Plot.SeriesCollection.count -
3).DataPoints.Item(-1).marker.Size = 1
      .Plot.SeriesCollection(.Plot.SeriesCollection.count -
3).DataPoints(-1).Brush.FillColor.Set 255, 255, 0

      .Plot.SeriesCollection(.Plot.SeriesCollection.count -
1).SeriesMarker.Show = True
      .Plot.SeriesCollection(.Plot.SeriesCollection.count -
1).DataPoints.Item(-1).marker.Size = 1
      .Plot.SeriesCollection(.Plot.SeriesCollection.count -
1).DataPoints(-1).Brush.FillColor.Set 255, 0, 255

   Next I

End With
End Sub

‘ Save Data to the text files
Private Sub saveDataNew()
Dim strFilePath As String
Dim strFile As String
Dim I, j, k As Integer
Dim totalCount As Integer

Screen.MousePointer = vbHourglass

strFilePath = App.Path + "\data"

Dim strFile1, strFile2, strFile3, strFile4, strFile5, strFile6,
strFile7, strFile8, strFile9, strFile10 As String
Dim tmp As String
For I = 0 To 3
   'strFile = strFilePath + "\" + Format(Now, "ddmmmyyyy")
+ CStr(i) + ".txt"
   strFile1 = strFilePath + "\" + "data" + CStr(I) + ".txt"

   If freqSweepFlag Then
      strFile2 = strFilePath + "\" + freq.Text + "_s11_" +
CStr(I) + ".txt"
      strFile10 = strFilePath + "\" + freq.Text +
"_s11_2_NL.txt"
   Else
      strFile2 = strFilePath + "\" + "s11_" + CStr(I) + ".txt"
      strFile10 = strFilePath + "\" + "s11_2_NL.txt"
   End If

   strFile3 = strFilePath + "\" + "dts_" + CStr(I) + ".txt"

   Open strFile1 For Output As #1 'open data file
   Open strFile2 For Output As #2 'open data file
   Open strFile3 For Output As #3 'open data file

   For j = 0 To zIn_Count(I) - 1
      Print #1, CStr(zIn(I, j).X) + " "; CStr(zIn(I, j).Y)
      Print #2, CStr(ssIn(I, j).X) + vbTab; CStr(ssIn(I, j).Y)
      Print #3, dts(I, j)
   Next j

   Close #3
   Close #2
   Close #1
Next I

If RunSweep Then
   strFile = strFilePath + "\" + "data4.txt"
   Open strFile For Output As #1 'open data file
   For j = 0 To zIn_Count(2) - 1
      Print #1, CStr(f(j))
   Next j
   Close #1
End If

Open strFile10 For Output As #10 'open data file
For I = 0 To sIn_Count(2) - 1
   tmp = CStr(sInNL(I).pwr) + vbTab +
CStr(sInNL(I).sIn.X) + vbTab + CStr(sInNL(I).sIn.Y)
   For j = 0 To (maxPwr - minPwr) / stepPwr
      tmp = tmp + vbTab
      tmp = tmp + CStr(sInNL(I).Data(j).pwr) + vbTab +
CStr(sInNL(I).Data(j).sIn.X) + vbTab +
CStr(sInNL(I).Data(j).sIn.Y)
   Next j
   Print #10, tmp
Next I
Close #10

strFile1 = strFilePath + "\" + "smithS.s1p"

Open strFile1 For Output As #1 'open data file
```

```
'Print #1, "# MHZ Z RI"
Print #1, "#MHZ S ri R 50"
For j = 0 To sIn_Count(3) - 1
   Print #1, CStr(j); vbTab;
CStr(cSmithChartGamma(ssIn(3, j)).X) & vbTab &
CStr(cSmithChartGamma(ssIn(3, j)).Y)
Next j
Close #1

Screen.MousePointer = vbDefault

End Sub

'Prepare data for the Histogram Chart
Function MakeHistogramData(ByRef hits() As Double,
ByVal numBins As Integer, ByRef binX() As Double,
ByRef binY() As Double)
ReDim binX(numBins - 1)
ReDim binY(numBins - 1)

'FIND MIN AND MAX X VALUES (NUMBER OF HITS
FOR THE BIN)
Dim hitMax As Double
Dim hitMin As Double

Dim I As Integer
Dim thisBin As Integer

If UBound(hits) <= 1 Then Exit Function

hitMax = 0
hitMin = 1000000000


For I = 0 To UBound(hits)
   If hits(I) > hitMax Then hitMax = hits(I)
   If hits(I) < hitMin Then hitMin = hits(I)
Next


For I = 0 To UBound(hits)
   binY(thisBin) = 0
   binX(thisBin) = 0
Next


'FILL IN Y DATA FOR binY ARRAY

For I = 0 To UBound(hits)
   'On Error Resume Next
   If hitMax - hitMin <> 0 Then
      thisBin = CInt((numBins - 1) * (hits(I) - hitMin) /
(hitMax - hitMin))
      binY(thisBin) = binY(thisBin) + 1
   End If

'On Error GoTo 0
Next

'FILL IN X DATA FOR binX ARRAY
For I = 0 To numBins - 1
   binX(I) = hitMin + I * (hitMax - hitMin) / numBins
Next

MakeHistogramData = binY

End Function

Private Sub save_Click()
Call saveDataNew
End Sub

Private Sub SSTab1_Click(PreviousTab As Integer)
Dim I As Integer
opt = SSTab1.Tab - 1

If SSTab1.Tab = 0 Then
   cmdGetData.Enabled = False
Else
   cmdGetData.Enabled = True
End If

End Sub
```

BIBLIOGRAPHY

[1] M. H. Mickle, M. Lovell, L. Mats, L. Neureuter, and D. Gorodetsky, "Energy Harvesting, Profiles, and Potential Sources" International Journal of Parallel and Distributed Systems and Networks," vol. 4, 2001.

[2] F. Thiesse, M. Dierkes, and E. Fleisch, "LotTrack: RFID-Based Process Control in the Semiconductor Industry," Pervasive Computing, IEEE, vol. 5, pp. 47-53, 2006.

[3] W. Shang-Wei, C. Wun-Hwa, O. Chorng-Shyong, L. Li, and C. Yun-Wen, "RFID Application in Hospitals: A Case Study on a Demonstration RFID Project in a Taiwan Hospital," 2006, pp. 184a-184a.

[4] B. Strassner and C. Kai, "Passive 5.8-GHz radio-frequency identification tag for monitoring oil drill pipe," Microwave Theory and Techniques, IEEE Transactions on, vol. 51, pp. 356-363, 2003.

[5] M. M. Ollivier, "RFID-a practical solution for problems you didn't even know you had!," IEE Colloquium on Wireless technology digest, pp. 3/1-3/6,1996.

[6] R. Glidden, C. Bockorick, S. Cooper, C. Diorio, D. Dressler, V. Gutnik, C. Hagen, D. Hara, T. Hass, T. Humes, J. Hyde, R. Oliver, O. Onen, A. Pesavento, K. Sundstrom, and M. Thomas, "Design of ultra-low-cost UHF RFID tags for supply chain applications," Communications Magazine, IEEE, vol. 42, pp. 140-151, 2004.

[7] K. Finkenzeller, RFID Handbook : Fundamentals and Applications in Contactless Smart Cards and Identification 2nd ed.: John Wiley & Sons, 2003.

[8] J. D. Kraus and R. J. Marhefka, Antennas For All Aplications, 3rd ed.: McGraw-Hill Science/Engineering/Math, 2001.

[9] J. Landt, "The history of RFID," Potentials, IEEE, vol. 24, pp. 8-11, 2005.

[10] K. V. S. Rao, "An overview of backscattered radio frequency identification system (RFID)," 1999, pp. 746-749 vol.3.

[11] S. Sarma, "WHITE PAPER: Towards the 5c Tag," Auto-ID Center, 2001.

[12] B. Trebilcock, "RFID: print and ship," Modern Materials Handling, January 1 2005.

[13] Omron Corporation, Available: http://www.omronrfid.com

[14] W. Kawai, "OMRON Technology To produce RFID Tags," 2005, Available: http://www.omronrfid.com

[15] Omron, "Jomful Technology," 2005, Available: http://www.omronrfid.com

[16] K. V. S. Rao, P. V. Nikitin, and S. F. Lam, "Antenna design for UHF RFID tags: a review and a practical application," Antennas and Propagation, IEEE Transactions on, vol. 53, pp. 3870-3876, 2005.

[17] I. J. Forster, "Method of variable position strap mounting for rfid transponder," United States Patent Application #20050282495, 2005.

[18] M. J. Brady, D. Dah-Weih, and K. V. S. Rao, "Transponder packaging techniques in radio frequency identification systems," 1999, pp. 956-957 vol.3.

[19] ZIH Corporation, Available: http://www.zebra.com

[20] Paxar Corporation, Available: http://www.paxar.com

[21] Omron, "V720-Series Electromagnetic Inductive RFID System Tag Inlets," 2003.

[22] G. W. Stimson, Introduction to Airborne Radar. Mendham, NJ: SciTech Publishing, 1998.

[23] C. Balanis, Antenna Theory Analysis and Design. New York: John Wiley & Sons, Inc., 1982.

[24] R. C. Hansen, "Relationships between antennas as scatterers and as radiators," Proceedings of the IEEE, vol. 77, pp. 659-662, 1989.

[25] Frost and Sullivan, Available: http://www.frost.com

[26] In-Stat, "RFID Tags And Chips: Changing The World For Less Than The Price Of A Cup Of Coffee," p. 42, December 2005. Available: http://www.in-stat.com

[27] U. Karthaus and M. Fischer, "Fully integrated passive UHF RFID transponder IC with 16.7-/spl mu/W minimum RF input power," Solid-State Circuits, IEEE Journal of, vol. 38, pp. 1602-1608, 2003.

[28] EPCglobal, "EPC Radio-Frequency Identity Protocols, Class-1 Generation-2 UHF Air Interface Protocol Standard Version 1.0.9," January 2005.

[29] Kulicke&Soffa, "4523 Manual Wedge Bonder," 2001.

[30] Ansoft Corporation, Available: http://www.ansoft.com

[31] Sonnet Software, Inc., Available: http://www.sonnetusa.com

[32] Zeland Software, Inc., Available: http://www.zeland.com

[33] MOSIS, http://www.mosis.org/Technical/Packaging/Ceramic/pkg-dip40-char.pdf

[34] Omron, "Manufacturing Method for High Reliability Inlay," June 30 2005.

[35] J. Rasul and W. Olson, "Flip chip on paper assembly utilizing anisotropic conductive adhesive," 2002, pp. 90-94.

[36] G. Prophet, "RFID and the smart label: bye bye bar code," EDN Europe, June 2000.

[37] J. S. Smith, "RFID inlay assembly technologies," in Smart Labels Conference, Baltimore, USA, 2005.

[38] J. Kawai; Wakahiro (Kyoto, "Method of mounting a semiconductor chip, circuit board for flip-chip connection and method of manufacturing the same, electromagnetic wave readable data carrier and method of manufacturing the same, and electronic component module for an electromagnetic wave readable data carrier.," Omron Corporation (Kyoto, JP) 2003.

[39] J. Kawai; Wakahiro (Kyoto, "Method of mounting a semiconductor chip, circuit board for flip-chip connection and method of manufacturing the same, electromagnetic wave readable data carrier and method of manufacturing the same, and electronic component module for an electromagnetic wave readable data carrier.," Omron Corporation (Kyoto, JP), 2002.

[40] R. Harrington, "Electromagnetic scattering by antennas," Antennas and Propagation, IEEE Transactions on [legacy, pre - 1988], vol. 11, pp. 595-596, 1963.

[41] D. D. King, "Measurement and interpretation of antenna scattering," Proceedings of the I.R.E., vol. 37, pp. 770-777, July 1949.

[42] E. F. Knott, J. F. Shaeffer, and M. T. Tuley, Radar Cross Section 2nd ed.: Artech House Publishers, 1993.

[43] R. J. Garbacz, "Determination of antenna parameters by scattering cross section measurements," Proceedings of the IEEE, vol. 111, October 1964.

[44] R. Green, "Scattering from conjugate-matched antennas," IEEE Transactions on Antennas and Propagation, vol. 14, pp. 17-21, 1966.

[45] H. Yueh-Ying, "Back-scattering cross section of a center-loaded cylindrical antenna," IEEE Transactions on Antennas and Propagation, vol. 6, pp. 140-148, 1958.

[46] D. M. Pozar, Microwave Engineering, 2nd ed. New York: John Wiley and Sons, 1998.

[47] K. S. Peat and J. G. Ih, "An analytical investigantion of the indirect measurements method of estimating the acoustic impidance of a time-varying source," Journal of Sound and Vibration, vol. 244, pp. 821-835, 2001.

[48] L. Hsin-Chia and C. Tah-Hsiung, "Antenna gain and scattering measurement using reflective three-antenna method," 1999, pp. 374-377 vol.1.

[49] P. V. Nikitin and K. V. S. Rao, "Measurement of Backscattering from RFID Tags," in Antennas Measurement Techniques Association Symposium, Newport, RI, 2005.

[50] M. A. Gilbert, "Parallel plate scattering range measurements utilizing an automatic network analyzer," 1989, pp. 343-346 vol.1.

[51] C. Icheln, P. Vainikainen, and P. Haapala, "Application of a GTEM cell to small antenna measurements," 1997, pp. 546-549 vol.1.

[52] H. Ping, "Small antenna measurements using a GTEM cell," 2003, pp. 715-718 vol.4.

[53] Y. V. Prokopenko, Y. M. Poplavko, A. M. Shevchuk, and N. Bahtina, "Influence of absorber termination quality in the GTEM cell on the RF radiation measurement," 2005, pp. 766-767 Vol. 2.

[54] Avery Dennison Corporation, Available: http://www.rfid.averydennison.com

[55] Alien Technology Corporation, Available: http://www.alientechnology.com

[56] Texas Instruments Inc., Available: http://www.ti.com

[57] UPM Raflatac, Available: http://www.rafsec.com

[58] Impinj, Inc. Available: http://www.impinj.com

[59] Ted Pella, Inc Available: http://www.tedpella.com

[60] J. P. Curty, N. Joehl, F. Krummenacher, C. Dehollain, and M. J. Declercq, "A Model for μ-Power Rectifier Analysis and Design," Circuits and Systems I: Regular Papers, IEEE Transactions on [see also Circuits and Systems I: Fundamental Theory and Applications, IEEE Transactions on], vol. 52, pp. 2771-2779, 2005.

[61] P. V. Nikitin, S. Lam, and K. V. S. Rao, "Low cost silver ink RFID tag antennas," 2005, pp. 353-356 vol. 2B.

[62] P. Berry, M. Dwane, G. Butch, and D. Baghurst, "Novel Conductive Inks for Smart. Label Applications," The Journal for Surface Mount and Electronic Assembly, December 2005.

[63] T. H. Lee, The Design of CMOS Radio-Frequency Integrated Circuits, 1 ed.: Cambridge University Press, 1998.

[64] G. Gonzalez, Microwave Transistor Amplifiers: Analysis and Design 2nd ed.: Prentice Hall, 1996.

[65] ISO, "Guide to the Expression of Uncertainty in Measurement," 2nd ed: International Organization for Standardization, 1995.

[66] B. N. Taylor and C. E. Kuyatt, "Guidelines for Evaluating and Expressing the Uncertainty of NIST Measurement Results " Technical Note 1297, National Institute of Standards and Technology (NIST), 1994.

[67] A. G. Morgan, N. M. Ridler, and M. J. Salter, "Generalised calibration schemes for precision RF vector network analyser measurements," IEEE Instrumentation and Measurement, 2002, pp. 1355-1358 vol.2.

[68] B. D. Hall, "Calculations of measurement uncertainty in complex-valued quantities involving 'uncertainty in the uncertainty'," ARFTG Microwave Measurements Conference, 2004, pp. 15-22.

[69] N. M. Ridler and M. J. Salter, "A generalised approach to the propagation of uncertainty in complex S-parameter measurements," ARFTG Microwave Measurements Conference, 2004, pp. 1-14.

[70] R. A. Johnson and D. W. Wichern, Applied Multivariate Statistical Analysis 5th ed.: Prentice Hall, 2002.

[71] A. C. Rencher, Multivariate Statistical Inference and Applications vol. 2: Wiley-Interscience, 1997.

[72] T. W. Anderson, An Introduction to Multivariate Statistical Analysis, 3rd ed., 2003.

[73] H. Hotelling, "The Generalization of Student's Ratio," The Annals of Mathematical Statistics, vol. 2, pp. 360-378, 1931.

[74] Statistical Consulting Services, Available: http://www.stat.pitt.edu/consulting

[75] A. Hastings, The Art of Analog Layout 1st ed.: Prentice Hall, 2000.

[76] A. Cinar and C. Undey, "Statistical process and controller performance monitoring. A tutorial on current methods and future directions," 1999, pp. 2625-2639 vol.4.

[77] Statistical and Power Analysis Software (NCSS), Available: http://www.ncss.com

[78] M. L. Tiku, "Tables of the Power of the F-Test," Journal of the American Statistical Association, vol. 62, No. 318, pp. 525-539, June 1967.